Statistical Analysis and Spectral Methods for Signal-Plus-Noise Matrix Models

by

Joshua R. Cape

A dissertation submitted to The Johns Hopkins University in conformity with the requirements for the degree of Doctor of Philosophy.

Baltimore, Maryland

May, 2019

Abstract

The singular value matrix decomposition plays a ubiquitous role in statistics and related fields. Myriad applications including clustering, classification, and dimensionality reduction involve studying and understanding the geometric structure of singular values and singular vectors.

Chapter 2 of this dissertation presents an initial analysis of local (e.g., entrywise) singular vector (resp., eigenvector) perturbations for signal-plus-noise matrix models of the form $\widehat{\mathbf{M}} := \mathbf{M} + \mathbf{E}$. We obtain both deterministic and probabilistic upper bounds on singular vector perturbations that complement and in certain settings improve upon classical, well-established benchmark bounds in the literature. We then apply our tools and methods of analysis to problems involving (spike) principal subspace estimation for high-dimensional covariance matrices and network models exhibiting community structure. Subsequently, Chapter 3 obtains precise local eigenvector estimation results under stronger assumptions involving signal strength, probabilistic concentration, and homogeneity. We provide *in silico* simulation examples to illustrate our theoretical bounds and distributional limit theory. Chapter 4 tran-

ABSTRACT

sitions to the investigation of singular value (resp., eigenvalue) perturbations, still in the signal-plus-noise matrix model framework. There, our results are leveraged for the purpose of better understanding hypothesis testing and change-point detection in statistical random graph analysis. Chapter 5 builds upon recent joint analysis of singular (resp., eigen) values and vectors in order to investigate the asymptotic relationship between spectral embedding performance and underlying network structure for stochastic block model graphs.

The content of this dissertation corresponds to several contemporary statistics publications and preprints, namely the works Cape et al. (2017, 2018, 2019a,b).

Primary Reader: Carey E. Priebe

Secondary Reader: Minh Tang

Acknowledgments

I am deeply grateful to my advisors Carey E. Priebe and Minh Tang for their holistic, multifaceted approaching to mentoring. Words alone are woefully inadequate for conveying the formative role that Carey and Minh have played in my professional and personal development. It has been a privilege to learn from them and to write this dissertation under their supervision.

Over the years, the Department of Applied Mathematics and Statistics at Johns Hopkins University has provided me with a consistently excellent environment in which to pursue a doctoral degree. The harmonious atmosphere among and between faculty, students, and staff has been a great source of productivity and enjoyment during my graduate studies.

I am indebted to many people for their guidance, help, and friendship. It is unfortunately impossible to name everyone here. I want to especially thank faculty members Avanti Athreya, James A. Fill, Donniell E. Fishkind, Vince Lyzinski, James C. Spall, and John C. Wierman for their instruction and insight over the years. I thank members of my qualifying exam and dissertation defense panels for their

suggestions and feedback, in particular Raman Arora, Amitabh Basu, Brian Caffo, Edinah Gnang, Chikako Mese, Daniel Robinson, and Yanxun Xu. I also want to thank Kristin Bechtel, Ann Gibbins, Sandra Kirt, Youngser Park, and Lindsay Tarner for all of their behind-the-scenes technical and organizational assistance throughout my Ph.D. studies. I am deeply grateful to Diane Clark, Eric Gottlieb, Jeff Hamrick, Anna Hinkle, Qin Lu, Christopher Seaton, Steve Schutts, and Reid Wightman for serving as formative teacher-mentors at various junctures throughout my education.

Last but not least, I am indebted to my family and close friends for their steadfast support and encouragement. Thank you all.

Dedication

This dissertation is dedicated to Corinna, Ruth, and Robert.

Contents

List of Tables

List of Figures

Chapter 1

Introduction

Consider the setting in which an experimental outcome y is modeled as a "noisy" realization of an underlying ground-truth "signal" quantity μ, namely

$$y = \mu + \epsilon, \tag{1.1}$$

where ϵ represents a noise term (deterministic or stochastic). The signal-plus-noise model displayed in Eq. (1.1), together with its generalizations, lies at the heart of scientific modeling and statistical analysis. Indeed, one need not look far to find examples and applications in reference texts and scholarly publications.

In this work we shall replace the scalar quantities (elements) μ and ϵ with matrices $\mathbf{M}$ and $\mathbf{E}$, respectively. Matrices can be viewed simply as rectangular arrays of elements, but matrices can also be thought of structurally in terms the factorizations

and decompositions that they admit. Importantly, even though entry (i, j) in $\mathbf{M}$ and in $\mathbf{M} + \mathbf{E}$ satisfy a simple relationship, the structural relationship between $\mathbf{M}$ and $\mathbf{M}+\mathbf{E}$ in terms of singular values and singular vectors may be quite complicated. More specifically, it is well-known that in general, matrix spectral perturbations behave highly non-linearly even in simple additive matrix models (Bhatia, 1997).

Given matrices $\mathbf{M}$ and $\mathbf{E}$ with the same dimensions, the ordered singular values $\sigma_i(\cdot)$ of $\mathbf{M}+\mathbf{E}$ and $\mathbf{M}$ satisfy a well-known perturbation inequality due to Weyl (Weyl, 1912); namely, in terms of the matrix operator norm $\|\cdot\|_2$, for each index i,

$$|\sigma_i(\mathbf{M} + \mathbf{E}) - \sigma_i(\mathbf{M})| \leq \|\mathbf{E}\|_2. \tag{1.2}$$

When $\mathbf{M} + \mathbf{E}$ and $\mathbf{M}$ are both symmetric, their corresponding principal subspaces $\widehat{\mathbf{U}}$ and $\mathbf{U}$ are "close to each other" as a function of the noise strength and the magnitude of a so-called *spectral gap* (i.e., *eigengap*) $\delta_{\text{gap}} > 0$, provided the latter exists. In particular, it follows from the classical Davis–Kahan $\sin\boldsymbol{\Theta}$ theorem (Bhatia, 1997; Davis and Kahan, 1970) that there exists an orthogonal matrix $\mathbf{W}$ and an absolute constant $C > 0$ such that

$$\|\widehat{\mathbf{U}} - \mathbf{U}\mathbf{W}\|_2 \leq C \left(\frac{\|\mathbf{E}\|_2}{\delta_{\text{gap}}} \right). \tag{1.3}$$

The classical results summarized in Eqs. (1.2)–(1.3) shall serve as baselines for the purpose of evaluating and understanding the results presented in this dissertation.

Here, we obtain stronger results as a function of the signal-to-noise level that improve upon these classical results in settings exhibiting additional structure. Loosely speaking, our results quantifying $\widehat{\mathbf{U}} \approx \mathbf{U}$ will be shown to hold in a strong local sense (e.g., entrywise). Contrast this with Eq. (1.3) which via $\|\cdot\|_2$ can be interpreted as a global (i.e., basis independent) result. For an extended discussion of classical perturbation theory and Eqs. (1.2)–(1.3), see Bhatia (1997); Horn and Johnson (2012); Stewart and Sun (1990).

1.1 Overview

Chapter 2 provides a novel collection of technical and theoretical tools for studying the geometry of singular subspaces using the two-to-infinity norm. Motivated by preliminary deterministic Procrustes analysis, we consider a general matrix perturbation setting in which we derive a new Procrustean matrix decomposition. Together with flexible machinery developed for the two-to-infinity norm, this allows us to conduct a refined analysis of the induced perturbation geometry with respect to the underlying singular vectors even in the presence of singular value multiplicity. Our analysis yields singular vector entrywise perturbation bounds for a range of popular matrix noise models, each of which has a meaningful associated statistical inference task. In addition, we demonstrate how the two-to-infinity norm is the preferred norm in certain statistical settings. Specific applications discussed in Chapter 2 include co-

variance estimation, singular subspace recovery, and multiple graph inference. This chapter has given rise to the paper Cape et al. (2019b).

Chapter 3 characterizes the behavior of perturbed eigenvectors for a range of signal-plus-noise matrix models encountered in both statistical and random matrix theoretic settings. In this chapter, we prove both first-order approximation results (i.e., sharp deviations) as well as second-order distributional limit theory (i.e., fluctuations). The concise methodology considered in this chapter synthesizes tools rooted in two core concepts, namely (i) deterministic decompositions of matrix perturbations and (ii) probabilistic matrix concentration phenomena. We illustrate our theoretical results via simulation examples involving stochastic block model random graphs and spiked matrix models. This chapter has given rise to the paper Cape et al. (2019a).

Chapter 4 presents an adaptation of the Kato–Temple inequality for bounding perturbations of eigenvalues with applications to statistical inference for random graphs, specifically hypothesis testing and change-point detection. We obtain high-probability bounds for the individual distances between certain spike eigenvalues of a graph's adjacency matrix and the corresponding eigenvalues of the model's edge probability matrix, even when the latter eigenvalues have multiplicity. Our results extend more broadly to the perturbation of singular values in the presence of quite general random matrix noise. This chapter has given rise to the paper Cape et al. (2017).

Chapter 5 analyzes the asymptotic information-theoretic relative performance of Laplacian spectral embedding and adjacency spectral embedding for block assign-

ment recovery in stochastic block model graphs by way of Chernoff information. We investigate the relationship between spectral embedding performance and underlying network structure (e.g., homogeneity, affinity, core-periphery, (un)balancedness) via a comprehensive treatment of the two-block stochastic block model and the class of K-block models exhibiting homogeneous balanced affinity structure. Our findings support the claim that, for a particular notion of sparsity, loosely speaking, "Laplacian spectral embedding favors relatively sparse graphs, whereas adjacency spectral embedding favors not-too-sparse graphs." We also provide evidence in support of the claim that "adjacency spectral embedding favors core-periphery network structure." This chapter has given rise to the paper Cape et al. (2018).

1.2 Notation

All vectors and matrices in this dissertation are taken to be real-valued. The symbols $:=$ and $\equiv$ are used to assign definitions and to denote formal equivalence. For any positive integer n, let $[n] := \{1, 2, \ldots, n\}$. We use C_α to denote a general constant that may change from line to line unless otherwise specified and that possibly depends only on α (either a parameter or an indexing value). Let $\mathcal{O}(\cdot)$ (and sometimes $O(\cdot)$) denote standard big-O notation, possibly with an underlying probabilistic qualifying statement. These conventions are simultaneously upheld when we write $\mathcal{O}_\alpha(\cdot)$. We let $\mathbb{O}_{p,r}$ denote the set of all $p \times r$ real matrices with orthonormal columns so that

$\mathbb{O}_p \equiv \mathbb{O}_{p,p}$ denotes the set of orthogonal matrices in $\mathbb{R}^{p\times p}$.

For (column) vectors $\mathbf{x}, \mathbf{y} \in \mathbb{R}^{p_1}$ where $\mathbf{x} \equiv (x_1, \ldots, x_{p_1})^\top$, the standard Euclidean inner product between $\mathbf{x}$ and $\mathbf{y}$ is denoted by $\langle \mathbf{x}, \mathbf{y} \rangle := \sum_i x_i y_i$. The classical ℓ_p vector norms are given by $\|\mathbf{x}\|_p := (\sum_{i=1}^{p} |x_i|^p)^{1/p}$ for $1 \leq p < \infty$, and $\|\mathbf{x}\|_\infty := \max_i |x_i|$. We also make use of several standard matrix norms. Letting $\sigma_i(\mathbf{A})$ denote the ith largest singular value of $\mathbf{A}$, then $\|\mathbf{A}\|_2 := \sigma_1(\mathbf{A})$ denotes the spectral norm of $\mathbf{A}$, $\|\mathbf{A}\|_{\mathrm{F}} := \sqrt{\sum_i \sigma_i^2(\mathbf{A})}$ denotes the Frobenius norm of $\mathbf{A}$, $\|\mathbf{A}\|_1 := \max_j \sum_i |a_{ij}|$ denotes the maximum absolute column sum of $\mathbf{A}$, and $\|\mathbf{A}\|_\infty := \max_i \sum_j |a_{ij}|$ denotes the maximum absolute row sum of $\mathbf{A}$. Additionally, we consider $\|\mathbf{A}\|_{\max} := \max_{i,j} |a_{ij}|$.

1.3 Norm relations

This dissertation prominently features the two-to-infinity norm, which for $\mathbf{A} \in \mathbb{R}^{p_1\times p_2}$ is given by

$$\|\mathbf{A}\|_{2\to\infty} := \sup_{\|\mathbf{x}\|_2=1} \|\mathbf{A}\mathbf{x}\|_\infty. \tag{1.4}$$

Proposition 1 establishes the simple fact that this norm corresponds to the maximum Euclidean row norm of $\mathbf{A}$. As such, the two-to-infinity norm of a matrix is easy to interpret and straightforward to compute. In certain settings, $\|\cdot\|_{2\to\infty}$ will be shown to serve as an attractive surrogate for $\|\cdot\|_{\max}$ in light of dimensionality considerations and additional algebraic properties that $\|\cdot\|_{2\to\infty}$ enjoys.

We now verify several basic properties of the two-to-infinity norm. Below, let $\mathbf{e}_i$ denote the ith standard basis vector, and let $\mathbf{a}_i \in \mathbb{R}^{p_2}$ denote the ith row of $\mathbf{A}$.

Proposition 1. *For $\mathbf{A} \in \mathbb{R}^{p_1 \times p_2}$, then $\|\mathbf{A}\|_{2\to\infty} = \max_{i\in[p_1]} \| \mathbf{a}_i \|_2$.*

Proof. The definition of $\|\cdot\|_{2\to\infty}$ and the Cauchy–Schwarz inequality together yield that $\|\mathbf{A}\|_{2\to\infty} \leq \max_{i\in[p_1]} \|\mathbf{a}_i\|_2$, since

$$\begin{aligned}\|\mathbf{A}\|_{2\to\infty} &:= \sup_{\|\mathbf{x}\|_2=1} \|\mathbf{A}\mathbf{x}\|_\infty = \sup_{\|\mathbf{x}\|_2=1} \max_{i\in[p_1]} \big|\langle \mathbf{A}\mathbf{x}, \mathbf{e}_i\rangle\big| \\ &\leq \max_{i\in[p_1]} \|\mathbf{a}_i\|_2.\end{aligned}$$

Barring the trivial case $\mathbf{A} \equiv \mathbf{0}$, let $\mathbf{e}_\star$ denote the standard basis vector in $\mathbb{R}^{p_1}$ with index given by $\operatorname{argmax}_{i\in[p_1]} \|\mathbf{a}_i\|_2$, noting that for each $i \in [p_1]$, $\mathbf{a}_i = \mathbf{A}^\top \mathbf{e}_i$. For the unit Euclidean norm vector $\mathbf{x}_\star := \|\mathbf{A}^\top \mathbf{e}_\star\|_2^{-1} (\mathbf{A}^\top \mathbf{e}_\star)$, then

$$\begin{aligned}\|\mathbf{A}\|_{2\to\infty} &= \sup_{\|\mathbf{x}\|_2=1} \max_{i\in[p_1]} \big|\langle \mathbf{A}\mathbf{x}, \mathbf{e}_i\rangle\big| \\ &\geq \big|\langle \mathbf{A}\mathbf{x}_\star, \mathbf{e}_\star\rangle\big| = \big\|\mathbf{A}^\top \mathbf{e}_\star\big\|_2 = \max_{i\in[p_1]} \|\mathbf{a}_i\|_2.\end{aligned}$$

This establishes the stated equivalence. □

Remark 1. The two-to-infinity norm is subordinate with respect to the ℓ_2 and ℓ_∞ vector norms in the sense that for any $\mathbf{x} \in \mathbb{R}^{p_2}$, $\|\mathbf{A}\mathbf{x}\|_\infty \leq \|\mathbf{A}\|_{2\to\infty} \|\mathbf{x}\|_2$. However, $\|\cdot\|_{2\to\infty}$ is not sub-multiplicative for matrices in general. For example, $\|\mathbf{A}\mathbf{B}\|_{2\to\infty} =$

$\sqrt{5} > \sqrt{4} = \|\mathbf{A}\|_{2\to\infty}\|\mathbf{B}\|_{2\to\infty}$ when

$$\mathbf{A} \equiv \mathbf{B} := \begin{bmatrix} 1 & 1 \\ 0 & 1 \end{bmatrix} \quad \text{and so} \quad \mathbf{AB} = \begin{bmatrix} 1 & 2 \\ 0 & 1 \end{bmatrix}.$$

Proposition 2. *For* $\mathbf{A} \in \mathbb{R}^{p_1 \times p_2}$*, then*

$$\|\mathbf{A}\|_{2\to\infty} \le \|\mathbf{A}\|_2 \le \min\big\{\sqrt{p_1}\|\mathbf{A}\|_{2\to\infty}, \sqrt{p_2}\big\|\mathbf{A}^\top\big\|_{2\to\infty}\big\}. \tag{1.5}$$

Proof. The first inequality is obvious since

$$\begin{aligned} \|\mathbf{A}\|_{2\to\infty} &= \sup_{\|\mathbf{x}\|_2=1} \max_{i\in[p_1]} \big|\langle \mathbf{Ax}, \mathbf{e}_i\rangle\big| \le \sup_{\|\mathbf{x}\|_2=1} \sup_{\|\mathbf{y}\|_2=1} \big|\langle \mathbf{Ax}, \mathbf{y}\rangle\big| \\ &= \|\mathbf{A}\|_2. \end{aligned}$$

The second inequality holds by an application of the Cauchy–Schwarz inequality together with the vector norm relationship $\|\mathbf{Ax}\|_2 \le \sqrt{p_1}\|\mathbf{Ax}\|_\infty$ for $\mathbf{Ax} \in \mathbb{R}^{p_1}$. In particular,

$$\begin{aligned} \sup_{\|\mathbf{x}\|_2=1} \sup_{\|\mathbf{y}\|_2=1} \big|\langle \mathbf{Ax}, \mathbf{y}\rangle\big| &\le \sup_{\|\mathbf{x}\|_2=1} \|\mathbf{Ax}\|_2 \le \sqrt{p_1} \sup_{\|\mathbf{x}\|_2=1} \|\mathbf{Ax}\|_\infty \\ &= \sqrt{p_1}\|\mathbf{A}\|_{2\to\infty}. \end{aligned}$$

By the transpose-invariance of the spectral norm, similarly

$$\|\mathbf{A}\|_2 = \left\|\mathbf{A}^\top\right\|_2 \leq \sqrt{p_2}\left\|\mathbf{A}^\top\right\|_{2\to\infty}. \qquad \square$$

Remark 2. Proposition 2 is sharp. Indeed, for the second inequality, take $\mathbf{A} := \{1/\sqrt{p_2}\}^{p_1\times p_2}$. Then $\|\mathbf{A}\|_{2\to\infty} = 1$ and $\|\mathbf{A}^\top\|_{2\to\infty} = \sqrt{p_1/p_2}$ while $\|\mathbf{A}\|_2 = \sqrt{p_1}$. For "tall, skinny" rectangular matrices, the two-to-infinity norm can be much smaller than the spectral norm.

Proposition 3. *For* $\mathbf{A} \in \mathbb{R}^{p_1\times p_2}$, $\mathbf{B} \in \mathbb{R}^{p_2\times p_3}$ *and* $\mathbf{C} \in \mathbb{R}^{p_4\times p_1}$, *then*

$$\|\mathbf{AB}\|_{2\to\infty} \leq \|\mathbf{A}\|_{2\to\infty}\|\mathbf{B}\|_2, \tag{1.6}$$

$$\|\mathbf{CA}\|_{2\to\infty} \leq \|\mathbf{C}\|_\infty\|\mathbf{A}\|_{2\to\infty}. \tag{1.7}$$

Proof. The subordinate property of $\|\cdot\|_{2\to\infty}$ yields that for all $\mathbf{x} \in \mathbb{R}^{p_3}$, $\|\mathbf{ABx}\|_\infty \leq \|\mathbf{A}\|_{2\to\infty}\|\mathbf{Bx}\|_2$, hence maximizing over all unit vectors $\mathbf{x}$ yields Eq. (1.6). Equation (1.7) follows from Hölder's inequality coupled with the fact that the vector norms

ℓ_1 and ℓ_∞ are dual to one another. Explicitly,

$$\begin{aligned}\|\mathbf{CA}\|_{2\to\infty} &= \sup_{\|\mathbf{x}\|_2=1} \max_{i\in[p_1]} \big|\langle \mathbf{CAx}, \mathbf{e}_i\rangle\big| \\ &\le \sup_{\|\mathbf{x}\|_2=1} \max_{i\in[p_1]} \big\|\mathbf{C}^\top \mathbf{e}_i\big\|_1 \|\mathbf{Ax}\|_\infty \\ &\le \left(\sup_{\|\mathbf{y}\|_1=1} \big\|\mathbf{C}^\top \mathbf{y}\big\|_1\right)\left(\sup_{\|\mathbf{x}\|_2=1} \|\mathbf{Ax}\|_\infty\right) = \big\|\mathbf{C}^\top\big\|_1 \|\mathbf{A}\|_{2\to\infty} \\ &= \|\mathbf{C}\|_\infty \|\mathbf{A}\|_{2\to\infty}. \end{aligned}$$ □

Proposition 4. *For* $\mathbf{A} \in \mathbb{R}^{r\times s}$, $\mathbf{U} \in \mathbb{O}_{p_1,r}$, *and* $\mathbf{V} \in \mathbb{O}_{p_2,s}$,

$$\|\mathbf{A}\|_2 = \|\mathbf{UA}\|_2 = \big\|\mathbf{AV}^\top\big\|_2 = \big\|\mathbf{UAV}^\top\big\|_2, \tag{1.8}$$

$$\|\mathbf{A}\|_{2\to\infty} = \big\|\mathbf{AV}^\top\big\|_{2\to\infty}. \tag{1.9}$$

However, $\|\mathbf{UA}\|_{2\to\infty}$ *need not equal* $\|\mathbf{A}\|_{2\to\infty}$.

Proof. The first statement follows from Proposition 3, the fact that the spectral norm is sub-multiplicative, and since $\mathbf{U}^\top\mathbf{U}$ and $\mathbf{V}^\top\mathbf{V}$ are both simply identity matrices. As for the final claim, consider the matrices

$$\mathbf{U} := \begin{bmatrix} 1/\sqrt{2} & 1/\sqrt{2} \\ 1/\sqrt{2} & -1/\sqrt{2} \end{bmatrix}, \qquad \mathbf{A} := \begin{bmatrix} 1 & 1 \\ 0 & 1 \end{bmatrix}, \qquad \mathbf{UA} = \begin{bmatrix} 1/\sqrt{2} & \sqrt{2} \\ 1/\sqrt{2} & 0 \end{bmatrix}, \tag{1.10}$$

for which $\|\mathbf{UA}\|_{2\to\infty} = \sqrt{5/2} > \sqrt{2} = \|\mathbf{A}\|_{2\to\infty}$. □

For $\mathbf{A} \in \mathbb{R}^{p_1 \times p_2}$, the standard relations between the ℓ_p norms for $p \in \{1, 2, \infty\}$ permit a quantitative comparison of $\|\cdot\|_{2\to\infty}$ to $\|\cdot\|_{\max}$ and $\|\cdot\|_\infty$. In particular, these matrix norms are related through matrix column dimension via

$$\frac{1}{\sqrt{p_2}}\|\mathbf{A}\|_{2\to\infty} \leq \|\mathbf{A}\|_{\max} \leq \|\mathbf{A}\|_{2\to\infty} \leq \|\mathbf{A}\|_\infty \leq \sqrt{p_2}\|\mathbf{A}\|_{2\to\infty}.$$

In contrast, the relationship between $\|\cdot\|_{2\to\infty}$ and $\|\cdot\|_2$ depends on the matrix row dimension (see Proposition 2) via

$$\|\mathbf{A}\|_{2\to\infty} \leq \|\mathbf{A}\|_2 \leq \sqrt{p_1}\|\mathbf{A}\|_{2\to\infty}.$$

As an example, consider the rectangular matrix $\mathbf{A} := \{1/\sqrt{p_2}\}^{p_1 \times p_2}$, for which $\|\mathbf{A}\|_{2\to\infty} = 1$ while $\|\mathbf{A}\|_2 = \|\mathbf{A}\|_{\mathrm{F}} = \sqrt{p_1}$. This example, together with the above norm relations, demonstrates that possibly $\|\mathbf{A}\|_{2\to\infty} \ll \|\mathbf{A}\|_2$ when the row dimension of $\mathbf{A}$ is large relative to the column dimension, that is, $p_1 \gg p_2$. Bounding $\|\mathbf{A}\|_{2\to\infty}$ would then be preferred to bounding $\|\mathbf{A}\|_2$ when seeking more refined (e.g., entrywise) control of $\mathbf{A}$. The same observation holds with respect to the Frobenius norm which satisfies the well-known, rank-based relation with the spectral norm given by

$$\|\mathbf{A}\|_2 \leq \|\mathbf{A}\|_{\mathrm{F}} \leq \sqrt{\mathrm{rank}(\mathbf{A})}\|\mathbf{A}\|_2.$$

The two-to-infinity norm is not in general sub-multiplicative for matrices. More-

over, the "constrained" sub-multiplicative behavior of $\|\cdot\|_{2\to\infty}$ (see Proposition 3), when taken together with the non-commutativity of matrix multiplication and standard properties of more common matrix norms, yields substantial flexibility when bounding matrix products and passing between norms. For this reason, a host of bounds beyond those presented in this dissertation follow naturally from the matrix decomposition results in Section 2.2.1. The relative strength of derived bounds will depend upon underlying, application-specific properties and assumptions.

1.4 Singular subspaces and Procrustes analysis

Let $\mathcal{U}$ and $\widehat{\mathcal{U}}$ denote the subspaces for which the columns of $\mathbf{U}, \widehat{\mathbf{U}} \in \mathbb{O}_{p,r}$ form orthonormal bases, respectively. From the classical cosine-sine (CS) matrix decomposition, a natural measure of distance between these subspaces (corresp., matrices) is given via the canonical (i.e., principal) angles between $\mathcal{U}$ and $\hat{\mathcal{U}}$. More specifically, for the singular values of $\mathbf{U}^\top\widehat{\mathbf{U}}$, denoted by $\{\sigma_i(\mathbf{U}^\top\widehat{\mathbf{U}})\}_{i=1}^r$ and indexed in non-increasing order, the canonical angles are the main diagonal elements of the $r\times r$ diagonal matrix

$$\boldsymbol{\Theta}(\widehat{\mathbf{U}},\mathbf{U}) := \operatorname{diag}\big(\cos^{-1}\big(\sigma_1\big(\mathbf{U}^\top\widehat{\mathbf{U}}\big)\big), \cos^{-1}\big(\sigma_2\big(\mathbf{U}^\top\widehat{\mathbf{U}}\big)\big), \ldots, \cos^{-1}\big(\sigma_r\big(\mathbf{U}^\top\widehat{\mathbf{U}}\big)\big)\big).$$

For an in-depth review of the CS decomposition and canonical angles see, for example, Bhatia (1997) and Stewart and Sun (1990). An extensive summary of the relationships between $\sin\boldsymbol{\Theta}$ distances, specifically $\|\sin\boldsymbol{\Theta}(\widehat{\mathbf{U}},\mathbf{U})\|_2$ and $\|\sin\boldsymbol{\Theta}(\widehat{\mathbf{U}},\mathbf{U})\|_{\mathrm{F}}$, as well as various other distance measures, is provided in Cai and Zhang (2018). This dissertation primarily focuses on $\sin\boldsymbol{\Theta}$ distance in relation to Procrustes analysis.

Given two matrices $\mathbf{A}$ and $\mathbf{B}$ together with a set of matrices $\mathbb{S}$ and a norm $\|\cdot\|$, a general version of the Procrustes problem is to investigate

$$\inf_{\mathbf{S}\in\mathbb{S}} \|\mathbf{A}-\mathbf{B}\mathbf{S}\|.$$

For $\mathbf{U},\widehat{\mathbf{U}}\in\mathbb{O}_{p,r}$ and $\eta\in\{\max, 2\to\infty, 2, \mathrm{F}\}$, this dissertation specifically considers

$$\inf_{\mathbf{W}\in\mathbb{O}_r} \|\widehat{\mathbf{U}}-\mathbf{U}\mathbf{W}\|_\eta. \tag{1.11}$$

For each choice of η, the corresponding infimum in Eq. (1.11) is provably achieved by the compactness of $\mathbb{O}_r$ together with properties of norms in finite-dimensional vector spaces. As such, let $\mathbf{W}_\eta^\star\in\mathbb{O}_r$ denote a corresponding Procrustes solution under η (where dependence upon the underlying matrices $\mathbf{U}$ and $\widehat{\mathbf{U}}$ is implicit from context). Unfortunately, these solutions are not analytically tractable in general, save under the Frobenius norm, in which case $\mathbf{W}_\mathbf{U}\equiv\mathbf{W}_{\mathrm{F}}^\star(\mathbf{U},\widehat{\mathbf{U}})$ corresponds to the the classical orthogonal Procrustes problem solution given explicitly by $\mathbf{W}_\mathbf{U}\equiv\mathbf{W}_1\mathbf{W}_2^\top$ when the singular value decomposition of $\mathbf{U}^\top\widehat{\mathbf{U}}\in\mathbb{R}^{r\times r}$ is written as $\mathbf{U}^\top\widehat{\mathbf{U}}\equiv\mathbf{W}_1\boldsymbol{\Sigma}_\mathbf{U}\mathbf{W}_2^\top$

(Gower and Dijksterhuis, 2004).

For each η, it is therefore natural to study the behavior of

$$\|\widehat{\mathbf{U}} - \mathbf{U}\mathbf{W}_{\mathbf{U}}\|_{\eta}. \tag{1.12}$$

To this end, $\sin\boldsymbol{\Theta}$ distances and the above Procrustes problems are related in the sense that (e.g., Cai and Zhang (2018))

$$\big\|\sin\boldsymbol{\Theta}(\widehat{\mathbf{U}},\mathbf{U})\big\|_{\mathrm{F}} \le \|\widehat{\mathbf{U}} - \mathbf{U}\mathbf{W}_{\mathbf{U}}\|_{\mathrm{F}} \le \sqrt{2}\big\|\sin\boldsymbol{\Theta}(\widehat{\mathbf{U}},\mathbf{U})\big\|_{\mathrm{F}},$$

and

$$\big\|\sin\boldsymbol{\Theta}(\widehat{\mathbf{U}},\mathbf{U})\big\|_{2} \le \big\|\widehat{\mathbf{U}} - \mathbf{U}\mathbf{W}_{2}^{\star}\big\|_{2} \le \|\widehat{\mathbf{U}} - \mathbf{U}\mathbf{W}_{\mathbf{U}}\|_{2} \le \sqrt{2}\big\|\sin\boldsymbol{\Theta}(\widehat{\mathbf{U}},\mathbf{U})\big\|_{2}.$$

By Lemma 40, $\|\widehat{\mathbf{U}} - \mathbf{U}\mathbf{W}_{\mathbf{U}}\|_2$ can be bounded differently in a manner suggesting that the performance of $\mathbf{W}_{\mathbf{U}}$ is "close" to the performance of $\mathbf{W}_2^{\star}$ under $\|\cdot\|_2$, namely

$$\|\widehat{\mathbf{U}} - \mathbf{U}\mathbf{W}_{\mathbf{U}}\|_{2} \le \big\|\sin\boldsymbol{\Theta}(\widehat{\mathbf{U}},\mathbf{U})\big\|_{2} + \big\|\sin\boldsymbol{\Theta}(\widehat{\mathbf{U}},\mathbf{U})\big\|_{2}^{2}.$$

Loosely speaking, it follows that the discrepancy between $\mathbf{W}_{\mathbf{U}}$ and $\mathbf{W}_2^{\star}$ in the spectral norm Procrustes problem behaves as $\mathcal{O}(\|\sin\boldsymbol{\Theta}(\widehat{\mathbf{U}},\mathbf{U})\|_2^2)$.

As for the two-to-infinity norm, simply considering the naïve relationship between

$\|\cdot\|_{2\to\infty}$ and $\|\cdot\|_2$ yields

$$\frac{1}{\sqrt{p}}\big\|\sin\boldsymbol{\Theta}(\widehat{\mathbf{U}},\mathbf{U})\big\|_2 \leq \big\|\widehat{\mathbf{U}}-\mathbf{U}\mathbf{W}^{\star}_{2\to\infty}\big\|_{2\to\infty} \leq \|\widehat{\mathbf{U}}-\mathbf{U}\mathbf{W}_{\mathbf{U}}\|_{2\to\infty}.$$

These observations collectively suggest that direct analysis of $\widehat{\mathbf{U}}-\mathbf{U}\mathbf{W}_{\mathbf{U}}$ may yield meaningfully tighter bounds on $\|\widehat{\mathbf{U}}-\mathbf{U}\mathbf{W}_{\mathbf{U}}\|_{2\to\infty}$ in settings wherein $p \gg r$ and $\|\widehat{\mathbf{U}}-\mathbf{U}\mathbf{W}_{\mathbf{U}}\|_{2\to\infty} \ll \|\widehat{\mathbf{U}}-\mathbf{U}\mathbf{W}_{\mathbf{U}}\|_2$. In such a regime, $\|\cdot\|_{2\to\infty}$ and $\|\cdot\|_{\max}$ differ by at most a (relatively small) r-dependent factor, so it is conceivable that $\|\cdot\|_{2\to\infty}$ may serve as a decent proxy for $\|\cdot\|_{\max}$.

We now proceed to introduce a matrix perturbation framework in which $\widehat{\mathbf{U}}$ represents a perturbation (i.e., estimate) of $\mathbf{U}$. We then formulate a Procrustean matrix decomposition in Section 2.2.1 by further decomposing the underlying matrices whose spectral norm bounds give rise to the above quantities $\|\sin\boldsymbol{\Theta}(\widehat{\mathbf{U}},\mathbf{U})\|_2$ and $\|\sin\boldsymbol{\Theta}(\widehat{\mathbf{U}},\mathbf{U})\|_2^2$. Together with two-to-infinity norm machinery and model-based analysis, we subsequently derive a collection of perturbation bounds and demonstrate their utility in problems of statistical estimation.

1.5 Signal-plus-noise matrix perturbation framework

For rectangular matrices $\mathbf{M}, \mathbf{E} \in \mathbb{R}^{p_1 \times p_2}$, let $\mathbf{M}$ denote an unobserved matrix, let $\mathbf{E}$ denote an unobserved perturbation (i.e., error) matrix, and let $\widehat{\mathbf{M}} := \mathbf{M} + \mathbf{E}$ denote an observed matrix that amounts to an additive perturbation of $\mathbf{M}$ by $\mathbf{E}$. For $\mathbf{M}$ and $\widehat{\mathbf{M}}$, their respective partitioned singular value decompositions are given in block matrix form by

$$\mathbf{M} = \begin{bmatrix} \mathbf{U} & \mathbf{U}_\perp \end{bmatrix} \cdot \begin{bmatrix} \mathbf{\Sigma} & \mathbf{0} \\ \mathbf{0} & \mathbf{\Sigma}_\perp \end{bmatrix} \cdot \begin{bmatrix} \mathbf{V}^\top \\ \mathbf{V}_\perp^\top \end{bmatrix} = \mathbf{U}\mathbf{\Sigma}\mathbf{V}^\top + \mathbf{U}_\perp \mathbf{\Sigma}_\perp \mathbf{V}_\perp^\top$$

and

$$\begin{aligned} \widehat{\mathbf{M}} := \mathbf{M} + \mathbf{E} &= \begin{bmatrix} \widehat{\mathbf{U}} & \widehat{\mathbf{U}}_\perp \end{bmatrix} \cdot \begin{bmatrix} \widehat{\mathbf{\Sigma}} & \mathbf{0} \\ \mathbf{0} & \widehat{\mathbf{\Sigma}}_\perp \end{bmatrix} \cdot \begin{bmatrix} \widehat{\mathbf{V}}^\top \\ \widehat{\mathbf{V}}_\perp^\top \end{bmatrix} \\ &= \widehat{\mathbf{U}}\widehat{\mathbf{\Sigma}}\widehat{\mathbf{V}}^\top + \widehat{\mathbf{U}}_\perp \widehat{\mathbf{\Sigma}}_\perp \widehat{\mathbf{V}}_\perp^\top. \end{aligned}$$

Above, $\mathbf{U} \in \mathbb{O}_{p_1,r}$, $\mathbf{V} \in \mathbb{O}_{p_2,r}$, $[\mathbf{U}|\mathbf{U}_\perp] \in \mathbb{O}_{p_1}$, and $[\mathbf{V}|\mathbf{V}_\perp] \in \mathbb{O}_{p_2}$. The matrices $\mathbf{\Sigma} \in \mathbb{R}^{r \times r}$ and $\mathbf{\Sigma}_\perp \in \mathbb{R}^{(p_1-r)\times(p_2-r)}$ contain the singular values of $\mathbf{M}$, where $\mathbf{\Sigma} = \mathrm{diag}(\sigma_1(\mathbf{M}), \ldots, \sigma_r(\mathbf{M}))$ and $\mathbf{\Sigma}_\perp$ contains the remaining singular values $\sigma_{r+1}(\mathbf{M}), \ldots$ on its main diagonal, possibly padded with additional zeros, such that $\sigma_1(\mathbf{M}) \geq \cdots \geq$

$\sigma_r(\mathbf{M}) > \sigma_{r+1}(\mathbf{M}) \geq \cdots \geq 0$. The matrices $\widehat{\mathbf{U}}, \widehat{\mathbf{U}}_\perp, \widehat{\mathbf{V}}, \widehat{\mathbf{V}}_\perp, \widehat{\mathbf{\Sigma}}$, and $\widehat{\mathbf{\Sigma}}_\perp$ are defined analogously.

This dissertation is primarily interested in the situation when $\sigma_r(\mathbf{M}) \gg \sigma_{r+1}(\mathbf{M})$, although our results and framework hold more generally when $\mathbf{\Sigma}$ is redefined to contain a collection of sequential singular values that are separated from the remaining singular values in $\mathbf{\Sigma}_\perp$. In such a modified setting, one would have

$$\mathbf{\Sigma} = \operatorname{diag}(\sigma_s(\mathbf{M}), \ldots, \sigma_{s+t}(\mathbf{M}))$$

for some positive integers s and t, where subsequent bounds and necessary bookkeeping would depend both on the two-sided gap

$$\min\{\sigma_{s-1}(\mathbf{M}) - \sigma_s(\mathbf{M}), \sigma_{s+t}(\mathbf{M}) - \sigma_{s+t+1}(\mathbf{M})\}$$

and on the magnitude of the perturbation $\mathbf{E}$, as in Yu et al. (2015).

1.6 Preliminary matrix analysis

For matrices $\widehat{\mathbf{U}}, \mathbf{U} \in \mathbb{O}_{p_1,r}$ and each choice of norm $\eta \in \{2, \mathrm{F}\}$, it holds that (e.g., Lemma 1 in Cai and Zhang (2018)),

$$\|\sin\mathbf{\Theta}(\widehat{\mathbf{U}}, \mathbf{U})\|_\eta \leq \inf_{\mathbf{W}\in\mathbb{O}_r} \|\widehat{\mathbf{U}} - \mathbf{U}\mathbf{W}\|_\eta \leq \sqrt{2}\|\sin\mathbf{\Theta}(\widehat{\mathbf{U}}, \mathbf{U})\|_\eta.$$

Simultaneously, the relationships between $\sin\boldsymbol{\Theta}$ distances and differences of orthogonal projections are given by

$$\|\sin\boldsymbol{\Theta}(\widehat{\mathbf{U}},\mathbf{U})\|_2 \leq \|\widehat{\mathbf{U}}\widehat{\mathbf{U}}^\top - \mathbf{U}\mathbf{U}^\top\|_2 \leq \sqrt{2}\|\sin\boldsymbol{\Theta}(\widehat{\mathbf{U}},\mathbf{U})\|_2,$$
$$\|\widehat{\mathbf{U}}\widehat{\mathbf{U}}^\top - \mathbf{U}\mathbf{U}^\top\|_{\mathrm{F}} = \sqrt{2}\|\sin\boldsymbol{\Theta}(\widehat{\mathbf{U}},\mathbf{U})\|_{\mathrm{F}}.$$

In this dissertation, we decompose the matrix $\widehat{\mathbf{U}} - \mathbf{U}\mathbf{W}$ as

$$\begin{aligned}\widehat{\mathbf{U}} - \mathbf{U}\mathbf{W} &= \widehat{\mathbf{U}} - \mathbf{U}\mathbf{U}^\top\widehat{\mathbf{U}} + \mathbf{U}\mathbf{U}^\top\widehat{\mathbf{U}} - \mathbf{U}\mathbf{W} \\ &= \underbrace{(\mathbf{I} - \mathbf{U}\mathbf{U}^\top)\widehat{\mathbf{U}}}_{\text{dominant term}} + \underbrace{\mathbf{U}(\mathbf{U}^\top\widehat{\mathbf{U}} - \mathbf{W})}_{\text{residual term}}.\end{aligned}$$

For $\mathbf{W}_{\mathbf{U}} := \underset{\mathbf{W}\in\mathbb{O}_r}{\arg\inf} \|\widehat{\mathbf{U}} - \mathbf{U}\mathbf{W}\|_{\mathrm{F}}$, subsequent analysis demonstrates that

$$\overbrace{\tfrac{1}{\sqrt{p_1}}\|\sin\boldsymbol{\Theta}(\widehat{\mathbf{U}},\mathbf{U})\|_2}^{\text{lower bound}} \leq \inf_{\mathbf{W}\in\mathbb{O}_r}\|\widehat{\mathbf{U}} - \mathbf{U}\mathbf{W}\|_{2\to\infty} \leq \|\widehat{\mathbf{U}} - \mathbf{U}\mathbf{W}_{\mathbf{U}}\|_{2\to\infty}$$

and

$$\|\widehat{\mathbf{U}} - \mathbf{U}\mathbf{W}_{\mathbf{U}}\|_{2\to\infty} \leq \overbrace{\underbrace{\|(\mathbf{I} - \mathbf{U}\mathbf{U}^\top)\widehat{\mathbf{U}}\|_{2\to\infty}}_{\text{dominant term}} + \underbrace{\|\mathbf{U}\|_{2\to\infty}\|\sin\boldsymbol{\Theta}(\widehat{\mathbf{U}},\mathbf{U})\|_2^2}_{\text{residual term}}}^{\text{upper bound}}.$$

In the statistically interesting settings considered here, both $\|\mathbf{U}\|_{2\to\infty} \ll 1$ and $\|\sin\boldsymbol{\Theta}(\widehat{\mathbf{U}},\mathbf{U})\|_2^2 \ll \|\sin\boldsymbol{\Theta}(\widehat{\mathbf{U}},\mathbf{U})\|_2$. The bulk of our technical analysis will involve carefully analyzing the dominant term in the upper bound.

We remark that straightforward algebraic considerations yield

$$\sqrt{\tfrac{r}{p_1}} \leq \|\widehat{\mathbf{U}}\|_{2\to\infty} \leq \inf_{\mathbf{W}\in\mathbb{O}_r} \|\widehat{\mathbf{U}} - \mathbf{U}\mathbf{W}\|_{2\to\infty} + \|\mathbf{U}\|_{2\to\infty}, \tag{1.13}$$

where $\|\mathbf{U}\mathbf{W}\|_{2\to\infty} \equiv \|\mathbf{U}\|_{2\to\infty}$ and possibly $\|\mathbf{U}\|_{2\to\infty} \to 0$ (as a function of r and p_1). For this reason, it will be important in our analysis to obtain bounds of the form

$$\|\widehat{\mathbf{U}} - \mathbf{U}\mathbf{W}_{\mathbf{U}}\|_{2\to\infty} = o(\|\mathbf{U}\|_{2\to\infty})$$

in order to establish that $\widehat{\mathbf{U}}$ indeed provides strong local estimates of $\mathbf{U}$ up to an appropriate orthogonal transformation.

It is worth pointing out that bounding $\|\widehat{\mathbf{U}}\widehat{\mathbf{U}}^\top - \mathbf{U}\mathbf{U}^\top\|_{\max}$ is related to bounding $\|\mathbf{U}\|_{2\to\infty}$ and $\|\widehat{\mathbf{U}} - \mathbf{U}\mathbf{W}\|_{2\to\infty}$ for any $r \times r$ orthogonal matrix $\mathbf{W}$, since

$$\|\widehat{\mathbf{U}}\widehat{\mathbf{U}}^\top - \mathbf{U}\mathbf{U}^\top\|_{\max} \leq \Big(2\|\mathbf{U}\|_{2\to\infty} + \|\widehat{\mathbf{U}} - \mathbf{U}\mathbf{W}\|_{2\to\infty}\Big)\, \|\widehat{\mathbf{U}} - \mathbf{U}\mathbf{W}\|_{2\to\infty}. \tag{1.14}$$

Chapter 2

Singular subspace geometry and high-dimensional statistics

2.1 Overview of Chapter 2

This chapter provides a collection of technical and theoretical tools for studying the perturbations of singular vectors and subspaces with respect to the two-to-infinity norm. Our main theoretical results are first presented quite generally and then followed by concrete consequences thereof to facilitate direct statistical applications. We establish perturbation bounds for both low and high rank matrices. Among the advantages of our methods is that we allow singular value multiplicity and merely leverage a population singular value gap assumption.

As a special case of our general framework and methods, we improve upon results

in Fan et al. (2018) wherein the authors obtain an ℓ_∞ norm perturbation bound for singular vectors of low rank matrices exhibiting specific coherence structure. In this way, beyond the stated theorems in this chapter, our results can be applied analogously to robust covariance estimation involving heavy-tailed random variables.

Our Procrustes analysis complements the study of perturbation bounds for singular subspaces in Cai and Zhang (2018). When considered in tandem, we demonstrate a Procrustean setting in which one recovers nearly rate-matching upper and lower bounds with respect to the two-to-infinity norm.

Another contribution of this chapter is that we extend and complement spectral methodology for graph inference and embedding (Levin et al., 2017; Lyzinski et al., 2014; Tang et al., 2017). To the best of our knowledge, we obtain among the first-ever estimation bounds for multiple graph inference in the presence of edge correlation.

2.1.1 Problem setting for Chapter 2

This chapter formulates and analyzes a general matrix decomposition for the aligned difference between real-valued matrices $\mathbf{U}$ and $\widehat{\mathbf{U}}$, each consisting of r orthonormal columns (i.e., partial isometries; Stiefel matrices; orthogonal r-frames), given by

$$\widehat{\mathbf{U}} - \mathbf{U}\mathbf{W}, \tag{2.1}$$

where $\mathbf{W}$ denotes an $r \times r$ orthogonal matrix. We focus on (but are strictly speaking not limited to) a certain "nice" choice of $\mathbf{W}$ which corresponds to an "optimal" Procrustes transformation in a sense that will be made precise.

Chapter 1 of this dissertation provides technical machinery for the two-to-infinity subordinate vector norm on matrices, which for $\mathbf{A} \in \mathbb{R}^{p_1 \times p_2}$ is given by

$$\|\mathbf{A}\|_{2\to\infty} := \sup_{\|\mathbf{x}\|_2=1} \|\mathbf{A}\mathbf{x}\|_\infty.$$

By combining two-to-infinity norm tools with the matrix decomposition considerations presented in this chapter, we obtain a suite of perturbation bounds within an additive perturbation framework of the singular value decomposition.

The two-to-infinity norm yields finer uniform control on the entries of a matrix than the more common spectral and Frobenius norms. We shall demonstrate that, in certain settings, the two-to-infinity norm is preferable to these and to other norms. In particular, matrices exhibiting bounded coherence in the sense of Candès and Recht (2009) form a popular and widely-encountered class of matrices for which the two-to-infinity norm is demonstrably an excellent choice.

The two-to-infinity norm has previously appeared in the statistics literature, including in Lyzinski et al. (2014) wherein it is leveraged to prove that adjacency spectral embedding achieves perfect clustering for certain stochastic block model graphs. More recently, it has also appeared in the study of random matrices when a fraction of

the matrix entries are modified (Rebrova and Vershynin, 2018). In general, however, the two-to-infinity norm has received far less attention than other norms. Among the aims of this dissertation is to advocate for the more widespread consideration of the two-to-infinity norm.

2.1.2 Sample application: covariance estimation

We pause here to present an application of our work and methods to estimating the top singular vectors of a structured covariance matrix.

Denote a random vector Y and its entries by $Y := (Y^{(1)}, Y^{(2)}, \ldots, Y^{(d)})^\top \in \mathbb{R}^d$, and let $Y, Y_1, Y_2, \ldots, Y_n$ be independent and identically distributed (i.i.d.) mean zero multivariate Gaussian random (column) vectors with common covariance matrix $\mathbf{\Gamma} \in \mathbb{R}^{d\times d}$. Denote the singular value decomposition of $\mathbf{\Gamma}$ by $\mathbf{\Gamma} \equiv \mathbf{U}\mathbf{\Sigma}\mathbf{U}^\top + \mathbf{U}_\perp\mathbf{\Sigma}_\perp\mathbf{U}_\perp^\top$, where $[\mathbf{U}|\mathbf{U}_\perp] \equiv [\mathbf{u}_1|\mathbf{u}_2|\ldots|\mathbf{u}_d] \in \mathbb{R}^{d\times d}$ is an orthogonal matrix. The singular values of $\mathbf{\Gamma}$ are indexed in non-increasing order, $\sigma_1(\mathbf{\Gamma}) \geq \sigma_2(\mathbf{\Gamma}) \geq \cdots \geq \sigma_d(\mathbf{\Gamma})$, with $\mathbf{\Sigma} := \mathrm{diag}(\sigma_1(\mathbf{\Gamma}), \sigma_2(\mathbf{\Gamma}), \ldots, \sigma_r(\mathbf{\Gamma})) \in \mathbb{R}^{r\times r}$, $\mathbf{\Sigma}_\perp := \mathrm{diag}(\sigma_{r+1}(\mathbf{\Gamma}), \sigma_{r+2}(\mathbf{\Gamma}), \ldots, \sigma_d(\mathbf{\Gamma})) \in \mathbb{R}^{(d-r)\times(d-r)}$, $\delta_r(\mathbf{\Gamma}) := \sigma_r(\mathbf{\Gamma}) - \sigma_{r+1}(\mathbf{\Gamma} > 0$, and $r \ll d$. Here, $\mathbf{\Sigma}$ may be viewed as containing the "signal" (i.e., spike) singular values of interest, while $\mathbf{\Sigma}_\perp$ contains the remaining "noise" (i.e., bulk) singular values. The singular values of $\mathbf{\Gamma}$ are not assumed to be distinct; rather, the assumption $\delta_r(\mathbf{\Gamma}) > 0$ simply specifies a singular value population gap between $\mathbf{\Sigma}$ and $\mathbf{\Sigma}_\perp$.

Let $\widehat{\mathbf{\Gamma}}_n$ denote the empirical covariance matrix $\widehat{\mathbf{\Gamma}}_n := \frac{1}{n}\sum_{k=1}^n Y_k Y_k^\top$ with decompo-

sition $\widehat{\mathbf{\Gamma}}_n \equiv \widehat{\mathbf{U}}\widehat{\mathbf{\Sigma}}\widehat{\mathbf{U}}^\top + \widehat{\mathbf{U}}_\perp\widehat{\mathbf{\Sigma}}_\perp\widehat{\mathbf{U}}_\perp^\top$. Let $\mathbf{E}_n := \widehat{\mathbf{\Gamma}}_n - \mathbf{\Gamma}$ denote the difference between the empirical and theoretical covariance matrices. Below, $C, c, c_1, c_2, \ldots$ are positive constants (possibly related) of minimal interest. We use $\mathrm{Var}(Y^{(i)})$ to denote the variance of $Y^{(i)}$ and $o(\cdot)$ to denote little-o notation.

We are interested in the regime where the sample size n and the covariance matrix dimension d are simultaneously allowed to grow. In this regime, an important measure of complexity is given by the effective rank of $\mathbf{\Gamma}$, defined as $\mathfrak{r}(\mathbf{\Gamma}) := \mathrm{trace}(\mathbf{\Gamma})/\sigma_1(\mathbf{\Gamma})$ (e.g., see Koltchinskii and Lounici (2017b)).

Theorem 5 (Application: covariance estimation)**.** *In Section 2.1.2, assume that* $\max\{\mathfrak{r}(\mathbf{\Gamma}), \log d\} = o(n)$, $\sigma_1(\mathbf{\Gamma})/\sigma_r(\mathbf{\Gamma}) \leq c_1$, $\delta_r(\mathbf{\Gamma}) \geq c_2\sigma_r(\mathbf{\Gamma}) > 0$, *and* $\|\mathbf{U}\|_{2\to\infty} \leq c_3\sqrt{r/d}$. *Let* $\nu(Y) := \max_{1\leq i\leq d}\sqrt{\mathrm{Var}(Y^{(i)})}$. *Then, there exists an* $r \times r$ *orthogonal matrix* $\mathbf{W}_\mathbf{U}$ *and a constant* $C > 0$ *such that with probability at least* $1 - d^{-2}$,

$$\|\widehat{\mathbf{U}} - \mathbf{U}\mathbf{W}_\mathbf{U}\|_{2\to\infty} \leq C\sqrt{\frac{\max\{\mathfrak{r}(\mathbf{\Gamma}), \log d\}}{n}}\left(\frac{\nu(Y)r}{\sqrt{\sigma_r(\mathbf{\Gamma})}} + \frac{\sigma_{r+1}(\mathbf{\Gamma})}{\sigma_r(\mathbf{\Gamma})}\right) + C\left(\frac{\max\{\mathfrak{r}(\mathbf{\Gamma}), \log d\}}{n}\right)\left(\sqrt{\frac{\sigma_{r+1}(\mathbf{\Gamma})}{\sigma_r(\mathbf{\Gamma})}} + \sqrt{\frac{r}{d}}\right).$$

Remark 3. In the setting of Theorem 5, spectral norm probabilistic concentration via Koltchinskii and Lounici (2017a,b) can be applied to yield a naïve two-to-infinity norm bound of the form

$$\|\widehat{\mathbf{U}} - \mathbf{U}\mathbf{W}_\mathbf{U}\|_{2\to\infty} \leq C\sqrt{\frac{\max\{\mathfrak{r}(\mathbf{\Gamma}), \log d\}}{n}}. \tag{2.2}$$

When $\mathbf{\Gamma}$ exhibits the additional spike structure $\mathbf{\Gamma} \equiv \mathbf{U}(\mathbf{\Lambda} + c^2\mathbf{I})\mathbf{U}^\top + c^2\mathbf{U}_\perp\mathbf{U}_\perp^\top$ with $\sigma_1(\mathbf{\Gamma}) \geq c_4(d/r)$, then $\sqrt{\sigma_{r+1}(\mathbf{\Gamma})}, \nu(Y) \leq c_5\sqrt{\sigma_1(\mathbf{\Gamma})}\sqrt{r/d}$, and so the bound in Theorem 5 simplifies to the form

$$\|\widehat{\mathbf{U}} - \mathbf{U}\mathbf{W}_\mathbf{U}\|_{2\to\infty} \leq C\sqrt{\frac{\max\{\mathfrak{r}(\mathbf{\Gamma}), \log d\}}{n}}\sqrt{\frac{r^3}{d}}. \tag{2.3}$$

The bound in Eq. (2.3) manifestly improves upon Eq. (2.2) since here $r \ll d$ and d is taken to be large.

2.2 Main results for singular subspace perturbations

This section presents our main deterministic Procrustes analysis and general perturbation bounds.

2.2.1 A Procrustean matrix decomposition and its variants

Below, Theorem 6 states the main matrix decomposition of this chapter in general form. Remark 4 subsequently provides accompanying discussion and is designed to offer a more intuitive, high-level explanation of the decomposition considerations

presented here. The formal procedure for deriving Theorem 6 is based on geometric considerations presented in Section 6.1.3.

Theorem 6 (Procrustean matrix decomposition)**.** *In the setting of Sections 1.4 and 1.5, if* $\widehat{\mathbf{M}}$ *has rank at least* r*, then* $\widehat{\mathbf{U}} - \mathbf{U}\mathbf{W}_{\mathbf{U}} \in \mathbb{R}^{p_1 \times r}$ *admits the decomposition*

$$\widehat{\mathbf{U}} - \mathbf{U}\mathbf{W}_{\mathbf{U}} = \big(\mathbf{I} - \mathbf{U}\mathbf{U}^\top\big)\mathbf{E}\mathbf{V}\mathbf{W}_{\mathbf{V}}\widehat{\mathbf{\Sigma}}^{-1} \tag{2.4}$$

$$+ \big(\mathbf{I} - \mathbf{U}\mathbf{U}^\top\big)\mathbf{E}(\widehat{\mathbf{V}} - \mathbf{V}\mathbf{W}_{\mathbf{V}})\widehat{\mathbf{\Sigma}}^{-1} \tag{2.5}$$

$$+ \big(\mathbf{I} - \mathbf{U}\mathbf{U}^\top\big)\mathbf{M}\big(\widehat{\mathbf{V}} - \mathbf{V}\mathbf{V}^\top\widehat{\mathbf{V}}\big)\widehat{\mathbf{\Sigma}}^{-1} \tag{2.6}$$

$$+ \mathbf{U}\big(\mathbf{U}^\top\widehat{\mathbf{U}} - \mathbf{W}_{\mathbf{U}}\big). \tag{2.7}$$

This decomposition still holds when replacing the $r \times r$ *orthogonal matrices* $\mathbf{W}_{\mathbf{U}}$ *and* $\mathbf{W}_{\mathbf{V}}$ *with any real* $r \times r$ *matrices* $\mathbf{T}_1$ *and* $\mathbf{T}_2$*, respectively. The analogous decomposition for* $\widehat{\mathbf{V}} - \mathbf{V}\mathbf{W}_{\mathbf{V}}$ *is given by replacing* $\mathbf{U}, \widehat{\mathbf{U}}, \mathbf{V}, \widehat{\mathbf{V}}, \mathbf{E}, \mathbf{M}, \mathbf{W}_{\mathbf{U}}$*, and* $\mathbf{W}_{\mathbf{V}}$ *above with* $\mathbf{V}, \widehat{\mathbf{V}}, \mathbf{U}, \widehat{\mathbf{U}}, \mathbf{E}^\top, \mathbf{M}^\top, \mathbf{W}_{\mathbf{V}}$*, and* $\mathbf{W}_{\mathbf{U}}$*, respectively.*

Remark 4 (Intuition for Theorem 6)**.** The decomposition presented in Theorem 6 can be loosely motivated in the following way. When $\mathbf{M}$ and $\widehat{\mathbf{M}}$ have rank at least r, then by Section 1.5, $\mathbf{U} \equiv \mathbf{M}\mathbf{V}\mathbf{\Sigma}^{-1}$ and $\widehat{\mathbf{U}} \equiv \widehat{\mathbf{M}}\widehat{\mathbf{V}}\widehat{\mathbf{\Sigma}}^{-1} = \mathbf{M}\widehat{\mathbf{V}}\widehat{\mathbf{\Sigma}}^{-1} + \mathbf{E}\widehat{\mathbf{V}}\widehat{\mathbf{\Sigma}}^{-1}$. It is thus conceivable that the difference between $\mathbf{U}$ and $\widehat{\mathbf{U}}$ behaves to leading order as $\mathbf{E}\mathbf{V}\mathbf{\Sigma}^{-1}$ (modulo proper orthogonal transformation) under suitable perturbation and structural assumptions. Indeed, we repeatedly observe such first-order behavior via the matrix term $(\mathbf{I} - \mathbf{U}\mathbf{U}^\top)\mathbf{E}\mathbf{V}\mathbf{W}_{\mathbf{V}}\widehat{\mathbf{\Sigma}}^{-1}$ when $\|\mathbf{U}\|_{2\to\infty} \ll 1$.

For the purpose of obtaining upper bounds, passing from $\widehat{\mathbf{\Sigma}}^{-1}$ to $\mathbf{\Sigma}^{-1}$ amounts to transitioning from $\sigma_r(\widehat{\mathbf{M}})$ to $\sigma_r(\mathbf{M})$; this can be achieved via Weyl's inequality (Bhatia, 1997) provided the perturbation $\mathbf{E}$ is suitably small in norm relative to $\sigma_r(\mathbf{M})$ (i.e., when the singular value "spike signal" is sufficiently informative relative to the noise level $\mathbf{E}$ in norm).

Subsequent results in Section 2.2.2 will demonstrate that lines (2.5)–(2.7) amount to situational residual and approximation error terms. Namely, with respect to the two-to-infinity norm:

- Line (2.5) can be much smaller than $\|\sin\mathbf{\Theta}(\widehat{\mathbf{V}},\mathbf{V})\|_2$ as a function of the relative magnitudes of $\mathbf{E}$ and $\hat{\mathbf{\Sigma}}^{-1}$.
- Line (2.6) can be much smaller than $\|\sin\mathbf{\Theta}(\widehat{\mathbf{V}},\mathbf{V})\|_2$ as a function of the multiplicative singular value gap $\sigma_{r+1}(\mathbf{M})/\sigma_r(\widehat{\mathbf{M}})$.
- Line (2.7) can be much smaller than $\|\sin\mathbf{\Theta}(\widehat{\mathbf{U}},\mathbf{U})\|_2^2$ as a function of $\|\mathbf{U}\|_{2\to\infty}$, specifically when $\|\mathbf{U}\|_{2\to\infty} \ll 1$.

Theorem 6 can be rewritten in terms of the spectral matrix decomposition when $\mathbf{M}$ and $\mathbf{E}$ are both symmetric matrices. For ease of reference, we state this special case in the form of a corollary.

Corollary 7. *Let $\mathbf{M},\mathbf{E}\in\mathbb{R}^{p\times p}$ be symmetric matrices. Rephrase Section 1.5 to hold for the spectral matrix decomposition in terms of the eigenvalues and eigenvectors of $\mathbf{M}$ and $\widehat{\mathbf{M}}$. Provided $\widehat{\mathbf{M}}$ has rank at least r, then $\widehat{\mathbf{U}}-\mathbf{U}\mathbf{W}_{\mathbf{U}}\in\mathbb{R}^{p\times r}$ admits the*

decomposition

$$\begin{aligned}\widehat{\mathbf{U}} - \mathbf{U}\mathbf{W}_{\mathbf{U}} = &\big(\mathbf{I} - \mathbf{U}\mathbf{U}^{\top}\big)\mathbf{E}\mathbf{U}\mathbf{W}_{\mathbf{U}}\widehat{\mathbf{\Sigma}}^{-1} \\ &+ \big(\mathbf{I} - \mathbf{U}\mathbf{U}^{\top}\big)\mathbf{E}(\widehat{\mathbf{U}} - \mathbf{U}\mathbf{W}_{\mathbf{U}})\widehat{\mathbf{\Sigma}}^{-1} \\ &+ \big(\mathbf{I} - \mathbf{U}\mathbf{U}^{\top}\big)\mathbf{M}\big(\widehat{\mathbf{U}} - \mathbf{U}\mathbf{U}^{\top}\widehat{\mathbf{U}}\big)\widehat{\mathbf{\Sigma}}^{-1} \\ &+ \mathbf{U}\big(\mathbf{U}^{\top}\widehat{\mathbf{U}} - \mathbf{W}_{\mathbf{U}}\big). \end{aligned} \tag{2.8}$$

Remark 5 (The orthogonal matrix $\mathbf{W}_{\mathbf{U}}$)**.** This chapter does not assume that the leading r singular values of $\mathbf{M}$ or $\widehat{\mathbf{M}}$ are distinct. As such, in general $\widehat{\mathbf{U}}$ alone cannot hope to recover $\mathbf{U}$ in the presence of singular value multiplicity. Indeed, $\widehat{\mathbf{U}}$ can only be viewed as an estimate of $\mathbf{U}$ up to an orthogonal transformation, and our specific choice of $\mathbf{W}_{\mathbf{U}}$ is based upon the aforementioned Procrustes-based considerations.

To reiterate, $\mathbf{W}_{\mathbf{U}}$ depends upon $\widehat{\mathbf{U}}$, which in turn depends upon the perturbation $\mathbf{E}$. Consequently, $\mathbf{W}_{\mathbf{U}}$ is unknown (resp., random) when $\mathbf{E}$ is assumed unknown (resp., random). We note that statistical inference methodologies and applications are often either invariant under or equivalent modulo orthogonal transformations as a source of non-identifiability. For example, K-means clustering applied to the rows of $\mathbf{U}$ in Euclidean space is equivalent to clustering the rows of $\mathbf{U}\mathbf{W}_{\mathbf{U}}$.

It will subsequently prove convenient to work with the following modified versions of Theorem 6 which are stated below as corollaries.

Corollary 8. *The decomposition in Theorem 6 can be rewritten as*

$$\begin{aligned}\widehat{\mathbf{U}} - \mathbf{U}\mathbf{W}_{\mathbf{U}} = &\big(\mathbf{I} - \mathbf{U}\mathbf{U}^\top\big)\mathbf{E}\big(\mathbf{V}\mathbf{V}^\top\big)\mathbf{V}\mathbf{W}_{\mathbf{V}}\widehat{\mathbf{\Sigma}}^{-1} \\ &+ \big(\mathbf{I} - \mathbf{U}\mathbf{U}^\top\big)(\mathbf{E} + \mathbf{M})(\widehat{\mathbf{V}} - \mathbf{V}\mathbf{W}_{\mathbf{V}})\hat{\mathbf{\Sigma}}^{-1} \\ &+ \mathbf{U}\big(\mathbf{U}^\top\widehat{\mathbf{U}} - \mathbf{W}_{\mathbf{U}}\big). \end{aligned} \tag{2.9}$$

Corollary 9. *Corollary 8 can be equivalently written as*

$$\begin{aligned}\widehat{\mathbf{U}} - \mathbf{U}\mathbf{W}_{\mathbf{U}} = &\big(\mathbf{U}_\perp\mathbf{U}_\perp^\top\big)\mathbf{E}\big(\mathbf{V}\mathbf{V}^\top\big)\mathbf{V}\mathbf{W}_{\mathbf{V}}\hat{\mathbf{\Sigma}}^{-1} \\ &+ \big(\mathbf{U}_\perp\mathbf{U}_\perp^\top\big)\mathbf{E}\big(\mathbf{V}\mathbf{V}^\top\big)\mathbf{V}\big(\mathbf{V}^\top\widehat{\mathbf{V}} - \mathbf{W}_{\mathbf{V}}\big)\widehat{\mathbf{\Sigma}}^{-1} \\ &+ \big(\mathbf{U}_\perp\mathbf{U}_\perp^\top\big)\mathbf{E}\big(\mathbf{V}_\perp\mathbf{V}_\perp^\top\big)\big(\widehat{\mathbf{V}} - \mathbf{V}\mathbf{V}^\top\widehat{\mathbf{V}}\big)\widehat{\mathbf{\Sigma}}^{-1} \\ &+ \big(\mathbf{U}_\perp\mathbf{U}_\perp^\top\big)\mathbf{M}\big(\mathbf{V}_\perp\mathbf{V}_\perp^\top\big)\big(\widehat{\mathbf{V}} - \mathbf{V}\mathbf{V}^\top\widehat{\mathbf{V}}\big)\widehat{\mathbf{\Sigma}}^{-1} \\ &+ \mathbf{U}\big(\mathbf{U}^\top\widehat{\mathbf{U}} - \mathbf{W}_{\mathbf{U}}\big). \end{aligned} \tag{2.10}$$

For Corollaries 8 and 9, the first term following the equality sign in each display equation is shown in practice to be the leading order term of interest. This point shall be made more precise and quantitative below.

2.2.2 General perturbation theorems

This section presents a collection of perturbation theorems derived via a unified methodology that combines Theorem 6, its variants, the two-to-infinity norm ma-

chinery in Section 1.3, and the geometric observations in Section 6.1.1. We bound $\widehat{\mathbf{U}} - \mathbf{U}\mathbf{W}_{\mathbf{U}}$, while similar bounds hold for $\widehat{\mathbf{V}} - \mathbf{V}\mathbf{W}_{\mathbf{V}}$ under the appropriate modifications detailed in Theorem 6.

Theorem 10 (Baseline two-to-infinity norm bound)**.** *Provided* $\sigma_r(\mathbf{M}) > \sigma_{r+1}(\mathbf{M}) \geq 0$ *and* $\sigma_r(\mathbf{M}) \geq 2\|\mathbf{E}\|_2$*, then*

$$\begin{aligned}\|\widehat{\mathbf{U}} - \mathbf{U}\mathbf{W}_{\mathbf{U}}\|_{2\to\infty} \leq\ & 2\left(\frac{\|(\mathbf{U}_\perp\mathbf{U}_\perp^\top)\mathbf{E}(\mathbf{V}\mathbf{V}^\top)\|_{2\to\infty}}{\sigma_r(\mathbf{M})}\right) \\ & + 2\left(\frac{\|(\mathbf{U}_\perp\mathbf{U}_\perp^\top)\mathbf{E}(\mathbf{V}_\perp\mathbf{V}_\perp^\top)\|_{2\to\infty}}{\sigma_r(\mathbf{M})}\right)\left\|\sin\boldsymbol{\Theta}(\widehat{\mathbf{V}},\mathbf{V})\right\|_2 \\ & + 2\left(\frac{\|(\mathbf{U}_\perp\mathbf{U}_\perp^\top)\mathbf{M}(\mathbf{V}_\perp\mathbf{V}_\perp^\top)\|_{2\to\infty}}{\sigma_r(\mathbf{M})}\right)\left\|\sin\boldsymbol{\Theta}(\widehat{\mathbf{V}},\mathbf{V})\right\|_2 \\ & + \left\|\sin\boldsymbol{\Theta}(\widehat{\mathbf{U}},\mathbf{U})\right\|_2^2\|\mathbf{U}\|_{2\to\infty}. \end{aligned} \tag{2.11}$$

Let $C_{\mathbf{M},\mathbf{U}}$ and $C_{\mathbf{M},\mathbf{V}}$ denote upper bounds on the quantities $\|(\mathbf{U}_\perp\mathbf{U}_\perp^\top)\mathbf{M}\|_\infty$ and $\|(\mathbf{V}_\perp\mathbf{V}_\perp^\top)\mathbf{M}^\top\|_\infty$, respectively, and define $C_{\mathbf{E},\mathbf{U}}$ and $C_{\mathbf{E},\mathbf{V}}$ analogously. Theorem 11 provides a uniform perturbation bound for $\|\widehat{\mathbf{U}} - \mathbf{U}\mathbf{W}_{\mathbf{U}}\|_{2\to\infty}$ and $\|\widehat{\mathbf{V}} - \mathbf{V}\mathbf{W}_{\mathbf{V}}\|_{2\to\infty}$. When $\mathrm{rank}(\mathbf{M}) = r$, Corollary 12 states a weaker but simpler version of the bound in Theorem 11.

Theorem 11 (Uniform perturbation bound for rectangular matrices)**.** *Suppose that* $\sigma_r(\mathbf{M}) > \sigma_{r+1}(\mathbf{M}) > 0$ *and that*

$$\sigma_r(\mathbf{M}) \geq \max\left\{2\|\mathbf{E}\|_2, (2/\alpha)C_{\mathbf{E},\mathbf{U}}, \left(2/\alpha'\right)C_{\mathbf{E},\mathbf{V}}, (2/\beta)C_{\mathbf{M},\mathbf{U}}, \left(2/\beta'\right)C_{\mathbf{M},\mathbf{V}}\right\}$$

for constants $0 < \alpha, \alpha', \beta, \beta' < 1$ *such that* $\delta := (\alpha + \beta)(\alpha' + \beta') < 1$. *Then*

$$\begin{aligned}(1-\delta)\|\widehat{\mathbf{U}} - \mathbf{U}\mathbf{W}_{\mathbf{U}}\|_{2\to\infty} \leq\ & 2\left(\frac{\|(\mathbf{U}_\perp\mathbf{U}_\perp^\top)\mathbf{E}(\mathbf{V}\mathbf{V}^\top)\|_{2\to\infty}}{\sigma_r(\mathbf{M})}\right) \\ & + 2\left(\frac{\|(\mathbf{V}_\perp\mathbf{V}_\perp^\top)\mathbf{E}^\top(\mathbf{U}\mathbf{U}^\top)\|_{2\to\infty}}{\sigma_r(\mathbf{M})}\right) \\ & + \left\|\sin\boldsymbol{\Theta}(\widehat{\mathbf{U}},\mathbf{U})\right\|_2^2\|\mathbf{U}\|_{2\to\infty} \\ & + \left\|\sin\boldsymbol{\Theta}(\widehat{\mathbf{V}},\mathbf{V})\right\|_2^2\|\mathbf{V}\|_{2\to\infty}. \end{aligned} \tag{2.12}$$

If $\mathrm{rank}(\mathbf{M}) = r$ *so that* $\sigma_{r+1}(\mathbf{M}) = 0$, *then the above bound holds for the value* $\delta := \alpha \times \alpha' < 1$ *under the weaker assumption that*

$$\sigma_r(\mathbf{M}) \geq \max\big\{2\|\mathbf{E}\|_2, (2/\alpha)C_{\mathbf{E},\mathbf{U}}, \big(2/\alpha'\big)C_{\mathbf{E},\mathbf{V}}\big\}.$$

Corollary 12 (Uniform perturbation bound for low rank matrices)**.** *Suppose that* $\sigma_r(\mathbf{M}) > \sigma_{r+1}(\mathbf{M}) = 0$ *and that*

$$\sigma_r(\mathbf{M}) \geq \max\big\{2\|\mathbf{E}\|_2, (2/\alpha)C_{\mathbf{E},\mathbf{U}}, \big(2/\alpha'\big)C_{\mathbf{E},\mathbf{V}}\big\}$$

for some constants $0 < \alpha, \alpha' < 1$ *such that* $\delta := \alpha \times \alpha' < 1$. *Then*

$$(1-\delta)\|\widehat{\mathbf{U}} - \mathbf{U}\mathbf{W}_{\mathbf{U}}\|_{2\to\infty} \leq 12 \times \max_{\eta\in\{1,\infty\}}\left\{\frac{\|\mathbf{E}\|_\eta}{\sigma_r(\mathbf{M})}\right\} \times \max_{\mathbf{Z}\in\{\mathbf{U},\mathbf{V}\}}\big\{\|\mathbf{Z}\|_{2\to\infty}\big\}. \tag{2.13}$$

2.3 Applications in high-dimensional statistics

This section applies our perturbation theorems and two-to-infinity norm machinery to three statistical settings corresponding to, among others, the results in Cai and Zhang (2018); Fan et al. (2018); Lyzinski et al. (2014), thereby yielding Theorem 14, Theorem 15, and Theorem 18. Each of these theorems (including Theorem 5 presented earlier) is obtained by combining general considerations with application-specific analysis.

Moving forward, consider the following structural matrix property which arises within the context of low rank matrix recovery.

Definition 13 (Coherence (Candès and Recht, 2009))**.** Let $\mathcal{U}$ be a subspace of dimension r in $\mathbb{R}^p$, and let $\mathbf{P}_{\mathcal{U}}$ be the orthogonal projection onto $\mathcal{U}$. Then the *coherence* of $\mathcal{U}$ (vis-à-vis the standard basis $\{\mathbf{e}_i\}$) is defined to be

$$\mu(\mathcal{U}) := \left(\frac{p}{r}\right) \max_{i \in [p]} \|\mathbf{P}_{\mathcal{U}} \mathbf{e}_i\|_2^2. \tag{2.14}$$

For $\mathbf{U} \in \mathbb{O}_{p,r}$, the (orthonormal) columns of $\mathbf{U}$ span a subspace of dimension r in $\mathbb{R}^p$, so it is natural to abuse notation and to interchange $\mathbf{U}$ with its underlying subspace $\mathcal{U}$. In this case, $\mathbf{P}_{\mathcal{U}} \equiv \mathbf{U}\mathbf{U}^\top$, and so Propositions 1 and 4 lead to the

equivalent formulation

$$\mu(\mathbf{U}) := \left(\frac{p}{r}\right)\|\mathbf{U}\|_{2\to\infty}^2.$$

Observe that $1 \leq \mu(\mathbf{U}) \leq p/r$, where the upper and lower bounds are achieved for $\mathbf{U}$ consisting of all standard basis vectors and of vectors whose entries each have magnitude $1/\sqrt{p}$, respectively. Since the columns of $\mathbf{U}$ are mutually orthogonal with unit Euclidean norm, the magnitude of $\mu(\mathbf{U})$ can be viewed as quantifying the row-wise accumulation of "mass" in $\mathbf{U}$.

The bounded coherence property (Candès and Recht, 2009) corresponds to the existence of a positive constant $C_\mu \geq 1$ such that

$$\|\mathbf{U}\|_{2\to\infty} \leq C_\mu\sqrt{\frac{r}{p}}. \tag{2.15}$$

Bounded coherence arises naturally in the random orthogonal (matrix) model and influences the recoverability of low rank matrices via nuclear norm minimization when sampling only a subset of the matrix entries (Candès and Recht, 2009). Bounded coherence is also closely related to the notion of eigenvector delocalization in random matrix theory (Rudelson and Vershynin, 2015). Examples of matrices whose row and column space factors exhibit bounded coherence can be found, for example, in the study of networks. Specifically, it is not difficult to check that bounded coherence holds for the top eigenvectors of the (non-random) low rank edge probability matrices corresponding to the Erdős–Rényi random graph model and the balanced K-block

stochastic block model.

2.3.1 Singular vector perturbation bound

In Fan et al. (2018), the authors consider low rank matrices exhibiting bounded coherence. For such matrices, the results therein provide singular vector perturbation bounds under the ℓ_∞ vector norm, which are then applied to robust covariance estimation.

In this dissertation, Corollary 12 states a perturbation bound that is similar in kind to those in Fan et al. (2018). Note that upper bounding $\|\widehat{\mathbf{U}} - \mathbf{U}\mathbf{W}_{\mathbf{U}}\|_{2\to\infty}$ immediately bounds both $\|\widehat{\mathbf{U}} - \mathbf{U}\mathbf{W}_{\mathbf{U}}\|_{\max}$ and $\inf_{\mathbf{W}\in\mathbb{O}_r} \|\widehat{\mathbf{U}} - \mathbf{U}\mathbf{W}\|_{\max}$, thereby providing ℓ_∞-type bounds for the perturbed singular vectors up to orthogonal transformation, the analogue of sign flips for well-separated, distinct singular values (similarly for $\mathbf{V}$, $\widehat{\mathbf{V}}$ and $\mathbf{W}_{\mathbf{V}}$). The joint, symmetric nature of the singular value gap assumption controls the dependence of $\|\widehat{\mathbf{U}} - \mathbf{U}\mathbf{W}_{\mathbf{U}}\|_{2\to\infty}$ and $\|\widehat{\mathbf{V}} - \mathbf{V}\mathbf{W}_{\mathbf{V}}\|_{2\to\infty}$ on one another and takes into account the underlying matrix dimensions.

For symmetric matrices, Theorem 14 improves upon Fan et al. (2018) and implicitly applies to the applications discussed therein.

Theorem 14 (Application: eigenvector (entrywise) perturbation bound)**.** *Let* $\mathbf{M}, \mathbf{E} \in \mathbb{R}^{p\times p}$ *be symmetric matrices where* $\operatorname{rank}(\mathbf{M}) = r$ *and* $\mathbf{M}$ *has spectral decomposition* $\mathbf{M} = \mathbf{U}\mathbf{\Lambda}\mathbf{U}^\top + \mathbf{U}_\perp\mathbf{\Lambda}_\perp\mathbf{U}_\perp^\top \equiv \mathbf{U}\mathbf{\Lambda}\mathbf{U}^\top$ *with leading eigenvalues* $|\lambda_1| \geq |\lambda_2| \geq \cdots \geq |\lambda_r| > 0$. *If* $|\lambda_r| \geq 4\|\mathbf{E}\|_\infty$, *then there exists an orthogonal matrix* $\mathbf{W}_{\mathbf{U}} \in \mathbb{O}_r$ *such*

that

$$\|\widehat{\mathbf{U}} - \mathbf{U}\mathbf{W}_{\mathbf{U}}\|_{2\to\infty} \leq 14\left(\frac{\|\mathbf{E}\|_{\infty}}{|\lambda_r|}\right)\|\mathbf{U}\|_{2\to\infty}. \tag{2.16}$$

Theorem 14 provides a user-friendly, deterministic perturbation bound that permits repeated eigenvalues in $\mathbf{M}$ and makes no assumption on the behavior of $\|\mathbf{U}\|_{2\to\infty}$. When bounded coherence does hold, combining Eq. (2.15) with Theorem 14 immediately yields the bound

$$\|\widehat{\mathbf{U}} - \mathbf{U}\mathbf{W}_{\mathbf{U}}\|_{2\to\infty} \leq 14C_{\mu}\left(\frac{\sqrt{r}\|\mathbf{E}\|_{\infty}}{\sqrt{p}|\lambda_r|}\right).$$

It is worth emphasizing that stronger (albeit more complicated) bounds are obtained in the proof leading up to the statement of Theorem 14.

2.3.2 Singular subspace perturbation and random matrices

This section interfaces the results in this dissertation with the spectral and Frobenius norm rate-optimal singular subspace perturbation bounds obtained in Cai and Zhang (2018).

Consider the setting wherein $\mathbf{M} \in \mathbb{R}^{p_1\times p_2}$ is a fixed rank r matrix with $r \ll p_1 \ll p_2$ and $\sigma_r(\mathbf{M}) \geq C(p_2/\sqrt{p_1})$. Let $\mathbf{E} \in \mathbb{R}^{p_1\times p_2}$ be a random matrix with independent

standard normal entries. Then by Cai and Zhang (2018), the following bounds hold for the left and right singular subspaces with high probability:

$$\left\|\sin\boldsymbol{\Theta}(\widehat{\mathbf{U}},\mathbf{U})\right\|_2 \leq C\left(\frac{\sqrt{p_1}}{\sigma_r(\mathbf{M})}\right) \quad \text{and} \quad \left\|\sin\boldsymbol{\Theta}(\widehat{\mathbf{V}},\mathbf{V})\right\|_2 \leq C\left(\frac{\sqrt{p_2}}{\sigma_r(\mathbf{M})}\right).$$

Here, working with $\mathbf{V}$ and $\widehat{\mathbf{V}}$ is desirable though comparatively more difficult. Theorem 15 demonstrates how (even relatively coarse) two-to-infinity norm analysis allows one to recover upper and lower bounds for $\|\widehat{\mathbf{V}} - \mathbf{V}\mathbf{W}_{\mathbf{V}}\|_{2\to\infty}$ that at times nearly match. For ease of presentation, Theorem 15 is stated simply as holding with high probability.

Theorem 15 (Application: singular subspace recovery)**.** *Let* $\mathbf{M}, \mathbf{E} \in \mathbb{R}^{p_1\times p_2}$ *be as in Section 2.3.2. There exists an orthogonal matrix* $\mathbf{W}_{\mathbf{V}} \in \mathbb{O}_r$ *and* $C_r > 0$ *such that with high probability,*

$$\begin{aligned}&\|\widehat{\mathbf{V}} - \mathbf{V}\mathbf{W}_{\mathbf{V}}\|_{2\to\infty} \\ &\quad \leq C_r\left(\frac{\log(p_2)}{\sigma_r(\mathbf{M})}\right)\left(1 + \left(\frac{p_1}{\sigma_r(\mathbf{M})}\right) + \left(\frac{\sqrt{p_1}}{\log(p_2)}\right)\|\mathbf{V}\|_{2\to\infty}\right). \end{aligned} \tag{2.17}$$

If in addition $\sigma_r(\mathbf{M}) \geq cp_1$ *and* $\|\mathbf{V}\|_{2\to\infty} \leq c_r/\sqrt{p_2}$ *for some* $c, c_r > 0$*, then with high probability*

$$\|\widehat{\mathbf{V}} - \mathbf{V}\mathbf{W}_{\mathbf{V}}\|_{2\to\infty} \leq C_r\left(\frac{\log(p_2)}{\sigma_r(\mathbf{M})}\right). \tag{2.18}$$

The lower bound $\frac{1}{\sqrt{p_2}}\|\sin\boldsymbol{\Theta}(\widehat{\mathbf{V}},\mathbf{V})\|_2 \leq \|\widehat{\mathbf{V}} - \mathbf{V}\mathbf{W}_{\mathbf{V}}\|_{2\to\infty}$ *always holds by Proposi-*

tion 2 and Lemma 39.

2.3.3 Statistical inference for random graphs

In the study of networks, community detection and clustering are tasks of central interest. A network (i.e., a graph $\mathcal{G} \equiv (\mathcal{V}, \mathcal{E})$ consisting of a vertex set $\mathcal{V}$ and edge set $\mathcal{E}$) may be represented by its adjacency matrix, $\mathbf{A} \equiv \mathbf{A}_{\mathcal{G}}$, which captures the edge connectivity of the nodes in the network. For inhomogeneous independent edge random graph models, the adjacency matrix can be viewed as a random perturbation of an underlying (often low rank) edge probability matrix $\mathbf{P}$, where in expectation $\mathbf{P} \equiv \mathbb{E}[\mathbf{A}]$. In the notation of Section 1.5, the matrix $\mathbf{P}$ corresponds to $\mathbf{M}$, the matrix $\mathbf{A}-\mathbf{P}$ corresponds to $\mathbf{E}$, and the matrix $\mathbf{A}$ corresponds to $\widehat{\mathbf{M}}$. By viewing $\widehat{\mathbf{U}}$ (here the matrix of leading eigenvectors of $\mathbf{A}$) as an estimate of $\mathbf{U}$ (here the matrix of leading eigenvectors of $\mathbf{P}$), the results in Section 2.2 immediately apply.

Spectral methods and related optimization problems for random graphs employ the spectral decomposition of the (adjacency or Laplacian) matrix (Rohe et al., 2011; Sarkar and Bickel, 2015; Sussman et al., 2012; Tang and Priebe, 2018). For example, Le et al. (2016) presents a general spectral-based, dimension-reduction community detection framework which incorporates the spectral norm distance between the leading eigenvectors of $\mathbf{A}$ and $\mathbf{P}$. Taken in the context of Le et al. (2016) and indeed the wider statistical network analysis literature, this chapter complements existing work and paves the way for expanding the toolkit of network analysts to include more

Procrustean considerations and two-to-infinity norm machinery.

Much of the existing literature for graphs and network models concerns the popular stochastic block model (SBM) (Holland et al., 1983) and its variants. The related random dot product graph model (RDPG model) (Young and Scheinerman, 2007) has recently been developed in a series of papers as both a tractable and flexible random graph model amenable to spectral methods (Fishkind et al., 2013; Sussman et al., 2012, 2014; Tang et al., 2017,?; Tang and Priebe, 2018). In the RDPG model, the graph's eigenvalues and eigenvectors are closely related to the model's generative latent positions. In particular, the leading eigenvectors of the adjacency matrix can be used to estimate the latent positions when properly scaled by the leading eigenvalues.

In the context of the wider RDPG literature, this dissertation extends both the treatment of the two-to-infinity norm in Lyzinski et al. (2014) and Procrustes matching for graphs in Tang et al. (2017). Our bounds in Section 2.2 imply an eigenvector version of Lemma 5 in Lyzinski et al. (2014) that does not require the matrix-valued model parameter $\mathbf{P}$ to have distinct eigenvalues. Our Procrustes analysis also suggests a refinement of the test statistic formulation in the two-sample graph inference hypothesis testing framework of Tang et al. (2017).

Our level of generality permits the consideration of random graph models that allow edge dependence structure, such as the (C, c, γ) property (O'Rourke et al., 2018) (see below). Indeed, moving beyond independent edge models represents an important direction for future work in the field of statistical network analysis.

Definition 16 ((C, c, γ) concentration (O'Rourke et al., 2018))**.** A $p_1 \times p_2$ random matrix $\mathbf{E}$ is said to be (C, c, γ)-*concentrated* if, given a trio of positive constants (C, c, γ), for all unit vectors $\mathbf{u} \in \mathbb{R}^{p_1}$, $\mathbf{v} \in \mathbb{R}^{p_2}$, and for every $t > 0$,

$$\mathbb{P}\big[\big|\langle \mathbf{E}\mathbf{v}, \mathbf{u}\rangle\big| > t\big] \leq C \exp\big(-ct^{\gamma}\big). \tag{2.19}$$

Remark 6 (Probabilistic concentration and the perturbation $\mathbf{E}$)**.** The proofs of our main results demonstrate the importance of bounding $\|\mathbf{E}\mathbf{V}\|_{2\to\infty}$ and $\|\mathbf{U}^{\top}\mathbf{E}\mathbf{V}\|_2$ in the perturbation framework of Section 1.5. When $\mathbf{E}$ satisfies the (C, c, γ) concentration property in Definition 16, these quantities can be easily controlled via standard Bernstein and Hoeffding-type probabilistic bounds encountered throughout statistics.

In the statistical network analysis literature, current active research directions include the development of random graph models exhibiting edge correlation and the development of inference methodology for multiple graphs. Here, we briefly consider the ρ-correlated stochastic block model (Lyzinski et al., 2015) and the omnibus embedding matrix for multiple graphs (Priebe et al., 2013) employed in Chen et al. (2016); Levin et al. (2017); Lyzinski (2018). The ρ-correlated stochastic block model provides a simple yet easily interpretable and tractable model for dependent random graphs, while the omnibus embedding matrix provides a framework for performing spectral analysis on multiple graphs by leveraging graph (dis)similarities.

Definition 17 (ρ-correlated SBM graphs (Lyzinski, 2018))**.** Let $\mathcal{G}^n$ denote the set of

labeled, n-vertex, simple, undirected graphs. Two n-vertex random graphs $(G^1, G^2) \in \mathcal{G}^1 \times \mathcal{G}^2$ are said to be *ρ-correlated SBM$(\kappa, \vec{n}, b, \mathbf{\Lambda})$ graphs* (abbreviated ρ-SBM) if:

1. $G^1 := (\mathcal{V}, \mathcal{E}(G^1))$ and $G^2 := (\mathcal{V}, \mathcal{E}(G^2))$ are marginally SBM$(\kappa, \vec{n}, b, \Lambda)$ random graphs; that is, for each $i = 1, 2$,

   (a) The vertex set $\mathcal{V}$ is the union of κ blocks $\mathcal{V}_1, \mathcal{V}_2, \ldots, \mathcal{V}_\kappa$, which are disjoint sets with respective cardinalities $n_1, n_2, \ldots, n_\kappa$;

   (b) The block membership function $b : \mathcal{V} \mapsto [\kappa]$ is such that for each $v \in \mathcal{V}$, $b(v)$ denotes the block of v; that is, $v \in \mathcal{V}_{b(v)}$;

   (c) The block adjacency probabilities are given by the symmetric matrix $\mathbf{\Lambda} \in [0,1]^{\kappa \times \kappa}$; that is, for each pair of vertices $\{j, l\} \in \binom{\mathcal{V}}{2}$, the adjacency of j and l is an independent Bernoulli trial with probability of success $\Lambda_{b(j),b(l)}$.

2. The random variables

$$\left\{\mathbb{I}\left[\{j,k\} \in \mathcal{E}\left(G^i\right)\right]\right\}_{i=1,2;\{j,k\}\in\binom{\mathcal{V}}{2}}$$

   are collectively independent except that for each $\{j, k\} \in \binom{\mathcal{V}}{2}$, the correlation between $\mathbb{I}[\{j, k\} \in \mathcal{E}(G^1)]$ and $\mathbb{I}[\{j, k\} \in \mathcal{E}(G^2)]$ is $\rho \geq 0$.

The following theorem provides a guarantee for estimating the leading eigenvectors of a multiple graph omnibus matrix when the graphs are not independent. Theorem 18 is among the first of its kind and complements the recent, concurrent work on joint

graph embedding in Levin et al. (2017).

Theorem 18 (Application: multiple graph inference)**.** *Let* (G^1, G^2) *be a pair of* ρ*-correlated SBM*$(\kappa, \vec{n}, b, \mathbf{\Lambda})$ *graphs as in Definition 17 with* $n \times n$ *(symmetric, binary) adjacency matrices* $(\mathbf{A}^1, \mathbf{A}^2)$*. Let the model omnibus matrix* $\mathfrak{O}$ *and adjacency omnibus matrix* $\widehat{\mathfrak{O}}$ *be given by*

$$\mathfrak{O} := \begin{bmatrix} 1 & 1 \\ & \\ 1 & 1 \end{bmatrix} \otimes \mathfrak{Z}\mathbf{\Lambda}\mathfrak{Z}^\top \quad \text{and} \quad \widehat{\mathfrak{O}} := \begin{bmatrix} \mathbf{A}^1 & \frac{\mathbf{A}^1+\mathbf{A}^2}{2} \\ & \\ \frac{\mathbf{A}^1+\mathbf{A}^2}{2} & \mathbf{A}^2 \end{bmatrix},$$

where $\otimes$ *denotes the matrix Kronecker product and* $\mathfrak{Z}$ *is the* $n \times \kappa$ *matrix of vertex-to-block assignments such that* $\mathbf{P} := \mathfrak{Z}\mathbf{\Lambda}\mathfrak{Z}^\top \in [0,1]^{n \times n}$ *denotes the edge probability matrix. Let* $\operatorname{rank}(\mathbf{\Lambda}) = r$*, and hence* $\operatorname{rank}(\mathfrak{O}) = r$*. For* $i = 1, 2$*, suppose that the maximum expected degree of* G^i*,* Δ*, satisfies* $\Delta \gg \log^4(n)$*, along with* $\sigma_r(\mathfrak{O}) \geq c\Delta$ *for some* $c > 0$*. Let* $\mathbf{U}, \widehat{\mathbf{U}} \in \mathbb{O}_{2n,r}$ *denote the matrices whose columns are the normalized eigenvectors corresponding to the largest eigenvalues of* $\mathfrak{O}$ *and* $\widehat{\mathfrak{O}}$ *given by the diagonal matrices* $\mathbf{\Sigma}$ *and* $\widehat{\mathbf{\Sigma}}$*, respectively. For* $\mathbf{W}_\mathbf{U} \in \mathbb{O}_r$ *as in Section 1.4, with probability* $1 - o(1)$ *as* $n \to \infty$*,*

$$\|\widehat{\mathbf{U}} - \mathbf{U}\mathbf{W}_\mathbf{U}\|_{2\to\infty} = \mathcal{O}_r\left(\frac{\log n}{\Delta}\right).$$

In contrast, spectral norm analysis implies the weaker two-to-infinity norm bound $\|\widehat{\mathbf{U}} - \mathbf{U}\mathbf{W}_\mathbf{U}\|_{2\to\infty} = \mathcal{O}_r(\frac{1}{\sqrt{\Delta}})$.

Remark 7 (Edge correlation)**.** The implicit dependence upon the correlation factor ρ in Theorem 18 can be made explicit by a more careful analysis of constant factors and the probability statement. This is not our present concern.

2.4 Discussion

This chapter develops a flexible Procrustean matrix decomposition and its variants together with machinery for the two-to-infinity norm in order to study the perturbation of singular vectors and subspaces. We have demonstrated both implicitly and explicitly the widespread applicability of our framework and results to a host of popular matrix noise models, namely matrices that have:

- independent and identically distributed entries (Section 2.3.2);
- independent and identically distributed rows (Section 2.1.2);
- independent but not identically distributed entries (Section 2.3.3);
- neither independent nor identically distributed entries (Section 2.3.1).

Each application presented in this chapter requires problem-specific analysis. One must determine which formulation of the Procrustean matrix decomposition to use, how to effectively transition between norms, and how to analyze the resulting quantities. For example, in Section 2.3.1 the product term $\|\mathbf{E}\|_{\infty}\|\mathbf{U}\|_{2\to\infty}$ is meaningful when coupled with the bounded coherence assumption, whereas the term $\|\mathbf{EU}\|_{2\to\infty}$ is

analyzed directly in order to prove Theorem 18. Similarly, with respect to covariance estimation (Theorems 5 and 14), context-specific differences motivate idiosyncratic approaches when deriving the stated bounds.

This chapter focuses on decomposing the matrix $\widehat{\mathbf{U}} - \mathbf{U}\mathbf{W}_{\mathbf{U}}$ and on establishing the two-to-infinity norm as a useful tool for matrix perturbation analysis. Among the observations made earlier in this dissertation, it is useful to keep in mind that

$$\inf_{\mathbf{W} \in \mathbb{O}_r} \|\widehat{\mathbf{U}} - \mathbf{U}\mathbf{W}\|_{\max} \leq \|\widehat{\mathbf{U}} - \mathbf{U}\mathbf{W}_{\mathbf{U}}\|_{\max} \leq \|\widehat{\mathbf{U}} - \mathbf{U}\mathbf{W}_{\mathbf{U}}\|_{2 \to \infty}.$$

Ample open problems and applications exist for which it is and will be productive to utilize the two-to-infinity norm and matrix decompositions in the future. It is our hope that the level of generality and flexibility presented in this chapter will facilitate the more widespread use of the two-to-infinity norm in statistics.

Chapter 3

Eigenvector deviations and fluctuations

3.1 Overview of Chapter 3

This chapter considers the setting where $\mathbf{M}$ and $\mathbf{E}$ are large $n \times n$ symmetric real-valued matrices with $\widehat{\mathbf{M}} = \mathbf{M} + \mathbf{E}$ representing an additive perturbation of $\mathbf{M}$ by $\mathbf{E}$. For $n \times r$ matrices $\mathbf{U}$ and $\widehat{\mathbf{U}}$ whose columns are orthonormal eigenvectors corresponding to the $r \ll n$ leading eigenvalues of $\mathbf{M}$ and $\widehat{\mathbf{M}}$, respectively, we ask:

Question 1. How entrywise close are the matrices of eigenvectors $\mathbf{U}$ and $\widehat{\mathbf{U}}$?

Under quite general structural assumptions on $\mathbf{U}$, $\mathbf{M}$, and $\mathbf{E}$, our main results address Question 1 both at the level of first-order deviations and at the level of second-order fluctuations. Theorems 19 and 20 quantify the entrywise closeness of

$\widehat{\mathbf{U}}$ to $\mathbf{U}$ modulo a necessary orthogonal transformation $\mathbf{W}$ (corresponding to $\mathbf{W}_{\mathbf{U}}$ in Chapter 2). Theorem 21 states a multivariate distributional limit result for the rows of the matrix $\widehat{\mathbf{U}} - \mathbf{U}\mathbf{W}$.

Numerous problems in statistics consider the eigenstructure of large symmetric matrices. Prominent examples of such problems include (spike) population and covariance matrix estimation (Johnstone, 2001; Silverstein, 1984, 1989; Yu et al., 2015) as well as principal component analysis (Jolliffe, 1986; Nadler, 2008; Paul, 2007), problems which have received additional attention and windfall as a result of advances in random matrix theory (Bai and Silverstein, 2010; Benaych-Georges and Nadakuditi, 2011; Paul and Aue, 2014). Within the study of networks, the problem of community detection and success of spectral clustering methodologies have also led to widespread interest in understanding spectral perturbations of large matrices, in particular graph Laplacian and adjacency matrices (Le et al., 2017; Lei and Rinaldo, 2015; Rohe et al., 2011; Sarkar and Bickel, 2015; Tang and Priebe, 2018). Towards these ends, recent ongoing and concurrent efforts in the statistics, computer science, and mathematics communities have been devoted to obtaining precise entrywise bounds on eigenvector perturbations (Cape et al., 2019b; Eldridge et al., 2018; Fan et al., 2018). See also Mao et al. (2017), Abbe et al. (2017), and Tang et al. (2017).

The content in this chapter distinguishes itself from the existing literature by presenting both deviation and fluctuation results within a concise yet flexible signal-plus-noise matrix model framework amenable to statistical applications. We extend

the machinery and perturbation considerations introduced in Chapters 1 and 2 in order to obtain more precise first-order bounds. We then demonstrate how careful analysis within a unified framework leads to second-order multivariate distributional limit theory. Our characterization of eigenvector perturbations relies upon a matrix perturbation series expansion together with an approximate commutativity argument for certain matrix products.

The results in this chapter apply to principal component analysis in spike matrix models, including those of the form $\mathbf{Y} = \lambda \mathbf{u}\mathbf{u}^\top + n^{-1/2}\mathbf{E}$ where $\mathbf{u} \in \mathbb{R}^n$ denotes a spike (signal) unit vector and $\mathbf{E} \in \mathbb{R}^{n \times n}$ denotes a random symmetric (noise) matrix. We consider the super-critical regime, $\lambda > 1$, for which it is known, for example, that the leading eigenvector $\widehat{\mathbf{u}}$ of $\mathbf{Y}$ has non-trivial correlation with $\mathbf{u}$ when $\mathbf{E}$ is drawn from the Gaussian orthogonal ensemble, namely $|\langle \widehat{\mathbf{u}}, \mathbf{u} \rangle|^2 \to 1 - 1/\lambda^2$ almost surely (Benaych-Georges and Nadakuditi, 2011). This chapter obtains stronger local results for spike estimation in the presence of sufficient eigenvector delocalization and provided the signal in $\lambda \gg 1$ is sufficiently informative with respect to $\mathbf{E}$. Loosely speaking, we establish that $\|\widehat{\mathbf{u}} - \mathbf{u}\|_\infty \leq C(\log n)^c \lambda^{-1} \|\mathbf{u}\|_\infty$ with high probability for some positive constants C and c, and we prove that $n(\widehat{\mathbf{u}}_i - \mathbf{u}_i)$ is asymptotically normally distributed. Our results hold more generally for r-dimensional spike models exhibiting eigenvalue multiplicity and for $\mathbf{E}$ exhibiting a heterogeneous variance profile.

3.2 Main results for eigenvector deviations and fluctuations

Let $\mathbf{M} \equiv \mathbf{M}_n \in \mathbb{R}^{n\times n}$ be a symmetric matrix with block spectral decomposition

$$\mathbf{M} \equiv [\mathbf{U}|\mathbf{U}_\perp][\mathbf{\Lambda} \oplus \mathbf{\Lambda}_\perp][\mathbf{U}|\mathbf{U}_\perp]^\top = \mathbf{U}\mathbf{\Lambda}\mathbf{U}^\top + \mathbf{U}_\perp\mathbf{\Lambda}_\perp\mathbf{U}_\perp^\top, \tag{3.1}$$

where the diagonal matrix $\mathbf{\Lambda} \in \mathbb{R}^{r\times r}$ contains the r largest-in-magnitude nonzero eigenvalues of $\mathbf{M}$ with $|\mathbf{\Lambda}_{1,1}| \geq \cdots \geq |\mathbf{\Lambda}_{r,r}| > 0$, and where $\mathbf{U} \in \mathbb{O}_{n,r}$ is an $n \times r$ matrix whose orthonormal columns are the corresponding eigenvectors of $\mathbf{M}$. The diagonal matrix $\mathbf{\Lambda}_\perp \in \mathbb{R}^{(n-r)\times(n-r)}$ contains the remaining $n - r$ eigenvalues of $\mathbf{M}$ with the associated matrix of orthonormal eigenvectors $\mathbf{U}_\perp \in \mathbb{O}_{n,(n-r)}$. Let $\mathbf{E} \in \mathbb{R}^{n\times n}$ be a symmetric matrix, and write the perturbation of $\mathbf{M}$ by $\mathbf{E}$ as $\widehat{\mathbf{M}} \equiv \mathbf{M} + \mathbf{E} = \widehat{\mathbf{U}}\widehat{\mathbf{\Lambda}}\widehat{\mathbf{U}}^\top + \widehat{\mathbf{U}}_\perp\widehat{\mathbf{\Lambda}}_\perp\widehat{\mathbf{U}}_\perp^\top$.

Assumption 1. Let ρ_n denote an n-dependent scaling parameter where $(0, 1] \ni \rho_n \to c_\rho \in [0, 1]$ as $n \to \infty$, with $n\rho_n \geq c_1(\log n)^{c_2}$ for some constants $c_1, c_2 \geq 1$.

Assumption 2. There exist constants $C, c > 0$ such that for all $n \geq n_0(C, c)$, $|\mathbf{\Lambda}_{r,r}| \geq c(n\rho_n)$ and $|\mathbf{\Lambda}_{1,1}||\mathbf{\Lambda}_{r,r}|^{-1} \leq C$, while $\mathbf{\Lambda}_\perp \equiv \mathbf{0}$.

Assumption 3. There exist constants $C, c > 0$ such that $\|\mathbf{E}\|_2 \leq C(n\rho_n)^{1/2}$ with probability at least $1 - n^{-c}$ for $n \geq n_0(C, c)$, written as $\|\mathbf{E}\|_2 = O_{\mathbb{P}}\{(n\rho_n)^{1/2}\}$.

Assumption 1 introduces a sparsity scaling factor ρ_n for additional flexibility. This chapter considers the large-n regime and often suppresses the dependence of (sequences of) matrices on n for notational convenience.

Assumption 2 specifies the magnitude of the leading eigenvalues corresponding to the leading eigenvectors of interest. For simplicity and specificity, all leading eigenvalues are taken to be of the same prescribed order, and the remaining eigenvalues are assumed to vanish. Remark 9 briefly addresses the situation when the leading eigenvalues differ in order of magnitude, when $\mathbf{\Lambda}_\perp \neq \mathbf{0}$, and when the (spike) dimension r is unknown.

Assumption 3 specifies that the random matrix $\mathbf{E}$ is concentrated in spectral norm in the classical probabilistic sense. Such concentration holds widely for random matrix models where $\mathbf{E}$ is centered, in which case $\widehat{\mathbf{M}}$ has low rank expectation equal to $\mathbf{M}$. The advantage of Assumption 3 when coupled with Assumption 2 is that, together with an application of Weyl's inequality (Bhatia, 1997, Corollary 3.2.6), the implicit signal-to-noise ratio terms behave as $\|\mathbf{E}\|_2|\mathbf{\Lambda}_{r,r}|^{-1}, \|\mathbf{E}\|_2|\widehat{\mathbf{\Lambda}}_{r,r}|^{-1} = O_{\mathbb{P}}\{(n\rho_n)^{-1/2}\}$. It is straightforward to adapt our analysis and results under less explicit assumptions, albeit at the expense of succinctness and clarity.

Below, Assumption 4 specifies an additional probabilistic concentration requirement that arises in conjunction with the model flexibility introduced via the sparsity scaling factor ρ_n in Assumption 1. The notation $\lceil \cdot \rceil$ used below denotes the ceiling function.

Assumption 4. There exist constants $C_{\mathbf{E}}, \nu > 0$, $\xi > 1$ such that for all $1 \leq k \leq k(n) = \lceil \log n / \log(n\rho_n) \rceil$, for each standard basis vector $\mathbf{e}_i$, and for each column vector $\mathbf{u}$ of $\mathbf{U}$,

$$|\langle \mathbf{E}^k \mathbf{u}, \mathbf{e}_i \rangle| \leq (C_{\mathbf{E}} n\rho_n)^{k/2} (\log n)^{k\xi} \|\mathbf{u}\|_\infty \tag{3.2}$$

with probability at least $1 - \exp\{-\nu(\log n)^\xi\}$ provided $n \geq n_0(C_{\mathbf{E}}, \nu, \xi)$.

Assumption 4 states a higher-order concentration estimate that reflects behavior exhibited by a broad class of random symmetric matrices including Wigner matrices whose entries exhibit sub-exponential decay and nonidentical variances (Erdős et al., 2013, modification of Lemma 7.10; Remark 2.4); see also Mao et al. (2017). For example, using our notation, the proof of Lemma 7.10 in Erdős et al. (2013) establishes that $|\langle (C_{\mathbf{E}} n\rho_n)^{-k/2} \mathbf{E}^k \mathbf{e}, \mathbf{e}_i \rangle| \leq (\log n)^{k\xi}$ with high probability, where $\mathbf{e}$ is the vector of all ones and the symmetric matrix $\mathbf{E}$ has independent mean zero entries with bounded variances. Taking a union bound collectively over $1 \leq k \leq k(n)$, the standard basis vectors in $\mathbb{R}^n$, and the columns of $\mathbf{U}$, yields an event that holds with probability at least $1 - n^{-c}$ for some constant $c > 0$ for sufficiently large n.

The function $k(n)$ is fundamentally model-dependent through its connection with the sparsity factor ρ_n and satisfies $(n\rho_n)^{-k(n)/2} \leq n^{-1/2}$ for n sufficiently large. In the case when $\rho_n \equiv 1$, then $k(n) \equiv 1$, and the behavior reflected in Eq. (3.2) reduces to commonly-encountered Bernstein-type probabilistic concentration. In contrast, when $\rho_n \to 0$ and, for example, $(n\rho_n) = n^\epsilon$ for some $\epsilon \in (0, 1)$, then $k(n) \equiv \epsilon^{-1}$. If instead

$(n\rho_n) = (\log n)^{c_2}$ for some $c_2 \geq 1$, then $k(n) = \lceil \log n/(c_2 \log\log n) \rceil$. We remark that all regimes in which $\rho_n \to c_\rho > 0$ functionally correspond to the regime where $\rho_n \equiv 1$ by appropriate rescaling.

3.2.1 First-order approximation (deviations)

Under Assumptions 2 and 3, spectral norm analysis via the Davis-Kahan $\sin\boldsymbol{\Theta}$ theorem (Bhatia, 1997, Section 7.3) yields that for large n there exists $\mathbf{W} \equiv \mathbf{W}_n \in \mathbb{O}_r$ such that

$$\|\widehat{\mathbf{U}} - \mathbf{U}\mathbf{W}\|_2 = O_{\mathbb{P}}\left\{(n\rho_n)^{-1/2}\right\}. \tag{3.3}$$

Equation (3.3) provides a coarse benchmark bound for the quantity $\|\widehat{\mathbf{U}} - \mathbf{U}\mathbf{W}\|_{2\to\infty}$ (since $\|\cdot\|_{2\to\infty} \leq \|\cdot\|_2$), a quantity which is shown below to at times be much smaller.

Theorem 19. *Suppose that Assumptions 1–4 hold and that* $n\rho_n = \omega\{(\log n)^{2\xi}\}$ *with* $r^{1/2} \leq (\log n)^{\xi}$. *Then there exists* $\mathbf{W} \equiv \mathbf{W}_n \in \mathbb{O}_r$ *such that*

$$\|\widehat{\mathbf{U}} - \mathbf{U}\mathbf{W}\|_{2\to\infty} = O_{\mathbb{P}}\left[(n\rho_n)^{-1/2} \times \min\left\{r^{1/2}(\log n)^{\xi}\|\mathbf{U}\|_{2\to\infty}, 1\right\}\right]. \tag{3.4}$$

The bound obtained by two-to-infinity norm methods in Eq. (3.4) is demonstrably superior to the bound implied by Eq. (3.3) when $r^{1/2}(\log n)^{\xi}\|\mathbf{U}\|_{2\to\infty} \to 0$ as $n \to \infty$, namely when $\|\mathbf{U}\|_{2\to\infty} \to 0$ sufficiently quickly. Such behavior arises both in theory and in applications, including under the guise of eigenvector delocalization (Erdős

et al., 2013; Rudelson and Vershynin, 2015) and of subspace basis coherence (Candès and Recht, 2009).

The proof of Theorem 19 first proceeds by way of refined deterministic matrix decompositions and then subsequently leverages the aforementioned probabilistic concentration assumptions. Our proof framework further permits second-order analysis, culminating in Theorem 21 in Section 3.2.2. In the process of proving Theorem 21 we also prove Theorem 20, an extension and refinement of Theorem 19. Proof details are provided Section 6.2.

Theorem 20. *Suppose that Assumptions 1–4 hold and that Eq. (3.2) holds for k up to $k(n)+1$. Suppose $n\rho_n = \omega\{(\log n)^{2\xi}\}$ and $r^{1/2} \leq (\log n)^{\xi}$. Then there exists $\mathbf{W} \equiv \mathbf{W}_n \in \mathbb{O}_r$ such that*

$$\widehat{\mathbf{U}} - \mathbf{U}\mathbf{W} = \mathbf{E}\mathbf{U}\mathbf{\Lambda}^{-1}\mathbf{W} + \mathbf{R} \tag{3.5}$$

for some matrix $\mathbf{R} \in \mathbb{R}^{n\times r}$ satisfying

$$\|\mathbf{R}\|_{2\to\infty} = O_{\mathbb{P}}\left[(n\rho_n)^{-1} \times r \times \max\left\{(\log n)^{2\xi}, \|\mathbf{U}^\top\mathbf{E}\mathbf{U}\|_2 + 1\right\} \times \|\mathbf{U}\|_{2\to\infty}\right].$$

Moreover,

$$\|\mathbf{E}\mathbf{U}\mathbf{\Lambda}^{-1}\mathbf{W}\|_{2\to\infty} = O_{\mathbb{P}}\left\{(n\rho_n)^{-1/2} \times r^{1/2}(\log n)^{\xi}\|\mathbf{U}\|_{2\to\infty}\right\}.$$

Theorem 20 provides a collective eigenvector (i.e., subspace) characterization of the relationship between the leading eigenvectors of $\mathbf{M}$ and $\widehat{\mathbf{M}}$ via the perturbation $\mathbf{E}$, summarized as

$$\widehat{\mathbf{U}} \approx \widehat{\mathbf{M}}\mathbf{U}\mathbf{\Lambda}^{-1}\mathbf{W} = \mathbf{U}\mathbf{W} + \mathbf{E}\mathbf{U}\mathbf{\Lambda}^{-1}\mathbf{W}.$$

The unperturbed eigenvectors satisfy $\mathbf{U}\mathbf{W} \equiv \mathbf{M}\mathbf{U}\mathbf{\Lambda}^{-1}\mathbf{W}$, leading to the striking observation that the eigenvector perturbation characterization is approximately linear in the perturbation $\mathbf{E}$.

Remark 8. It always holds that $\|\mathbf{U}^\top\mathbf{E}\mathbf{U}\|_2 \leq \|\mathbf{E}\|_2$, where "$\leq$" can be replaced by "$\ll$" upon invoking Hoeffding-type concentration or more generally (C, c, γ) *concentration* for suitable choices of $\mathbf{E}$ (O'Rourke et al., 2018). Moreover, $\|\mathbf{R}\|_{2\to\infty} \ll \|\mathbf{E}\mathbf{U}\mathbf{\Lambda}^{-1}\mathbf{W}\|_{2\to\infty}$ holds with high probability in Theorem 20 for numerous regimes in which $n\rho_n \to \infty$ and $\|\mathbf{U}\|_{2\to\infty} \to 0$.

Remark 9. Strictly speaking, Eq. (3.3) holds even when the leading eigenvalues of $\mathbf{M}$ are not of the same order of magnitude, for the bound is fundamentally given by $C\|\mathbf{E}\|(|\mathbf{\Lambda}_{r,r}| - \|\mathbf{\Lambda}_\perp\|_2)^{-1}$. Similarly, the first-order bounds in this chapter still hold for $\mathbf{\Lambda}_\perp \neq 0$ provided $\|\mathbf{\Lambda}_\perp\|_2$ is sufficiently small, in which case naïve analysis introduces additional terms of the form $\|\mathbf{\Lambda}_\perp\|_2\|\mathbf{\Lambda}^{-1}\|_2\|\sin\mathbf{\Theta}(\widehat{\mathbf{U}}, \mathbf{U})\|_2$. In practice the exact spike dimension may be unknown, though it can often be consistently estimated via the "elbow in the scree plot" approach (Zhu and Ghodsi, 2006) provided $\|\mathbf{E}\|_2$ is sufficiently small relative to the leading nonzero eigenvalues of $\mathbf{M}$.

3.2.2 Second-order limit theory (fluctuations)

This section specifies additional structure on $\mathbf{M}$ and $\mathbf{E}$ for the purpose of establishing second-order limit theory. Here, $\mathbf{M}$ is assumed to have strictly positive leading eigenvalues, reminiscent of a spike covariance or kernel population matrix setting. It is possible though more involved to obtain similar second-order results when $\mathbf{M}$ is allowed to have both strictly positive and strictly negative leading eigenvalues of the same order. Specifically, such modifications would give rise to considerations involving structured orthogonal matrices and the indefinite orthogonal group.

Assumption 5. Suppose that $\mathbf{M}$ can be written as $\mathbf{M} \equiv \rho_n \mathbf{X}\mathbf{X}^\top \equiv \mathbf{U}\mathbf{\Lambda}\mathbf{U}^\top$ with $\mathbf{X} = [X_1|\ldots|X_n]^\top \in \mathbb{R}^{n\times r}$ and $(n^{-1}\mathbf{X}^\top\mathbf{X}) \to \mathbf{\Xi} \in \mathbb{R}^{r\times r}$ as $n \to \infty$ for some symmetric invertible matrix $\mathbf{\Xi}$. Also suppose that for a fixed index i, the scaled i-th row of $\mathbf{EX}$, written as $(n\rho_n)^{-1/2}(\mathbf{EX})_i = (n\rho_n)^{-1/2}(\sum_{j=1}^n \mathbf{E}_{ij}X_j)$, converges in distribution to a centered multivariate normal random vector $Y_i \in \mathbb{R}^r$ with second moment matrix $\mathbf{\Gamma}_i \in \mathbb{R}^{r\times r}$.

Theorem 21. *Suppose that Assumptions 1–5 hold and that Eq. (3.2) holds for k up to $k(n)+1$. Suppose in addition that $n\rho_n = \omega\{(\log n)^{2\xi}\}$, $r^{1/2} \le (\log n)^{\xi}$, and*

$$\rho_n^{-1/2} \times r \times \max\left\{(\log n)^{2\xi}, \|\mathbf{U}^\top\mathbf{E}\mathbf{U}\|_2 + 1\right\} \times \|\mathbf{U}\|_{2\to\infty} \to 0 \tag{3.6}$$

in probability as $n \to \infty$. Let $\widehat{\mathbf{U}}_i$ and $\mathbf{U}_i$ be column vectors denoting the i-th rows of $\widehat{\mathbf{U}}$ and $\mathbf{U}$, respectively. Then there exist sequences of orthogonal matrices $(\mathbf{W})$ and

($\mathbf{W}_{\mathbf{X}}$) *depending on* n *such that the random vector* $n\rho_n^{1/2}\mathbf{W}_{\mathbf{X}}^\top(\mathbf{W}\widehat{\mathbf{U}}_i - \mathbf{U}_i)$ *converges in distribution to a centered multivariate normal random vector with covariance matrix* $\mathbf{\Sigma}_i = \mathbf{\Xi}^{-3/2}\mathbf{\Gamma}_i\mathbf{\Xi}^{-3/2}$, *i.e.*

$$n\rho_n^{1/2}\mathbf{W}_{\mathbf{X}}^\top\left(\mathbf{W}\widehat{\mathbf{U}}_i - \mathbf{U}_i\right) \Rightarrow \mathcal{N}_r(\mathbf{0}, \mathbf{\Sigma}_i). \tag{3.7}$$

Equation (3.6) amounts to a mild regularity condition ensuring $n\rho_n^{1/2}\|\mathbf{R}\|_{2\to\infty} \to 0$ in probability for $\mathbf{R} \equiv \mathbf{R}_n \in \mathbb{R}^{n\times r}$ as in Theorem 20. This condition holds, for example, when $\|\mathbf{U}\|_{2\to\infty} = O\{(\log n)^{c_3} n^{-1/2}\}$, in which case the left-hand side of Eq. (3.6) can often be shown to behave as $O_{\mathbb{P}}\{(\log n)^{c_4}(n\rho_n)^{-1/2}\}$ where $(\log n)^{c_4}(n\rho_n)^{-1/2} \to 0$ as $n \to \infty$. Such bounds on $\|\mathbf{U}\|_{2\to\infty}$ arise when $(\max_i \|X_i\|_2)/(\min_i \|X_i\|_2)$ is at most polylogarithmic in n.

Remark 10 (Example: matrix $\mathbf{M}$ with kernel-type structure)**.** Let F be a probability distribution defined on $\mathcal{X} \subseteq \mathbb{R}^r$, and let $X_1, \ldots, X_n \sim F$ be independent random vectors with invertible second moment matrix $\mathbf{\Xi} \in \mathbb{R}^{r\times r}$. For $\mathbf{X} = [X_1|\ldots|X_n]^\top \in \mathbb{R}^{n\times r}$, let $\mathbf{M} = \rho_n\mathbf{X}\mathbf{X}^\top \equiv \mathbf{U}\mathbf{\Lambda}\mathbf{U}^\top$, so for each n there exists an $r\times r$ orthogonal matrix $\mathbf{W}_{\mathbf{X}}$ such that $\rho_n^{1/2}\mathbf{X} = \mathbf{U}\mathbf{\Lambda}^{1/2}\mathbf{W}_{\mathbf{X}}$. The strong law of large numbers guarantees that $(n^{-1}\mathbf{X}^\top\mathbf{X}) \to \mathbf{\Xi}$ almost surely as $n \to \infty$, and so $\mathbf{M}$ has r eigenvalues of order $\Theta(n\rho_n)$ asymptotically almost surely. Moreover, $\|\mathbf{U}\|_{2\to\infty} \le Cn^{-1/2}\|\mathbf{X}\|_{2\to\infty}$ asymptotically almost surely for some constant $C > 0$, where $\|\mathbf{X}\|_{2\to\infty}$ can be suitably controlled by imposing additional assumptions, such as taking $\mathcal{X}$ to be bounded or imposing

moment assumptions on $\|X_1\|_2$. Conditioning on $\mathbf{X}$ yields a deterministic choice of $\mathbf{M}$ for the purposes of Assumption 5.

Remark 11 (Example: matrix $\mathbf{E}$ and multivariate normality)**.** To continue the discussion from Remark 10, let all the entries of $\mathbf{E}$ be centered and independent up to symmetry with common variance $\sigma_{\mathbf{E}}^2 > 0$. Then, by the classical multivariate central limit theorem, the asymptotic normality condition in Assumption 5 holds and $n\rho_n^{1/2}\mathbf{W}_{\mathbf{X}}^\top(\mathbf{W}\widehat{\mathbf{U}}_i - \mathbf{U}_i) \Rightarrow \mathcal{N}_r(\mathbf{0}, \sigma_{\mathbf{E}}^2\boldsymbol{\Xi}^{-2})$ by Theorem 21. There are a variety of other regimes in which the multivariate central limit theorem can be invoked for $(n\rho_n)^{-1/2}(\sum_{j=1}^n \mathbf{E}_{ij}X_j)$ in order to satisfy the normality condition in Assumption 5, including when the entries of $\mathbf{E}$ have heterogeneous variances. In practice, we remark that Assumption 5 is structurally milder than Assumption 4 with respect to $\mathbf{E}$.

3.3 Simulation examples

3.3.1 Stochastic block models

The K-block stochastic block model (Holland et al., 1983) is a simple yet ubiquitous random graph model in which vertices are assigned to one of K possible communities (blocks) and where the adjacency of any two vertices is conditionally independent given the two vertices' community memberships. For stochastic block model graphs on n vertices, the binary symmetric adjacency matrix $\mathbf{A} \in \{0,1\}^{n\times n}$ can be

viewed as an additive perturbation of a (low rank) population edge probability matrix $\mathbf{P} \in [0,1]^{n \times n}$, $\mathbf{A} = \mathbf{P} + \mathbf{E}$, where for K-block model graphs the matrix $\mathbf{P}$ corresponds to an appropriate dilation of the block edge probability matrix $\mathbf{B} \in [0,1]^{K \times K}$. In the language of this chapter, $\widehat{\mathbf{M}} = \mathbf{A}$ and $\mathbf{M} = \mathbf{P}$. It can be verified that versions of the aforementioned assumptions and hypotheses hold for the following examples. Here we set $\rho_n \equiv 1$.

Consider n-vertex graphs arising from the three-block stochastic block model with equal block sizes where the within-block and between-block Bernoulli edge probabilities are given by $\mathbf{B}_{i,i} = 0.5$ for $i = 1, 2, 3$ and $\mathbf{B}_{i,j} = 0.3$ for $i \neq j$, respectively. Here $\operatorname{rank}(\mathbf{M}) = 3$, and the second-largest eigenvalue of $\mathbf{M}$ has multiplicity two. Figure 3.1 (left) plots the empirical mean and 95% empirical confidence interval for $\|\widehat{\mathbf{U}} - \mathbf{U}\mathbf{W}\|_{2 \to \infty}$ computed from 100 independent simulated adjacency matrices for each value of n. Figure 3.1 (left) also plots the function $\phi(n) = \{\lambda_3^{-1/2}(\mathbf{M})\}(\log n) n^{-1/2}$ which for large n captures the behavior of the leading order term in Theorem 20. This illustration does not pursue optimal constants or logarithmic factors. Here $\lambda_3(\mathbf{M}) = \Theta(n\rho_n) = \Theta\{(n\rho_n)^{1/2}\lambda\}$ with respect to λ at the end of Section 3.1.

Figure 3.1 (right) shows a scatter plot of the (uncentered, block-conditional) scaled leading eigenvector components for an $n = 200$ vertex graph arising from a two-block model with 40% of the vertices belonging to the first block and where the block edge probability matrix $\mathbf{B}$ has entries $\mathbf{B}_{1,1} = 0.5$, $\mathbf{B}_{1,2} = \mathbf{B}_{2,1} = 0.3$, and $\mathbf{B}_{2,2} = 0.3$. This

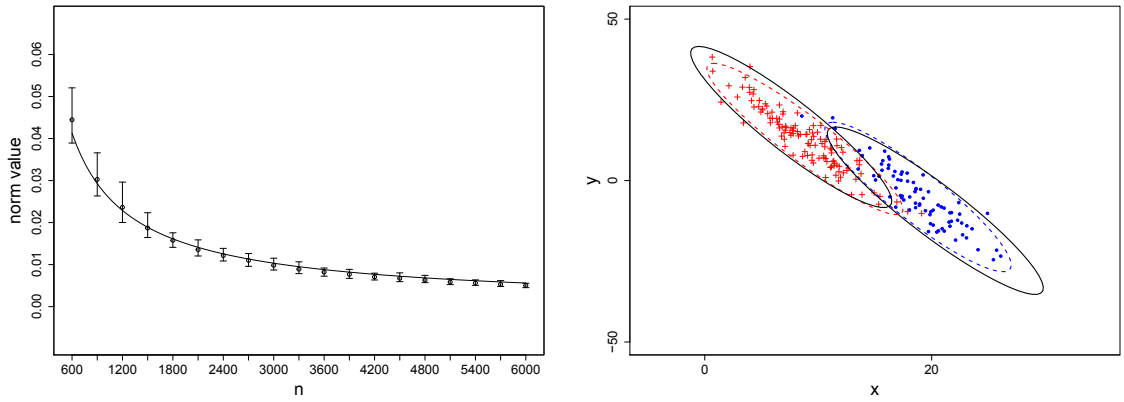

Figure 3.1: (Left plot) First-order simulations for the three-block model with number of vertices n on the x-axis and values of $\|\widehat{\mathbf{U}}-\mathbf{U}\mathbf{W}\|_{2\to\infty}$ on the y-axis. Vertical bars depict 95% empirical confidence intervals, and the solid line reflects Theorem 20. (Right plot) Second-order simulations for the two-block model with $n = 200$ where point shape reflects the block membership of the corresponding vertices. Dashed ellipses give the 95% level curves for the empirical distributions. Solid ellipses give the 95% level curves for the theoretical distributions according to Theorem 21.

small-n example is complemented by additional simulation results provided below. Table 3.1 shows block-conditional sample covariance matrix estimates for the centered random vectors $n\rho_n^{1/2}\mathbf{W}_{\mathbf{X}}^{\top}(\mathbf{W}\widehat{\mathbf{U}}_i - \mathbf{U}_i)$. Also shown are the corresponding theoretical covariance matrices.

We remark that the normalized random (row) vectors are jointly dependent but with decaying pairwise correlations; rows within any fixed finite collection are provably asymptotically independent as $n \to \infty$.

Table 3.1: SBM example: empirical and theoretical covariance matrices

n	1000	2000	∞
$\widehat{\mathbf{\Sigma}}_1$	$\begin{bmatrix} 14.11 & -36.08 \\ -36.08 & 110.13 \end{bmatrix}$	$\begin{bmatrix} 14.94 & -36.85 \\ -36.85 & 108.55 \end{bmatrix}$	$\begin{bmatrix} 15.14 & -38.05 \\ -38.05 & 112.34 \end{bmatrix}$
$\widehat{\mathbf{\Sigma}}_2$	$\begin{bmatrix} 11.76 & -30.09 \\ -30.09 & 93.07 \end{bmatrix}$	$\begin{bmatrix} 12.91 & -33.04 \\ -33.04 & 101.64 \end{bmatrix}$	$\begin{bmatrix} 13.12 & -33.93 \\ -33.93 & 103.94 \end{bmatrix}$

3.3.2 Spiked matrix models

Figure 3.2 provides two additional examples illustrating Theorem 21 for one and two-dimensional spiked matrix models, written in the rescaled form $\widehat{\mathbf{M}} = \lambda \mathbf{U}\mathbf{U}^\top + \mathbf{E}$ with $\rho_n \equiv 1$. In the left plot, $\lambda = n$, $\mathbf{U} = n^{-1/2}\mathbf{e} \in \mathbb{R}^n$, and $\mathbf{E}_{ij} \sim \text{Laplace}(0, 2^{-1/2})$ independently for $i \leq j$ with $\mathbf{E}_{ij} = \mathbf{E}_{ji}$. Here $\mathbf{\Xi}$ is the one-dimensional identity matrix, i.e. $\mathbf{\Xi} = \mathbf{I}_1$, and $(n\rho_n)^{-1/2}(\mathbf{E}\mathbf{X})_i \Rightarrow \mathcal{N}_1(0,1)$ by the central limit theorem, so for each fixed row i Theorem 21 yields convergence in distribution to $\mathcal{N}_1(0,1)$. In the right plot, $\lambda = n$ and $\mathbf{U}_{ij} = n^{-1/2}$ for $1 \leq i \leq n, j = 1$, $1 \leq i \leq n/2, j = 2$ with $\mathbf{U}_{ij} = -n^{-1/2}$ otherwise. In addition, $\mathbf{E}_{ij} \sim \text{Uniform}[-1,1]$ independently for $i \leq j$ with $\mathbf{E}_{ij} = \mathbf{E}_{ji}$, so $\text{Var}(\mathbf{E}_{ij}) = 1/3$. Here $(n\rho_n)^{-1/2}(\mathbf{E}\mathbf{X})_i$ converges in distribution to a centered multivariate normal random variable with covariance matrix $\mathbf{\Gamma}_i = (1/3)\mathbf{I}_2 \in \mathbb{R}^{2\times 2}$ by the multivariate central limit theorem, while the second moment matrix for the rows X_i in Assumption 5 is simply $\mathbf{\Xi} = \mathbf{I}_2$. Theorem 21 therefore yields $n\rho_n^{1/2}\mathbf{W}_\mathbf{X}^\top(\mathbf{W}\widehat{\mathbf{U}}_i - \mathbf{U}_i) \Rightarrow \mathcal{N}_2(\boldsymbol{\mu}, \mathbf{\Sigma}_i)$, where $\boldsymbol{\mu} = (0,0)^\top \in \mathbb{R}^2$ and $\mathbf{\Sigma}_i = (1/3)\mathbf{I}_2 \in \mathbb{R}^{2\times 2}$. Plots depict all vectors computed from a single simulated adjacency matrix.

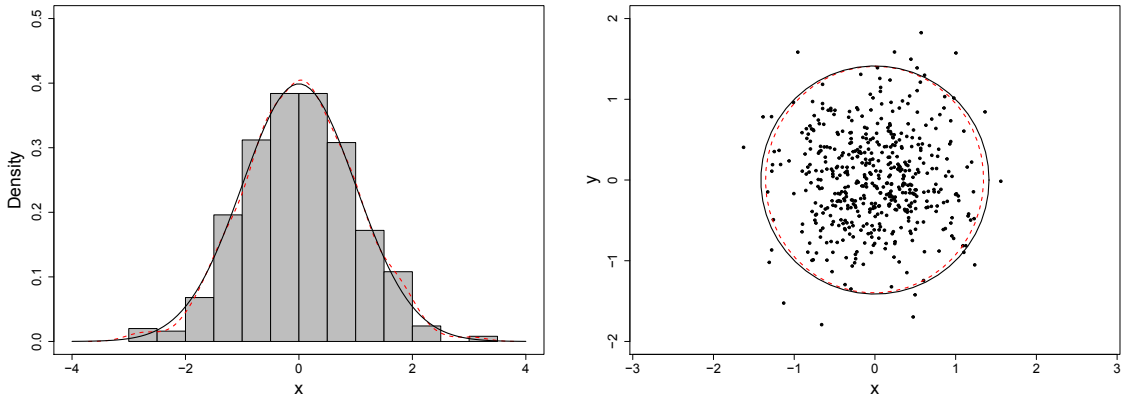

Figure 3.2: (Left plot) One-dimensional simulation for $n = 500$ with empirical (dashed line) and theoretical (solid line) eigenvector fluctuation density. (Right plot) Two-dimensional simulation for $n = 500$ where the dashed ellipse gives the 95% level curve for the empirical distribution, and the solid ellipse gives the 95% level curve for the row-wise theoretical distribution.

Chapter 4

Eigenvalue concentration and graph inference

4.1 Overview of Chapter 4

Eigenvalues and eigenvectors are structurally fundamental quantities associated with matrices and are widely studied throughout mathematics, statistics, and engineering disciplines. For example, given an observed graph, the eigenvalues and eigenvectors of associated matrix representations, such as the adjacency matrix or Laplacian matrix, encode structural information about the graph (e.g., community structure, connectivity (Chung, 1997)). In the context of certain random graph models, the eigenvalues and eigenvectors associated with the underlying matrix-valued model parameter, the edge probability matrix, exhibit similar information. It is

therefore natural to study how "close" the eigenvalues and eigenvectors of a graph are to the underlying model quantities.

In this chapter we consider simple, undirected random graphs on n vertices generated via the *inhomogeneous Erdős–Rényi model* (IERM) (Bollobás et al., 2007; Hoff et al., 2002), $\mathbb{G}(n, \mathbf{P})$, where $\mathbf{P} := (\mathbf{P}_{ij}) \in [0,1]^{n \times n}$ denotes the (symmetric) edge probability matrix. This independent edge model generalizes numerous widely-studied random graph models including the classical Erdős–Rényi model (Erdős and Rényi, 1959), the stochastic block model (Holland et al., 1983), and the random dot product graph model (Nickel, 2006; Young and Scheinerman, 2007). For $G \sim \mathbb{G}(n, \mathbf{P})$, the (symmetric) adjacency matrix, $\mathbf{A} \equiv \mathbf{A}_G \in \{0,1\}^{n \times n}$, has entries that are independently distributed according to $\mathbf{A}_{ij} \sim \text{Bernoulli}(\mathbf{P}_{ij})$ for all $i \leq j$. This yields $\mathbf{P} \equiv \mathbb{E}[\mathbf{A}]$, where $\mathbb{E}[\cdot]$ denotes probabilistic expectation.

We focus our attention on the eigenvalues of $\mathbf{A}$ and $\mathbf{P}$. Specifically, we consider the eigenvalues in pairs (e.g., the largest eigenvalues of $\mathbf{A}$ and of $\mathbf{P}$ form a pair, as do the second-largest eigenvalues of each matrix, etc.). We obtain bounds on the distance between eigenvalues in certain "signal pairs", thereby and therein demonstrating a local sense in which random graphs concentrate. Note that in the random graph literature, the term *concentration* is primarily used to describe global, uniform behavior via the spectral norm quantity $\|\mathbf{A} - \mathbb{E}[\mathbf{A}]\|_2$.

The following description provides an overview of our results for the IERM setting. Given a collection of consecutive, ordered eigenvalues of $\mathbf{P}$ which are sufficiently

separated from the remainder of the spectrum and conditional on that the corresponding eigenvalues of $\mathbf{A}$ are not near the remainder of the spectrum of either $\mathbf{A}$ or $\mathbf{P}$, then Theorems 26 and 27 yield high-probability bounds on the distances between the eigenvalues in each pair. The individual, pair-specific (i.e., local) bounds we obtain stand in contrast to weaker bounds which hold uniformly for all eigenvalue pairs (e.g., bounds implied by Weyl's inequality (Horn and Johnson, 2012)). Our results hold even in the presence of eigenvalue multiplicity.

We demonstrate that when the matrix $\mathbf{P}$ has low rank, our results compare favorably with the recent study of low rank matrices undergoing random perturbation in O'Rourke et al. (2018) (e.g., see our Example 1). We also demonstrate that our results can lead to meaningful estimation in high rank settings (e.g., see our Example 2).

After presenting our main theoretical results, we then apply the theory in this chapter to both hypothesis testing and change-point detection for random graphs. Moreover, we generalize our results beyond the IERM setting to obtain high-probability bounds for perturbations of singular values of rectangular matrices in a quite general random matrix noise setting.

Broadly speaking, we adapt the original, deterministic setting in a paper by T. Kato (Kato, 1950) to a new setting involving randomness, and this approach is novel in the context of random graphs, random matrix theory, and statistical inference for random graphs. We further detail the key modifications and differences between our work and Kato (1950) in our subsequent remarks and proofs. The present

chapter also stands in contrast to a deterministic generalization of the Kato–Temple inequality in Harrell (1978).

4.1.1 Inhomogeneous random graphs

In the inhomogeneous random graph literature, concentration bounds have been known for some time for each eigenvalue of $\mathbf{A}$, denoted $\lambda_i(\mathbf{A})$, both around its median and around its expectation, $\mathbb{E}[\lambda_i(\mathbf{A})]$ (Alon et al., 2002). Unfortunately, since the latter quantities are inaccessible in practice, such bounds are of limited practical use. Moreover, in general $\mathbb{E}[\lambda_i(\mathbf{A})] \neq \lambda_i(\mathbb{E}[\mathbf{A}])$.

By way of contrast, numerous results in the literature bound the spectral norm matrix difference $\|\mathbf{A} - \mathbb{E}[\mathbf{A}]\|_2$, thereby immediately and uniformly bounding each of the eigenvalue differences $|\lambda_i(\mathbf{A}) - \lambda_i(\mathbb{E}[\mathbf{A}])|$ via an application of Weyl's inequality. For example, Oliveira (2010) proved an asymptotically almost surely spectral norm bound of $\|\mathbf{A} - \mathbb{E}[\mathbf{A}]\|_2 = O(\sqrt{\Delta \log n})$ for $\Delta = \Omega(\log(n))$ where $\Delta \equiv \Delta(n)$ denotes the maximum expected degree of a graph. In Lu and Peng (2013) the above bound is improved to $\|\mathbf{A} - \mathbb{E}[\mathbf{A}]\|_2 \leq (2 + o(1))\sqrt{\Delta}$ under the stronger assumption that $\Delta = \omega(\log^4 n)$ with further refinement being subsequently obtained in Lei and Rinaldo (2015). We on the other hand show that under certain conditions, for particular eigenvalue pairs, one can obtain tighter and non-uniform high probability bounds of the form $|\lambda_i(\mathbf{A}) - \lambda_i(\mathbb{E}[\mathbf{A}])| = O(\log^{\delta} n)$ for small $\delta > 0$.

Spectral theory for random graphs overlaps with the random matrix theory liter-

ature. There, asymptotic analysis includes proving, for example, convergence of the empirical spectral distribution to a limiting measure (Ding and Jiang, 2010). Related approaches to studying the spectrum of random graphs consider normalized versions of the adjacency matrix (Le et al., 2017) and employ standard random matrix theory techniques such as the Stieltjes transform method (Avrachenkov et al., 2015; Zhang et al., 2014). In contrast, we do not study normalized versions of the adjacency or the edge probability matrix. In this chapter, our aim is to demonstrate the usefulness of adapting and applying the eigenvalue-centric Kato–Temple framework.

The stochastic block model (SBM) offers an example of an inhomogeneous random graph model which is wildly popular in the literature (Bickel and Sarkar, 2013; Karrer and Newman, 2011; Lei, 2016; Lei and Rinaldo, 2015; Zhao et al., 2012) and in which our results apply to the top (signal) eigenvalues of $\mathbf{A}$ and $\mathbf{P}$. Previously, the authors in Athreya et al. (2016) obtained a collective deviation bound on the top eigenvalues of $\mathbf{A}$ and $\mathbf{P}$ for certain stochastic block model graphs in order to prove the main limit theorem therein. Our Theorem 26 improves upon Lemma 2 in Athreya et al. (2016) by removing a distinct eigenvalue assumption and by obtaining stronger high-probability deviation bounds for pairs of top eigenvalues of $\mathbf{A}$ and $\mathbf{P}$ which are of the same order. This implies a statistical hypothesis testing regime for random graphs which is discussed further in Section 4.4.

The remainder of this chapter is organized as follows. In Section 4.2 we introduce notation and the Kato–Temple eigenvalue perturbation framework. In Section 4.3

we present our results for random graphs and more generally for matrix perturbation theory. There we also include illustrative examples together with comparative analysis involving recent results in the literature. In Section 4.4 we discuss applications to problems involving graph inference. Section 6.3 contains the proofs of our results.

4.2 Problem setup for eigenvalue concentration

Let $\langle \cdot, \cdot \rangle$ denote the standard Euclidean inner (dot) product between two vectors, $\| \cdot \|$ denote the vector norm induced by the dot product, and $\| \cdot \|_2$ denote the spectral norm of a matrix. The identity matrix is implicitly understood when we write the difference of a matrix with a scalar. In this chapter, $\mathcal{O}(\cdot)$, $\Omega(\cdot)$, and $\Theta(\cdot)$ denote standard big-O, big-Omega, and big-Theta notation, respectively, while $o(\cdot)$ and $\omega(\cdot)$ denote standard little-o and little-omega notation, respectively.

As prefaced in Section 4.1, we consider simple, undirected random graphs on n vertices generated by the inhomogeneous Erdős–Rényi model, $G \sim \mathbb{G}(n, \mathbf{P})$, via the corresponding (binary, symmetric) adjacency matrix $\mathbf{A} \equiv \mathbf{A}_G$. Given an open interval in the positive half of the real line, $(\alpha, \beta) \subset \mathbb{R}_{>0}$, we denote the d eigenvalues of $\mathbf{P}$ that lie in this interval (locally) by

$$\alpha < \lambda_1(\mathbf{P}) \leq \lambda_2(\mathbf{P}) \leq \cdots \leq \lambda_d(\mathbf{P}) < \beta, \tag{4.1}$$

and similarly for $\mathbf{A}$, noting that for $\mathbf{A}$ this amounts to a probabilistic statement. By symmetry one can handle the case when the interval lies in the negative half of the real line. We are principally interested in eigenvalues that are large in magnitude, so we do not consider the case when the underlying interval contains the origin.

To highlight the Kato–Temple framework for bounding eigenvalues, we now reproduce two lemmas from Kato (1950) along with the Kato–Temple inequality as stated in Harrell (1978) (see Theorem 24 below).[1] These results all hold in the following common setting.

> Let $\mathbf{H}$ be a self-adjoint operator on a Hilbert space. Assume a unit vector $\mathbf{w}$ is in the domain of $\mathbf{H}$ and define $\eta := \langle \mathbf{H}\mathbf{w}, \mathbf{w} \rangle$ along with $\epsilon := \|(\mathbf{H} - \eta\mathbf{I})\mathbf{w}\|$, noting that $\eta^2 + \epsilon^2 = \|\mathbf{H}\mathbf{w}\|^2$. The quantity η may be viewed as an "approximate eigenvalue" of $\mathbf{H}$ corresponding to the "approximate eigenvector" $\mathbf{w}$, while ϵ represents a scalar residual term.

Lemma 22 (Lemma 1 in Kato (1950))**.** *For every α such that $\alpha < \eta$ (where $\alpha = -\infty$ is permitted), the interval $(\alpha, \eta + \frac{\epsilon^2}{\eta - \alpha}]$ contains a point in the spectrum of $\mathbf{H}$.*

Lemma 23 (Lemma 2 in Kato (1950))**.** *For every β such that $\beta > \eta$ (where $\beta = \infty$ is permitted), the interval $[\eta - \frac{\epsilon^2}{\beta - \eta}, \beta)$ contains a point in the spectrum of H.*

Theorem 24 (Kato–Temple inequality; Theorem 2 in Harrell (1978))**.** *Suppose that $\epsilon^2 < (\beta - \eta)(\eta - \alpha)$ where $\alpha < \beta$. Then* spectrum$(\mathbf{H}) \cap (\alpha, \beta) \neq \emptyset$*. Moreover, if the*

[1] Of primary importance in this chapter is the extension of Theorem 24 to multiple eigenvalues as presented in Kato (1950). The original statement of the extension to multiple eigenvalues is more involved and therefore omitted for simplicity.

only point of the spectrum of $\mathbf{H}$ *in the interval* (α, β) *is the eigenvalue* $\lambda(\mathbf{H})$*, then*

$$-\frac{\epsilon^2}{\beta - \eta} \leq \lambda(\mathbf{H}) - \eta \leq \frac{\epsilon^2}{\eta - \alpha}.$$

Remark 12 (Hermitian dilation)**.** Given an $m \times n$ real matrix $\mathbf{M}$, it will be useful to consider the corresponding real symmetric $(m+n) \times (m+n)$ Hermitian dilation matrix $\tilde{\mathbf{M}}$ given by

$$\tilde{\mathbf{M}} := \begin{bmatrix} \mathbf{0} & \mathbf{M} \\ \mathbf{M}^\top & \mathbf{0} \end{bmatrix}.$$

It is well-known that the non-zero eigenvalues of $\tilde{\mathbf{M}}$ correspond to the signed singular values of $\mathbf{M}$ (see Theorem 7.3.3 in Horn and Johnson (2012)). This correspondence between the singular values of arbitrary matrices and the eigenvalues of Hermitian matrices allows our results to generalize beyond the IERM setting to the more general study of matrix perturbation theory for singular values in a straightforward manner.

4.3 Results for eigenvalue concentration

4.3.1 Results for random graphs

In the IERM setting, a graph's adjacency matrix can be written as $\mathbf{A} = \mathbf{P} + \mathbf{E}$ where $\mathbf{E} := \mathbf{A} - \mathbf{P}$ is a random matrix and $\mathbf{P}$ is the (deterministic) expectation of $\mathbf{A}$. We begin with a preliminary observation concerning the tail behavior of $\mathbf{A} - \mathbf{P}$ which

will subsequently be invoked for the purpose of obtaining standard union bounds. The proof follows from a straightforward application of Hoeffding's inequality.

Proposition 25 (General IERM concentration)**.** *Let* $\mathbf{u}, \mathbf{v} \in \mathbb{R}^n$ *denote (non-random) unit vectors. Then for any* $t > 0$*,*

$$\mathbb{P}[|\langle(\mathbf{A} - \mathbf{P})\mathbf{u}, \mathbf{v}\rangle| > t] \leq 2\exp(-t^2). \tag{4.2}$$

It is indeed possible to invoke more refined concentration inequalities than Proposition 25 in the presence of additional structure (e.g., when all entries of $\mathbf{P}$ have uniformly very small magnitude). Doing so is particularly useful when it is simultaneously possible to obtain a strong bound on $\|\mathbf{A} - \mathbf{P}\|_2$. This observation will be made clearer in the context of Theorem 26 below. Furthermore, consideration of Proposition 25 will facilitate the subsequent presentation of our generalized results which extend beyond the IERM setting.

Remark 13. In this chapter the main diagonal elements of $\mathbf{P}$ are allowed to be strictly positive, in which case realizations of $\mathbf{A}$ need not necessarily be hollow (i.e., observed graphs may have self-loops). To avoid graphs with self-loops, one may either condition on the event that $\mathbf{A}$ is hollow or set the main diagonal of $\mathbf{P}$ to be zero. In the former case, note that $\mathbf{P} \equiv \mathbb{E}[\mathbf{A}]$ no longer holds on the main diagonal. In the latter case, a modified version of Proposition 25 holds.

We now present our main results for the IERM setting. The proofs, which are

located in Section 6.3, also formulate a bound for the special case when the upper bound threshold β may be chosen to be infinity. This special case is particularly useful in applications.

Theorem 26 (IERM eigenvalue perturbation bounds, conditional version)**.** *Let the matrices* $\mathbf{A} \in \{0,1\}^{n\times n}$ *and* $\mathbf{P} \in [0,1]^{n\times n}$ *correspond to the IERM setting described in Section 4.2. Suppose the interval* $(\alpha, \beta) \subset \mathbb{R}_{>0}$ *contains precisely* d *eigenvalues of* $\mathbf{P}$*,* $\lambda_1(\mathbf{P}) \leq \lambda_2(\mathbf{P}) \leq \cdots \leq \lambda_d(\mathbf{P})$ *(possibly with multiplicity). Condition on the event that* (α, β) *contains precisely* d *eigenvalues of* $\mathbf{A}$*,* $\{\lambda_i(\mathbf{A})\}_{i=1}^d$*, as well as the set* $\{\langle \mathbf{A}\boldsymbol{w}_i, \boldsymbol{w}_i\rangle\}_{i=1}^d$ *where* $\{\boldsymbol{w}_i\}_{i=1}^d$ *is an orthonormal collection of eigenvectors of* $\mathbf{P}$ *corresponding to the eigenvalues* $\{\lambda_i(\mathbf{P})\}_{i=1}^d$*. Fix* $k \in [d]$*. Define* $l := (d-k+1)$*. Then, for* $t > 0$*,*

$$\lambda_k(\mathbf{A}) \geq \lambda_k(\mathbf{P}) - t - \zeta^-, \tag{4.3}$$

where $\zeta^- := \frac{l\|\mathbf{E}\|_2^2 + ((\beta - \lambda_k(\mathbf{P})) + (\lambda_d(\mathbf{P}) - \lambda_k(\mathbf{P})) + 3t)l(l-1)t}{\beta - \lambda_d(\mathbf{P}) - (l(l-1)+1)t}$ *holds with probability at least* $1 - \left(l + \binom{l}{2}\right) 2\exp(-t^2)$*. Also, for* $t > 0$*,*

$$\lambda_k(\mathbf{A}) \leq \lambda_k(\mathbf{P}) + t + \zeta^+, \tag{4.4}$$

where $\zeta^+ := \frac{k\|\mathbf{E}\|_2^2 + (3\lambda_k(\mathbf{P}) - \alpha + 3t)k(k-1)t}{\lambda_1(\mathbf{P}) - \alpha - (k(k-1)+1)t}$ *with probability at least* $1 - \left(k + \binom{k}{2}\right) 2\exp(-t^2)$*. Moreover, the upper and lower bounds hold collectively with probability at least* $1 - \left(d + \binom{d}{2}\right) 2\exp(-t^2)$*.*

Remark 14. Our proof depends upon several new observations with respect to Kato's original argument. In particular, for $\mathbf{w}_i$ as defined above, the matrix $[\langle \mathbf{A}\mathbf{w}_i, \mathbf{w}_j \rangle]_{i,j=1}^d$ need not be diagonal, so $\{\mathbf{w}_i\}_{i=1}^d$ need not constitute an orthonormal collection of "approximate eigenvectors" of $\mathbf{A}$ in the sense of Kato (1950). Instead, here the notion of "approximate" may be interpreted via Proposition 25 as the source of randomness which allows for Kato–Temple methodology to be adapted beyond the original deterministic setting. Of additional note is that the vectors $\mathbf{w}_i$ as defined in this chapter agree in function and notation with Kato's original paper, the operational distinction being that our setting provides a canonical choice for these vectors.

Remark 15. We note that the term $\|\mathbf{E}\|_2^2$ in the formulation of both ζ^+ and ζ^- can be replaced by an appropriate maximum over quantities of the form $\|\mathbf{E}\mathbf{w}_i\|^2$ (see Eq. (6.29)). That is to say, in the presence of additional local structure and knowledge, one can refine the above bounds in Theorem 26.

Remark 16. In settings wherein the eigenvalues of interest have disparate orders of magnitude, Kato–Temple methodology is not guaranteed to yield useful bounds. This can be seen in the bounds' dependence on the ratio of the eigenvalues of $\mathbf{P}$ in Theorem 26. Moreover, within the Kato–Temple framework, poor separation from the remainder of the spectrum also deteriorates the bounds, as is evident in the denominators' dependence on the interval endpoints α and β along with the smallest and largest local eigenvalues of $\mathbf{P}$. On the other hand, by further localizing, i.e. by restricting to a subset of $d' < d$ eigenvalues in a particular interval, applying

Theorem 26 to said fewer eigenvalue pairs may yield improved bounds (e.g., see Example 1 and Remark 15).

Next, we formulate an unconditional version of Theorem 26. For both simplicity and the purpose of applications, Theorem 27 is stated in terms of the largest singular values in the IERM setting.

Theorem 27 (IERM singular value perturbation bounds, unconditional version)**.** *Let the matrices* $\mathbf{A} \in \{0,1\}^{n\times n}$ *and* $\mathbf{P} \in [0,1]^{n\times n}$ *correspond to the IERM setting described in Section 4.2 with maximum expected degree (via* $\mathbf{P}$*) given by* $\Delta \equiv \Delta(n)$*. Denote the* $d+1$ *largest singular values of* $\mathbf{A}$ *by* $0 \le \hat{\sigma}_0 < \hat{\sigma}_1 \le \cdots \le \hat{\sigma}_d$*, and denote the* $d+1$ *largest singular values of* $\mathbf{P}$ *by* $0 \le \sigma_0 < \sigma_1 \le \cdots \le \sigma_d$*. Suppose that* $\Delta = \omega(\log^4 n)$*,* $\sigma_1 \ge C\Delta$*, and* $\sigma_0 \le c\Delta$ *for some absolute constants* $C > c > 0$*. Let* $\delta \in (0,1]$*. Then for each* $k \in [d]$*, there exists some positive constant* $c_{k,d}$ *such that as* $n \to \infty$*, with probability* $1 - o(1)$ *involving* δ*,*

$$|\hat{\sigma}_k - \sigma_k| \le c_{k,d}\left(\log^{\delta} n\right). \tag{4.5}$$

A similar version of Theorem 30 holds when $\Delta = \Omega(\log n)$ under slightly different assumptions on the entries of P for which one still has $\|\mathbf{A} - \mathbf{P}\|_2 = O(\sqrt{\Delta})$ with high probability (Lei and Rinaldo, 2015). On a related yet different note, see Le et al. (2017) for discussion of the sparsity regime $\Delta = O(1)$ in which graphs fail to concentrate in the classical sense.

Remark 17 (Random dot product graph model)**.** When the edge probability matrix $\mathbf{P}$ can be written as $\mathbf{P} = \mathbf{X}\mathbf{X}^\top$ for some matrix $\mathbf{X} \in \mathbb{R}^{n\times d}$ with $d \ll n$, then the IERM corresponds to the popular *random dot product graph (RDPG) model* (Young and Scheinerman, 2007). In the random dot product graph model, the largest eigenvalues of $\mathbf{A}$ and $\mathbf{P}$ are of statistical interest in that they represent spectral "signal" in the model. These eigenvalues are separated from the remainder of their respective spectra and lie in an interval of the form (α, ∞) where, for example, α may be taken to be $O(\|\mathbf{A} - \mathbf{P}\|_2)$.

Among its applications, the RDPG model has been used as a platform for modeling graphs with hierarchical and community structure (Lyzinski et al., 2017). A central limit theorem is known for the behavior of the top eigenvectors of adjacency matrices arising from the RDPG model (Athreya et al., 2016), and this limit theorem relies upon a lemma which collectively bounds the differences between top eigenvalues of $\mathbf{A}$ and $\mathbf{P}$ but requires a stringent eigengap assumption. Namely, Lemma 2 in Athreya et al. (2016) states that with high probability,

$$\sqrt{\sum_{i=1}^{d} |\lambda_i(\mathbf{A}) - \lambda_i(\mathbf{P})|^2} = O(\delta_{\text{gap}}^{-2} \log n). \tag{4.6}$$

In contrast, using Theorem 27 with $\sigma_0 := 0$, we do not require the gap assumption

$\delta_{\text{gap}} > 0$ and still obtain that with high probability,

$$\sqrt{\sum_{i=1}^{d} |\lambda_i(\mathbf{A}) - \lambda_i(\mathbf{P})|^2} = O(\log n). \tag{4.7}$$

In practice, models involving repeated or arbitrarily close eigenvalues are prevalent and of interest (e.g., Section 4.4.2). As such, the above improvement is nontrivial and of practical significance.

Remark 18 (Latent position random graphs)**.** Theorem 26 further extends to the more general setting of latent position random graphs. There, the matrix $\mathbf{P}$ is viewed as an operator $[\kappa(X_i, X_j)]_{i,j=1}^{n}$ where X_i and X_j are independent, identically distributed latent positions with distribution F, and the positive definite kernel, κ (viewed as an integral operator), is not necessarily of finite fixed rank as n increases (Hoff et al., 2002; Tang et al., 2013). Note that for the RDPG model, the kernel κ is simply the standard Euclidean inner product between (latent position) vectors.

4.3.2 Results for matrix perturbation theory

The behavior of the random matrix $\mathbf{A} - \mathbf{P}$ (i.e., see Proposition 25) represents a specific instance of more general, widely-encountered probabilistic concentration as discussed in O'Rourke et al. (2018) and formulated in the following definition (which previously appeared in Chapter 2).

Definition 28 ((C, c, γ) concentration (O'Rourke et al., 2018))**.** A $m \times n$ random matrix $\mathbf{E}$ is said to be (C, c, γ)-*concentrated* if, given a trio of positive constants (C, c, γ), for all unit vectors $\mathbf{u} \in \mathbb{R}^n$, $\mathbf{v} \in \mathbb{R}^m$, and for every $t > 0$,

$$\mathbb{P}\big[\big|\langle \mathbf{E}\mathbf{u}, \mathbf{v}\rangle\big| > t\big] \leq C \exp\big(-ct^{\gamma}\big). \tag{4.8}$$

In particular, the IERM setting corresponds to (C, c, γ) concentration where $m = n$, $C = \gamma = 2$, and $c = 1$. For the Hermitian dilation discussed in Remark 12, one has the following correspondence between $\mathbf{E}$ and $\tilde{\mathbf{E}}$.

Lemma 29 (O'Rourke et al. (2018))**.** *Let $\mathbf{E} \in \mathbb{R}^{m\times n}$ be (C, c, γ)-concentrated. Define $\tilde{C} := 2C$ and $\tilde{c} := c/2^{\gamma}$. Then the matrix $\tilde{\mathbf{E}} \in \mathbb{R}^{m+n\times m+n}$ is $(\tilde{C}, \tilde{c}, \gamma)$-concentrated.*

Definition 28 and Lemma 29 together with Remark 12 allow for Theorem 26 to be generalized in a straightforward manner. We frame the generalization in the context of a signal-plus-noise matrix model with tail probability bounds. In particular, replace $\mathbf{A}$ with $\widehat{\mathbf{M}} := \mathbf{M} + \mathbf{E}$, thought of as an observed data matrix. Also replace $\mathbf{P}$ with $\mathbf{M}$, thought of as an underlying signal matrix, so that the matrix $\mathbf{A} - \mathbf{P}$ becomes $\mathbf{E}$, thought of as an additive error matrix. We emphasize that the following generalization is in terms of the singular values of $\mathbf{M}$ and $\widehat{\mathbf{M}}$. This generalization resembles the formulation of a result obtained in O'Rourke et al. (2018) using different methods; however, unlike our Theorem 30, the bound in O'Rourke et al. (2018) depends upon the rank of $\mathbf{M}$ and assumes that the rank is known.

Given a matrix $\mathbf{M} \in \mathbb{R}^{m\times n}$, write its singular value decomposition as $\mathbf{M} \equiv \mathbf{U}\mathbf{\Sigma}\mathbf{V}^\top$ where $\mathbf{M}\mathbf{v}_i = \sigma_i \mathbf{u}_i$ holds for the normalized left (resp., right) singular vectors $\mathbf{v}_i$ (resp., $\mathbf{u}_i$) and singular values $\sigma_i = \mathbf{\Sigma}_{ii}$. For each i such that $\sigma_i > 0$, define $\tilde{\mathbf{w}}_i \in \mathbb{R}^{m+n}$ to be the concatenated unit vector $\mathbf{w}_i := \frac{1}{\sqrt{2}}(\mathbf{u}_i^\top, \mathbf{v}_i^\top)^\top$. Note that $\tilde{\mathbf{w}}_i$ is an eigenvector for $\tilde{\mathbf{M}}$ with $\tilde{\mathbf{M}}\tilde{\mathbf{w}}_i = \sigma_i \tilde{\mathbf{w}}_i$.

Theorem 30 (Singular value perturbation bounds, conditional version)**.** *For matrices $\mathbf{M}, \mathbf{E} \in \mathbb{R}^{m\times n}$ and $\widehat{\mathbf{M}} := \mathbf{M} + \mathbf{E}$, suppose that $\mathbf{E}$ is (C, c, γ)-concentrated for positive constants $C, c, \gamma > 0$. Suppose the interval $(\alpha, \beta) \subset \mathbb{R}_{>0}$ contains the largest d singular values of $\mathbf{M}$, denoted by $0 < \sigma_1 \le \sigma_2 \le \cdots \le \sigma_d$. Condition on the event that the interval (α, β) contains precisely d singular values of $\widehat{\mathbf{M}}$, denoted $0 < \hat{\sigma}_1 \le \hat{\sigma}_2 \le \cdots \le \hat{\sigma}_d$, as well as $\langle \widehat{\tilde{\mathbf{M}}}\tilde{\boldsymbol{w}}_i, \tilde{\boldsymbol{w}}_i\rangle$ for $1 \le i \le d$ and unit vector $\tilde{\boldsymbol{w}}_i$ as defined above. Fix $k \in [d]$. Define $l := (d - k + 1)$. Then for $t > 0$,*

$$\hat{\sigma}_k \ge \sigma_k - t - \zeta^-, \tag{4.9}$$

where $\zeta^- := \frac{l\|\mathbf{E}\|_2^2 + ((\beta-\sigma_k)+(\sigma_d-\sigma_k)+3t)l(l-1)t}{\beta-\sigma_d-(l(l-1)+1)t}$ with probability at least $1 - \left(l + \binom{l}{2}\right)\tilde{C}\exp(-\tilde{c}t^\gamma)$. Also, for $t > 0$,

$$\hat{\sigma}_k \le \sigma_k + t + \zeta^+, \tag{4.10}$$

where $\zeta^+ := \frac{k\|\mathbf{E}\|_2^2 + (3\sigma_k-\alpha+3t)k(k-1)t}{\sigma_1-\alpha-(k(k-1)+1)t}$ with probability at least $1 - \left(k + \binom{k}{2}\right)\tilde{C}\exp(-\tilde{c}t^\gamma)$. Moreover, the upper and lower bound hold collectively with

probability at least $1 - \left(d + \binom{d}{2}\right) \tilde{C} \exp(-\tilde{c}t^{\gamma})$.

As with the results in Section 4.3.1, Theorem 30 can be formulated unconditionally and for collections of not–necessarily–the–largest singular values. Both of these aspects are explored in greater detail in Example 2. The following technical lemma will subsequently be employed in applications.

Lemma 31. *Let* $\mathbf{E} \in \mathbb{R}^{m \times n}$ *be a* (C, c, γ)*-concentrated random matrix. Choose* $\epsilon > 0$ *such that* $2 + \epsilon > 2\,(2\log(9)/c)^{1/\gamma}$. *Define* $c_{\epsilon,c,\gamma} := (c(1+\epsilon/2)^{\gamma} - 2\log(9)) > 0$. *Then,*

$$\mathbb{P}\left[\|\mathbf{E}\|_2 > (2+\epsilon)\max\{m,n\}^{1/\gamma}\right] \leq C\exp(-c_{\epsilon,c,\gamma}\max\{m,n\}). \tag{4.11}$$

If in addition $m = n$ *and* $\mathbf{E}$ *is assumed to be symmetric, then the quantity* $2\log(9)$ *above may be replaced by* $\log(9)$*, an improvement.*

4.3.3 Two illustrative examples

In the remainder of this section, we present two examples that highlight the usefulness and flexibility of Kato–Temple methodology. We begin with Example 1 which presents a simple stochastic block model setting wherein our results compare favorably with those in the recent work of O'Rourke et al. (2018), noting that in general for similar settings, the corresponding results are often comparable.

Example 1 (Balanced affinity two block stochastic block model)**.** Consider an n vertex realization from a two block stochastic block model in which $0 < q < p < 1$ where

p and q denote the within–block and between–block edge probabilities, respectively. Suppose each block contains $n/2$ of the graph's vertices. The signal singular values and maximum expected degree of this rank two model are given by

$$\sigma_1(\mathbf{P}) = \frac{n}{2}(p-q), \sigma_2(\mathbf{P}) = \frac{n}{2}(p+q), \text{ and } \Delta = \sigma_2(\mathbf{P}). \tag{4.12}$$

For the purposes of large n comparison, view $\|\mathbf{E}\|_2 \approx 2\sqrt{\Delta}$ from Lu and Peng (2013) and set the lower threshold α to be $\|\mathbf{E}\|_2$. Define $r_{p,q}$ to be the edge probability-dependent parameter $r_{p,q} := (p+q)/(p-q)$. Then via Kato–Temple methodology applied jointly to $\sigma_1(\mathbf{P})$ and $\sigma_2(\mathbf{P})$, with probability approximately 0.99 when $t_{KT} \geq 2.55$, for each singular value, respectively,

$$-3t_{KT} \leq \hat{\sigma}_1(\mathbf{A}) - \sigma_1(\mathbf{P}) \leq 4r_{p,q} + t_{KT},$$
$$-t_{KT} \leq \hat{\sigma}_2(\mathbf{A}) - \sigma_2(\mathbf{P}) \leq (8+6t)r_{p,q} + t_{KT}.$$

By the same approach, the bounds obtained in O'Rourke et al. (2018) are given by

$$-t_{OVW} \leq \hat{\sigma}_1(\mathbf{A}) - \sigma_1(\mathbf{P}) \leq 8\sqrt{2}r_{p,q} + \sqrt{2}t_{OVW},$$
$$-t_{OVW} \leq \hat{\sigma}_2(\mathbf{A}) - \sigma_2(\mathbf{P}) \leq 8 + \sqrt{2}t_{OVW}.$$

Direct application of the results in O'Rourke et al. (2018) yields probability approximately at least 0.99 for $t_{OVW} \geq 11.6$, though it appears upon further inspection

that this can be improved to, for example, $t_{OVW} \geq 5.6$. The above joint analysis demonstrates that our bounds are favorable for the pair $\{\hat{\sigma}_1(\mathbf{A}), \sigma_1(\mathbf{P})\}$ whereas the opposite is true for the pair $\{\hat{\sigma}_2(\mathbf{A}), \sigma_2(\mathbf{P})\}$.

We emphasize that here the upper bounds are of primary importance and interest. Indeed, the (C, c, γ) property allows for straightforward lower bounds to be obtained by epsilon net techniques together with the Courant–Fisher–Weyl min-max principle. For example, note that a single application of (C, c, γ)-concentration yields that $\hat{\sigma}_2(\mathbf{A}) - \sigma_2(\mathbf{P}) \geq -t$ with probability at least $1 - C\exp(-ct^{\gamma})$.

Among the advantages of Kato–Temple methodology is the ability to, in certain cases, refine one's initial analysis by further localizing the underlying interval (α, β). This is possible in the current example wherein we can "zoom in" further on the largest signal singular value. In particular, keeping the same indexing as above and setting α to be $\|\mathbf{E}\|_2 + \sigma_1(\mathbf{P})$, then for n large and with probability approximately 0.99, we have

$$-t_{KT} \leq \hat{\sigma}_2(\mathbf{A}) - \sigma_2(\mathbf{P}) \leq 2\left(\tfrac{p}{q} + 1\right) + t_{KT}. \qquad \blacktriangle$$

In contrast to the low rank setting of Example 1, Example 2 shows how our results can be applied to the problem of estimating signal in a high rank matrix setting.

Example 2 (Estimating signal in a high rank spike model)**.** Let $m, n, p \in \mathbb{N}$ and set

$q := m + n + p$. Let $\mathbf{M} \in \mathbb{R}^{q \times q}$ be full rank with singular values given by the set

$$\{\underbrace{1, \ldots, 1}_{m \text{ times}}, \underbrace{\kappa + 1, \ldots, \kappa + 1}_{n \text{ times}}, \underbrace{\tau + \kappa + 1, \ldots, \tau + \kappa + 1}_{p \text{ times}}\},$$

where $\tau, \kappa > 0$. By slight abuse of notation, denote the singular values of $\mathbf{M}$ up to multiplicity by $\sigma_1 := 1$, $\sigma_2 := \kappa + 1$, and $\sigma_3 := \tau + \kappa + 1$.

Further suppose that $\mathbf{E} \in \mathbb{R}^{q \times q}$ has entries which are independent, identically distributed standard normal random variables. It follows by Gaussian concentration that $\mathbf{E}$ is (C, c, γ)-concentrated with parameters $C = 2$, $c = \frac{1}{2}$, and $\gamma = 2$, and so by an application of Lemma 31 for $\epsilon = 4$, then

$$\mathbb{P}\left[\|\mathbf{E}\|_2 > 6\sqrt{q}\right] \leq 2 \exp\left(-\tfrac{1}{10} q\right).$$

Define $\widehat{\mathbf{M}} := \mathbf{M} + \mathbf{E}$ and organize the singular values of $\widehat{\mathbf{M}}$ in correspondence with the repeated singular values of $\mathbf{M}$, namely write

$$\left\{\{\hat{\sigma}_{1,i_1}\}_{i_1=1}^{m}, \{\hat{\sigma}_{2,i_2}\}_{i_2=1}^{n}, \{\hat{\sigma}_{3,i_3}\}_{i_3=1}^{p}\right\}.$$

Suppose that $\tau, \kappa > (2 \times (6\sqrt{q}) + 1)$. Then we can use Weyl's inequality as a preliminary tool for selecting the threshold values α and β. In particular, such analysis

yields that with high probability,

$$\begin{aligned}
|\hat{\sigma}_{1,i_1} - 1| \leq \|\mathbf{E}\|_2 \implies & \quad 0 \leq \hat{\sigma}_{1,i_1} \leq 6\sqrt{q} + 1, \\
|\hat{\sigma}_{2,i_2} - (\kappa + 1)| \leq \|\mathbf{E}\|_2 \implies & \quad 6\sqrt{q} + 2 < \hat{\sigma}_{2,i_2} < \tau + \kappa - 6\sqrt{q}, \\
|\hat{\sigma}_{3,i_3} - (\tau + \kappa + 1)| \leq \|\mathbf{E}\|_2 \implies & \quad \tau + \kappa + 1 - 6\sqrt{q} \leq \hat{\sigma}_{3,i_3} \leq \tau + \kappa + 1 + 6\sqrt{q}.
\end{aligned}$$

For the choices $\alpha = 6\sqrt{q}+2$ and $\beta = \tau+\kappa-6\sqrt{q}$, observe that $\{\hat{\sigma}_{2,i_2}\}_{i_2=1}^{n} \subset (\alpha, \beta) \subset \mathbb{R}_{>0}$ while simultaneously $\{1, \kappa+1, \tau+\kappa+1\} \bigcap (\alpha, \beta) = \{\kappa+1\}$. In this setting our perturbation theorems apply for κ sufficiently large. Namely, choosing $\delta \in (0, 1]$ and setting $t = \Theta(\log^{\delta} q)$ yields that for each $k \in [n]$ there exist positive constants c' and c'' such that with high probability,

$$|\hat{\sigma}_{2,k} - \sigma_2| \leq c't + c''.$$

To reiterate, this bound improves upon the bound implied by a naïve, terminal application of Weyl's inequality. Moreover, Example 2 demonstrates how Weyl's inequality may be invoked for the preliminary purpose of establishing threshold values when the paired singular values (eigenvalues) correspond to the same index after ordering. ▲

4.4 Applications to graph inference

4.4.1 Methods of graph inference

The field of statistical inference and modeling for graphs represents a burgeoning area of research with implications for the social and natural sciences among other disciplines (Goldenberg et al., 2010; Kolaczyk, 2009). Within the current body of research, the pursuit of identifying and studying community structure within real–world networks continues to receive widespread attention (Arias-Castro and Verzelen, 2014; Bickel and Sarkar, 2013; Fortunato, 2010; Newman and Girvan, 2004; Newman, 2006; Verzelen and Arias-Castro, 2015). Still another area of investigation involves anomaly detection for time series of graphs by considering graph statistics such as the total degree, number of triangles, and various scan statistics (Rukhin, 2009; Wang et al., 2014). Here we apply our results to two such detection tasks.

4.4.2 Community detection via hypothesis testing

Here we view the problem of community detection through the lens of hypothesis testing as in Arias-Castro and Verzelen (2014); Verzelen and Arias-Castro (2015). We consider the simple setting of a balanced three block stochastic block model and the problem of detecting differences in between-block communication. Namely, consider

the block edge probability matrix and block assignment vector given by

$$\text{Null model: } \mathbf{B}_0 = \begin{bmatrix} p & q & q \\ q & p & q \\ q & q & p \end{bmatrix} \text{ and } \boldsymbol{\pi}_0 = \left(\tfrac{1}{3}, \tfrac{1}{3}, \tfrac{1}{3}\right)^\top, \tag{4.13}$$

where $p = 0.81$ and $q = 0.2025$. In this model, vertices have an equal probability of belonging to each of the three blocks. Vertices within the same block have probability p of being connected by an edge, whereas vertices in different blocks have probability q of being connected by an edge.

As an aside, we note that this SBM may be cast in the language of random dot product graphs for which the underlying distribution of latent positions F is a mixture of point masses. Specifically, take F to be the discrete uniform distribution on the vectors $\mathbf{x}_1 \approx (0.55, 0.32, 0.64)^\top$, $\mathbf{x}_2 \approx (-0.55, 0.32, 0.64)^\top$, and $\mathbf{x}_3 \approx (0, -0.64, 0.64)^\top$ in $\mathbb{R}^3$ (see Remarks 17 and 18).

For a graph on n vertices from this three block model, condition on the graph exhibiting equal block sizes, i.e., $n_1 = n_2 = n_3 = n/3$. For the corresponding $\mathbf{P}$ matrix, denoted $\mathbf{P}_n(\mathbf{B}_0)$, the non-trivial (signal) model eigenvalues themselves exhibit multiplicity (hence Eq. (4.6) via Athreya et al. (2016) does not apply) and are

$$\lambda_1(\mathbf{P}_n(\mathbf{B}_0)) = \lambda_2(\mathbf{P}_n(\mathbf{B}_0)) = \frac{n}{3}(p - q) \text{ and } \lambda_3(\mathbf{P}_n(\mathbf{B}_0)) = \frac{n}{3}(p + 2q). \tag{4.14}$$

In contrast, consider an alternative model in which the first and second blocks exhibit stronger between-block communication. This stronger communication is represented by an additional additive factor $\epsilon \in (0, p-q)$ in the block edge probability matrix $\mathbf{B}_\epsilon$, where ϵ is assumed to be bounded away from $p-q$ for convenience.

$$\text{Alternative model: } \mathbf{B}_\epsilon = \begin{bmatrix} p & q+\epsilon & q \\ q+\epsilon & p & q \\ q & q & p \end{bmatrix} \text{ and } \boldsymbol{\pi}_1 = \left(\tfrac{1}{3}, \tfrac{1}{3}, \tfrac{1}{3}\right)^\top. \tag{4.15}$$

Under $\mathbf{B}_\epsilon$, the signal eigenvalues of $\mathbf{P}_n(\mathbf{B}_\epsilon)$ (equiv., singular values) can be explicitly computed as functions of p, q, n, and ϵ. They are given by

$$\lambda_1(\mathbf{P}_n(\mathbf{B}_\epsilon)) = \frac{n}{3}(p-q-\epsilon), \quad \lambda_2(\mathbf{P}_n(\mathbf{B}_\epsilon)) = \frac{n}{6}(2p+q+\epsilon-\sqrt{9q^2+2q\epsilon+\epsilon^2}),$$
$$\lambda_3(\mathbf{P}_n(\mathbf{B}_\epsilon)) = \frac{n}{6}(2p+q+\epsilon+\sqrt{9q^2+2q\epsilon+\epsilon^2}).$$

Furthermore, the maximum expected degree of the model corresponding to $\mathbf{B}_\epsilon$ is given by $\Delta_\epsilon = \frac{n}{3}(p+2q+\epsilon)$.

For $\epsilon > 0$, now consider a simple null versus simple alternative hypothesis test written as

$$\mathbb{H}_0 : \mathbf{B} = \mathbf{B}_0 \text{ against } \mathbb{H}_\text{A} : \mathbf{B} = \mathbf{B}_\epsilon. \tag{4.16}$$

In what follows we choose the smallest signal eigenvalue as our test statistic and denote it by Λ_1. We compare our bounds obtained via Kato–Temple methodology

with the large-sample approximation bounds implied by Lu and Peng (2013) for the specified values $n \in \{6000, 9000, 12000, 15000\}$. Similar comparison can be carried out with respect to the results in O'Rourke et al. (2018). Our bounds are competitive even for conservative choices of t.

By Lemma 31 and Proposition 25, irrespective of $\epsilon > 0$ above, we have the concentration inequality $\mathbb{P}\left[\|\mathbf{E}\|_2 > 3\sqrt{n}\right] \leq 2\exp\left(-\frac{1}{20}n\right)$. This spectral norm bound allows us to invoke an unconditional version of Theorem 26. Specifically, for moderate choices of $t > 0$, the bounds in Theorem 26 hold with probability at least $1 - 12\exp(-t^2) - 2\exp\left(-\frac{1}{20}n\right)$. When $n \geq 6000$, the choice $t \approx 2.66$ yields probability at least 0.99.

Using these concentration inequality results, we determine confidence intervals which hold for Λ_1 with probability at least 0.99 under $\mathbb{H}_0$ and $\mathbb{H}_\mathrm{A}$, respectively. We compute the value ϵ_n such that the confidence intervals under $\mathbb{H}_0$ and $\mathbb{H}_\mathrm{A}$ no longer overlap for $\epsilon \in (\epsilon_n, 0.2]$, emphasizing that smaller values of ϵ_n indicate superior performance. This provides us with a region of the alternative in which the statistical test has power at least 0.99. Our results are summarized in the numerical table below. It is not too difficult to realize that the eigenvalue-based test considered here has asymptotic power equal to one as $n \to \infty$ for any choice of $0 < q < p < 1$ and $\epsilon \in (0, p - q)$. Moreover, as a consequence of Theorem 27 and subsequent discussion, we make the following observation.

Proposition 32. *Consider testing the hypothesis in Equation (4.16). Assume that*

Table 4.1: Local approximate confidence intervals for eigenvalues

n	ϵ_n via Lu and Peng (2013)	ϵ_n via this chapter
6000	0.1006	0.0407
9000	0.0818	0.0256
12000	0.0707	0.0187
15000	0.0631	0.0147

$q \equiv q_n = \omega(\frac{\log n}{n})$ *with* $q_n < p_n$. *Then for* $n\epsilon_n = \omega(\log n)$ *and* $\epsilon_n < p_n - q_n$, *the above test using* Λ_1 *has asymptotically full power.*

Note that the above analysis investigates testing performance as a function of ϵ for graphs with fixed block proportions. Next we investigate a setting wherein ϵ is fixed and the sizes of the graph communities change.

4.4.3 Change-point detection

We now consider a stylized example of change-point detection via hypothesis testing. Let $T^* \geq 1$ and suppose that $G_1, G_2, \ldots, G_T$ for $T < T^*$ are Erdős–Rényi graphs on n vertices, while for $T \geq T^*$ the graph G_T is sampled according to a two block stochastic block model with block edge probability matrix $\mathbf{B} = \left[\begin{smallmatrix} p_\epsilon & p \\ p & p \end{smallmatrix}\right]$ for $p_\epsilon := p + \epsilon$ and $\epsilon > 0$, with m vertices assigned to the first block and $n - m$ vertices assigned to the second block. We note that $\mathbf{B}$ encapsulates a notion of chatter anomaly, i.e., a subset of the vertices in $[n]$ exhibit altered communication behavior in an otherwise stationary setting. For a given value of T, we are interested in testing the hypothesis that T is a change-point in the collection $\{G_1, G_2, \ldots, G_T\}$. Given two graphs with

adjacency matrices, $\mathbf{A}^{(T-1)}$ and $\mathbf{A}^{(T)}$, this can be formulated as the problem of testing the two-sample hypotheses

$$\mathbb{H}_0 \colon \mathbf{A}^{(T-1)} \sim \mathrm{ER}(n,p), \mathbf{A}^{(T)} \sim \mathrm{ER}(n,p) \quad \text{against}$$

$$\mathbb{H}_\mathrm{A} \colon \mathbf{A}^{(T-1)} \sim \mathrm{ER}(n,p), \mathbf{A}^{(T)} \sim \mathrm{SBM}(\mathbf{B}, m, n-m).$$

We emphasize that in the above formulation, the parameter p in $\mathrm{ER}(n,p)$, the size m of the chatter community, and the associated communication probability p_ϵ are generally assumed to be unknown.

Many test statistics are available for this change-point detection problem, including those based on graph invariant statistics (such as number of edges or number of triangles) or those based on locality statistics (such as max degree or scan statistics). For a given graph with adjacency matrix $\mathbf{A}$, let $N(i) = \{j \colon \mathbf{A}_{i,j} = 1\}$ denote the collection of vertices adjacent to vertex i. Furthermore,

- let $\mathcal{T}_k$ count the number of k-cliques in $\mathbf{A}$ for $k \geq 2$;
- let $\delta(\mathbf{A}) := \max_i \sum_j \mathbf{A}_{i,j}$ be the max degree statistic of $\mathbf{A}$;
- let $\Psi(\mathbf{A}) := \max_i \sum_{j,k \in N(i)} \mathbf{A}_{j,k}$ be the scan statistic of $\mathbf{A}$.

These test statistics are widely used in anomaly detection for time series of graphs; see Arias-Castro and Verzelen (2014); Priebe et al. (2005); Ranshous et al. (2015); Wang et al. (2014) and the references therein for a survey of results and applications.

One can then show that the test statistics based on $\mathcal{T}_2$ and $\mathcal{T}_3$ are consistent for the above hypothesis test when $m = \Omega(\sqrt{n})$ (Rukhin and Priebe, 2011; Tang et al., 2013). More precisely, under the null hypothesis,

$$\frac{\mathcal{T}_2(\mathbf{A}^{(T)}) - \mathcal{T}_2(\mathbf{A}^{(T-1)})}{n\sqrt{p(1-p)}} \Rightarrow \mathcal{N}(0,1); \quad \frac{\mathcal{T}_3(\mathbf{A}^{(T)}) - \mathcal{T}_3(\mathbf{A}^{(T-1)})}{n^2p^2\sqrt{pp_\epsilon}} \Rightarrow \mathcal{N}(0,1),$$

as $n \to \infty$, while under the alternative hypothesis,

$$\begin{aligned}\frac{\mathcal{T}_2(\mathbf{A}^{(T)}) - \mathcal{T}_2(\mathbf{A}^{(T-1)})}{n\sqrt{p(1-p)}} &\Rightarrow \mathcal{N}\Big(\frac{m(m-1)\epsilon}{n\sqrt{p(1-p)}}, C_1\Big);\\ \frac{\mathcal{T}_3(\mathbf{A}^{(T)}) - \mathcal{T}_3(\mathbf{A}^{(T-1)})}{n^2p^2\sqrt{pp_\epsilon}} &\Rightarrow \mathcal{N}\Big(\frac{\mu_{n,m,p,\epsilon}}{n^2p^2\sqrt{pp_\epsilon}}, C_2\Big),\end{aligned}$$

as $n \to \infty$ for some positive constants C_1 and C_2 together with $\mu_{n,m,p,\epsilon} := m^3p_\epsilon^3/6 + m^2(n-m)p^2p_\epsilon + (m(n-m)^2/2 + (n-m)^3/6)p^3 - n^3p^3/6$. Now, if $m = \omega(\sqrt{n})$, then

$$\frac{m(m-1)\epsilon}{n\sqrt{p(1-p)}} \to \infty; \quad \frac{\mu_{n,m,p,\epsilon}}{n^2p^2\sqrt{pp_\epsilon}} \to \infty,$$

as $n \to \infty$, and thus both $\mathcal{T}_2$ and $\mathcal{T}_3$ are consistent for the above hypothesis test when $m = \Omega(\sqrt{n})$. Furthermore, Theorem 2 and Proposition 2 of Arias-Castro and Verzelen (2014) indicate that $\mathcal{T}_2$ is asymptotically optimal, i.e., if $m = o(\sqrt{n})$ then provided that

$$\lim_{n\to\infty} \mathcal{I}(m,n,p,\epsilon) := \lim_{n\to\infty} \frac{m\big(p_\epsilon \log \frac{p_\epsilon}{p} + (1-p_\epsilon)\log\frac{1-p_\epsilon}{1-p}\big)}{2\log(n/m)} < 1, \tag{4.17}$$

no test statistic is consistent for testing the above hypotheses. Similarly, one can also show that the test statistics based on $\delta(A)$ and $\Psi(A)$ are consistent for the above hypothesis test when $m = \Omega(\sqrt{n \log n})$; in particular, the (normalized) limiting distributions of both $\delta(\mathbf{A}^{(T)}) - \delta(\mathbf{A}^{(T-1)})$ and $\Psi(\mathbf{A}^{(T)}) - \Psi(\mathbf{A}^{(T-1)})$ is the Gumbel distribution (Rukhin and Priebe, 2011; Tang et al., 2013).

In the context of this chapter, one could also use a test statistic based on the largest eigenvalue. Our earlier results indicate that, under the null hypothesis, with high probability the largest eigenvalues of $\mathbf{A}^{(T)}$ and $\mathbf{A}^{(T-1)}$ satisfy

$$|\lambda_{\max}(\mathbf{A}^{(T)}) - \lambda_{\max}(\mathbf{P}^{(T)})| = O(1) \text{ and } |\lambda_{\max}(\mathbf{A}^{(T-1)}) - \lambda_{\max}(\mathbf{P}^{(T-1)})| = O(1),$$

along with $|\lambda_{\max}(\mathbf{A}^{(T)}) - \lambda_{\max}(\mathbf{A}^{(T-1)})| = O(1)$. Meanwhile, under the alternative hypothesis, when $m = o(n)$, then with high probability

$$\left| \left| \lambda_{\max}(\mathbf{A}^{(T)}) - \lambda_{\max}(\mathbf{A}^{(T-1)}) \right| - \frac{m^2 p \epsilon}{np - m\epsilon} \right| = O(1).$$

Thus the largest eigenvalue test statistic is also consistent when $m = \Omega(\sqrt{n})$.

The previous test statistics are all global test statistics in the sense that, if $\mathbb{H}_0$ is rejected, the resulting test procedures do not extract the subset of the vertices which exhibits anomalous behavior between $\mathbf{A}^{(T)}$ and $\mathbf{A}^{(T-1)}$. One can construct related local test statistics which do extract the subset of anomalous vertices, although the resulting test procedure is computationally prohibitive. For example, assuming that

m is known, we could replace $\Psi(\mathbf{A})$ with the (modified) scan statistic $\Upsilon_m(\mathbf{A}) = \max_{|S|=m} \mathcal{T}_2(\mathbf{A}_{|S})$ where $\mathbf{A}_{|S}$ is the subgraph of A induced by the vertices in S and the maximum is taken over all subsets $S \subset [n]$ with $|S| = m$. Thus $\Upsilon_m(\mathbf{A})$ is the maximum number of edges in any subgraph induced by m vertices of $\mathbf{A}$. By Arias-Castro and Verzelen (2014), the test statistic $\Upsilon_m(\mathbf{A}^{(T)}) - \Upsilon_m(\mathbf{A}^{(T-1)})$ is consistent for the hypothesis test considered in this section whenever

$$\lim_{n\to\infty} \mathcal{J}(m, n, p, \epsilon) > 1.$$

Thus, for any fixed p and ϵ, the (modified) scan statistic is consistent when $m = \Omega(\log n)$ as $n \to \infty$. Using a similar idea, one can define a local variant of the largest eigenvalue statistic as $\Lambda_m(\mathbf{A}) = \max_{|S|=m} \lambda_{\max}(\mathbf{A}_{|S})$. By Theorem 26 and a union bound over all $\binom{n}{m} = O(n^m)$ subsets $S \subseteq [n]$ with $|S| = m$, we have that there exists a constant $C > 0$ such that if $T = C\sqrt{m \log n}$, then with high probability

$$|\Lambda_m(\mathbf{A}^{(T)}) - \Lambda_m(\mathbf{A}^{(T-1)})| = O(\sqrt{m \log n})$$

under the null hypothesis, whereas under the alternative hypothesis, with high probability

$$\left| |\Lambda_m(\mathbf{A}^{(T)}) - \Lambda_m(\mathbf{A}^{(T-1)})| - m\epsilon \right| = O(\sqrt{m \log n}).$$

Thus for any fixed p and ϵ, the test statistic based on Λ_m is also consistent for the

above hypothesis test whenever $m = \Omega(\log n)$ as $n \to \infty$.

In summary, the results in Section 4.3 facilitate eigenvalue-based test statistics for the change-point detection problem as presented in this section. Furthermore, the resulting procedure is consistent whenever the size of the chatter community m exceeds the threshold of detectability given in Arias-Castro and Verzelen (2014).

Chapter 5

Spectral embedding performance and elucidating network structure in stochastic block model graphs

5.1 Preface to Chapter 5

The stochastic block model (SBM) (Holland et al., 1983) is a simple yet ubiquitous network model capable of reflecting community structure that has been widely studied via spectral methods in the mathematics, statistics, physics, and engineering communities. Each vertex in an n-vertex K-block SBM graph belongs to one of the K blocks (communities), and the probability of any two vertices sharing an edge depends exclusively on the vertices' block assignments (memberships).

This chapter provides a detailed comparison of two popular spectral embedding procedures by synthesizing recent advances in random graph limit theory. We undertake an extensive investigation of network structure for stochastic block model graphs by considering sub-models exhibiting various functional relationships, symmetries, and geometric properties within the inherent parameter space consisting of block membership probabilities and block edge probabilities. We also provide a collection of figures depicting relative spectral embedding performance as a function of the SBM parameter space for a range of sub-models exhibiting different forms of network structure, specifically homogeneous community structure, affinity structure, core-periphery structure, and (un)balanced block sizes (see Section 5.5).

The rest of this chapter is organized as follows.

- Section 5.2 introduces the formal setting under consideration and contextualizes this work with respect to the existing statistical network analysis literature.
- Section 5.3 establishes notation, presents the generalized random dot product graph model (of which the stochastic block model is a special case), defines the adjacency and Laplacian spectral embeddings, presents the corresponding spectral embedding limit theorems, and specifies the notion of sparsity considered in this chapter.
- Section 5.4 motivates and formulates a measure of large-sample relative spectral embedding performance via Chernoff information.

- Section 5.5 presents a treatment of the two-block SBM and certain K-block SBMs whereby we elucidate the relationship between spectral embedding performance and network model structure.

- Section 5.6 offers further discussion and some concluding remarks.

Later in Chapter 6, Section 6.4 provides additional supplementary technical material and proof details.

5.2 Stochastic block models

Formally, we consider the following stochastic block model setting.

Definition 33 (K-block stochastic block model)**.** Let $K \geq 2$ be a positive integer and $\boldsymbol{\pi}$ be a vector in the interior of the $(K-1)$-dimensional unit simplex in $\mathbb{R}^K$. Let $\mathbf{B} \in (0,1)^{K \times K}$ be a symmetric matrix with distinct rows. We say $(\mathbf{A}, \boldsymbol{\tau}) \sim \text{SBM}(\mathbf{B}, \boldsymbol{\pi})$ with scaling factor $0 < \rho_n \leq 1$ provided the following conditions hold. Firstly, $\boldsymbol{\tau} \equiv (\tau_1, \ldots, \tau_n)^\top$ where τ_i are independent and identically distributed (i.i.d.) random variables with $\mathbb{P}[\tau_i = k] = \pi_k$. Then, $\mathbf{A} \in \{0,1\}^{n \times n}$ denotes a symmetric (adjacency) matrix such that, conditioned on $\boldsymbol{\tau}$, for all $i \leq j$, the entries $\mathbf{A}_{ij}$ are independent Bernoulli random variables with $\mathbb{E}[\mathbf{A}_{ij}] = \rho_n \mathbf{B}_{\tau_i, \tau_j}$. If only $\mathbf{A}$ is observed, namely if $\boldsymbol{\tau}$ is integrated out from $(\mathbf{A}, \boldsymbol{\tau})$, then we write $\mathbf{A} \sim \text{SBM}(\mathbf{B}, \boldsymbol{\pi})$.[1] ▲

[1]The distinct row assumption removes potential redundancy with respect to block connectivity and labeling. Namely, if rows k and k' of $\mathbf{B}'$ are identical, then their corresponding blocks are indistinguishable and can without loss of generality be merged to form a reduced block edge probability

The SBM is an example of an inhomogeneous Erdős–Rényi random graph model (Bollobás et al., 2007) and reduces to the classical Erdős–Rényi model (Erdős and Rényi, 1959) in the degenerate case when all the entries of $\mathbf{B}$ are identical. This model enjoys an extensive body of literature focused on spectral methods (Von Luxburg, 2007) for statistical estimation, inference, and community detection (Fishkind et al., 2013; Lei and Rinaldo, 2015; McSherry, 2001; Rohe et al., 2011; Sarkar and Bickel, 2015; Sussman et al., 2012). Considerable effort has also been devoted to the information theoretic and computational investigation of the SBM as a result of interest in the community detection problem; for an overview see Abbe (2018). Popular variants of the SBM include the mixed-membership stochastic block model (Airoldi et al., 2008) and the degree-corrected stochastic block model (Karrer and Newman, 2011).

Within the statistics literature, substantial attention has been paid to the class of K-block SBMs with positive semidefinite block edge probability matrices $\mathbf{B}$. This is due in part to the extensive study of the *random dot product graph* (RDPG) *model* (Athreya et al., 2018; Nickel, 2006; Young and Scheinerman, 2007), a latent position random graph model (Hoff et al., 2002) which includes positive semidefinite SBMs as a special case. Notably, it was recently shown that for the random dot product graph model, both Laplacian spectral embedding (LSE; see Definition 35) and adjacency spectral embedding (ASE; see Definition 35) behave approximately as random sam-

matrix $\mathbf{B}$ with corresponding combined block membership probability $\pi_k + \pi_{k'}$. We also remark that Definition 33 implicitly permits vertex self-loops, a choice that we make for mathematical expediency. Whether or not self-loops are disallowed does not alter the asymptotic results and conclusions presented here.

ples from Gaussian mixture models (Athreya et al., 2016; Tang and Priebe, 2018). In tandem with these limit results, the concept of Chernoff information (Chernoff, 1952) was employed in Tang and Priebe (2018) to demonstrate that neither Laplacian nor adjacency spectral embedding dominates the other for subsequent inference as a spectral embedding method when the underlying inference task is to recover vertices' latent block assignments. In doing so, the results in Tang and Priebe (2018) clarify and complete the groundbreaking work in Sarkar and Bickel (2015) on comparing spectral clusterings for stochastic block model graphs.

In Tang and Priebe (2018) the authors leave open the problem of comprehensively investigating Chernoff information as a measure of relative spectral embedding performance for stochastic block model graphs. Moreover, they do not investigate how relative spectral embedding performance corresponds to underlying network model structure. This is understandable, since the positive semidefinite restriction on $\mathbf{B}$ limits the possible network structure that can be investigated under the random dot product graph model.

More recently, the limit theory in Tang and Priebe (2018) was extended in Rubin-Delanchy et al. (2017) to hold for *all* SBMs within the more flexible framework of the *generalized random dot product graph* (GRDPG) *model*. These developments now make it possible to conduct a more comprehensive Chernoff-based analysis, and that is precisely the aim of this chapter. We set forth to formulate and analyze a criterion based on Chernoff information for quantifying relative spectral embedding

performance which we then further consider in conjunction with underlying network model structure. The investigation carried out in this chapter is, to the best of our knowledge, among the first of its kind in the study of statistical network analysis and random graph inference.

This chapter focuses on the following two models which have garnered widespread interest (e.g., see Abbe (2018) and the references therein).

1. The two-block SBM with $\mathbf{B} = \left[\begin{smallmatrix} a & b \\ b & c \end{smallmatrix}\right]$ and $\boldsymbol{\pi} = (\pi_1, 1-\pi_1)^\top$ where $a, b, c, \pi_1 \in (0, 1)$;

2. The $K \geq 2$ block SBM exhibiting homogeneous balanced affinity structure, i.e. $\mathbf{B}_{ij} = a$ for all $i = j$, $\mathbf{B}_{ij} = b$ for all $i \neq j$, $0 < b < a < 1$, and $\boldsymbol{\pi} = (\frac{1}{K}, \ldots, \frac{1}{K})^\top \in \mathbb{R}^K$.

Using Chernoff information (see Section 5.4), we obtain an information-theoretic summary characteristic $\rho^\star \equiv \rho^\star(\mathbf{B}, \boldsymbol{\pi})$ such that the cases $\rho^\star > 1$, $\rho^\star < 1$, and $\rho^\star = 1$ correspond to the preference of spectral embedding procedure based on approximate large-sample relative performance, summarized as ASE $>$ LSE, ASE $<$ LSE, and ASE $=$ LSE, respectively. The above models' low-dimensional parameter spaces facilitate visualizing and analyzing the relationship between network structure (i.e., SBM$(\mathbf{B}, \boldsymbol{\pi})$) and embedding performance (i.e., $\rho^\star(\mathbf{B}, \boldsymbol{\pi})$).

This chapter considers the task of performing inference on a single large graph. As such, we interpret the notion of *sparsity* in reference to the magnitudes of probability

parameters, namely the magnitudes of the entries of $\mathbf{B}$. This notion of sparsity corresponds to the interpretation and intuition of a practitioner wanting to do statistics with an observed graph. With this understanding in mind, we shall demonstrate that LSE is preferred as an embedding method in relatively sparse regimes, whereas ASE is preferred as an embedding method in not-too-sparse regimes.

By way of contrast, the scaling factor ρ_n in Definition 33, which is included for the purpose of general presentation, indexes a sequence of models wherein edge probabilities change with n. We take ρ_n to be constant in n which by rescaling is equivalent to setting $\rho_n \equiv 1$. Limit theorems are known for regimes where $\rho_n \to 0$ as $n \to \infty$, but these regimes are uninteresting for single graph inference from the perspective of relative spectral embedding performance (Tang and Priebe, 2018).

5.3 Preliminaries and existing results

Given a symmetric positive definite $n \times n$ matrix $\mathbf{M}$, let $\langle \cdot, \cdot \rangle_{\mathbf{M}} : \mathbb{R}^n \times \mathbb{R}^n \to \mathbb{R}$ denote the real inner product induced by $\mathbf{M}$. Similarly, define the induced norm as $\| \cdot \|_{\mathbf{M}} := \sqrt{\langle \cdot, \cdot \rangle_{\mathbf{M}}}$. In particular, given the $n \times n$ identity matrix $\mathbf{I}$, denote the standard Euclidean inner product and Euclidean norm by $\langle \cdot, \cdot \rangle \equiv \langle \cdot, \cdot \rangle_{\mathbf{I}}$ and $\| \cdot \|_2 := \sqrt{\langle \cdot, \cdot \rangle}$, respectively. Given an underlying matrix, $\det(\cdot)$ and $\mathrm{tr}(\cdot)$ denote the matrix determinant and matrix trace operator, respectively. Given a diagonal matrix $\mathbf{D} := \mathrm{diag}(d_{11}, d_{22}, \ldots, d_{nn}) \in \mathbb{R}^{n \times n}$, $|\mathbf{D}|$ denotes the entrywise absolute value

(matrix) of $\mathbf{D}$.

The vector of all ones in $\mathbb{R}^n$ is denoted by $\mathbf{1}_n$, whereas the zero matrix in $\mathbb{R}^{m\times n}$ is denoted by $\mathbf{0}_{m,n}$. We suppress the indices for convenience when the underlying dimensions are understood, writing instead $\mathbf{1}$ and $\mathbf{0}$.

Let $\mathbb{N} := \{1, 2, 3, \dots\}$ denote the set of natural numbers so that for $n \in \mathbb{N}$, $[n] := \{1, 2, \dots, n\}$. For integers $d^+ \geq 1$, $d^- \geq 0$, and $d := d^+ + d^- \geq 1$, let $\mathbf{I}_{d^-}^{d^+} := \mathbf{I}_{d^+} \bigoplus (-\mathbf{I}_{d^-}) \in \mathbb{R}^{d\times d}$ be the direct sum (diagonal) matrix with identity matrices $\mathbf{I}_{d^+} \in \mathbb{R}^{d^+\times d^+}$ and $\mathbf{I}_{d^-} \in \mathbb{R}^{d^-\times d^-}$ together with the convention that $\mathbf{I}_0^{d^+} \equiv \mathbf{I}_{d^+}$. For example, $\mathbf{I}_1^1 \equiv \mathrm{diag}(1, -1) \in \mathbb{R}^{2\times 2}$.

For integers $n \geq d \geq 1$, the set of all $n \times d$ real matrices with orthonormal columns shall be denoted by $\mathbb{O}_{n,d}$. Let $\mathbb{O}(d^+, d^-)$ denote the indefinite orthogonal group with signature (d^+, d^-), and let $\mathbb{O}_{d^+} \equiv \mathbb{O}_{d^+,d^+} \equiv \mathbb{O}(d^+, 0)$ denote the orthogonal group in $\mathbb{R}^{d^+\times d^+}$. In particular, $\mathbf{M} \in \mathbb{O}(d^+, d^-)$ has the characterization $\mathbf{M}^\top \mathbf{I}_{d^-}^{d^+} \mathbf{M} = \mathbf{I}_{d^-}^{d^+}$. For the orthogonal group, this characterization reduces to the relationship $\mathbf{M}^\top \equiv \mathbf{M}^{-1}$.

5.3.1 Generalized random dot product graphs

A growing corpus has emerged within the statistics literature focused on the development of theory and applications for the *random dot product graph* (RDPG) *model* (Nickel, 2006; Young and Scheinerman, 2007). This latent position random graph model associates to each vertex in a graph an underlying low-dimensional vector. These vectors may be viewed as encoding structural information or attributes pos-

sessed by their corresponding vertices. In turn, the probability of two vertices sharing an edge is specified through the standard Euclidean inner (dot) product of the vertices' latent position vectors. While simple in concept and design, this model has proven successful in real-world applications in the areas of neuroscience and social networks (Lyzinski et al., 2017). On the theoretical side, the RDPG model enjoys some of the first-ever statistical theory for two-sample hypothesis testing on random graphs, both semiparametric (Tang et al., 2017) and nonparametric (Tang et al., 2017). For more on the RDPG model, see the survey Athreya et al. (2018) and the references therein.

More recently, the *generalized random dot product graph* (GRDPG) *model* was introduced as an extension of the RDPG model that includes as special cases the mixed membership stochastic block model as well as *all* (single membership) stochastic block models (Rubin-Delanchy et al., 2017). Effort towards the development of theory for the GRDPG model has already raised new questions and produced new findings related to the geometry of spectral methods, embeddings, and random graph inference. The present chapter further contributes to these efforts.

Definition 34 (The generalized random dot product graph (GRDPG) model)**.** For integers $d^+ \geq 1$ and $d^- \geq 0$ such that $d := d^+ + d^- \geq 1$, let F be a distribution on a set $\mathcal{X} \subset \mathbb{R}^d$ such that $\langle \mathbf{I}_{d^-}^{d^+} \mathbf{x}, \mathbf{y} \rangle \in [0, 1]$ for all $\mathbf{x}, \mathbf{y} \in \mathcal{X}$. We say that $(\mathbf{X}, \mathbf{A}) \sim$ GRDPG(F) with signature (d^+, d^-) and scaling factor $0 < \rho_n \leq 1$ if the following hold. Let $X_1, \ldots, X_n \sim F$ be independent and identically distributed random (latent

position) vectors with

$$\mathbf{X} := [X_1|\cdots|X_n]^\top \in \mathbb{R}^{n\times d} \text{ and } \mathbf{P} := \rho_n \mathbf{X}\mathbf{I}_{d^-}^{d^+}\mathbf{X}^\top \in [0,1]^{n\times n}. \tag{5.1}$$

For each $i \leq j$, the entries $\mathbf{A}_{ij}$ of the symmetric adjacency matrix $\mathbf{A} \in \{0,1\}^{n\times n}$ are generated in a conditionally independent fashion given the latent positions, i.e.,

$$\{\mathbf{A}_{ij}|X_i, X_j\} \sim \text{Bernoulli}(\rho_n \langle \mathbf{I}_{d^-}^{d^+} X_i, X_j\rangle). \tag{5.2}$$

In this setting, the conditional probability $\mathbb{P}[\mathbf{A}|\mathbf{X}]$ can be computed explicitly as a product of Bernoulli probabilities. ▲

To reiterate, we consider the regime $\rho_n \equiv 1$ and therefore suppress dependencies on ρ_n later in the text. When no confusion can arise, we also use adorned versions of the symbol ρ to denote Chernoff-related quantities (and unrelated to ρ_n) in a manner consistent with the notation in Tang and Priebe (2018) (see Section 5.4).

When $d^- = 0$, the GRDPG model reduces to the RDPG model. When the distribution F is a discrete distribution on a finite collection of vectors in $\mathbb{R}^d$, then the GRDPG model coincides with the SBM, in which case the $n \times n$ edge probability matrix $\mathbf{P}$ arises as an appropriate dilation of the $K \times K$ block edge probability matrix $\mathbf{B}$. Given any valid $\mathbf{B} \in (0,1)^{K\times K}$ as in Definition 33, there exist integers d^+, d^-, and a matrix $\mathbf{X} \in \mathbb{R}^{K\times K}$ such that $\mathbf{B}$ has the (not necessarily unique) factorization $\mathbf{B} \equiv \mathbf{X}\mathbf{I}_{d^-}^{d^+}\mathbf{X}^\top$, which follows since the spectral decomposition of $\mathbf{B}$ can be written

as $\mathbf{B} \equiv \mathbf{U_B}\mathbf{\Lambda}\mathbf{U_B}^\top = (\mathbf{U_B}|\mathbf{\Lambda}|^{1/2})\mathbf{I}_{d^-}^{d^+}(\mathbf{U_B}|\mathbf{\Lambda}|^{1/2})^\top$. This demonstrates the ability of the GRDPG framework in Definition 34 to model all possible stochastic block models formulated in Definition 33.

Remark 19 (Non-identifiability in the GRDPG model)**.** The GRDPG model possesses two intrinsic sources of non-identifiability, summarized as "uniqueness up to indefinite orthogonal transformations" and "uniqueness up to artificial dimension blow-up". More precisely, for $(\mathbf{X}, \mathbf{A}) \sim \text{GRDPG}(F)$ with signature (d^+, d^-), the following considerations must be taken into account.

1. For any $\mathbf{Q} \in \mathbb{O}(d^+, d^-)$, $(\mathbf{X}, \mathbf{A}) \overset{\text{d}}{=} (\mathbf{Y}, \mathbf{B})$ whenever $(\mathbf{Y}, \mathbf{B}) \sim \text{GRDPG}(F \circ \mathbf{Q})$, where $F \circ \mathbf{Q}$ denotes the distribution of the latent position vector $Y = \mathbf{Q}X$ and $\overset{\text{d}}{=}$ denotes equality in distribution. This source of non-identifiability cannot be mitigated. See Eq. (5.2).

2. There exists a distribution F' on $\mathbb{R}^{d'}$ for some $d' > d$ such that $(\mathbf{X}, \mathbf{A}) \overset{\text{d}}{=} (\mathbf{Y}, \mathbf{B})$ where $(\mathbf{Y}, \mathbf{B}) \sim \text{GRDPG}(F')$. This source of non-identifiability can be avoided by assuming, as we do here, that F is non-degenerate in the sense that for $X_1 \sim F$, the second moment matrix $\mathbb{E}[X_1 X_1^\top] \in \mathbb{R}^{d \times d}$ is full rank.

Definition 35 (Adjacency and Laplacian spectral embeddings)**.** Let $\mathbf{A} \in \{0, 1\}^{n \times n}$ be a symmetric adjacency matrix with eigendecomposition $\mathbf{A} \equiv \sum_{i=1}^n \lambda_i \mathbf{u}_i \mathbf{u}_i^\top$ and with ordered eigenvalues $|\lambda_1| \geq |\lambda_2| \geq \cdots \geq |\lambda_n|$ corresponding to orthonormal eigenvectors $\mathbf{u}_1, \mathbf{u}_2, \ldots, \mathbf{u}_n$. Given a positive integer d such that $d \leq n$, let $\mathbf{S_A} :=$

$\text{diag}(\lambda_1, \ldots, \lambda_d) \in \mathbb{R}^{d \times d}$ and $\mathbf{U_A} := [\mathbf{u}_1 | \ldots | \mathbf{u}_d] \in \mathbb{O}_{n,d}$. The *adjacency spectral embedding* (ASE) of $\mathbf{A}$ into $\mathbb{R}^d$ is then defined to be the $n \times d$ matrix $\hat{\mathbf{X}} := \mathbf{U_A}|\mathbf{S_A}|^{1/2}$. The matrix $\hat{\mathbf{X}}$ serves as a consistent estimator for $\mathbf{X}$ up to indefinite orthogonal transformation as $n \to \infty$.

Along similar lines, define the normalized Laplacian of $\mathbf{A}$ as

$$\mathcal{L}(\mathbf{A}) := (\text{diag}(\mathbf{A}\mathbf{1}_n))^{-1/2}\mathbf{A}(\text{diag}(\mathbf{A}\mathbf{1}_n))^{-1/2} \in \mathbb{R}^{n \times n}, \tag{5.3}$$

whose eigendecomposition is given by $\mathcal{L}(\mathbf{A}) \equiv \sum_{i=1}^{n} \tilde{\lambda}_i \tilde{\mathbf{u}}_i \tilde{\mathbf{u}}_i^\top$ with ordered eigenvalues $|\tilde{\lambda}_1| \geq |\tilde{\lambda}_2| \geq \cdots \geq |\tilde{\lambda}_n|$ corresponding to orthonormal eigenvectors $\tilde{\mathbf{u}}_1, \tilde{\mathbf{u}}_2, \ldots, \tilde{\mathbf{u}}_n$. Given a positive integer d such that $d \leq n$, let $\tilde{\mathbf{S}}_\mathbf{A} := \text{diag}(\tilde{\lambda}_1, \ldots, \tilde{\lambda}_d) \in \mathbb{R}^{d \times d}$ and let $\tilde{\mathbf{U}}_\mathbf{A} := [\tilde{\mathbf{u}}_1 | \ldots | \tilde{\mathbf{u}}_d] \in \mathbb{O}_{n,d}$. The *Laplacian spectral embedding* (LSE) of $\mathbf{A}$ into $\mathbb{R}^d$ is then defined to be the $n \times d$ matrix $\breve{\mathbf{X}} := \tilde{\mathbf{U}}_\mathbf{A}|\tilde{\mathbf{S}}_\mathbf{A}|^{1/2}$. The matrix $\breve{\mathbf{X}}$ serves as a consistent estimator for the matrix $(\text{diag}(\mathbf{X}\mathbf{I}_{d^-}^{d^+}\mathbf{X}^\top\mathbf{1}_n))^{-1/2}\mathbf{X}$ up to indefinite orthogonal transformation as $n \to \infty$. ▲

Remark 20 (Consistent estimation and parametrization involving latent positions)**.** The matrices $\mathbf{X}$ and $(\text{diag}(\mathbf{X}\mathbf{I}_{d^-}^{d^+}\mathbf{X}^\top\mathbf{1}_n))^{-1/2}\mathbf{X}$, which are one-to-one invertible transformations of each other, may be viewed as providing different parametrizations of GRDPG graphs. As such, comparing $\hat{\mathbf{X}}$ and $\breve{\mathbf{X}}$ as estimators is non-trivial. In order to carry out such a comparison, we subsequently adopt an information-theoretic approach in which we consider a particular choice of f-divergence which is both an-

alytically tractable and statistically interpretable in the current setting.

For the subsequent purposes of the present work, Theorems 36 and 37 (below) state slightly weaker formulations of the corresponding limit theorems obtained in Rubin-Delanchy et al. (2017) for adjacency and Laplacian spectral embedding.

Theorem 36 (ASE limit theorem for GRDPG, adapted from Rubin-Delanchy et al. (2017))**.** *Assume the d-dimensional GRDPG setting in Definition 34 with* $\rho_n \equiv 1$*. Let* $\hat{\mathbf{X}}$ *be the adjacency spectral embedding into* $\mathbb{R}^d$ *with i-th row denoted by* $\hat{X}_i$*. Let* $\Phi(\cdot, \mathbf{\Sigma})$ *denote the cumulative distribution function of the centered multivariate normal distribution in* $\mathbb{R}^d$ *with covariance matrix* $\mathbf{\Sigma}$*. Then, with respect to the adjacency spectral embedding, there exists a sequence of matrices* $\mathbf{Q} \equiv \mathbf{Q}_n \in \mathbb{O}(d^+, d^-)$ *such that, for any* $\boldsymbol{z} \in \mathbb{R}^d$*,*

$$\Pr\left[\sqrt{n}\left(\mathbf{Q}\hat{X}_i - X_i\right) \leq \boldsymbol{z}\right] \to \int_{\mathcal{X}} \Phi(\boldsymbol{z}, \mathbf{\Sigma}(\boldsymbol{x}))dF(\boldsymbol{x}) \tag{5.4}$$

as $n \to \infty$*. Here, for* $X_1 \sim F$*,* $\mathbf{\Delta} := \mathbb{E}[X_1 X_1^\top]$*, and the scalar quantity* $g(\boldsymbol{x}, X_1) := \langle \mathbf{I}_{d^-}^{d^+}\boldsymbol{x}, X_1\rangle(1 - \langle \mathbf{I}_{d^-}^{d^+}\boldsymbol{x}, X_1\rangle)$*, the covariance matrix* $\mathbf{\Sigma}(\boldsymbol{x})$ *is given by*

$$\mathbf{I}_{d^-}^{d^+}\mathbf{\Delta}^{-1}\mathbb{E}\left[g(\boldsymbol{x}, X_1)X_1X_1^\top\right]\mathbf{\Delta}^{-1}\mathbf{I}_{d^-}^{d^+}.$$

Theorem 37 (LSE limit theorem for GRDPG, adapted from Rubin-Delanchy et al. (2017))**.** *Assume the d-dimensional GRDPG setting in Definition 34 with* $\rho_n \equiv 1$*.*

Let $\breve{\mathbf{X}}$ *be the Laplacian spectral embedding into* $\mathbb{R}^d$ *with* i*-th row denoted by* $\breve{X}_i$*. Let* $\Phi(\cdot, \mathbf{\Sigma})$ *denote the cumulative distribution function of the centered multivariate normal distribution in* $\mathbb{R}^d$ *with covariance matrix* $\mathbf{\Sigma}$*. Then, with respect to the Laplacian spectral embedding, there exists a sequence of matrices* $\tilde{\mathbf{Q}} \equiv \tilde{\mathbf{Q}}_n \in \mathbb{O}(d^+, d^-)$ *such that, for any* $\boldsymbol{z} \in \mathbb{R}^d$*,*

$$\Pr\left[n\left(\tilde{\mathbf{Q}}\breve{X}_i - \frac{X_i}{\sqrt{\sum_j \langle \mathbf{I}_{d^-}^{d^+} X_i, X_j\rangle}}\right) \leq z\right] \to \int_{\mathcal{X}} \Phi(\boldsymbol{z}, \tilde{\mathbf{\Sigma}}(\boldsymbol{x}))dF(\boldsymbol{x}) \tag{5.5}$$

as $n \to \infty$*. Here, for* $X_1 \sim F$*,* $\boldsymbol{\mu} := \mathbb{E}[X_1]$*, and* $\tilde{\mathbf{\Delta}} := \mathbb{E}\left[\langle \mathbf{I}_{d^-}^{d^+}\boldsymbol{\mu}, X_1\rangle^{-1} X_1 X_1^\top\right]$*, then* $\tilde{g}(\boldsymbol{x}, X_1) := \left(\langle \mathbf{I}_{d^-}^{d^+}\boldsymbol{\mu}, \boldsymbol{x}\rangle^{-1}\langle \mathbf{I}_{d^-}^{d^+}\boldsymbol{x}, X_1\rangle(1 - \langle \mathbf{I}_{d^-}^{d^+}\boldsymbol{x}, X_1\rangle)\right)$*, and* $\tilde{\mathbf{\Sigma}}(\boldsymbol{x})$ *is given by*

$$\mathbf{I}_{d^-}^{d^+}\tilde{\mathbf{\Delta}}^{-1}\mathbb{E}\left[\tilde{g}(\boldsymbol{x}, X_1)\left(\frac{X_1}{\langle \mathbf{I}_{d^-}^{d^+}\boldsymbol{\mu}, X_1\rangle} - \frac{\tilde{\mathbf{\Delta}}\mathbf{I}_{d^-}^{d^+}\boldsymbol{x}}{2\langle \mathbf{I}_{d^-}^{d^+}\boldsymbol{\mu}, \boldsymbol{x}\rangle}\right)\left(\frac{X_1}{\langle \mathbf{I}_{d^-}^{d^+}\boldsymbol{\mu}, X_1\rangle} - \frac{\tilde{\mathbf{\Delta}}\mathbf{I}_{d^-}^{d^+}\boldsymbol{x}}{2\langle \mathbf{I}_{d^-}^{d^+}\boldsymbol{\mu}, \boldsymbol{x}\rangle}\right)^\top\right]\tilde{\mathbf{\Delta}}^{-1}\mathbf{I}_{d^-}^{d^+}.$$

5.4 Spectral embedding performance

We desire to compare the large-n sample relative performance of adjacency and Laplacian spectral embedding for subsequent inference, where the subsequent inference task is naturally taken to be the problem of recovering latent block assignments. Here, measuring spectral embedding performance will correspond to estimating the large-sample optimal error rate for recovering the underlying block assignments following each of the spectral embeddings. Towards this end, we now introduce Chernoff information and Chernoff divergence as appropriate information-theoretic quantities.

Given independent and identically distributed random vectors Y_i arising from one of two absolutely continuous multivariate distributions F_1 and F_2 on $\Omega = \mathbb{R}^d$ with density functions f_1 and f_2, respectively, we are interested in testing the simple null hypothesis $\mathbb{H}_0 : F = F_1$ against the simple alternative hypothesis $\mathbb{H}_\text{A} : F = F_2$. In this framework, a statistical test T can be viewed as a sequence of mappings $T_m : \Omega^m \to \{1, 2\}$ indexed according to sample size m such that T_m returns the value two when $\mathbb{H}_0$ is rejected in favor of $\mathbb{H}_\text{A}$ and correspondingly returns the value one when $\mathbb{H}_0$ is favored. For each m, the corresponding significance level and type-II error are denoted by α_m and β_m, respectively.

Assume that the prior probability of $\mathbb{H}_0$ being true is given by $\pi \in (0, 1)$. For a given $\alpha_m^\star \in (0, 1)$, let $\beta_m^\star \equiv \beta_m^\star(\alpha_m^\star)$ denote the type-II error associated with the corresponding likelihood ratio test when the type-I error is at most $\alpha_m^\star$. Then, the *Bayes risk* in deciding between $\mathbb{H}_0$ and $\mathbb{H}_\text{A}$ given m independent random vectors $Y_1, Y_2, \ldots, Y_m$ is given by

$$\inf_{\alpha_m^\star \in (0,1)} \pi\alpha_m^\star + (1 - \pi)\beta_m^\star. \tag{5.6}$$

The Bayes risk is intrinsically related to *Chernoff information* (Chernoff, 1952, 1956), $C(F_1, F_2)$, namely

$$\lim_{m\to\infty} \tfrac{1}{m} \left[\inf_{\alpha_m^\star \in (0,1)} \log(\pi\alpha_m^\star + (1 - \pi)\beta_m^\star) \right] = -C(F_1, F_2), \tag{5.7}$$

where

$$C(F_1, F_2) := -\log\left[\inf_{t\in(0,1)} \int_{\mathbb{R}^d} f_1^t(\mathbf{x}) f_2^{1-t}(\mathbf{x}) d\mathbf{x}\right] = \sup_{t\in(0,1)} \left[-\log \int_{\mathbb{R}^d} f_1^t(\mathbf{x}) f_2^{1-t}(\mathbf{x}) d\mathbf{x}\right].$$

In words, the Chernoff information between F_1 and F_2 is the exponential rate at which the Bayes risk decreases as $m \to \infty$. Note that the Chernoff information is independent of the prior probability π. A version of Eq. (5.7) also holds when considering $K \geq 3$ hypothesis with distributions $F_1, F_2, \ldots, F_K$, thereby introducing the quantity $\min_{k\neq l} C(F_k, F_l)$; more discussion is provided in Tang and Priebe (2018).

Chernoff information can be expressed in terms of the *Chernoff divergence* between distributions F_1 and F_2, defined for $t \in (0, 1)$ as

$$C_t(F_1, F_2) = -\log \int_{\mathbb{R}^d} f_1^t(\mathbf{x}) f_2^{1-t}(\mathbf{x}) d\mathbf{x}, \tag{5.8}$$

which yields the relation

$$C(F_1, F_2) = \sup_{t\in(0,1)} C_t(F_1, F_2). \tag{5.9}$$

The Chernoff divergence is an example of an f-divergence and as such satisfies the data processing lemma (Liese and Vajda, 2006) and is invariant with respect to invertible transformations (Devroye et al., 2013). One could instead use another f-divergence for the purpose of comparing the two embedding methods, such as the

Kullback-Liebler divergence. Our choice is motivated by the aforementioned relationship with Bayes risk in Eq. (5.7).

In this chapter we explicitly consider multivariate normal distributions as a consequence of Theorems 36 and 37 when conditioning on the individual underlying latent positions for stochastic block model graphs. In particular, given $F_1 = \mathcal{N}(\boldsymbol{\mu}_1, \boldsymbol{\Sigma}_1)$, $F_2 = \mathcal{N}(\boldsymbol{\mu}_2, \boldsymbol{\Sigma}_2)$, and $t \in (0,1)$, then for $\boldsymbol{\Sigma}_t := t\boldsymbol{\Sigma}_1 + (1-t)\boldsymbol{\Sigma}_2$, the Chernoff information between F_1 and F_2 is given by

$$\begin{aligned} C(F_1, F_2) &= \sup_{t\in(0,1)} \left[\tfrac{t(1-t)}{2} (\boldsymbol{\mu}_2 - \boldsymbol{\mu}_1)^\top \boldsymbol{\Sigma}_t^{-1} (\boldsymbol{\mu}_2 - \boldsymbol{\mu}_1) + \tfrac{1}{2} \log \left(\tfrac{\det(\boldsymbol{\Sigma}_t)}{\det(\boldsymbol{\Sigma}_1)^t \det(\boldsymbol{\Sigma}_2)^{1-t}} \right) \right] \\ &= \sup_{t\in(0,1)} \left[\tfrac{t(1-t)}{2} \|\boldsymbol{\mu}_2 - \boldsymbol{\mu}_1\|^2_{\boldsymbol{\Sigma}_t^{-1}} + \tfrac{1}{2} \log \left(\tfrac{\det(\boldsymbol{\Sigma}_t)}{\det(\boldsymbol{\Sigma}_1)^t \det(\boldsymbol{\Sigma}_2)^{1-t}} \right) \right]. \end{aligned}$$

Let $\mathbf{B} \in (0,1)^{K\times K}$ and $\boldsymbol{\pi}$ denote the matrix of block edge probabilities and the vector of block assignment probabilities for a K-block stochastic block model as before. This corresponds to a special case of the GRDPG model with signature (d^+, d^-), $d^+ + d^- = \operatorname{rank}(\mathbf{B})$, and latent positions $\boldsymbol{\nu}_k \in \mathbb{R}^{\operatorname{rank}(\mathbf{B})}$. For an n-vertex SBM graph with parameters $(\mathbf{B}, \boldsymbol{\pi})$, the large-sample optimal error rate for recovering block assignments when performing adjacency spectral embedding can be characterized by the quantity $\rho_{\mathrm{A}} \equiv \rho_{\mathrm{A}}(\mathbf{B}, \boldsymbol{\pi}, n)$ defined by

$$\rho_{\mathrm{A}} := \min_{k\neq l} \sup_{t\in(0,1)} \left[\tfrac{nt(1-t)}{2} \|\boldsymbol{\nu}_k - \boldsymbol{\nu}_l\|^2_{\boldsymbol{\Sigma}_{kl}^{-1}(t)} + \tfrac{1}{2} \log \left(\tfrac{\det(\boldsymbol{\Sigma}_{kl}(t))}{\det(\boldsymbol{\Sigma}_k)^t \det(\boldsymbol{\Sigma}_l)^{1-t}} \right) \right], \tag{5.10}$$

where $\mathbf{\Sigma}_{kl}(t) := t\mathbf{\Sigma}_k + (1-t)\mathbf{\Sigma}_l$ for $t \in (0,1)$.

Similarly for Laplacian spectral embedding, $\rho_{\mathrm{L}} \equiv \rho_{\mathrm{L}}(\mathbf{B}, \boldsymbol{\pi}, n)$, where

$$\rho_{\mathrm{L}} := \min_{k \neq l} \sup_{t \in (0,1)} \left[\tfrac{nt(1-t)}{2} \|\tilde{\boldsymbol{\nu}}_k - \tilde{\boldsymbol{\nu}}_l\|^2_{\tilde{\mathbf{\Sigma}}_{kl}^{-1}(t)} + \tfrac{1}{2} \log \left(\tfrac{\det(\tilde{\mathbf{\Sigma}}_{kl}(t))}{\det(\tilde{\mathbf{\Sigma}}_k)^t \det(\tilde{\mathbf{\Sigma}}_l)^{1-t}} \right) \right], \tag{5.11}$$

with $\tilde{\mathbf{\Sigma}}_{kl}(t) := t\tilde{\mathbf{\Sigma}}_k + (1-t)\tilde{\mathbf{\Sigma}}_l$ and $\tilde{\boldsymbol{\nu}}_k := \boldsymbol{\nu}_k / (\sum_{k'} \pi_{k'} \langle \mathbf{I}_{d^-}^{d^+} \boldsymbol{\nu}_{k'}, \boldsymbol{\nu}_k \rangle)^{1/2}$.

The factor n in Eqs. (5.10)–(5.11) arises from the implicit consideration of the appropriate (non-singular) theoretical sample covariance matrices. To assist in the comparison and interpretation of the quantities ρ_{A} and ρ_{L}, we assume throughout that $n_k = n\pi_k$ for $\tilde{\boldsymbol{\nu}}_k$. The logarithmic terms in Eqs. (5.10–5.11) as well as the deviations of each term n_k from $n\pi_k$ are negligible for large n, collectively motivating the following large-sample measure of relative performance, $\rho^\star$, where

$$\frac{\rho_{\mathrm{A}}}{\rho_{\mathrm{L}}} \equiv \frac{\rho_{\mathrm{A}}(n)}{\rho_{\mathrm{L}}(n)} \to \rho^\star \equiv \frac{\rho_{\mathrm{A}}^\star}{\rho_{\mathrm{L}}^\star} := \frac{\min_{k \neq l} \sup_{t \in (0,1)} \left[t(1-t) \|\boldsymbol{\nu}_k - \boldsymbol{\nu}_l\|^2_{\mathbf{\Sigma}_{kl}^{-1}(t)} \right]}{\min_{k \neq l} \sup_{t \in (0,1)} \left[t(1-t) \|\tilde{\boldsymbol{\nu}}_k - \tilde{\boldsymbol{\nu}}_l\|^2_{\tilde{\mathbf{\Sigma}}_{kl}^{-1}(t)} \right]}. \tag{5.12}$$

Here we have suppressed the functional dependence on the underlying model parameters $\mathbf{B}$ and $\boldsymbol{\pi}$. For large n, observe that as $\rho_{\mathrm{A}}^\star$ increases, ρ_{A} also increases, and therefore the large-sample optimal error rate corresponding to adjacency spectral embedding decreases in light of Eq. (5.7) and its generalization. Similarly, large values of $\rho_{\mathrm{L}}^\star$ correspond to good theoretical performance of Laplacian spectral embedding. Thus, if $\rho^\star > 1$, then ASE is to be preferred to LSE, whereas if $\rho^\star < 1$, then LSE

is to be preferred to ASE. The case when $\rho^\star = 1$ indicates that neither ASE nor LSE is superior for the given parameters $\mathbf{B}$ and $\boldsymbol{\pi}$. To reiterate, we summarize these preferences as ASE $>$ LSE, ASE $<$ LSE, and ASE $=$ LSE, respectively.

In what follows, we fixate on the asymptotic quantity $\rho^\star$. For the two-block SBM and certain K-block SBMs exhibiting symmetry, Eq. (5.12) reduces to the form

$$\rho^\star = \frac{\sup_{t\in(0,1)} \left[t(1-t) \|\boldsymbol{\nu}_1 - \boldsymbol{\nu}_2\|^2_{\boldsymbol{\Sigma}^{-1}_{1,2}(t)} \right]}{\sup_{t\in(0,1)} \left[t(1-t) \|\tilde{\boldsymbol{\nu}}_1 - \tilde{\boldsymbol{\nu}}_2\|^2_{\tilde{\boldsymbol{\Sigma}}^{-1}_{1,2}(t)} \right]} \tag{5.13}$$

for canonically specified latent positions $\boldsymbol{\nu}_1$ and $\boldsymbol{\nu}_2$. In some cases it is possible to concisely obtain analytic expressions (in t) for both the numerator and denominator. In other cases this is not possible. A related challenge with respect to Eq. (5.12) is analytically inverting the interpolated block conditional covariance matrices $\boldsymbol{\Sigma}_{1,2}(t)$ and $\tilde{\boldsymbol{\Sigma}}_{1,2}(t)$. Section 6.4 provides additional technical details and discussion.

5.5 Elucidating network structure

5.5.1 The two-block stochastic block model

Consider the set of two-block SBMs with parameters $\boldsymbol{\pi} \equiv (\pi_1, 1-\pi_1)^\top$ and $\mathbf{B} \in \mathcal{B} := \left\{ \mathbf{B} = \left[\begin{smallmatrix} a & b \\ b & c \end{smallmatrix}\right] : a, b, c \in (0,1) \right\}$. For $\boldsymbol{\pi} = (\frac{1}{2}, \frac{1}{2})^\top$, then $a \geq c$ without loss of generality by symmetry. In general, for any fixed choice of $\boldsymbol{\pi}$, the class of models $\mathcal{B}$

can be partitioned according to matrix rank, namely

$$\begin{aligned}\mathcal{B} &\equiv \mathcal{B}_1 \bigsqcup \mathcal{B}_2 \\ &:= \{\mathbf{B} : \operatorname{rank}(\mathbf{B}) = 1; a, b, c \in (0,1)\} \bigsqcup \{\mathbf{B} : \operatorname{rank}(\mathbf{B}) = 2; a, b, c \in (0,1)\}.\end{aligned}$$

The collection of sub-models $\mathcal{B}_1$ further decomposes into the disjoint union of the Erdős–Rényi model with homogeneous edge probability $a = b = c \in (0,1)$ and its relative complement in $\mathcal{B}_1$ satisfying the determinant constraint $\det(\mathbf{B}) \equiv ac - b^2 = 0$. These partial sub-models can be viewed as one-dimensional and two-dimensional (parameter) regions in the open unit cube, $(0,1)^3$, respectively.

Similarly, the collection of sub-models $\mathcal{B}_2$ further decomposes into the disjoint union of $\mathbb{PD}_2 \cap \mathcal{B}_2$ and $\mathbb{IND}_2 \cap \mathcal{B}_2$, where $\mathbb{PD}_2$ denotes the set of positive definite matrices in $\mathbb{R}^{2\times 2}$ and $\mathbb{IND}_2 := \{\mathbf{B} \in \mathcal{B}_2 : \exists \mathbf{X} \in \mathbb{R}^{2\times 2}, \operatorname{rank}(\mathbf{X}) = 2, \mathbf{B} = \mathbf{X}\mathbf{I}_1^1\mathbf{X}^\top\}$. Here only $\mathbf{I}_0^2 \equiv \mathbf{I}_2$ and $\mathbf{I}_1^1$ are necessary for computing edge probabilities via inner products of the latent positions. Both of these partial sub-models can be viewed as three-dimensional (parameter) regions in $(0,1)^3$.

Remark 21 (Latent position parametrization)**.** One might ask whether or not for our purposes there exists a "best" latent position representation for some or even every SBM. To this end and more generally, for any $K \geq 2$ and $\mathbf{M} \in \mathbb{PD}_K \subset \mathbb{R}^{K\times K}$, there exists a unique lower-triangular matrix $\mathbf{L} \in \mathbb{R}^{K\times K}$ with positive diagonal entries such that $\mathbf{M} = \mathbf{L}\mathbf{L}^\top$ by the Cholesky matrix decomposition. This yields a canonical choice

for the matrix of latent positions $\mathbf{X}$ when $\mathbf{B}$ is positive definite. In particular, for $\mathbf{B} \in \mathbb{PD}_2$, then $\mathbf{B} = \mathbf{X}\mathbf{I}_2\mathbf{X}^\top$ with $\mathbf{X} := \begin{bmatrix} \sqrt{a} & 0 \\ b/\sqrt{a} & \sqrt{ac-b^2}/\sqrt{a} \end{bmatrix}$. In contrast, for $\mathbf{B} \in \mathbb{IND}_2$, then $\mathbf{B} = \mathbf{X}\mathbf{I}_1^1\mathbf{X}^\top$ with $\mathbf{X} := \begin{bmatrix} \sqrt{a} & 0 \\ b/\sqrt{a} & \sqrt{b^2-ac}/\sqrt{a} \end{bmatrix}$, keeping in mind that in this case $b^2 - ac > 0$. The latter factorization may be viewed informally as an indefinite Cholesky decomposition under $\mathbf{I}_1^1$. For the collection of rank one sub-models $\mathcal{B}_1$, the latent positions $\boldsymbol{\nu}_1$ and $\boldsymbol{\nu}_2$ are simply taken to be scalar-valued.

5.5.1.1 Homogeneous balanced network structure

We refer to the two-block SBM sub-model with $\mathbf{B} = \begin{bmatrix} a & b \\ b & a \end{bmatrix}$ and $\boldsymbol{\pi} = (\frac{1}{2}, \frac{1}{2})^\top$ as the *homogeneous balanced two-block SBM*. The cases when $a > b$, $a < b$, and $a = b$ correspond to the cases when $\mathbf{B}$ is positive definite, indefinite, and reduces to Erdős–Rényi, respectively. The positive definite parameter regime has the network structure interpretation of being *assortative* in the sense that the within-block edge probability a is larger than the between-block edge probability b, consistent with the affinity-based notion of community structure. In contrast, the indefinite parameter regime has the network structure interpretation of being *disassortative* in the sense that between-block edge density exceeds within-block edge density, consistent with the "opposites attract" notion of community structure.

For this SBM sub-model, $\rho^\star$ can be simplified analytically (see Section 6.4 for additional details) and can be expressed as a translation with respect to the value

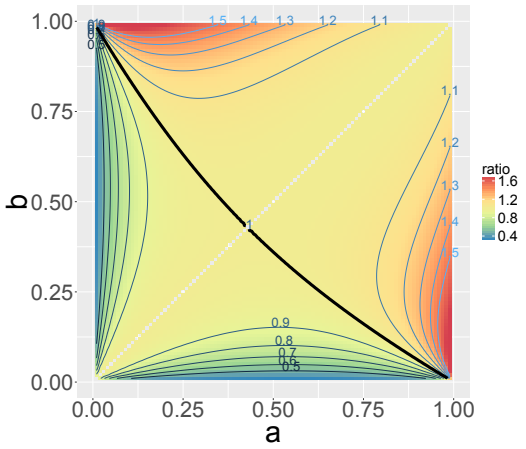

Figure 5.1: The ratio $\rho^\star$ for the homogeneous balanced sub-model in Section 5.5.1.1. The empty diagonal depicts the Erdős–Rényi model singularity.

one, namely

$$\rho^\star \equiv \rho^\star_{a,b} = 1 + \frac{(a-b)^2(3a(a-1)+3b(b-1)+8ab)}{4(a+b)^2(a(1-a)+b(1-b))} := 1 + c_{a,b} \times \psi_{a,b}, \qquad (5.14)$$

where $\psi_{a,b} := 3a(a-1)+3b(b-1)+8ab$ and $c_{a,b} > 0$. By recognizing that $\psi_{a,b}$ functions as a discriminating term, it is straightforward to read off the relative performance of ASE and LSE according to Table 5.1.

Table 5.1: Summary of embedding performance in Section 5.5.1.1

$\rho^\star = 1 \iff \psi_{a,b} = 0$; (ASE = LSE)
$\rho^\star > 1 \iff \psi_{a,b} > 0$; (ASE > LSE)
$\rho^\star < 1 \iff \psi_{a,b} < 0$; (ASE < LSE)

Further investigation of Eq. (5.14) leads to the observation that ASE < LSE for all $0 < b < a \leq \frac{3}{7}$, thereby yielding a parameter region for which LSE dominates ASE. On the other hand, for any fixed $b \in (0,1)$ there exist values $a_1 < a_2$ such

that ASE $<$ LSE under a_1, whereas ASE $>$ LSE under a_2. Figure 5.1 demonstrates that for homogeneous balanced network structure, LSE is preferred to ASE when the entries in $\mathbf{B}$ are sufficiently small, whereas conversely ASE is preferred to LSE when the entries in $\mathbf{B}$ are not too small.

Remark 22 (Model spectrum and ASE dominance I)**.** Here $\lambda_{\max}(\mathbf{B}) = a + b$, hence $\lambda_{\max}(\mathbf{B}) > 1$ implies ASE $>$ LSE by Eq. (5.14). This observation amounts to a network structure-based (i.e., $\mathbf{B}$-based) spectral sufficient condition for determining when ASE is preferred to LSE.

Remark 23 (A balanced one-dimensional SBM restricted sub-model)**.** When $b = 1 - a$, the homogeneous balanced sub-model further reduces to a one-dimensional parameter space such that $\rho^\star$ simplifies to

$$\rho^\star = 1 + \tfrac{1}{4}(2a - 1)^2 \geq 1, \tag{5.15}$$

demonstrating that ASE uniformly dominates LSE for this restricted sub-model. Additionally, it is potentially of interest to note that in this setting the marginal covariance matrices from Theorem 36 for ASE coincide for each block. In contrast, the same behavior is not true for LSE.

5.5.1.2 Core-periphery network structure

We refer to the two-block SBM sub-model with $\mathbf{B} = \left[\begin{smallmatrix} a & b \\ b & b \end{smallmatrix}\right]$ and $\boldsymbol{\pi} = (\pi_1, 1-\pi_1)^\top$ as the *core-periphery two-block SBM*. We explicitly consider the balanced (block size) regime in which $\boldsymbol{\pi} = (\frac{1}{2}, \frac{1}{2})^\top$ and an unbalanced regime in which $\boldsymbol{\pi} = (\frac{1}{4}, \frac{3}{4})^\top$. Here, the cases $a > b$, $a < b$, and $a = b$ correspond to the cases when $\mathbf{B}$ is positive definite, indefinite, and reduces to the Erdős–Rényi model, respectively.

For this sub-model, the ratio $\rho^\star$ is not analytically tractable in general. That is to say, simple closed-form solutions do not simultaneously exist for the numerator and denominator in the definition of $\rho^\star$. As such, Figure 5.2 is obtained numerically by evaluating $\rho^\star$ on a grid of points in $(0,1)^2$ followed by smoothing.

For $a > b$, graphs generated from this SBM sub-model exhibit the popular interpretation of core-periphery structure in which vertices forming a dense core are attached to surrounding periphery vertices with comparatively smaller edge connectivity. Provided the core is sufficiently dense, namely for $a > \frac{1}{4}$ in the balanced regime and $a > \frac{1}{2}$ in the unbalanced regime, Figure 5.2 demonstrates that ASE $>$ LSE. Conversely, ASE $<$ LSE uniformly in $0 < b < a$ for small enough values of a in both the balanced and unbalanced regime.

In contrast, when $a < b$, the sub-model produces graphs whose network structure is interpreted as having a comparatively sparse induced subgraph which is strongly connected to all vertices in the graph but for which the subgraph vertices exhibit comparatively weaker connectivity. Alternatively, the second block may itself be

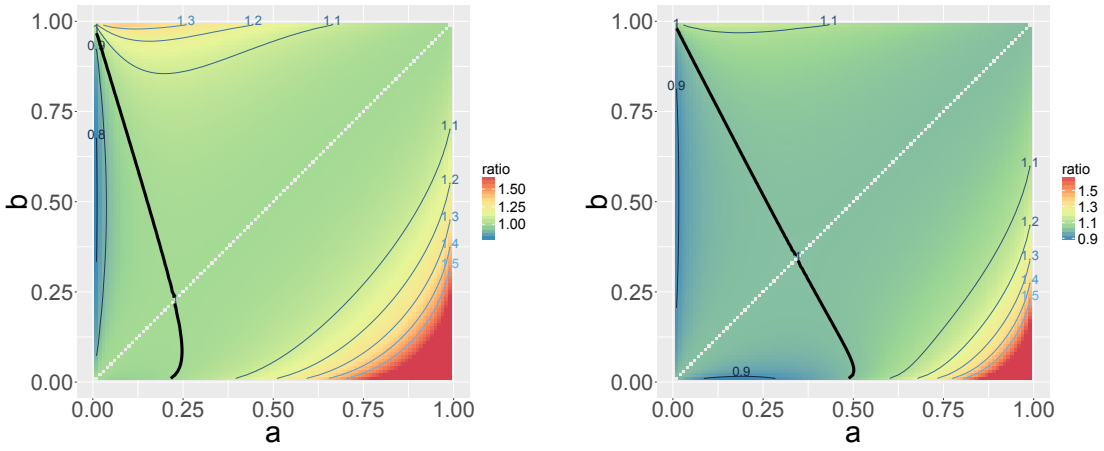

(a) $\rho^\star$ when $\boldsymbol{\pi} = (\frac{1}{2}, \frac{1}{2})^\top$ i.e., balanced **(b)** $\rho^\star$ when $\boldsymbol{\pi} = (\frac{1}{4}, \frac{3}{4})^\top$ i.e., unbalanced

Figure 5.2: The ratio $\rho^\star$ for the core-periphery sub-model in Section 5.5.1.2. The empty diagonal depicts the Erdős–Rényi model singularity.

viewed as a dense core which is simultaneously densely connected to all vertices in the graph. Figure 5.2 illustrates that for the balanced regime, LSE is preferred for sparser induced subgraphs. Put differently, for large enough dense core with dense periphery, then ASE is the preferable spectral embedding procedure. LSE is preferred to ASE in only a relatively small region corresponding approximately to the triangular region where $0 < b < 1 - 4a$, which as a subset of the unit square has area $\frac{1}{8}$. Similar behavior holds for the unbalanced regime for approximately the (enlarged) triangular region of the parameter space where $0 < b < 1 - 2a$, which as a subset of the unit square has area $\frac{1}{4}$.

Figure 5.2 suggests that as π_1 decreases from $\frac{1}{2}$ to $\frac{1}{4}$, LSE is favored in a growing region of the parameter space, albeit still in a smaller region than that for which ASE is to be preferred. Together with the observation that LSE dominates in the lower-left corner of the plots in Figure 5.2 where a and b have small magnitude, we are led to

say in summary that LSE favors relatively sparse core-periphery network structure. To reiterate, sparsity is interpreted with respect to the parameters a and b, keeping in mind the underlying simplifying assumption that $n_k = n\pi_k$ for $k = 1, 2$.

Remark 24 (Model spectrum and ASE dominance II)**.** For $0 < b < a < 1$, then $\lambda_{\max}(\mathbf{B}) = \frac{1}{2}\left(a + b + \sqrt{a^2 - 2ab + 5b^2}\right)$. Numerical evaluation (not shown) yields that $\lambda_{\max}(\mathbf{B}) > \frac{1}{2}$ implies ASE $>$ LSE. Along the same lines as the discussion in Section 5.5.1.1, this observation provides a network structure (i.e. $\mathbf{B}$-based) spectral sufficient condition for this sub-model for determining the relative embedding performance ASE $>$ LSE.

5.5.1.3 Two-block rank one sub-models

The sub-model for which $\mathbf{B} = \left[\begin{smallmatrix} a & b \\ b & c \end{smallmatrix}\right]$ with $a, b, c \in (0, 1)$ and $\det(\mathbf{B}) = 0$ can be re-parameterized according to the assignments $a \mapsto p^2$ and $c \mapsto q^2$, yielding $\mathbf{B} = \left[\begin{smallmatrix} p^2 & pq \\ pq & q^2 \end{smallmatrix}\right]$ with $p, q \in (0, 1)$. Here $\operatorname{rank}(\mathbf{B}) = 1$ and $\mathbf{B}$ is positive semidefinite, corresponding to the one-dimensional RDPG model with latent positions given by the scalars p and q with associated probabilities π_1 and π_2, respectively. Explicit computation yields the expression

$$\rho^\star = \frac{(\sqrt{p}+\sqrt{q})^2(\pi_1 p^2+\pi_2 q^2)^2\left(\sqrt{\pi_1 p(1-p^2)+\pi_2 q(1-pq)}+\sqrt{\pi_1 p(1-pq)+\pi_2 q(1-q^2)}\right)^2}{4(\pi_1 p+\pi_2 q)^2\left(\sqrt{\pi_1 p^4(1-p^2)+\pi_2 pq^3(1-pq)}+\sqrt{\pi_1 p^3 q(1-pq)+\pi_2 q^4(1-q^2)}\right)^2}, \tag{5.16}$$

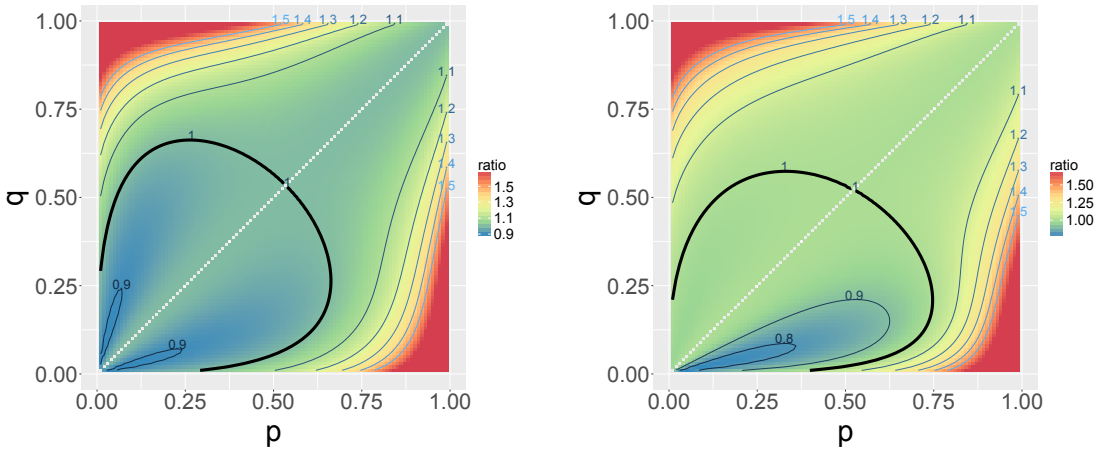

(a) $\rho^\star$ when $\boldsymbol{\pi} = (\frac{1}{2}, \frac{1}{2})^\top$ i.e. balanced **(b)** $\rho^\star$ when $\boldsymbol{\pi} = (\frac{1}{4}, \frac{3}{4})^\top$ i.e. unbalanced

Figure 5.3: The ratio $\rho^\star$ for the two-block rank one sub-model in Section 5.5.1.3. The empty diagonal depicts the Erdős–Rényi model singularity.

whereby $\rho^\star$ is given as an explicit, closed-form function of the parameter values p, q, and π_1 with $\pi_2 = 1 - \pi_1$. The simplicity of this sub-model together with its analytic tractability with respect to both $\mathbf{B}$ and $\boldsymbol{\pi}$ makes it particularly amenable to study for the purpose of elucidating network structure. Below, consideration of this sub-model further illustrates the relationship between (parameter-based) sparsity and relative embedding performance.

Figure 5.3 demonstrates how LSE favors sparse graphs in the sense of the edge probabilities, p and q, as well as how relative performance changes in light of block sizes, reflected by π_1. Here the underlying $\mathbf{B}$ matrix is always positive semidefinite, and each of the regions $p > q$ and $p < q$ corresponds to a modified notion of core-periphery structure. For example, when $p > q$, then $\mathbf{B} = \left[\begin{smallmatrix} p_1 & p_2 \\ p_2 & p_3 \end{smallmatrix}\right]$ with $p_1 > p_2 > p_3$, yielding a hierarchy of core-periphery structure when passing from vertices that are both in block one to vertices that are in different blocks and finally to vertices that are

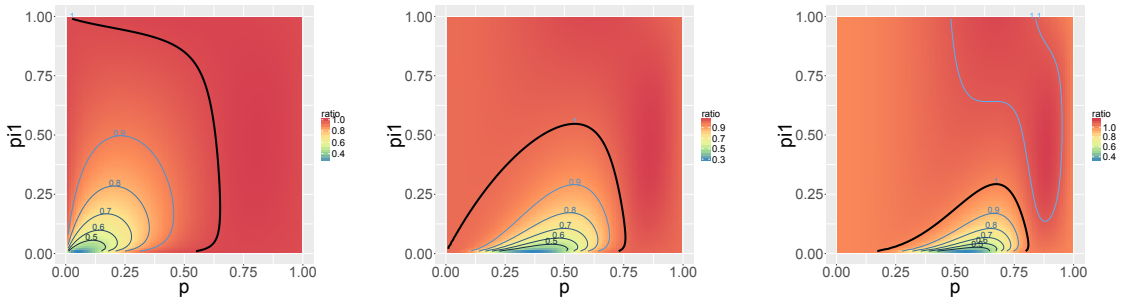

(a) $\rho^\star$ with quadratic q **(b)** $\rho^\star$ with quartic q **(c)** $\rho^\star$ with sextic q

Figure 5.4: The ratio $\rho^\star$ for $p, \pi_1 \in (0,1)$, $q = p^\gamma$, $\gamma \in \{2,4,6\}$ in Section 5.5.1.3.

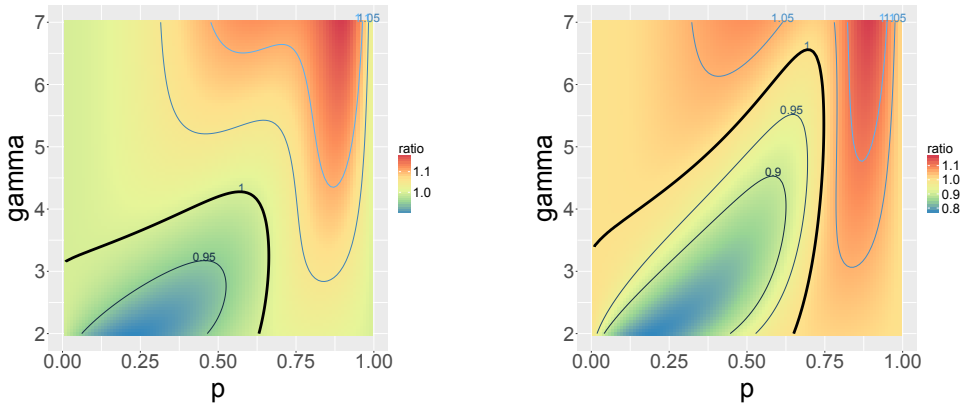

(a) $\rho^\star$ when $\boldsymbol{\pi} = (\frac{1}{2}, \frac{1}{2})^\top$ i.e. balanced **(b)** $\rho^\star$ when $\boldsymbol{\pi} = (\frac{1}{4}, \frac{3}{4})^\top$ i.e. unbalanced

Figure 5.5: The ratio $\rho^\star$ for $p \in (0,1), \gamma \in [2,7]$ when $q = p^\gamma$ in Section 5.5.1.3.

both in block two. Note the similar behavior in the bottom-right triangular regions in Figure 5.3a–5.3b and in the same bottom-right triangular region in Figure 5.2.

Remark 25 (The two-block polynomial p SBM restricted sub-model)**.** Consider the restricted sub-model in which $\mathbf{B} = \begin{bmatrix} p^2 & p^{\gamma+1} \\ p^{\gamma+1} & p^{2\gamma} \end{bmatrix}$, where $\gamma > 1$ and $\pi_1 \in (0,1)$. For $\gamma \gg 1$ and π_1 fixed, then $\rho^\star$ in Eq. (5.16) satisfies the approximate behavior

$$\rho^\star \approx \frac{\left(1+\sqrt{1-p^2}\right)^2}{4(1-p^2)}. \tag{5.17}$$

The above approximation exceeds the value one since $1 > \sqrt{1-p^2}$ for $p \in (0,1)$ and is simultaneously agnostic with respect to π_1. Moreover, for large values of γ, the block edge probability matrix is approximately of the form $\mathbf{B} \approx \left[\begin{smallmatrix} p_1 & p_2 \\ p_2 & p_3 \end{smallmatrix}\right]$ with $p_1 \gg p_2 \approx p_3$, where p_2 and p_3 are very small. This restricted sub-model can therefore be viewed as exhibiting an extremal version of core-periphery structure corresponding to the extremal regions in Figure 5.2 where ASE is preferred.

In Figure 5.4, the progression from left to right corresponds to tending towards the approximation presented in Eq. (5.17). For larger values of γ when $q = p^\gamma$ (not shown), the region where ASE > LSE continues to expand. We do not discuss or pursue the taking of limits within the parameter space(s) in light of degenerate boundary value behavior and in order to avoid possible misinterpretation.

Figure 5.5 offers a different perspective in which γ is allowed to vary continuously for both the balanced and the unbalanced regime. As in Figure 5.3, Figure 5.5 demonstrates that LSE is preferred for network structure wherein the block with comparatively higher edge probability exhibits smaller block membership size.

5.5.1.4 Full rank two-block stochastic block models

This section presents a macroscopic view of full rank two-block SBMs with $\mathbf{B} = \left[\begin{smallmatrix} a & b \\ b & c \end{smallmatrix}\right]$, $(a,b,c) \in (0,1)^3$, for the regimes $\boldsymbol{\pi} = (\frac{1}{2}, \frac{1}{2})^\top$ and $\boldsymbol{\pi} = (\frac{1}{4}, \frac{3}{4})^\top$. The parameter space is partitioned via the latent space geometry of $\mathbf{B}$, namely according to whether $\mathbf{B}$ is either positive definite or indefinite.

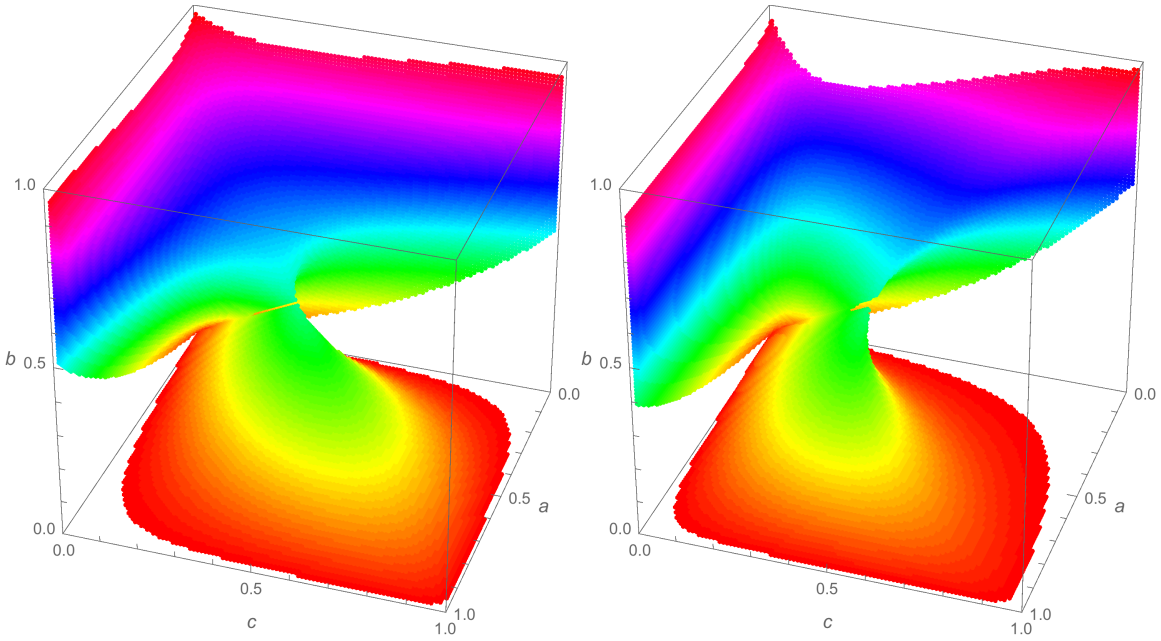

(a) $\rho^\star < 1$; $\text{rank}(\mathbf{B}) = 2$; $\boldsymbol{\pi} = (\frac{1}{2}, \frac{1}{2})^\top$ **(b)** $\rho^\star < 1$; $\text{rank}(\mathbf{B}) = 2$; $\boldsymbol{\pi} = (\frac{1}{4}, \frac{3}{4})^\top$

Figure 5.6: Parameter region where ASE $<$ LSE for full rank $\mathbf{B}$ in Section 5.5.1.4. The plots depict numerical evaluations of $\rho^\star$ for $a, b, c \in [0.01, 0.99]$ with step size 0.01.

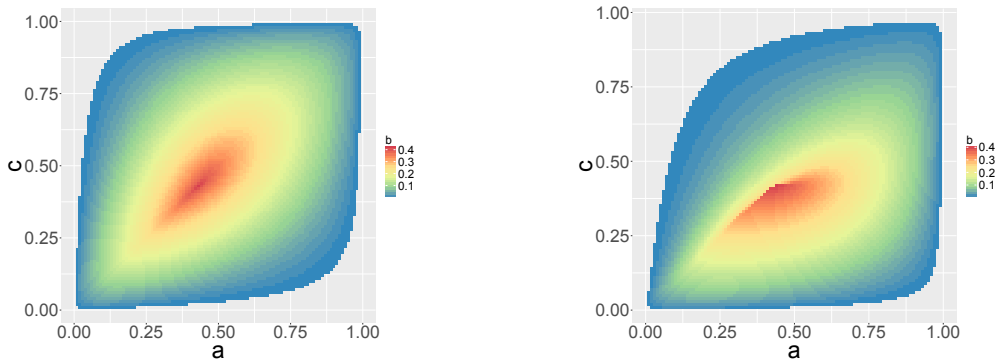

(a) $\rho^\star < 1$; $\mathbf{B} \in \mathbb{PD}_2$; $\boldsymbol{\pi} = (\frac{1}{2}, \frac{1}{2})^\top$ **(b)** $\rho^\star < 1$; $\mathbf{B} \in \mathbb{PD}_2$; $\boldsymbol{\pi} = (\frac{1}{4}, \frac{3}{4})^\top$

Figure 5.7: A top-down view of the positive definite region where ASE $<$ LSE in Section 5.5.1.4, with a, b, and c corresponding to length, depth, and width, respectively. The plots depict numerical evaluations of $\rho^\star$ for $a, b, c \in [0.01, 0.99]$ with step size 0.01.

Figure 5.6a and Figure 5.6b each present a three-dimensional view of the region in the parameter space where ASE $<$ LSE. The separate positive definite and indefinite parameter regions exhibiting ASE $<$ LSE can be seen extending from faces of the unit cube. Specifically, the conic-like region rising up from the $b = 0$ face corresponds to $\mathbf{B}$ for which $\mathbf{B} \in \mathbb{PD}_2$, whereas the hyperbolic-like regions extending from the $a = 0$ and $c = 0$ faces corresponds to $\mathbf{B}$ for which $\mathbf{B} \in \mathbb{IND}_2$.

For the balanced case reflected in Figure 5.6a, let $a \geq c$ without loss of generality by symmetry, and hence $\rho^\star$ is symmetric about the plane defined by $a = c$. For the unbalanced case shown in Figure 5.6b, symmetry no longer holds, and geometric warping behavior can be seen with respect to the $a = c$ plane. Figure 5.7a and Figure 5.7b provide a birds-eye view of the three-dimensional positive definite parameter region from the vantage point $b =$ "∞". The latter provides another view of the warping phenomenon observed for $\boldsymbol{\pi} = (\frac{1}{4}, \frac{3}{4})^\top$ that holds in general for all unbalanced regimes.

In both block size regimes depicted in Figure 5.6, the colored parameter region occupies less than one-fourth of the unit cube volumetrically, thereby quantitatively providing a coarse overall sense in which ASE is to be preferred to LSE for numerous two-block SBM models.

5.5.2 The K-block model with homogeneous balanced affinity network structure

This section generalizes the analysis in Section 5.5.1.1 to the setting of K-block homogeneous balanced affinity SBMs where $\mathbf{B}_{ij} = a$ for all $i = j$, $\mathbf{B}_{ij} = b$ for all $i \neq j$, $0 < b < a < 1$, and $\pi_i = \frac{1}{K}$ for $1 \leq i \leq K$.

Theorem 38. *For K-block homogeneous balanced affinity SBM models as in Section 5.5.2, the ratio $\rho^\star$ in Eq. (5.12) can be expressed analytically as*

$$\rho^\star = 1 + \frac{(a-b)^2(3a(a-1)+3b(b-1)(K-1)+4abK)}{4(a+(K-1)b)^2(a(1-a)+b(1-b))} := 1 + c_{a,b,K} \times \psi_{a,b,K}, \tag{5.18}$$

where $\psi_{a,b,K} := 3a(a-1) + 3b(b-1)(K-1) + 4abK$ and $c_{a,b,K} > 0$.

As in Table 5.1, the function $\psi_{a,b,K}$ is the discriminating term that explicitly characterizes the relative performance of ASE and LSE.

Here $\psi_{a,b,K}$ satisfies $(4ab - 3(a-b^2))K < \psi_{a,b,K} < (4ab)K$, and there are explicit constants $c^{(1)}_{a,b}$ and $c^{(2)}_{a,b}$ depending only on a and b such that $\frac{1}{K}c^{(1)}_{a,b} < c_{a,b,K} \times \psi_{a,b,K} < \frac{1}{K}c^{(2)}_{a,b}$. Taking a and b to be fixed, these observations allow Eq. (5.18) to be summarized in terms of K as

$$\rho^\star = 1 + \Theta_{a,b}\left(\tfrac{1}{K}\right), \tag{5.19}$$

demonstrating that $\rho^\star \to 1$ as $K \to \infty$. In words, for the class of SBMs under consideration, ASE and LSE in a sense have asymptotically (in K) equivalent embedding

performance (via $\rho^\star$). This amounts to a statement concerning a sequence of models with a necessarily growing number of vertices in order to ensure the underlying assumption of equal block sizes.

Rewriting the level-set $\psi_{a,b,K} = 0$, which holds if and only if $\rho^\star = 1$, yields

$$\left(\frac{1-a}{b}\right)\frac{1}{K} + \left(\frac{1-b}{a}\right)\frac{K-1}{K} = \frac{4}{3}, \tag{5.20}$$

together with the observation that ASE $>$ LSE (resp. ASE $<$ LSE) when the left-hand side of Eq. (5.20) is less than (resp. greater than) the value $\frac{4}{3}$. The above equation perhaps interestingly depicts a convex combination in K of a reparameterization in terms of the variables $\frac{1-a}{b}$ and $\frac{1-b}{a}$, where the value $\frac{4}{3}$ is interpretable as a Chernoff-based information theoretic threshold.

The observation that $\psi_{a,b,K} > (4ab - 3(a-b^2))K$ in the context of Eq. (5.18) implies a sufficient condition for determining a parameter region in which ASE $>$ LSE *uniformly in* K. Specifically, the condition $(4ab - 3(a-b^2)) > 0$, equivalently written as $\frac{a-b^2}{ab} < \frac{4}{3}$, ensures that $\psi_{a,b,K} > 0$ and hence that $\rho^\star > 1$.

Remark 26 (Detectability and phase transitions in random graph models)**.** With respect to the random graph literature, the setting considered in this chapter corresponds to a strong consistency regime (i.e., exact recovery) in which the block membership of each individual vertex is recovered almost surely for graphs on n vertices with $n \to \infty$. For different regimes where edge probabilities are allowed to

decrease as a function of n, numerous deep and fascinating detectability and phase transition phenomena are known, some of which also employ Chernoff divergence and related considerations (Abbe, 2018). In the context of homogeneous balanced affinity SBMs, the quantity SNR $:= \frac{(a-b)^2}{K(a+(K-1)b)}$ has been shown to function as an important information-theoretic signal-to-noise ratio. Here too the SNR appears, albeit with respect to $c_{a,b,K}$, in the sense that

$$c_{a,b,K} := \frac{(a-b)^2}{4(a+(K-1)b)^2(a(1-a)+b(1-b))} \equiv \left(\frac{(a-b)^2}{K(a+(K-1)b)}\right) \tilde{c}_{a,b,K}$$

for some constant $\tilde{c}_{a,b,K} > 0$. Perhaps more interestingly,

$$c_{a,b,K} \equiv \frac{1}{4}\left(\frac{\lambda_{\min}(\mathbf{B}(K))}{\lambda_{\max}(\mathbf{B}(K))}\right)^2 \left(\frac{1}{\sigma^2(\mathbf{B}_{11}(K)) + \sigma^2(\mathbf{B}_{12}(K))}\right),$$

where $\sigma^2(\mathbf{B}_{ij}(K))$ is the edge variance corresponding to a pair of vertices in blocks i and j, together with $\lambda_{\min}(\mathbf{B}(K)) = a - b$ and $\lambda_{\max}(\mathbf{B}(K)) = a + (K-1)b$, noting that the constant factor $\frac{1}{4}$ could just as easily be absorbed by redefining $\psi_{a,b,K}$. We believe that these observations warrant further investigation in future work.

5.6 Discussion

Loosely speaking, Laplacian spectral embedding may be viewed as a degree-normalized version of adjacency spectral embedding in light of Eq. (5.3). As such,

our analysis complements existing literature that seeks to understand normalization in the context of spectral methods (Sarkar and Bickel, 2015; Von Luxburg, 2007). Moreover, our work together with Rubin-Delanchy et al. (2017) addresses network models exhibiting indefinite geometry, an area that has received comparatively limited attention in the statistical network analysis literature. The ability of indefinite modeling considerations to reflect widely-observed disassortative community structure is encouraging and suggests future research activity in this and related directions.

Core-periphery network structure, broadly construed, is demonstrably ubiquitous in real-world networks (Csermely et al., 2013; Holme, 2005; Leskovec et al., 2009). With this understanding and the ability of the SBM to serve as a building block for hierarchically modeling complex network structure, our findings pertaining to spectral embedding for core-periphery structure may be of particular interest.

This chapter examines the information-theoretic relationship between the performance of two competing, widely popular graph embeddings and subsequent vertex clustering with an eye towards underlying network model structure. The findings presented in Section 5.5 support the claim that, for *sparsity* interpreted as $\mathbf{B}$ having entries that are small, loosely speaking, "Laplacian spectral embedding favors relatively sparse graphs, whereas adjacency spectral embedding favors not-too-sparse graphs." Moreover, our results provide evidence in support of the claim that "adjacency spectral embedding favors certain core-periphery network structure." Of course, caution must be exercised when making such general assertions, since our findings demonstrate in-

tricate and nuanced functional relationships linking spectral embedding performance to network model structure. Nevertheless, we believe such summary statements are both faithful and useful for conveying a high-level, macroscopic overview of the investigation presented in this chapter.

Chapter 6

Proofs and supplementary material

6.1 Proofs for Chapter 2

6.1.1 Singular subspace geometric bounds

Let $\mathbf{U}, \widehat{\mathbf{U}} \in \mathbb{O}_{p\times r}$ and $\mathbf{W}_{\mathbf{U}} \in \mathbb{O}_r$ denote the Frobenius-optimal Procrustes transformation. We shall use the fact that $\|\sin\boldsymbol{\Theta}(\widehat{\mathbf{U}}, \mathbf{U})\|_2 = \|\mathbf{U}_\perp^\top \widehat{\mathbf{U}}\|_2 = \|(\mathbf{I} - \mathbf{U}\mathbf{U}^\top)\widehat{\mathbf{U}}\widehat{\mathbf{U}}^\top\|_2$ (Bhatia (1997), Chapter 7).

Lemma 39. *Let $\mathbf{T} \in \mathbb{R}^{r\times r}$ be arbitrary. Then*

$$\left\|\sin\boldsymbol{\Theta}(\widehat{\mathbf{U}}, \mathbf{U})\right\|_2 = \left\|\widehat{\mathbf{U}} - \mathbf{U}\mathbf{U}^\top\widehat{\mathbf{U}}\right\|_2 \leq \|\widehat{\mathbf{U}} - \mathbf{U}\mathbf{T}\|_2, \tag{6.1}$$

$$\frac{1}{2}\left\|\sin\boldsymbol{\Theta}(\widehat{\mathbf{U}}, \mathbf{U})\right\|_2^2 \leq \left\|\mathbf{U}^\top\widehat{\mathbf{U}} - \mathbf{W}_{\mathbf{U}}\right\|_2 \leq \left\|\sin\boldsymbol{\Theta}(\widehat{\mathbf{U}}, \mathbf{U})\right\|_2^2. \tag{6.2}$$

Proof. The matrix difference $(\widehat{\mathbf{U}} - \mathbf{U}\mathbf{U}^\top\widehat{\mathbf{U}}) \in \mathbb{R}^{p\times r}$ represents the residual of $\widehat{\mathbf{U}}$ after orthogonally projecting onto the subspace spanned by the columns of $\mathbf{U}$. Note that $\|\mathbf{A}\|_2^2 = \|\mathbf{A}^\top\mathbf{A}\|_2 = \sup_{\|\mathbf{x}\|_2=1} |\langle \mathbf{A}^\top\mathbf{A}\mathbf{x}, \mathbf{x}\rangle|$, and so several intermediate steps of computation yield that for any $\mathbf{T} \in \mathbb{R}^{r\times r}$,

$$\begin{aligned}
\big\|\widehat{\mathbf{U}} - \mathbf{U}\mathbf{U}^\top\widehat{\mathbf{U}}\big\|_2^2 &= \sup_{\|\mathbf{x}\|_2=1} \big|\big\langle \big(\widehat{\mathbf{U}} - \mathbf{U}\mathbf{U}^\top\widehat{\mathbf{U}}\big)^\top \big(\widehat{\mathbf{U}} - \mathbf{U}\mathbf{U}^\top\widehat{\mathbf{U}}\big)\mathbf{x}, \mathbf{x}\big\rangle\big| \\
&= \sup_{\|\mathbf{x}\|_2=1} \big|\big\langle \big(\mathbf{I} - \widehat{\mathbf{U}}^\top\mathbf{U}\mathbf{U}^\top\widehat{\mathbf{U}}\big)\mathbf{x}, \mathbf{x}\big\rangle\big| \\
&\leq \sup_{\|\mathbf{x}\|_2=1} \Big(\big|\big\langle \big(\mathbf{I} - \widehat{\mathbf{U}}^\top\mathbf{U}\mathbf{U}^\top\widehat{\mathbf{U}}\big)\mathbf{x}, \mathbf{x}\big\rangle\big| + \big\|\big(\mathbf{T} - \mathbf{U}^\top\widehat{\mathbf{U}}\big)\mathbf{x}\big\|_2^2\Big) \\
&= \sup_{\|\mathbf{x}\|_2=1} \big|\big\langle (\widehat{\mathbf{U}} - \mathbf{U}\mathbf{T})^\top(\widehat{\mathbf{U}} - \mathbf{U}\mathbf{T})\mathbf{x}, \mathbf{x}\big\rangle\big| \\
&= \|\widehat{\mathbf{U}} - \mathbf{U}\mathbf{T}\|_2^2.
\end{aligned}$$

On the other hand, by Proposition 4 and the above observation,

$$\begin{aligned}
\big\|\widehat{\mathbf{U}} - \mathbf{U}\mathbf{U}^\top\widehat{\mathbf{U}}\big\|_2 = \big\|\widehat{\mathbf{U}}\widehat{\mathbf{U}}^\top - \mathbf{U}\mathbf{U}^\top\widehat{\mathbf{U}}\widehat{\mathbf{U}}^\top\big\|_2 &= \big\|\big(\mathbf{I} - \mathbf{U}\mathbf{U}^\top\big)\widehat{\mathbf{U}}\widehat{\mathbf{U}}^\top\big\|_2 \\
&= \big\|\sin\boldsymbol{\Theta}(\widehat{\mathbf{U}}, \mathbf{U})\big\|_2.
\end{aligned}$$

The matrix difference $(\mathbf{U}^\top\widehat{\mathbf{U}} - \mathbf{W}_\mathbf{U}) \in \mathbb{R}^{r\times r}$ represents the extent to which $\mathbf{U}^\top\widehat{\mathbf{U}}$ with singular value decomposition $\mathbf{W}_1\boldsymbol{\Sigma}_\mathbf{U}\mathbf{W}_2^\top$ is "almost" the Frobenius-optimal Procrustes transformation $\mathbf{W}_\mathbf{U} \equiv \mathbf{W}_1\mathbf{W}_2^\top$. The orthogonal invariance of the spectral norm together with the interpretation of canonical angles between $\widehat{\mathbf{U}}$ and $\mathbf{U}$, denoted by

$\{\theta_i\}$ with $\cos(\theta_i) = \sigma_i(\mathbf{U}^\top \widehat{\mathbf{U}}) \in [0,1]$, yields

$$\left\|\mathbf{U}^\top \widehat{\mathbf{U}} - \mathbf{W}_{\mathbf{U}}\right\|_2 = \left\|\mathbf{W}_1 \mathbf{\Sigma}_{\mathbf{U}} \mathbf{W}_2^\top - \mathbf{W}_1 \mathbf{W}_2^\top\right\|_2 = \|\mathbf{\Sigma}_{\mathbf{U}} - \mathbf{I}_r\|_2 = 1 - \min_i \cos(\theta_i).$$

Thus, both

$$\left\|\mathbf{U}^\top \widehat{\mathbf{U}} - \mathbf{W}_{\mathbf{U}}\right\|_2 \leq 1 - \min_i \cos^2(\theta_i) = \max_i \sin^2(\theta_i) = \left\|\sin \mathbf{\Theta}(\widehat{\mathbf{U}}, \mathbf{U})\right\|_2^2$$

and

$$\begin{aligned}\left\|\mathbf{U}^\top \widehat{\mathbf{U}} - \mathbf{W}_{\mathbf{U}}\right\|_2 &\geq \frac{1}{2}\big(1 - \min_i \cos^2(\theta_i)\big) = \frac{1}{2} \max_i \sin^2(\theta_i) \\ &= \frac{1}{2}\left\|\sin \mathbf{\Theta}(\widehat{\mathbf{U}}, \mathbf{U})\right\|_2^2.\end{aligned}$$

□

Lemma 40. *The quantity* $\|\widehat{\mathbf{U}} - \mathbf{U}\mathbf{W}_{\mathbf{U}}\|_2$ *satisfies the lower bound*

$$\left\|\sin \mathbf{\Theta}(\widehat{\mathbf{U}}, \mathbf{U})\right\|_2 \leq \left\|\widehat{\mathbf{U}} - \mathbf{U}\mathbf{W}_2^\star\right\|_2 \leq \|\widehat{\mathbf{U}} - \mathbf{U}\mathbf{W}_{\mathbf{U}}\|_2 \tag{6.3}$$

and satisfies the upper bound

$$\|\widehat{\mathbf{U}} - \mathbf{U}\mathbf{W}_{\mathbf{U}}\|_2 \leq \left\|\sin \mathbf{\Theta}(\widehat{\mathbf{U}}, \mathbf{U})\right\|_2 + \left\|\sin \mathbf{\Theta}(\widehat{\mathbf{U}}, \mathbf{U})\right\|_2^2. \tag{6.4}$$

Taken together with Lemma 1 in Cai and Zhang (2018), an improved upper bound is

given by

$$\|\widehat{\mathbf{U}} - \mathbf{U}\mathbf{W}_{\mathbf{U}}\|_2 \leq \min\{1 + \|\sin\boldsymbol{\Theta}(\widehat{\mathbf{U}}, \mathbf{U})\|_2, \sqrt{2}\}\|\sin\boldsymbol{\Theta}(\widehat{\mathbf{U}}, \mathbf{U})\|_2. \tag{6.5}$$

Proof. The lower bound follows from setting $\mathbf{T} = \mathbf{W}_2^\star$ in Lemma 39 together with the definition of $\mathbf{W}_2^\star$. Again by Lemma 39 and together with the triangle inequality,

$$\begin{aligned}\|\widehat{\mathbf{U}} - \mathbf{U}\mathbf{W}_{\mathbf{U}}\|_2 &\leq \|\widehat{\mathbf{U}} - \mathbf{U}\mathbf{U}^\top\widehat{\mathbf{U}}\|_2 + \|\mathbf{U}(\mathbf{U}^\top\widehat{\mathbf{U}} - \mathbf{W}_{\mathbf{U}})\|_2 \\ &\leq \|\sin\boldsymbol{\Theta}(\widehat{\mathbf{U}}, \mathbf{U})\|_2 + \|\sin\boldsymbol{\Theta}(\widehat{\mathbf{U}}, \mathbf{U})\|_2^2.\end{aligned}$$

The proof of Lemma 1 in Cai and Zhang (2018) establishes that

$$\inf_{\mathbf{W}\in\mathbb{O}_r} \|\widehat{\mathbf{U}} - \mathbf{U}\mathbf{W}\|_2 \leq \|\widehat{\mathbf{U}} - \mathbf{U}\mathbf{W}_{\mathbf{U}}\|_2 \leq \sqrt{2}\|\sin\boldsymbol{\Theta}(\widehat{\mathbf{U}}, \mathbf{U})\|_2,$$

which completes the proof. □

For ease of reference and notation, Theorem 41 below states a version of the Davis–Kahan $\sin\boldsymbol{\Theta}$ theorem Davis and Kahan (1970) in the language of Yu et al. (2015). This amounts to a recasting of Theorem VII.3.2 in Bhatia (1997), and so we omit the proof.

Theorem 41. *Let* $\mathbf{M}, \widehat{\mathbf{M}} \in \mathbb{R}^{p\times p}$ *be symmetric matrices with eigenvalues* $\lambda_1 \geq \cdots \geq \lambda_p$ *and* $\widehat{\lambda}_1 \geq \cdots \geq \widehat{\lambda}_p$*, respectively. Write* $\mathbf{E} := \widehat{\mathbf{M}} - \mathbf{M}$ *and fix* $1 \leq r \leq s \leq p$*. Assume that* $\delta_{\text{gap}} := \min(\lambda_{r-1} - \lambda_r, \lambda_s - \lambda_{s+1}) > 0$ *where* $\lambda_0 := \infty$ *and* $\lambda_{p+1} := -\infty$*. Let* $d =$

$s-r+1$ and let $\mathbf{V} := [\boldsymbol{v}_r|\boldsymbol{v}_{r+1}|\ldots|\boldsymbol{v}_s] \in \mathbb{R}^{p\times d}$ and $\widehat{\mathbf{V}} := [\widehat{\boldsymbol{v}}_r|\widehat{\boldsymbol{v}}_{r+1}|\ldots|\widehat{\boldsymbol{v}}_s] \in \mathbb{R}^{p\times d}$ have orthonormal columns satisfying $\mathbf{M}\boldsymbol{v}_j = \lambda_j \boldsymbol{v}_j$ and $\widehat{\mathbf{M}}\widehat{\boldsymbol{v}}_j = \widehat{\lambda}_j \widehat{\boldsymbol{v}}_j$ for $j = r, r+1, \ldots, s$. Then

$$\left\|\sin\boldsymbol{\Theta}(\widehat{\mathbf{V}}, \mathbf{V})\right\|_2 \leq \left(\frac{2\|\mathbf{E}\|_2}{\delta_{\text{gap}}}\right). \tag{6.6}$$

6.1.2 Proof of Theorem 5

Proof. For ease of presentation, we use $C > 0$ to denote various constants that are allowed to depend on one another. Both n and d are taken to be large.

By hypothesis $\max\{\mathfrak{r}(\boldsymbol{\Gamma}), \log d\} = o(n)$, where $\mathfrak{r}(\boldsymbol{\Gamma}) := \text{trace}(\boldsymbol{\Gamma})/\sigma_1(\boldsymbol{\Gamma})$ denotes the effective rank of $\boldsymbol{\Gamma}$. In the present multivariate Gaussian covariance matrix setting, it follows from Koltchinskii and Lounici (2017a,b) that there exists some constant $C > 0$ such that with probability at least $1 - \frac{1}{3}d^{-2}$,

$$\|\mathbf{E}_n\|_2 \leq C\sigma_1(\boldsymbol{\Gamma})\sqrt{\frac{\max\{\mathfrak{r}(\boldsymbol{\Gamma}), \log d\}}{n}}.$$

By hypothesis $\sigma_1(\boldsymbol{\Gamma})/\sigma_r(\boldsymbol{\Gamma}) \leq C$, and so together with the above observations, then

$\sigma_r(\mathbf{\Gamma}) \geq 2\|\mathbf{E}_n\|_2$ with high probability. Theorem 10 thus yields

$$\begin{aligned}\|\widehat{\mathbf{U}} - \mathbf{U}\mathbf{W}_{\mathbf{U}}\|_{2\to\infty} \leq\ & C\big\|\big(\mathbf{U}_\perp\mathbf{U}_\perp^\top\big)\mathbf{E}_n\big(\mathbf{U}\mathbf{U}^\top\big)\big\|_{2\to\infty}/\sigma_r(\mathbf{\Gamma}) \\ & + C\big\|\big(\mathbf{U}_\perp\mathbf{U}_\perp^\top\big)\mathbf{E}_n\big(\mathbf{U}_\perp\mathbf{U}_\perp^\top\big)\big\|_{2\to\infty}\big\|\sin\mathbf{\Theta}(\widehat{\mathbf{U}},\mathbf{U})\big\|_2/\sigma_r(\mathbf{\Gamma}) \\ & + C\big\|\big(\mathbf{U}_\perp\mathbf{U}_\perp^\top\big)\mathbf{\Gamma}\big(\mathbf{U}_\perp\mathbf{U}_\perp^\top\big)\big\|_{2\to\infty}\big\|\sin\mathbf{\Theta}(\widehat{\mathbf{U}},\mathbf{U})\big\|_2/\sigma_r(\mathbf{\Gamma}) \\ & + \big\|\sin\mathbf{\Theta}(\widehat{\mathbf{U}},\mathbf{U})\big\|_2^2\|\mathbf{U}\|_{2\to\infty}.\end{aligned}$$

Moving forward, we record several important observations:

- By Proposition 3, $\|(\mathbf{U}_\perp\mathbf{U}_\perp^\top)\mathbf{E}_n(\mathbf{U}\mathbf{U}^\top)\|_{2\to\infty} \leq \|\mathbf{U}_\perp\mathbf{U}_\perp^\top\|_\infty\|\mathbf{E}_n\mathbf{U}\|_{2\to\infty}$.
- By the (bounded coherence) assumption that $\|\mathbf{U}\|_{2\to\infty} \leq C\sqrt{r/d}$, then

$$\big\|\mathbf{U}_\perp\mathbf{U}_\perp^\top\big\|_\infty = \big\|\mathbf{I} - \mathbf{U}\mathbf{U}^\top\big\|_\infty \leq 1 + \sqrt{d}\big\|\mathbf{U}\mathbf{U}^\top\big\|_{2\to\infty} \leq (1+C)\sqrt{r}.$$

- The random (Gaussian) vector $\mathbf{U}_\perp^\top Y$ has covariance matrix $\mathbf{U}_\perp\mathbf{\Sigma}_\perp\mathbf{U}_\perp^\top$, so by Koltchinskii and Lounici (2017a,b) there exists some constant $C > 0$ such that with probability at least $1 - \frac{1}{3}d^{-2}$,

$$\begin{aligned}\big\|\big(\mathbf{U}_\perp\mathbf{U}_\perp^\top\big)\mathbf{E}_n\big(\mathbf{U}_\perp\mathbf{U}_\perp^\top\big)\big\|_2 &\leq C\sigma_{r+1}(\mathbf{\Gamma})\sqrt{\frac{\max\{\mathfrak{r}(\mathbf{\Sigma}_\perp),\log d\}}{n}} \\ &\leq C\sqrt{\sigma_{r+1}(\mathbf{\Gamma})}\sqrt{\sigma_1(\mathbf{\Gamma})}\sqrt{\frac{\max\{\mathfrak{r}(\mathbf{\Gamma}),\log d\}}{n}},\end{aligned}$$

where the final inequality holds since

$$\mathfrak{r}(\mathbf{\Sigma}_\perp) = \left(\frac{\sigma_1(\mathbf{\Gamma})}{\sigma_{r+1}(\mathbf{\Gamma})}\right)\left(\mathfrak{r}(\mathbf{\Gamma}) - \frac{\operatorname{tr}(\mathbf{\Sigma})}{\sigma_1(\mathbf{\Gamma})}\right) \leq \left(\frac{\sigma_1(\mathbf{\Gamma})}{\sigma_{r+1}(\mathbf{\Gamma})}\right)\mathfrak{r}(\mathbf{\Gamma}).$$

- Note that $\|(\mathbf{U}_\perp\mathbf{U}_\perp^\top)\mathbf{\Gamma}(\mathbf{U}_\perp\mathbf{U}_\perp^\top)\|_{2\to\infty} = \|\mathbf{U}_\perp\mathbf{\Sigma}_\perp\mathbf{U}_\perp^\top\|_{2\to\infty} \leq \sigma_{r+1}(\mathbf{\Gamma})$.
- Theorem 41 yields the bound $\|\sin\mathbf{\Theta}(\widehat{\mathbf{U}}, \mathbf{U})\|_2 \leq C\|\mathbf{E}_n\|_2/\delta_r(\mathbf{\Gamma})$ with population gap given by $\delta_r(\mathbf{\Gamma}) := \sigma_r(\mathbf{\Gamma}) - \sigma_{r+1}(\mathbf{\Gamma}) \geq c_2\sigma_r(\mathbf{\Gamma}) > 0$.

Together, these observations yield

$$\begin{aligned}\|\widehat{\mathbf{U}} - \mathbf{U}\mathbf{W}_{\mathbf{U}}\|_{2\to\infty} \leq\; & C\sqrt{r}\|\mathbf{E}_n\mathbf{U}\|_{2\to\infty}/\sigma_r(\mathbf{\Gamma}) \\ & + C\left(\frac{\max\{\mathfrak{r}(\mathbf{\Gamma}), \log d\}}{n}\right)\sqrt{\sigma_{r+1}(\mathbf{\Gamma})/\sigma_r(\mathbf{\Gamma})} \\ & + C\sqrt{\frac{\max\{\mathfrak{r}(\mathbf{\Gamma}), \log d\}}{n}}\big(\sigma_{r+1}(\mathbf{\Gamma})/\sigma_r(\mathbf{\Gamma})\big) \\ & + C\left(\frac{\max\{\mathfrak{r}(\mathbf{\Gamma}), \log d\}}{n}\right)\sqrt{r/d}.\end{aligned}$$

Now let $\mathbf{e}_i$ denote the ith standard basis vector in $\mathbb{R}^d$ and $\mathbf{u}_j$ denote the jth column of $\mathbf{U}$. The matrix $\mathbf{E}_n$ is symmetric, and $\mathbf{E}_n\mathbf{U} \in \mathbb{R}^{d\times r}$ can be bounded in two-to-infinity norm in the manner

$$\|\mathbf{E}_n\mathbf{U}\|_{2\to\infty} \leq \sqrt{r}\|\mathbf{E}_n\mathbf{U}\|_{\max} = \sqrt{r}\max_{i\in[d],j\in[r]}\big|\langle\mathbf{E}_n\mathbf{e}_i, \mathbf{u}_j\rangle\big|.$$

For each $(i,j) \in [d] \times [r]$, the scalar $\langle \mathbf{E}_n \mathbf{e}_i, \mathbf{u}_j \rangle$ can be expanded as

$$\langle \mathbf{E}_n \mathbf{e}_i, \mathbf{u}_j \rangle = \frac{1}{n} \sum_{k=1}^{n} \big(\big(\mathbf{u}_j^\top Y_k \big) \big(Y_k^\top \mathbf{e}_i \big) - \mathbf{u}_j^\top \mathbf{\Gamma} \mathbf{e}_i \big) = \frac{1}{n} \sum_{k=1}^{n} \big(\langle Y_k, \mathbf{u}_j \rangle Y_k^{(i)} - \langle \mathbf{\Gamma} \mathbf{e}_i, \mathbf{u}_j \rangle \big).$$

The product of (sub-)Gaussian random variables is sub-exponential, so for i and j fixed, $(\langle Y_k, \mathbf{u}_j \rangle Y_k^{(i)} - \langle \mathbf{\Gamma} \mathbf{e}_i, \mathbf{u}_j \rangle)$ with $1 \leq k \leq n$ is a collection of independent and identically distributed, centered sub-exponential random variables (Vershynin, 2018). To this end, the (univariate) sub-exponential norm, the (univariate) sub-Gaussian norm, and the vector sub-Gaussian norm are respectively,

$$\begin{aligned}
\big\| \big(Y^{(i)} \big)^2 \big\|_{\psi_1} &:= \sup_{p \geq 1} p^{-1} \big(\mathbb{E} \big[\big| \big(Y^{(i)} \big)^2 \big|^p \big] \big)^{1/p}; \\
\big\| Y^{(i)} \big\|_{\psi_2} &:= \sup_{p \geq 1} p^{-1/2} \big(\mathbb{E} \big[\big| Y^{(i)} \big|^p \big] \big)^{1/p}; \\
\| Y \|_{\psi_2} &:= \sup_{\|\mathbf{x}\|_2 = 1} \big\| \langle Y, \mathbf{x} \rangle \big\|_{\psi_2}.
\end{aligned}$$

By properties of these (Orlicz) norms (Vershynin, 2018), there exists some constant $C > 0$ such that the above sub-exponential random variables satisfy the bound

$$\big\| \langle Y_k, \mathbf{u}_j \rangle Y_k^{(i)} - \langle \mathbf{\Gamma} \mathbf{e}_i, \mathbf{u}_j \rangle \big\|_{\psi_1} \leq 2 \big\| \langle Y_k, \mathbf{u}_j \rangle Y_k^{(i)} \big\|_{\psi_1} \leq C \big\| \langle Y, \mathbf{u}_j \rangle \big\|_{\psi_2} \big\| Y^{(i)} \big\|_{\psi_2}.$$

The random vector Y is mean zero multivariate Gaussian, hence for each $1 \leq i \leq d$,

the norm of the ith component satisfies the variance-based bound

$$\left\|Y^{(i)}\right\|_{\psi_2} \leq C \max_{1 \leq i \leq d} \sqrt{\mathrm{Var}\left(Y^{(i)}\right)} \equiv C\nu(Y).$$

For each $j \in [r]$, $\mathrm{Var}(\langle Y, \mathbf{u}_j \rangle) = \mathbf{u}_j^\top \mathbf{\Gamma} \mathbf{u}_j = \sigma_j(\mathbf{\Gamma})$, where $\langle Y, \mathbf{u}_j \rangle$ is univariate Gaussian, so we have the spectral-based bound $\|\langle Y, \mathbf{u}_j \rangle\|_{\psi_2} \leq C\sqrt{\sigma_1(\mathbf{\Gamma})}$. Taken together, these observations establish a uniform bound over all i, j, k of the form

$$\left\|\langle Y_k, \mathbf{u}_j \rangle Y_k^{(i)} - \langle \mathbf{\Gamma} \mathbf{e}_i, \mathbf{u}_j \rangle\right\|_{\psi_1} \leq C\nu(Y)\sqrt{\sigma_1(\mathbf{\Gamma})}.$$

By combining a union bound with Bernstein's inequality for sub-exponential random variables (Vershynin, 2018), it follows that there exists a constant $C > 0$ such that with probability at least $1 - \frac{1}{3}d^{-2}$,

$$\|\mathbf{E}_n \mathbf{U}\|_{2 \to \infty} \leq C\nu(Y)\sqrt{\sigma_1(\mathbf{\Gamma})}\sqrt{r}\sqrt{\frac{\max\{\mathfrak{r}(\mathbf{\Gamma}), \log d\}}{n}}.$$

The r largest singular values of $\mathbf{\Gamma}$ bound each other up to absolute multiplicative constants for all values of d by assumption. Moreover, $\delta_r(\mathbf{\Gamma}) \geq c_2 \sigma_r(\mathbf{\Gamma})$ by assumption.

Aggregating the above observations yields that with probability at least $1 - d^{-2}$,

$$\|\widehat{\mathbf{U}} - \mathbf{U}\mathbf{W}_{\mathbf{U}}\|_{2\to\infty} \leq C\sqrt{\frac{\max\{\mathfrak{r}(\mathbf{\Gamma}), \log d\}}{n}}\left(\frac{\nu(Y)r}{\sqrt{\sigma_r(\mathbf{\Gamma})}} + \frac{\sigma_{r+1}(\mathbf{\Gamma})}{\sigma_r(\mathbf{\Gamma})}\right) + C\left(\frac{\max\{\mathfrak{r}(\mathbf{\Gamma}), \log d\}}{n}\right)\left(\sqrt{\frac{\sigma_{r+1}(\mathbf{\Gamma})}{\sigma_r(\mathbf{\Gamma})}} + \sqrt{\frac{r}{d}}\right),$$

which completes the proof. □

6.1.3 Proof of Theorem 6

Proof. The matrices $\mathbf{M}$ and $\widehat{\mathbf{M}}$ have rank at least r, so $\widehat{\mathbf{U}} \equiv \widehat{\mathbf{M}}\widehat{\mathbf{V}}\widehat{\mathbf{\Sigma}}^{-1}$ and $\mathbf{U}\mathbf{W}_{\mathbf{U}} \equiv \mathbf{M}\mathbf{V}\mathbf{\Sigma}^{-1}\mathbf{W}_{\mathbf{U}}$ by the block matrix formulation in Section 1.5. The explicit correspondence between $\mathbf{W}_{\mathbf{U}}$ and $\mathbf{U}^\top\widehat{\mathbf{U}}$ along with subsequent left-multiplication by the matrix $\mathbf{U}$ motivates the introduction of the projected quantity $\pm\mathbf{U}\mathbf{U}^\top\widehat{\mathbf{U}}$ and leads to

$$\begin{aligned}\widehat{\mathbf{U}} - \mathbf{U}\mathbf{W}_{\mathbf{U}} &= \big(\widehat{\mathbf{U}} - \mathbf{U}\mathbf{U}^\top\widehat{\mathbf{U}}\big) + \big(\mathbf{U}\mathbf{U}^\top\widehat{\mathbf{U}} - \mathbf{U}\mathbf{W}_{\mathbf{U}}\big) \\ &= \big(\mathbf{I} - \mathbf{U}\mathbf{U}^\top\big)\widehat{\mathbf{M}}\widehat{\mathbf{V}}\widehat{\mathbf{\Sigma}}^{-1} + \mathbf{U}\big(\mathbf{U}^\top\widehat{\mathbf{U}} - \mathbf{W}_{\mathbf{U}}\big).\end{aligned}$$

The matrix $\mathbf{U}(\mathbf{U}^\top\widehat{\mathbf{U}} - \mathbf{W}_{\mathbf{U}})$ can be meaningfully bounded in both spectral and two-to-infinity norm by Lemma 40 and Proposition 3. Ignoring $\mathbf{U}$ for the moment, the difference $\mathbf{U}^\top\widehat{\mathbf{U}} - \mathbf{W}_{\mathbf{U}}$ represents the geometric approximation error between $\mathbf{U}^\top\widehat{\mathbf{U}}$ and the orthogonal matrix $\mathbf{W}_{\mathbf{U}}$.

It is not immediately clear how to control $(\mathbf{I}-\mathbf{U}\mathbf{U}^\top)\widehat{\mathbf{M}}\widehat{\mathbf{V}}\widehat{\mathbf{\Sigma}}^{-1}$ given the dependence

on the perturbed quantity $\widehat{\mathbf{M}}$. If instead we replace $\widehat{\mathbf{M}}$ with $\mathbf{M}$ and consider the matrix $(\mathbf{I}-\mathbf{U}\mathbf{U}^\top)\mathbf{M}\widehat{\mathbf{V}}\widehat{\mathbf{\Sigma}}^{-1}$, then by the block matrix form in Section 1.5 one can check that $(\mathbf{I}-\mathbf{U}\mathbf{U}^\top)\mathbf{M} = \mathbf{M}(\mathbf{I}-\mathbf{V}\mathbf{V}^\top)$. Since $(\mathbf{I}-\mathbf{U}\mathbf{U}^\top)$ is an orthogonal projection and hence is idempotent, $(\mathbf{I}-\mathbf{U}\mathbf{U}^\top)\mathbf{M}\widehat{\mathbf{V}}\widehat{\mathbf{\Sigma}}^{-1} = (\mathbf{I}-\mathbf{U}\mathbf{U}^\top)\mathbf{M}(\widehat{\mathbf{V}}-\mathbf{V}\mathbf{V}^\top\widehat{\mathbf{V}})\widehat{\mathbf{\Sigma}}^{-1}$. Thus,

$$\big(\mathbf{I}-\mathbf{U}\mathbf{U}^\top\big)\widehat{\mathbf{M}}\widehat{\mathbf{V}}\widehat{\mathbf{\Sigma}}^{-1} = \big(\mathbf{I}-\mathbf{U}\mathbf{U}^\top\big)\mathbf{E}\widehat{\mathbf{V}}\widehat{\mathbf{\Sigma}}^{-1} + \big(\mathbf{I}-\mathbf{U}\mathbf{U}^\top\big)\mathbf{M}\big(\widehat{\mathbf{V}}-\mathbf{V}\mathbf{V}^\top\widehat{\mathbf{V}}\big)\widehat{\mathbf{\Sigma}}^{-1}.$$

By Lemma 39 and Proposition 3, the terms comprising the matrix product $(\mathbf{I}-\mathbf{U}\mathbf{U}^\top)\mathbf{M}(\widehat{\mathbf{V}}-\mathbf{V}\mathbf{V}^\top\widehat{\mathbf{V}})\widehat{\mathbf{\Sigma}}^{-1}$ can be suitably controlled in norm. At times, it shall be useful to further decompose $(\mathbf{I}-\mathbf{U}\mathbf{U}^\top)\mathbf{M}(\widehat{\mathbf{V}}-\mathbf{V}\mathbf{V}^\top\widehat{\mathbf{V}})\widehat{\mathbf{\Sigma}}^{-1}$ as

$$\big(\big(\mathbf{I}-\mathbf{U}\mathbf{U}^\top\big)\mathbf{M}(\widehat{\mathbf{V}}-\mathbf{V}\mathbf{W}_\mathbf{V})\widehat{\mathbf{\Sigma}}^{-1}\big) + \big(\big(\mathbf{I}-\mathbf{U}\mathbf{U}^\top\big)\mathbf{M}\mathbf{V}\big(\mathbf{W}_\mathbf{V}-\mathbf{V}^\top\widehat{\mathbf{V}}\big)\widehat{\mathbf{\Sigma}}^{-1}\big),$$

where the second term vanishes since $(\mathbf{I}-\mathbf{U}\mathbf{U}^\top)\mathbf{M}\mathbf{V}$ vanishes.

As for the matrix $(\mathbf{I}-\mathbf{U}\mathbf{U}^\top)\mathbf{E}\widehat{\mathbf{V}}\widehat{\mathbf{\Sigma}}^{-1}$, we do not assume explicit control of $\widehat{\mathbf{V}}$, so we rewrite the above matrix product in terms of $\mathbf{V}$ and a corresponding residual quantity. A natural choice is to incorporate the orthogonal factor $\mathbf{W}_\mathbf{V}$. Specifically, introducing $\pm(\mathbf{I}-\mathbf{U}\mathbf{U}^\top)\mathbf{E}\mathbf{V}\mathbf{W}_\mathbf{V}\widehat{\mathbf{\Sigma}}^{-1}$ yields

$$\big(\mathbf{I}-\mathbf{U}\mathbf{U}^\top\big)\mathbf{E}\widehat{\mathbf{V}}\widehat{\mathbf{\Sigma}}^{-1} = \big(\mathbf{I}-\mathbf{U}\mathbf{U}^\top\big)\mathbf{E}(\widehat{\mathbf{V}}-\mathbf{V}\mathbf{W}_\mathbf{V})\widehat{\mathbf{\Sigma}}^{-1} + \big(\mathbf{I}-\mathbf{U}\mathbf{U}^\top\big)\mathbf{E}\mathbf{V}\mathbf{W}_\mathbf{V}\widehat{\mathbf{\Sigma}}^{-1}.$$

Gathering right-hand sides of the above equations yields Theorem 6. Corollaries 7

and 8 are evident given that $\mathbf{U}^\top\mathbf{U}$ and $\mathbf{V}^\top\mathbf{V}$ are both simply the identity matrix. Corollary 9 is obtained from Corollary 8 by additional straightforward algebraic manipulations. In applications, $(\mathbf{I} - \mathbf{U}\mathbf{U}^\top)\mathbf{E}\mathbf{V}\mathbf{W}_\mathbf{V}\widehat{\mathbf{\Sigma}}^{-1} \approx \mathbf{E}\mathbf{V}\mathbf{W}_\mathbf{V}\widehat{\mathbf{\Sigma}}^{-1}$ can often be shown to function as the leading order term. □

6.1.4 Proof of Theorem 10

Proof. The assumption $\sigma_r(\mathbf{M}) \geq 2\|\mathbf{E}\|_2$ implies that $\sigma_r(\widehat{\mathbf{M}}) \geq \frac{1}{2}\sigma_r(\mathbf{M})$ since by Weyl's inequality for singular values, $\sigma_r(\widehat{\mathbf{M}}) \geq \sigma_r(\mathbf{M}) - \|\mathbf{E}\|_2 \geq \frac{1}{2}\sigma_r(\mathbf{M})$. The result then follows from Corollary 9 together with Proposition 3 and Lemma 39. □

6.1.5 Proof of Theorem 11

Proof. By Corollary 8, consider the decomposition

$$\begin{aligned}\widehat{\mathbf{U}} - \mathbf{U}\mathbf{W}_\mathbf{U} = &\big(\mathbf{I} - \mathbf{U}\mathbf{U}^\top\big)\mathbf{E}\big(\mathbf{V}\mathbf{V}^\top\big)\mathbf{V}\mathbf{W}_\mathbf{V}\widehat{\mathbf{\Sigma}}^{-1} \\ &+ \big(\mathbf{I} - \mathbf{U}\mathbf{U}^\top\big)(\mathbf{E} + \mathbf{M})(\widehat{\mathbf{V}} - \mathbf{V}\mathbf{W}_\mathbf{V})\widehat{\mathbf{\Sigma}}^{-1} \\ &+ \mathbf{U}\big(\mathbf{U}^\top\widehat{\mathbf{U}} - \mathbf{W}_\mathbf{U}\big).\end{aligned}$$

Applying Proposition 3 and Lemma 39 yields

$$\begin{aligned}\|\widehat{\mathbf{U}} - \mathbf{U}\mathbf{W}_{\mathbf{U}}\|_{2\to\infty} \leq{}& \big\|\big(\mathbf{U}_\perp\mathbf{U}_\perp^\top\big)\mathbf{E}\big(\mathbf{V}\mathbf{V}^\top\big)\big\|_{2\to\infty}/\sigma_r(\widehat{\mathbf{M}}) \\ &+ (C_{\mathbf{E},\mathbf{U}} + C_{\mathbf{M},\mathbf{U}})\|\widehat{\mathbf{V}} - \mathbf{V}\mathbf{W}_{\mathbf{V}}\|_{2\to\infty}/\sigma_r(\widehat{\mathbf{M}}) \\ &+ \big\|\sin\boldsymbol{\Theta}(\widehat{\mathbf{U}},\mathbf{U})\big\|_2^2\|\mathbf{U}\|_{2\to\infty}\end{aligned}$$

and similarly

$$\begin{aligned}\|\widehat{\mathbf{V}} - \mathbf{V}\mathbf{W}_{\mathbf{V}}\|_{2\to\infty} \leq{}& \big\|\big(\mathbf{V}_\perp\mathbf{V}_\perp^\top\big)\mathbf{E}^\top\big(\mathbf{U}\mathbf{U}^\top\big)\big\|_{2\to\infty}/\sigma_r(\widehat{\mathbf{M}}) \\ &+ (C_{\mathbf{E},\mathbf{V}} + C_{\mathbf{M},\mathbf{V}})\|\widehat{\mathbf{U}} - \mathbf{U}\mathbf{W}_{\mathbf{U}}\|_{2\to\infty}/\sigma_r(\widehat{\mathbf{M}}) \\ &+ \big\|\sin\boldsymbol{\Theta}(\widehat{\mathbf{V}},\mathbf{V})\big\|_2^2\|\mathbf{V}\|_{2\to\infty}.\end{aligned}$$

By assumption,

$$\sigma_r(\mathbf{M}) \geq \max\big\{2\|\mathbf{E}\|_2, (2/\alpha)C_{\mathbf{E},\mathbf{U}}, \big(2/\alpha'\big)C_{\mathbf{E},\mathbf{V}}, (2/\beta)C_{\mathbf{M},\mathbf{U}}, \big(2/\beta'\big)C_{\mathbf{M},\mathbf{V}}\big\}$$

for some constants $0 < \alpha, \alpha', \beta, \beta' < 1$ such that $\delta := (\alpha + \beta)(\alpha' + \beta') < 1$. The assumption $\sigma_r(\mathbf{M}) \geq 2\|\mathbf{E}\|_2$ implies that $\sigma_r(\widehat{\mathbf{M}}) \geq \sigma_r(\mathbf{M}) - \mathbf{E}\|_2 \geq \frac{1}{2}\sigma_r(\mathbf{M})$ by Weyl's inequality for singular values. Combining the above observations and rearranging

terms yields

$$
\begin{aligned}
(1-\delta)\|\widehat{\mathbf{U}}-\mathbf{U}\mathbf{W}_{\mathbf{U}}\|_{2\to\infty} \leq\ & 2\big\|\big(\mathbf{U}_\perp\mathbf{U}_\perp^\top\big)\mathbf{E}\big(\mathbf{V}\mathbf{V}^\top\big)\big\|_{2\to\infty}/\sigma_r(\mathbf{M}) \\
& + 2(\alpha+\beta)\big\|\big(\mathbf{V}_\perp\mathbf{V}_\perp^\top\big)\mathbf{E}^\top\big(\mathbf{U}\mathbf{U}^\top\big)\big\|_{2\to\infty}/\sigma_r(\mathbf{M}) \\
& + \big\|\sin\boldsymbol{\Theta}(\widehat{\mathbf{U}},\mathbf{U})\big\|_2^2\|\mathbf{U}\|_{2\to\infty} \\
& + (\alpha+\beta)\big\|\sin\boldsymbol{\Theta}(\widehat{\mathbf{V}},\mathbf{V})\big\|_2^2\|\mathbf{V}\|_{2\to\infty}.
\end{aligned}
$$

The first claim follows since $(\alpha+\beta)<1$. When $\mathrm{rank}(X)=r$, then $\mathbf{U}_\perp\mathbf{U}_\perp^\top\mathbf{M}$ vanishes. Corollary 7 then yields the simpler form

$$
\begin{aligned}
\widehat{\mathbf{U}}-\mathbf{U}\mathbf{W}_{\mathbf{U}} =\ & \big(\mathbf{I}-\mathbf{U}\mathbf{U}^\top\big)\mathbf{E}\big(\mathbf{V}\mathbf{V}^\top\big)\mathbf{V}\mathbf{W}_{\mathbf{V}}\widehat{\boldsymbol{\Sigma}}^{-1} \\
& + \big(\mathbf{I}-\mathbf{U}\mathbf{U}^\top\big)\mathbf{E}(\widehat{\mathbf{V}}-\mathbf{V}\mathbf{W}_{\mathbf{V}})\widehat{\boldsymbol{\Sigma}}^{-1} \\
& + \mathbf{U}\big(\mathbf{U}^\top\widehat{\mathbf{U}}-\mathbf{W}_{\mathbf{U}}\big),
\end{aligned}
$$

and similarly for $\widehat{\mathbf{V}}-\mathbf{V}\mathbf{W}_{\mathbf{V}}$. In this case, the bound holds without needing to consider either $C_{\mathbf{M},\mathbf{U}}$ or $C_{\mathbf{M},\mathbf{V}}$. □

6.1.6 Proof of Corollary 12

Proof. By Theorem 11, we have

$$\begin{aligned}(1-\delta)\|\widehat{\mathbf{U}}-\mathbf{U}\mathbf{W}_{\mathbf{U}}\|_{2\to\infty} \leq{}& 2\big\|\big(\mathbf{U}_\perp\mathbf{U}_\perp^\top\big)\mathbf{E}\big(\mathbf{V}\mathbf{V}^\top\big)\big\|_{2\to\infty}/\sigma_r(\mathbf{M})\\ &+2\big\|\big(\mathbf{V}_\perp\mathbf{V}_\perp^\top\big)\mathbf{E}^\top\big(\mathbf{U}\mathbf{U}^\top\big)\big\|_{2\to\infty}/\sigma_r(\mathbf{M})\\ &+\big\|\sin\boldsymbol{\Theta}(\widehat{\mathbf{U}},\mathbf{U})\big\|_2^2\|\mathbf{U}\|_{2\to\infty}\\ &+\big\|\sin\boldsymbol{\Theta}(\widehat{\mathbf{V}},\mathbf{V})\big\|_2^2\|\mathbf{V}\|_{2\to\infty}.\end{aligned}$$

Applying Wedin's $\sin\boldsymbol{\Theta}$ theorem with the assumption $\sigma_r(\mathbf{M}) \geq 2\|\mathbf{E}\|_2$ and the norm relation $\|\mathbf{E}\|_2 \leq \max\{\|\mathbf{E}\|_\infty, \|\mathbf{E}\|_1\}$ yields

$$\max_{\mathbf{Z}\in\{\mathbf{U},\mathbf{V}\}}\big\{\big\|\sin\boldsymbol{\Theta}(\widehat{\mathbf{Z}},\mathbf{Z})\big\|_2\big\} \leq \min\left\{\left(\frac{2\times\max\{\|\mathbf{E}\|_\infty,\|\mathbf{E}\|_1\}}{\sigma_r(\mathbf{M})}\right),1\right\}.$$

By invoking properties of the two-to-infinity norm, it follows that

$$\begin{aligned}\big\|\big(\mathbf{U}_\perp\mathbf{U}_\perp^\top\big)\mathbf{E}\big(\mathbf{V}\mathbf{V}^\top\big)\big\|_{2\to\infty} &\leq \big\|\mathbf{E}\big(\mathbf{V}\mathbf{V}^\top\big)\big\|_{2\to\infty}+\big\|\big(\mathbf{U}\mathbf{U}^\top\big)\mathbf{E}\big(\mathbf{V}\mathbf{V}^\top\big)\big\|_{2\to\infty}\\ &\leq \|\mathbf{E}\mathbf{V}\|_{2\to\infty}+\|\mathbf{U}\|_{2\to\infty}\big\|\mathbf{U}^\top\mathbf{E}\mathbf{V}\big\|_2\\ &\leq \|\mathbf{E}\|_\infty\|\mathbf{V}\|_{2\to\infty}+\|\mathbf{U}\|_{2\to\infty}\max\big\{\|\mathbf{E}\|_\infty,\|\mathbf{E}\|_1\big\}\\ &\leq 2\times\max_{\eta\in\{1,\infty\}}\big\{\|\mathbf{E}\|_\eta\big\}\times\max_{\mathbf{Z}\in\{\mathbf{U},\mathbf{V}\}}\big\{\|\mathbf{Z}\|_{2\to\infty}\big\}.\end{aligned}$$

Similarly,

$$\begin{aligned}
&\big\|(\mathbf{V}_\perp\mathbf{V}_\perp^\top)\mathbf{E}^\top(\mathbf{U}\mathbf{U}^\top)\big\|_{2\to\infty} \\
&\quad\le \|\mathbf{E}\|_1\|\mathbf{U}\|_{2\to\infty} + \|\mathbf{V}\|_{2\to\infty}\max\big\{\|\mathbf{E}\|_\infty, \|\mathbf{E}\|_1\big\} \\
&\quad\le 2\times \max_{\eta\in\{1,\infty\}}\big\{\|\mathbf{E}\|_\eta\big\}\times \max_{\mathbf{Z}\in\{\mathbf{U},\mathbf{V}\}}\big\{\|\mathbf{Z}\|_{2\to\infty}\big\}.
\end{aligned}$$

Hence

$$(1-\delta)\|\widehat{\mathbf{U}} - \mathbf{U}\mathbf{W}_\mathbf{U}\|_{2\to\infty} \le 12\times \max_{\eta\in\{1,\infty\}}\left\{\frac{\|\mathbf{E}\|_\eta}{\sigma_r(\mathbf{M})}\right\}\times \max_{\mathbf{Z}\in\{\mathbf{U},\mathbf{V}\}}\{\|\mathbf{Z}\|_{2\to\infty}\}. \qquad \square$$

6.1.7 Proof of Theorem 14

Proof. Specializing Corollary 8 to the case when $\mathbf{M}$ is symmetric with $\mathrm{rank}(\mathbf{M}) = r$ yields the decomposition

$$\begin{aligned}
\widehat{\mathbf{U}} - \mathbf{U}\mathbf{W}_\mathbf{U} = \mathbf{E}(\widehat{\mathbf{U}} - \mathbf{U}\mathbf{W}_\mathbf{U})\widehat{\mathbf{\Lambda}}^{-1} - \big(\mathbf{U}\mathbf{U}^\top\big)\mathbf{E}(\widehat{\mathbf{U}} - \mathbf{U}\mathbf{W}_\mathbf{U})\widehat{\mathbf{\Lambda}}^{-1} + \mathbf{E}\mathbf{U}\mathbf{W}_\mathbf{U}\widehat{\mathbf{\Lambda}}^{-1} \\
- \big(\mathbf{U}\mathbf{U}^\top\big)\mathbf{E}\mathbf{U}\mathbf{W}_\mathbf{U}\widehat{\mathbf{\Lambda}}^{-1} + \mathbf{U}\big(\mathbf{U}^\top\widehat{\mathbf{U}} - \mathbf{W}_\mathbf{U}\big).
\end{aligned}$$

Applying the technical results in Sections 1.3 and 6.1.1 yields the term-wise bounds

$$\begin{aligned}
\big\|\mathbf{E}(\widehat{\mathbf{U}}-\mathbf{U}\mathbf{W}_{\mathbf{U}})\widehat{\mathbf{\Lambda}}^{-1}\big\|_{2\to\infty} &\leq \|\mathbf{E}\|_{\infty}\|\widehat{\mathbf{U}}-\mathbf{U}\mathbf{W}_{\mathbf{U}}\|_{2\to\infty}|\widehat{\lambda}_r|^{-1},\\
\big\|\big(\mathbf{U}\mathbf{U}^{\top}\big)\mathbf{E}(\widehat{\mathbf{U}}-\mathbf{U}\mathbf{W}_{\mathbf{U}})\widehat{\mathbf{\Lambda}}^{-1}\big\|_{2\to\infty} &\leq \|\mathbf{U}\|_{2\to\infty}\|\mathbf{E}\|_2\|\widehat{\mathbf{U}}-\mathbf{U}\mathbf{W}_{\mathbf{U}}\|_2|\widehat{\lambda}_r|^{-1},\\
\big\|\mathbf{E}\mathbf{U}\mathbf{W}_{\mathbf{U}}\widehat{\mathbf{\Lambda}}^{-1}\big\|_{2\to\infty} &\leq \|\mathbf{E}\|_{\infty}\|\mathbf{U}\|_{2\to\infty}|\widehat{\lambda}_r|^{-1},\\
\big\|\big(\mathbf{U}\mathbf{U}^{\top}\big)\mathbf{E}\mathbf{U}\mathbf{W}_{\mathbf{U}}\widehat{\mathbf{\Lambda}}^{-1}\big\|_{2\to\infty} &\leq \|\mathbf{U}\|_{2\to\infty}\|\mathbf{E}\|_2||\widehat{\lambda}_r|^{-1},\\
\big\|\mathbf{U}\big(\mathbf{U}^{\top}\widehat{\mathbf{U}}-\mathbf{W}_{\mathbf{U}}\big)\big\|_{2\to\infty} &\leq \|\mathbf{U}\|_{2\to\infty}\big\|\mathbf{U}^{\top}\widehat{\mathbf{U}}-\mathbf{W}_{\mathbf{U}}\big\|_2.
\end{aligned}$$

The matrix $\mathbf{E}$ is symmetric by assumption, therefore, $\|\mathbf{E}\|_2 \leq \|\mathbf{E}\|_{\infty}$. Furthermore, $\|\widehat{\mathbf{U}}-\mathbf{U}\mathbf{W}_{\mathbf{U}}\|_2 \leq \sqrt{2}\|\sin\mathbf{\Theta}(\widehat{\mathbf{U}},\mathbf{U})\|_2$ by Lemma 40, and Theorem 41 guarantees that $\|\sin\mathbf{\Theta}(\widehat{\mathbf{U}},\mathbf{U})\|_2 \leq 2\|\mathbf{E}\|_2|\lambda_r|^{-1}$. Therefore,

$$\begin{aligned}
\big\|\mathbf{E}(\widehat{\mathbf{U}}-\mathbf{U}\mathbf{W}_{\mathbf{U}})\widehat{\mathbf{\Lambda}}^{-1}\big\|_{2\to\infty} &\leq \|\mathbf{E}\|_{\infty}\|\widehat{\mathbf{U}}-\mathbf{U}\mathbf{W}_{\mathbf{U}}\|_{2\to\infty}|\widehat{\lambda}_r|^{-1},\\
\big\|\big(\mathbf{U}\mathbf{U}^{\top}\big)\mathbf{E}(\widehat{\mathbf{U}}-\mathbf{U}\mathbf{W}_{\mathbf{U}})\widehat{\mathbf{\Lambda}}^{-1}\big\|_{2\to\infty} &\leq 4\|\mathbf{E}\|_{\infty}^2\|\mathbf{U}\|_{2\to\infty}|\widehat{\lambda}_r|^{-1}|\lambda_r|^{-1},\\
\big\|\mathbf{E}\mathbf{U}\mathbf{W}_{\mathbf{U}}\widehat{\mathbf{\Lambda}}^{-1}\big\|_{2\to\infty} &\leq \|\mathbf{E}\|_{\infty}\|\mathbf{U}\|_{2\to\infty}|\widehat{\lambda}_r|^{-1},\\
\big\|\big(\mathbf{U}\mathbf{U}^{\top}\big)\mathbf{E}\mathbf{U}\mathbf{W}_{\mathbf{U}}\widehat{\mathbf{\Lambda}}^{-1}\big\|_{2\to\infty} &\leq \|\mathbf{E}\|_{\infty}\|\mathbf{U}\|_{2\to\infty}|\widehat{\lambda}_r|^{-1},\\
\big\|\mathbf{U}\big(\mathbf{U}^{\top}\widehat{\mathbf{U}}-\mathbf{W}_{\mathbf{U}}\big)\big\|_{2\to\infty} &\leq 4\|\mathbf{E}\|_{\infty}^2\|\mathbf{U}\|_{2\to\infty}|\lambda_r|^{-2}.
\end{aligned}$$

By assumption $|\lambda_r| \geq 4\|\mathbf{E}\|_\infty$, so $|\widehat{\lambda}_r| \geq \frac{1}{2}|\lambda_r|$. As a consequence, it follows that $\|\mathbf{E}\|_\infty |\widehat{\lambda}_r|^{-1} \leq 2\|\mathbf{E}\|_\infty |\lambda_r|^{-1} \leq \frac{1}{2}$. Thus,

$$\begin{aligned}
\big\|\mathbf{E}(\widehat{\mathbf{U}} - \mathbf{U}\mathbf{W}_\mathbf{U})\widehat{\mathbf{\Lambda}}^{-1}\big\|_{2\to\infty} &\leq \frac{1}{2}\|\widehat{\mathbf{U}} - \mathbf{U}\mathbf{W}_\mathbf{U}\|_{2\to\infty}, \\
\big\|\big(\mathbf{U}\mathbf{U}^\top\big)\mathbf{E}(\widehat{\mathbf{U}} - \mathbf{U}\mathbf{W}_\mathbf{U})\widehat{\mathbf{\Lambda}}^{-1}\big\|_{2\to\infty} &\leq 2\|\mathbf{E}\|_\infty \|\mathbf{U}\|_{2\to\infty}|\lambda_r|^{-1}, \\
\big\|\mathbf{E}\mathbf{U}\mathbf{W}_\mathbf{U}\widehat{\mathbf{\Lambda}}^{-1}\big\|_{2\to\infty} &\leq 2\|\mathbf{E}\|_\infty \|\mathbf{U}\|_{2\to\infty}|\lambda_r|^{-1}, \\
\big\|\big(\mathbf{U}\mathbf{U}^\top\big)\mathbf{E}\mathbf{U}\mathbf{W}_\mathbf{U}\widehat{\mathbf{\Lambda}}^{-1}\big\|_{2\to\infty} &\leq 2\|\mathbf{E}\|_\infty \|\mathbf{U}\|_{2\to\infty}|\lambda_r|^{-1}, \\
\big\|\mathbf{U}\big(\mathbf{U}^\top\widehat{\mathbf{U}} - \mathbf{W}_\mathbf{U}\big)\big\|_{2\to\infty} &\leq \|\mathbf{E}\|_\infty \|\mathbf{U}\|_{2\to\infty}|\lambda_r|^{-1}.
\end{aligned}$$

Hence, $\|\widehat{\mathbf{U}} - \mathbf{U}\mathbf{W}_\mathbf{U}\|_{\max} \leq \|\widehat{\mathbf{U}} - \mathbf{U}\mathbf{W}_\mathbf{U}\|_{2\to\infty} \leq 14\big(\frac{\|\mathbf{E}\|_\infty}{|\lambda_r|}\big)\|\mathbf{U}\|_{2\to\infty}$. □

6.1.8 Proof of Theorem 15

Proof. Rewriting Corollary 8 in terms of the matrix $\widehat{\mathbf{V}} - \mathbf{V}\mathbf{W}_\mathbf{V}$ as described in Theorem 6 yields the decomposition

$$\begin{aligned}
\widehat{\mathbf{V}} - \mathbf{V}\mathbf{W}_\mathbf{V} = \big(\mathbf{V}_\perp\mathbf{V}_\perp^\top\big)\mathbf{E}^\top\big(\mathbf{U}\mathbf{U}^\top\big)\mathbf{U}\mathbf{W}_\mathbf{U}\widehat{\mathbf{\Sigma}}^{-1} \\
+ \big(\mathbf{V}_\perp\mathbf{V}_\perp^\top\big)\big(\mathbf{E}^\top + \mathbf{M}^\top\big)(\widehat{\mathbf{U}} - \mathbf{U}\mathbf{W}_\mathbf{U})\widehat{\mathbf{\Sigma}}^{-1} \\
+ \mathbf{V}\big(\mathbf{V}^\top\widehat{\mathbf{V}} - \mathbf{W}_\mathbf{V}\big).
\end{aligned}$$

Observe that $(\mathbf{U}\mathbf{U}^\top)\mathbf{U} \equiv \mathbf{U}$, while the assumption $\operatorname{rank}(\mathbf{M}) = r$ implies that the matrix $(\mathbf{V}_\perp\mathbf{V}_\perp^\top)\mathbf{M}^\top$ vanishes. Applying Proposition 3, Lemma 39, and Lemma 40 to

the remaining terms therefore yields

$$\begin{aligned}
&\big\|(\mathbf{V}_\perp\mathbf{V}_\perp^\top)\mathbf{E}^\top\mathbf{U}\mathbf{W}_\mathbf{U}\widehat{\mathbf{\Sigma}}^{-1}\big\|_{2\to\infty} \le \big\|(\mathbf{V}_\perp\mathbf{V}_\perp^\top)\mathbf{E}^\top\mathbf{U}\big\|_{2\to\infty}/\sigma_r(\widehat{\mathbf{M}}),\\
&\big\|(\mathbf{V}_\perp\mathbf{V}_\perp^\top)\mathbf{E}^\top(\widehat{\mathbf{U}}-\mathbf{U}\mathbf{W}_\mathbf{U})\widehat{\mathbf{\Sigma}}^{-1}\big\|_{2\to\infty}\\
&\quad\le C\big\|(\mathbf{V}_\perp\mathbf{V}_\perp^\top)\mathbf{E}^\top\big\|_{2\to\infty}\big\|\sin\mathbf{\Theta}(\widehat{\mathbf{U}},\mathbf{U})\big\|_2/\sigma_r(\widehat{\mathbf{M}}),\\
&\big\|\mathbf{V}\big(\mathbf{V}^\top\widehat{\mathbf{V}}-\mathbf{W}_\mathbf{V}\big)\big\|_{2\to\infty} \le \big\|\sin\mathbf{\Theta}(\widehat{\mathbf{V}},\mathbf{V})\big\|_2^2\|\mathbf{V}\|_{2\to\infty}.
\end{aligned}$$

The columns of $(\mathbf{V}_\perp\mathbf{V}_\perp^\top)\mathbf{E}^\top \in \mathbb{R}^{p_2\times p_1}$ are centered independent multivariate normal random vectors with covariance matrix $(\mathbf{V}_\perp\mathbf{V}_\perp^\top)$, so row i of $(\mathbf{V}_\perp\mathbf{V}_\perp^\top)\mathbf{E}^\top$ is a centered multivariate normal random vector with covariance matrix $\sigma_i^2\mathbf{I}$, where $\sigma_i^2 := (\mathbf{V}_\perp\mathbf{V}_\perp^\top)_{i,i} \le 1$ and $\mathbf{I} \in \mathbb{R}^{p_1\times p_1}$ denotes the identity matrix. By Gaussian concentration and applying a union bound with $p_2 \gg p_1$, then $\|(\mathbf{V}_\perp\mathbf{V}_\perp^\top)\mathbf{E}^\top\|_{2\to\infty} \le C_r\sqrt{p_1}\log(p_2)$ with high probability.

As for $(\mathbf{V}_\perp\mathbf{V}_\perp^\top)\mathbf{E}^\top\mathbf{U} \in \mathbb{R}^{p_2\times r}$, the above argument implies that entry (i,j) is $\mathcal{N}(0,\sigma_i^2)$. Hence by the same approach, $\|(\mathbf{V}_\perp\mathbf{V}_\perp^\top)\mathbf{E}^\top\mathbf{U}\|_{2\to\infty} \le C_r\log(p_2)$ with high probability.

By hypothesis $r \ll p_1 \ll p_2$ and $\sigma_r(\mathbf{M}) \ge Cp_2/\sqrt{p_1}$, where $\|\mathbf{E}\|_2 \le C\sqrt{p_2}$ with high probability. In this setting, via Cai and Zhang (2018),

$$\big\|\sin\mathbf{\Theta}(\widehat{\mathbf{U}},\mathbf{U})\big\|_2 \le C\left(\frac{\sqrt{p_1}}{\sigma_r(\mathbf{M})}\right) \quad\text{and}\quad \big\|\sin\mathbf{\Theta}(\widehat{\mathbf{V}},\mathbf{V})\big\|_2 \le C\left(\frac{\sqrt{p_2}}{\sigma_r(\mathbf{M})}\right).$$

Combining these observations yields

$$\left(\frac{\|(\mathbf{V}_\perp\mathbf{V}_\perp^\top)\mathbf{E}^\top\mathbf{U}\|_{2\to\infty}}{\sigma_r(\widehat{\mathbf{M}})}\right) \leq C_r\left(\frac{\log(p_2)}{\sigma_r(\mathbf{M})}\right),$$
$$\left(\frac{\|(\mathbf{V}_\perp\mathbf{V}_\perp^\top)\mathbf{E}^\top\|_{2\to\infty}}{\sigma_r(\widehat{\mathbf{M}})}\right)\left\|\sin\boldsymbol{\Theta}(\widehat{\mathbf{U}},\mathbf{U})\right\|_2 \leq C_r\left(\frac{\log(p_2)}{\sigma_r(\mathbf{M})}\right)\left(\frac{p_1}{\sigma_r(\mathbf{M})}\right),$$
$$\left\|\sin\boldsymbol{\Theta}(\widehat{\mathbf{V}},\mathbf{V})\right\|_2^2\|\mathbf{V}\|_{2\to\infty} \leq C_r\left(\frac{\log(p_2)}{\sigma_r(\mathbf{M})}\right)\left(\frac{\sqrt{p_1}}{\log(p_2)}\right)\|\mathbf{V}\|_{2\to\infty}.$$

Hence, with high probability

$$\|\widehat{\mathbf{V}}-\mathbf{V}\mathbf{W}_\mathbf{V}\|_{2\to\infty} \leq C_r\left(\frac{\log(p_2)}{\sigma_r(\mathbf{M})}\right)\left(1+\left(\frac{p_1}{\sigma_r(\mathbf{M})}\right)+\left(\frac{\sqrt{p_1}}{\log(p_2)}\right)\|\mathbf{V}\|_{2\to\infty}\right).$$

If in addition $\sigma_r(\mathbf{M}) \geq cp_1$ and $\|\mathbf{V}\|_{2\to\infty} \leq c_r/\sqrt{p_2}$ for some $c, c_r > 0$, then the above bound simplifies to the form

$$\|\widehat{\mathbf{V}}-\mathbf{V}\mathbf{W}_\mathbf{V}\|_{2\to\infty} \leq C_r\left(\frac{\log(p_2)}{\sigma_r(\mathbf{M})}\right),$$

which completes the proof. □

6.1.9 Proof of Theorem 18

Proof. We seek to bound $\|\widehat{\mathbf{U}}-\mathbf{U}\mathbf{W}_\mathbf{U}\|_{2\to\infty}$ and allow the constant $C > 0$ to change from line to line. Our analysis considers appropriate groupings of matrix elements in order to handle the graph correlation structure.

By assumption $\text{rank}(\mathfrak{O}) = r$ which implies that the matrix $(\mathbf{I} - \mathbf{U}\mathbf{U}^\top)\mathfrak{O}$ vanishes. Via Corollary 7, this yields the bound

$$\begin{aligned}\|\widehat{\mathbf{U}} - \mathbf{U}\mathbf{W}_\mathbf{U}\|_{2\to\infty} \leq & \left\|\left(\mathbf{I} - \mathbf{U}\mathbf{U}^\top\right)(\widehat{\mathfrak{O}} - \mathfrak{O})\mathbf{U}\mathbf{W}_\mathbf{U}\widehat{\mathbf{\Sigma}}^{-1}\right\|_{2\to\infty} \\ & + \left\|\left(\mathbf{I} - \mathbf{U}\mathbf{U}^\top\right)(\widehat{\mathfrak{O}} - \mathfrak{O})(\widehat{\mathbf{U}} - \mathbf{U}\mathbf{W}_\mathbf{U})\widehat{\mathbf{\Sigma}}^{-1}\right\|_{2\to\infty} \\ & + \|\mathbf{U}\|_{2\to\infty}\left\|\mathbf{U}^\top\widehat{\mathbf{U}} - \mathbf{W}_\mathbf{U}\right\|_2,\end{aligned}$$

which can be further weakened to the form

$$\begin{aligned}\|\widehat{\mathbf{U}} - \mathbf{U}\mathbf{W}_\mathbf{U}\|_{2\to\infty} \leq & \left\|(\widehat{\mathfrak{O}} - \mathfrak{O})\mathbf{U}\right\|_{2\to\infty}\left\|\widehat{\mathbf{\Sigma}}^{-1}\right\|_2 \\ & + \|\mathbf{U}\|_{2\to\infty}\left\|\mathbf{U}^\top(\widehat{\mathfrak{O}} - \mathfrak{O})\mathbf{U}\right\|_2\left\|\widehat{\mathbf{\Sigma}}^{-1}\right\|_2 \\ & + \|\widehat{\mathfrak{O}} - \mathfrak{O}\|_2\|\widehat{\mathbf{U}} - \mathbf{U}\mathbf{W}_\mathbf{U}\|_2\left\|\widehat{\mathbf{\Sigma}}^{-1}\right\|_2 \\ & + \|\mathbf{U}\|_{2\to\infty}\left\|\mathbf{U}^\top\widehat{\mathbf{U}} - \mathbf{W}_\mathbf{U}\right\|_2.\end{aligned}$$

Applying the triangle inequality to the block matrix $\widehat{\mathfrak{O}} - \mathfrak{O}$ yields a spectral norm bound of the form

$$\|\widehat{\mathfrak{O}} - \mathfrak{O}\|_2 \leq C \times \max\left\{\left\|\mathbf{A}^1 - \mathbf{P}\right\|_2, \left\|\mathbf{A}^2 - \mathbf{P}\right\|_2\right\}.$$

By assumption, for $i = 1, 2$, the maximum expected degree of G^i, Δ, satisfies $\Delta \gg \log^4(n)$, hence $\|\mathbf{A}^i - \mathbf{P}\|_2 = \mathcal{O}(\sqrt{\Delta})$ with probability $1 - o(1)$ by Lu and Peng (2013). The assumption $\sigma_r(\mathfrak{O}) \geq c\Delta$ implies that $\sigma_r(\widehat{\mathfrak{O}}) \geq C\Delta$ with probability

$1 - o(1)$ by Weyl's inequality, so $\|\widehat{\mathbf{\Sigma}}^{-1}\|_2 = \mathcal{O}(1/\Delta)$. Combining these observations with Theorem 41 and the proof of Lemma 40 produces

$$\|\widehat{\mathbf{U}} - \mathbf{U}\mathbf{W}_{\mathbf{U}}\|_2 \leq C\big\|\sin\mathbf{\Theta}(\widehat{\mathbf{U}}, \mathbf{U})\big\|_2 \leq C\|\widehat{\mathbf{\mathfrak{O}}} - \mathbf{\mathfrak{O}}\|_2/\sigma_r(\mathbf{\mathfrak{O}}) = \mathcal{O}(1/\sqrt{\Delta}),$$

which we note simultaneously provides a naïve bound for $\|\widehat{\mathbf{U}} - \mathbf{U}\mathbf{W}_{\mathbf{U}}\|_{2\to\infty}$. As for the matrix, $(\widehat{\mathbf{\mathfrak{O}}} - \mathbf{\mathfrak{O}})\mathbf{U} \in \mathbb{R}^{2n\times r}$,

$$\big\|(\widehat{\mathbf{\mathfrak{O}}} - \mathbf{\mathfrak{O}})\mathbf{U}\big\|_{2\to\infty} \leq \sqrt{r}\max_{i\in[2n],j\in[r]}\big|\big\langle(\widehat{\mathbf{\mathfrak{O}}} - \mathbf{\mathfrak{O}})\mathbf{u}_j, \mathbf{e}_i\big\rangle\big|.$$

For all $1 \leq k \leq n$, $u_{(k+n),j} = u_{k,j}$, and for each $1 \leq i \leq n$ and $1 \leq j \leq r$,

$$\big\langle(\widehat{\mathbf{\mathfrak{O}}} - \mathbf{\mathfrak{O}})\mathbf{u}_j, \mathbf{e}_i\big\rangle = \mathbf{e}_i^\top(\widehat{\mathbf{\mathfrak{O}}} - \mathbf{\mathfrak{O}})\mathbf{u}_j = \sum_{k=1}^{n}\left(\frac{3}{2}a_{i,k}^1 + \frac{1}{2}a_{i,k}^2 - 2p_{i,k}\right)u_{k,j}.$$

Above, the roles of $\mathbf{A}^1$ and $\mathbf{A}^2$ are interchanged for $n+1 \leq i \leq 2n$.

For any $1 \leq i \leq n$, the above expansion is a sum of independent (in k), bounded, mean zero random variables taking values in $[-2u_{k,j}, 2u_{k,j}]$.

Hence by Hoeffding's inequality, with probability $1 - o(1)$ in n,

$$\big\|(\widehat{\mathbf{\mathfrak{O}}} - \mathbf{\mathfrak{O}})\mathbf{U}\big\|_{2\to\infty} = \mathcal{O}_r(\log n).$$

Similarly, for the matrix $\mathbf{U}^\top(\widehat{\mathfrak{O}} - \mathfrak{O})\mathbf{U} \in \mathbb{R}^{r\times r}$,

$$\left\|\mathbf{U}^\top(\widehat{\mathfrak{O}} - \mathfrak{O})\mathbf{U}\right\|_2 \leq r \max_{i\in[r],j\in[r]} \left|\left\langle(\widehat{\mathfrak{O}} - \mathfrak{O})\mathbf{u}_j, \mathbf{u}_i\right\rangle\right|,$$

so for $1 \leq i, j \leq r$, then

$$\left\langle(\widehat{\mathfrak{O}} - \mathfrak{O})\mathbf{u}_j, \mathbf{u}_i\right\rangle = \mathbf{u}_i^\top(\widehat{\mathfrak{O}} - \mathfrak{O})\mathbf{u}_j = \sum_{1\leq l<k\leq n} 4\big(a^1_{l,k} + a^2_{l,k} - 2p_{l,k}\big)u_{k,j}u_{l,i}.$$

This sum decomposes as a sum of independent, mean zero, bounded random variables taking values in $[-8u_{k,j}u_{l,i}, 8u_{k,j}u_{l,i}]$. By another application of Hoeffding's inequality, with probability $1 - o(1)$,

$$\left\|\mathbf{U}^\top(\widehat{\mathfrak{O}} - \mathfrak{O})\mathbf{U}\right\|_2 = \mathcal{O}_r(\log n).$$

Lemma 39 bounds $\|\mathbf{U}^\top\widehat{\mathbf{U}} - \mathbf{W}_\mathbf{U}\|_2$ by $\|\sin\boldsymbol{\Theta}(\widehat{\mathbf{U}}, \mathbf{U})\|_2^2$ which is $\mathcal{O}(1/\Delta)$. Cumulatively, this demonstrates that $\|\widehat{\mathbf{U}} - \mathbf{U}\mathbf{W}_\mathbf{U}\|_{2\to\infty} = \mathcal{O}_r((\log n)/\Delta)$ with probability $1 - o(1)$ as $n \to \infty$. □

6.2 Proofs for Chapter 3

This section contains a joint proof of the theoretical results in Chapter 3 as well as additional simulation examples.

6.2.1 Proof of Theorems 19, 20, and 21

Proof. We begin with several important observations, namely that

$$\|(\mathbf{I} - \mathbf{U}\mathbf{U}^\top)\widehat{\mathbf{U}}\|_2 = \|\sin\boldsymbol{\Theta}(\widehat{\mathbf{U}}, \mathbf{U})\|_2 = O\left(\|\mathbf{E}\||\boldsymbol{\Lambda}_{r,r}|^{-1}\right) = O_{\mathbb{P}}\left\{(n\rho_n)^{-1/2}\right\}, \tag{6.7}$$

and that there exists $\mathbf{W} \in \mathbb{O}_r$ depending on $\widehat{\mathbf{U}}$ and $\mathbf{U}$ such that

$$\|\mathbf{U}^\top\widehat{\mathbf{U}} - \mathbf{W}\|_2 \leq \|\sin\boldsymbol{\Theta}(\widehat{\mathbf{U}}, \mathbf{U})\|_2^2 = O_{\mathbb{P}}\left\{(n\rho_n)^{-1}\right\}. \tag{6.8}$$

In particular, $\mathbf{W}$ can be taken to be the product of the left and right orthogonal factors in the singular value decomposition of $\mathbf{U}^\top\widehat{\mathbf{U}}$. See Section 1.4.

Importantly, the relation $\widehat{\mathbf{U}}\widehat{\boldsymbol{\Lambda}} = \widehat{\mathbf{M}}\widehat{\mathbf{U}} = (\mathbf{M} + \mathbf{E})\widehat{\mathbf{U}}$ yields the matrix equation $\widehat{\mathbf{U}}\widehat{\boldsymbol{\Lambda}} - \mathbf{E}\widehat{\mathbf{U}} = \mathbf{M}\widehat{\mathbf{U}}$. The spectra of $\widehat{\boldsymbol{\Lambda}}$ and $\mathbf{E}$ are disjoint from one another with high probability as a consequence of Assumptions 2 and 3, so it follows that $\widehat{\mathbf{U}}$ can be written as the matrix series (Bhatia, 1997, Section 7.2)

$$\widehat{\mathbf{U}} = \sum_{k=0}^{\infty} \mathbf{E}^k\mathbf{M}\widehat{\mathbf{U}}\widehat{\boldsymbol{\Lambda}}^{-(k+1)} = \sum_{k=0}^{\infty} \mathbf{E}^k\mathbf{U}\boldsymbol{\Lambda}\mathbf{U}^\top\widehat{\mathbf{U}}\widehat{\boldsymbol{\Lambda}}^{-(k+1)}, \tag{6.9}$$

where the second equality holds since $\operatorname{rank}(\mathbf{M}) = r$.

For any choice of $\mathbf{W} \in \mathbb{O}_r$, the matrix $\widehat{\mathbf{U}} - \mathbf{U}\mathbf{W}$ can be decomposed as

$$\begin{aligned}\widehat{\mathbf{U}} - \mathbf{U}\mathbf{W} &= \mathbf{E}\widehat{\mathbf{U}}\widehat{\mathbf{\Lambda}}^{-1} + \mathbf{U}\mathbf{\Lambda}(\mathbf{U}^\top\widehat{\mathbf{U}}\widehat{\mathbf{\Lambda}}^{-1} - \mathbf{\Lambda}^{-1}\mathbf{U}^\top\widehat{\mathbf{U}}) + \mathbf{U}(\mathbf{U}^\top\widehat{\mathbf{U}} - \mathbf{W}) \\ &= \mathbf{E}\widehat{\mathbf{U}}\widehat{\mathbf{\Lambda}}^{-1} + \mathbf{R}^{(1)} + \mathbf{R}^{(2)}_{\mathbf{W}}.\end{aligned}$$

For $\mathbf{R}^{(2)}_{\mathbf{W}} = \mathbf{U}(\mathbf{U}^\top\widehat{\mathbf{U}} - \mathbf{W})$, it follows that for $\mathbf{W}$ satisfying Eq. (6.8), then

$$\|\mathbf{R}^{(2)}_{\mathbf{W}}\|_{2\to\infty} \leq \|\mathbf{U}^\top\widehat{\mathbf{U}} - \mathbf{W}\|_2\|\mathbf{U}\|_{2\to\infty} = O_{\mathbb{P}}\left\{(n\rho_n)^{-1}\|\mathbf{U}\|_{2\to\infty}\right\}.$$

For $\mathbf{R}^{(1)} = \mathbf{U}\mathbf{\Lambda}\mathbf{R}^{(3)}$ where $\mathbf{R}^{(3)} = (\mathbf{U}^\top\widehat{\mathbf{U}}\widehat{\mathbf{\Lambda}}^{-1} - \mathbf{\Lambda}^{-1}\mathbf{U}^\top\widehat{\mathbf{U}}) \in \mathbb{R}^{r\times r}$, the entries of $\mathbf{R}^{(3)}$ satisfy

$$\mathbf{R}^{(3)}_{ij} = \langle \mathbf{u}_i, \widehat{\mathbf{u}}_j\rangle\left\{(\widehat{\mathbf{\Lambda}}_{j,j})^{-1} - (\mathbf{\Lambda}_{i,i})^{-1}\right\} = \langle \mathbf{u}_i, \widehat{\mathbf{u}}_j\rangle(\mathbf{\Lambda}_{i,i} - \widehat{\mathbf{\Lambda}}_{j,j})(\mathbf{\Lambda}_{i,i})^{-1}(\widehat{\mathbf{\Lambda}}_{j,j})^{-1}.$$

Define the matrix $\mathbf{H}_1 \in \mathbb{R}^{r\times r}$ entrywise according to $(\mathbf{H}_1)_{ij} = (\mathbf{\Lambda}_{i,i})^{-1}(\widehat{\mathbf{\Lambda}}_{j,j})^{-1}$. Then, with $\circ$ denoting the Hadamard matrix product,

$$\mathbf{R}^{(3)} = -\mathbf{H}_1 \circ (\mathbf{U}^\top\widehat{\mathbf{U}}\widehat{\mathbf{\Lambda}} - \mathbf{\Lambda}\mathbf{U}^\top\widehat{\mathbf{U}}).$$

The rightmost matrix factor can be expanded as

$$(\mathbf{U}^\top\widehat{\mathbf{U}}\widehat{\mathbf{\Lambda}} - \mathbf{\Lambda}\mathbf{U}^\top\widehat{\mathbf{U}}) = \mathbf{U}^\top\mathbf{E}\widehat{\mathbf{U}} = \mathbf{U}^\top\mathbf{E}\mathbf{U}\mathbf{U}^\top\widehat{\mathbf{U}} + \mathbf{U}^\top\mathbf{E}(\mathbf{I} - \mathbf{U}\mathbf{U}^\top)\widehat{\mathbf{U}},$$

and is therefore bounded in spectral norm using Eq. (6.7) in the manner

$$\|\mathbf{U}^\top \widehat{\mathbf{U}}\widehat{\mathbf{\Lambda}} - \mathbf{\Lambda}\mathbf{U}^\top \widehat{\mathbf{U}}\|_2 \leq \|\mathbf{U}^\top \mathbf{E}\mathbf{U}\|_2 + O_{\mathbb{P}}(1).$$

Combining the above observations together with properties of matrix norms yields the following two-to-infinity norm bound on $\mathbf{R}^{(1)}$.

$$\begin{aligned}\|\mathbf{R}^{(1)}\|_{2\to\infty} = \|\mathbf{U}\mathbf{\Lambda}\mathbf{R}^{(3)}\|_{2\to\infty} &\leq r\|\mathbf{U}\|_{2\to\infty}\|\mathbf{\Lambda}\|_2\|\mathbf{H}_1\|_{\max}\|\mathbf{U}^\top \widehat{\mathbf{U}}\widehat{\mathbf{\Lambda}} - \mathbf{\Lambda}\mathbf{U}^\top \widehat{\mathbf{U}}\|_2 \\ &= O_{\mathbb{P}}\left\{r(n\rho_n)^{-1}(\|\mathbf{U}^\top \mathbf{E}\mathbf{U}\|_2 + 1)\|\mathbf{U}\|_{2\to\infty}\right\}\end{aligned}$$

Assumptions 2 and 3 with an application of Weyl's inequality (Bhatia, 1997, Corollary 3.2.6) guarantee that there exist constants $C_1, C_2 > 0$ such that $\|\mathbf{E}\|_2 \leq C_1(n\rho_n)^{1/2}$ and $\|\widehat{\mathbf{\Lambda}}^{-1}\|_2 \leq C_2(n\rho_n)^{-1}$ with high probability for n sufficiently large. Therefore, by applying the earlier matrix series expansion,

$$\begin{aligned}\|\mathbf{E}\widehat{\mathbf{U}}\widehat{\mathbf{\Lambda}}^{-1}\|_{2\to\infty} &= \left\|\sum_{k=1}^{\infty} \mathbf{E}^k \mathbf{U}\mathbf{\Lambda}\mathbf{U}^\top \widehat{\mathbf{U}}\widehat{\mathbf{\Lambda}}^{-(k+1)}\right\|_{2\to\infty} \\ &\leq \sum_{k=1}^{k(n)} \|\mathbf{E}^k\mathbf{U}\|_{2\to\infty}\|\mathbf{\Lambda}\|_2\|\widehat{\mathbf{\Lambda}}^{-1}\|_2^{k+1} + \sum_{k=k(n)+1}^{\infty} \|\mathbf{E}\|^k\|\mathbf{\Lambda}\|_2\|\widehat{\mathbf{\Lambda}}^{-1}\|_2^{k+1} \\ &= O_{\mathbb{P}}\left\{r^{1/2}(n\rho_n)^{-1/2}(\log n)^{\xi}\|\mathbf{U}\|_{2\to\infty} + (n\rho_n)^{-1/2}\|\mathbf{U}\|_{2\to\infty}\right\},\end{aligned}$$

where we have used the fact that $n\rho_n = \omega\{(\log n)^{2\xi}\}$, $(n\rho_n)^{-k(n)/2} \leq n^{-1/2} \leq \|\mathbf{U}\|_{2\to\infty}$ for n sufficiently large, and that by Assumption 4, for each $k \leq k(n)$, with high

probability

$$\|\mathbf{E}^k\mathbf{U}\|_{2\to\infty} \leq r^{1/2} \max_{i\in[n],j\in[r]} |\langle \mathbf{E}^k\mathbf{u}_j, \mathbf{e}_i\rangle| \leq r^{1/2}(C_{\mathbf{E}} n\rho_n)^{k/2}(\log n)^{k\xi}\|\mathbf{U}\|_{2\to\infty}.$$

Since $\|\mathbf{U}^\top\mathbf{E}\mathbf{U}\|_2 \leq \|\mathbf{E}\|_2$ and $r^{1/2} \leq (\log n)^\xi$ with $n\rho_n = \omega\{(\log n)^{2\xi}\}$, then

$$\begin{aligned}\|\widehat{\mathbf{U}} - \mathbf{U}\mathbf{W}\|_{2\to\infty} &\leq \|\mathbf{E}\widehat{\mathbf{U}}\widehat{\mathbf{\Lambda}}^{-1}\|_{2\to\infty} + \|\mathbf{R}^{(1)}\|_{2\to\infty} + \|\mathbf{R}^{(2)}_{\mathbf{W}}\|_{2\to\infty} \\ &= O_{\mathbb{P}}\left\{r^{1/2}(n\rho_n)^{-1/2}(\log n)^{\xi}\|\mathbf{U}\|_{2\to\infty}\right\}.\end{aligned}$$

This completes the proof of Theorem 19.

Next, we further decompose the matrix $\mathbf{E}\widehat{\mathbf{U}}\widehat{\mathbf{\Lambda}}^{-1}$ by extending the above proof techniques in order to obtain second-order fluctuations. Using the matrix series form in Eq. (6.9) yields

$$\begin{aligned}\mathbf{E}\widehat{\mathbf{U}}\widehat{\mathbf{\Lambda}}^{-1} &= \mathbf{E}\mathbf{U}\mathbf{\Lambda}\mathbf{U}^\top\widehat{\mathbf{U}}\widehat{\mathbf{\Lambda}}^{-2} + \sum_{k=2}^{\infty}\mathbf{E}^k\mathbf{U}\mathbf{\Lambda}\mathbf{U}^\top\widehat{\mathbf{U}}\widehat{\mathbf{\Lambda}}^{-(k+1)} \\ &= \mathbf{E}\mathbf{U}\mathbf{\Lambda}^{-1}\mathbf{W} + \mathbf{E}\mathbf{U}\mathbf{\Lambda}(\mathbf{U}^\top\widehat{\mathbf{U}}\widehat{\mathbf{\Lambda}}^{-2} - \mathbf{\Lambda}^{-2}\mathbf{U}^\top\widehat{\mathbf{U}}) + \mathbf{E}\mathbf{U}\mathbf{\Lambda}^{-1}(\mathbf{U}^\top\widehat{\mathbf{U}} - \mathbf{W}) \\ &\quad + \sum_{k=2}^{\infty}\mathbf{E}^k\mathbf{U}\mathbf{\Lambda}\mathbf{U}^\top\widehat{\mathbf{U}}\widehat{\mathbf{\Lambda}}^{-(k+1)} \\ &= \mathbf{E}\mathbf{U}\mathbf{\Lambda}^{-1}\mathbf{W} + \mathbf{R}^{(1)}_2 + \mathbf{R}^{(2)}_{2,\mathbf{W}} + \mathbf{R}^{(\infty)}_2.\end{aligned}$$

The final term satisfies the bound

$$\|\mathbf{R}_2^{(\infty)}\|_{2\to\infty} = O_{\mathbb{P}}\left\{r^{1/2}(n\rho_n)^{-1}(\log n)^{2\xi}\|\mathbf{U}\|_{2\to\infty}\right\},$$

which follows from Assumption 4 holding up to $k(n)+1$, namely

$$\begin{aligned}\|\mathbf{R}_2^{(\infty)}\|_{2\to\infty} &\leq \sum_{k=2}^{k(n)+1} \|\mathbf{E}^k\mathbf{U}\|_{2\to\infty}\|\mathbf{\Lambda}\|_2\|\widehat{\mathbf{\Lambda}}^{-1}\|_2^{k+1} + \sum_{k=k(n)+2}^{\infty} \|\mathbf{E}\|_2^k\|\mathbf{\Lambda}\|_2\|\widehat{\mathbf{\Lambda}}^{-1}\|_2^{k+1} \\ &= O_{\mathbb{P}}\left\{r^{1/2}(n\rho_n)^{-1}(\log n)^{2\xi}\|\mathbf{U}\|_{2\to\infty} + (n\rho_n)^{-1}\|\mathbf{U}\|_{2\to\infty}\right\}.\end{aligned}$$

On the other hand, modifying the previous analysis used to bound $\mathbf{R}_{\mathbf{W}}^{(2)}$ yields

$$\begin{aligned}\|\mathbf{R}_{2,\mathbf{W}}^{(2)}\|_{2\to\infty} &\leq \|\mathbf{E}\mathbf{U}\|_{2\to\infty}\|\mathbf{\Lambda}^{-1}\|_2\|\mathbf{U}^\top\widehat{\mathbf{U}} - \mathbf{W}\|_2 \\ &= O_{\mathbb{P}}\left\{r^{1/2}(n\rho_n)^{-3/2}(\log n)^{\xi}\|\mathbf{U}\|_{2\to\infty}\right\}.\end{aligned}$$

We now bound $\mathbf{R}_2^{(1)} = \mathbf{E}\mathbf{U}\mathbf{\Lambda}(\mathbf{U}^\top\widehat{\mathbf{U}}\widehat{\mathbf{\Lambda}}^{-2} - \mathbf{\Lambda}^{-2}\mathbf{U}^\top\widehat{\mathbf{U}})$ by extending the previous argument used to bound $\mathbf{R}^{(1)}$. For $\mathbf{R}_2^{(1)} = \mathbf{E}\mathbf{U}\mathbf{\Lambda}\mathbf{R}_2^{(3)}$ where $\mathbf{R}_2^{(3)} = (\mathbf{U}^\top\widehat{\mathbf{U}}\widehat{\mathbf{\Lambda}}^{-2} - \mathbf{\Lambda}^{-2}\mathbf{U}^\top\widehat{\mathbf{U}}) \in \mathbb{R}^{r\times r}$, the entries of $\mathbf{R}_2^{(3)}$ satisfy

$$\mathbf{R}_{ij}^{(3)} = \langle\mathbf{u}_i, \widehat{\mathbf{u}}_j\rangle\left\{(\widehat{\mathbf{\Lambda}}_{j,j})^{-2} - (\mathbf{\Lambda}_{i,i})^{-2}\right\} = \langle\mathbf{u}_i, \widehat{\mathbf{u}}_j\rangle(\mathbf{\Lambda}_{i,i}^2 - \widehat{\mathbf{\Lambda}}_{j,j}^2)(\mathbf{\Lambda}_{i,i})^{-2}(\widehat{\mathbf{\Lambda}}_{j,j})^{-2}.$$

Define the matrix $\mathbf{H}_2 \in \mathbb{R}^{r\times r}$ entrywise according to $(\mathbf{H}_2)_{ij} = (\mathbf{\Lambda}_{i,i})^{-2}(\widehat{\mathbf{\Lambda}}_{j,j})^{-2}$. Then,

with $\circ$ denoting the Hadamard matrix product,

$$\mathbf{R}_2^{(3)} = -\mathbf{H}_2 \circ (\mathbf{U}^\top \widehat{\mathbf{U}} \widehat{\mathbf{\Lambda}}^2 - \mathbf{\Lambda}^2 \mathbf{U}^\top \widehat{\mathbf{U}}).$$

The rightmost matrix factor can be written as

$$(\mathbf{U}^\top \widehat{\mathbf{U}} \widehat{\mathbf{\Lambda}}^2 - \mathbf{\Lambda}^2 \mathbf{U}^\top \widehat{\mathbf{U}}) = \mathbf{U}^\top (\widehat{\mathbf{M}})^2 \widehat{\mathbf{U}} - \mathbf{U}^\top \mathbf{M}^2 \widehat{\mathbf{U}} = \mathbf{U}^\top (\mathbf{ME} + \mathbf{EM}) \widehat{\mathbf{U}},$$

and has spectral norm on the order of $O_{\mathbb{P}}\{(n\rho_n)^{3/2}\}$. Hence,

$$\begin{aligned} \|\mathbf{R}_2^{(1)}\|_{2\to\infty} = \|\mathbf{EU\Lambda R}_2^{(3)}\|_{2\to\infty} &\leq r\|\mathbf{EU}\|_{2\to\infty}\|\mathbf{\Lambda}\|_2\|\mathbf{H}_2\|_{\max}\|\mathbf{U}^\top \widehat{\mathbf{U}} \widehat{\mathbf{\Lambda}}^2 - \mathbf{\Lambda}^2 \mathbf{U}^\top \widehat{\mathbf{U}}\|_2 \\ &= O_{\mathbb{P}}\left\{r^{3/2}(n\rho_n)^{-1}(\log n)^{\xi}\|\mathbf{U}\|_{2\to\infty}\right\}. \end{aligned}$$

For $\mathbf{R} = \mathbf{R}^{(1)} + \mathbf{R}_{\mathbf{W}}^{(2)} + \mathbf{R}_2^{(1)} + \mathbf{R}_{2,\mathbf{W}}^{(2)} + \mathbf{R}_2^{(\infty)}$, we have therefore shown that

$$\widehat{\mathbf{U}} - \mathbf{UW} = \mathbf{EU\Lambda}^{-1}\mathbf{W} + \mathbf{R}, \tag{6.10}$$

where since $r^{1/2} \leq (\log n)^{\xi}$, the residual matrix $\mathbf{R}$ satisfies

$$\|\mathbf{R}\|_{2\to\infty} = O_{\mathbb{P}}\left[(n\rho_n)^{-1} \times r \times \max\left\{(\log n)^{2\xi}, \|\mathbf{U}^\top \mathbf{EU}\|_2 + 1\right\} \times \|\mathbf{U}\|_{2\to\infty}\right].$$

The leading term agrees with the order of the bound in Theorem 19, namely

$$\|\mathbf{E}\mathbf{U}\mathbf{\Lambda}^{-1}\mathbf{W}\|_{2\to\infty} = O_{\mathbb{P}}\left\{(n\rho_n)^{-1/2} \times r^{1/2}(\log n)^{\xi}\|\mathbf{U}\|_{2\to\infty}\right\}.$$

This establishes Theorem 20 en route to proving Theorem 21, which we now finish.

Since $\mathbf{M} = \rho_n \mathbf{X}\mathbf{X}^\top \equiv \mathbf{U}\mathbf{\Lambda}\mathbf{U}^\top$, there exists an orthogonal matrix $\mathbf{W}_{\mathbf{X}}$ (depending on n) such that $\rho_n^{1/2}\mathbf{X} = \mathbf{U}\mathbf{\Lambda}^{1/2}\mathbf{W}_{\mathbf{X}}$, hence $\rho_n \mathbf{X}^\top\mathbf{X} = \mathbf{W}_{\mathbf{X}}^\top\mathbf{\Lambda}\mathbf{W}_{\mathbf{X}}$. Following some algebraic manipulations, the matrix $\mathbf{E}\mathbf{U}\mathbf{\Lambda}^{-1}\mathbf{W}$ can therefore be written as

$$\mathbf{E}\mathbf{U}\mathbf{\Lambda}^{-1}\mathbf{W} = \rho_n^{-1}\mathbf{E}\mathbf{X}(\mathbf{X}^\top\mathbf{X})^{-3/2}(\mathbf{W}_{\mathbf{X}}^\top\mathbf{W}).$$

Plugging this observation into Eq. (6.10) and subsequent matrix multiplication together yield the relation

$$\left(\widehat{\mathbf{U}}\mathbf{W}^\top\mathbf{W}_{\mathbf{X}} - \mathbf{U}\mathbf{W}_{\mathbf{X}}\right) = \rho_n^{-1}\mathbf{E}\mathbf{X}(\mathbf{X}^\top\mathbf{X})^{-3/2} + \mathbf{R}\mathbf{W}^\top\mathbf{W}_{\mathbf{X}}.$$

For fixed i, let $\widehat{\mathbf{U}}_i$, $\mathbf{U}_i$, and $\mathbf{R}_i$ be column vectors denoting the i-th rows of $\widehat{\mathbf{U}}$, $\mathbf{U}$, and $\mathbf{R}$, respectively. By hypothesis, it follows that $n\rho_n^{1/2}\|\mathbf{R}_i\|_2 \to 0$ in probability. In addition, $(n^{-1}\mathbf{X}^\top\mathbf{X})^{-3/2} \to \mathbf{\Xi}^{-3/2}$ by Assumption 5 together with the continuous mapping theorem. The scaled i-th row of $\mathbf{E}\mathbf{X}$ converges in distribution to $Y_i \sim \mathcal{N}_r(\mathbf{0}, \mathbf{\Gamma}_i)$ by Assumption 5, so combining the above observations together with Slutsky's theorem

yields that there exist sequences of orthogonal matrices $(\mathbf{W})$ and $(\mathbf{W}_{\mathbf{X}})$ such that

$$n\rho_n^{1/2}\mathbf{W}_{\mathbf{X}}^{\top}\left(\mathbf{W}\widehat{\mathbf{U}}_i - \mathbf{U}_i\right) = \left(n^{-1}\mathbf{X}^{\top}\mathbf{X}\right)^{-3/2}\left\{(n\rho_n)^{-1/2}(\mathbf{E}\mathbf{X})_i\right\} + n\rho_n^{1/2}\mathbf{W}_{\mathbf{X}}^{\top}\mathbf{W}\mathbf{R}_i$$
$$\Rightarrow \boldsymbol{\Xi}^{-3/2}Y_i + \mathbf{0}.$$

In particular, we have the row-wise convergence in distribution

$$n\rho_n^{1/2}\mathbf{W}_{\mathbf{X}}^{\top}\left(\mathbf{W}\widehat{\mathbf{U}}_i - \mathbf{U}_i\right) \Rightarrow \mathcal{N}_r(\mathbf{0}, \boldsymbol{\Sigma}_i)$$

where $\boldsymbol{\Sigma}_i = \boldsymbol{\Xi}^{-3/2}\boldsymbol{\Gamma}_i\boldsymbol{\Xi}^{-3/2}$. This completes the proof of Theorem 21. □

6.3 Proofs for Chapter 4

6.3.1 Proof of Theorem 26

Proof. Let $\mathbf{P}, \mathbf{E} \in \mathbb{R}^{n\times n}$ be real symmetric matrices such that $\mathbf{E}$ satisfies Proposition 25. Denote the d largest eigenvalues of $\mathbf{P}$ and $\mathbf{A}$ by

$$0 < \lambda_1(\mathbf{P}) \leq \lambda_2(\mathbf{P}) \leq \cdots \leq \lambda_d(\mathbf{P}),$$
$$0 < \lambda_1(\mathbf{A}) \leq \lambda_2(\mathbf{A}) \leq \cdots \leq \lambda_d(\mathbf{A}).$$

Let $\{\mathbf{w}_i\}_{i=1}^d$ denote a collection of orthonormal eigenvectors of $\mathbf{P}$ corresponding to the collection of eigenvalues $\{\lambda_i(\mathbf{P})\}_{i=1}^d$. Similarly, let $\{\mathbf{u}_i\}_{i=1}^d$ denote a collection of orthonormal eigenvectors of $\mathbf{A}$ corresponding to the collection of eigenvalues $\{\lambda_i(\mathbf{A})\}_{i=1}^d$.

For each $i \in [d]$ define η_i to be an "approximate eigenvalue of $\mathbf{A}$ close to $\lambda_i(\mathbf{P})$" in the sense that

$$\eta_i := \langle \mathbf{A}\mathbf{w}_i, \mathbf{w}_i \rangle = \lambda_i(\mathbf{P}) + \langle \mathbf{E}\mathbf{w}_i, \mathbf{w}_i \rangle, \tag{6.11}$$

and define a corresponding "residual quantity" ϵ_i as

$$\epsilon_i := \|(\mathbf{A} - \eta_i \mathbf{I})\mathbf{w}_i\|. \tag{6.12}$$

6.3.1.1 Proof of Theorem 26: upper bound

Now for fixed $k \in [d]$ define the k-dimensional linear manifold $\mathcal{M}_k$ by

$$\mathcal{M}_k := \text{span}\{\mathbf{u}_1, \ldots, \mathbf{u}_k\}.$$

We now define a collection of "aggregate quantities":

- Define $\mathbf{w}$ to be an "aggregate approximate eigenvector of $\mathbf{A}$" in the sense that $\mathbf{w} := \sum_{i=1}^k r_i \mathbf{w}_i$ for a collection of normalized coefficients $\{r_i\}_{i=1}^k$ such that $\|\mathbf{w}\|^2 = \sum_{i=1}^k r_i \mathbf{w}_i = 1$, and satisfying the under-determined linear system

$\langle \mathbf{w}, \mathbf{u}_i \rangle = 0$ for $i = 1, 2, \ldots, k-1$.

- Define η to be an "aggregate approximate eigenvector of $\mathbf{A}$" in the sense that $\eta := \langle \mathbf{A}\mathbf{w}, \mathbf{w} \rangle$.
- Define ϵ to be the "aggregate residual quantity" $\epsilon := \|(\mathbf{A} - \eta \mathbf{I})\mathbf{w}\|$.

By Lemma 1 in Kato (1950), the interval $\left(\alpha, \eta + \frac{\epsilon^2}{\eta - \alpha}\right]$ contains a point in the spectrum of A. Note that by construction, $\mathbf{w} \in \mathcal{M}_{k-1}^{\perp} =: \mathcal{N}_{k-1}$; moreover, $\mathbf{A}\mathbf{w} \in \mathcal{N}_{k-1}$ as a function of $\{r_i\}_{i=1}^k$. In the Hilbert space $\mathcal{N}_{k-1}$, however, the spectrum of $\mathbf{A}$ does not contain $\lambda_1(\mathbf{A}), \ldots, \lambda_{k-1}(\mathbf{A})$ since $\mathbf{u}_1, \ldots, \mathbf{u}_{k-1} \notin \mathcal{N}_{k-1}$. Thus, by another application of Lemma 1 in Kato (1950), the eigenvalue of $\mathbf{A}$ in the interval given by $\left(\alpha, \eta + \frac{\epsilon^2}{\eta - \alpha}\right]$ must be $\lambda_k(\mathbf{A})$ with associated unit eigenvector $\mathbf{u}_k$. Hence,

$$\lambda_k(\mathbf{A}) \leq \eta + \frac{\epsilon^2}{\eta - \alpha} = \frac{\eta^2 + \epsilon^2 - \alpha\eta}{\eta - \alpha}. \tag{6.13}$$

We pause briefly to make several computational observations. First,

$$\eta^2 + \epsilon^2 = \langle \mathbf{A}\mathbf{w}, \mathbf{w} \rangle^2 + \|(\mathbf{A} - \langle \mathbf{A}\mathbf{w}, \mathbf{w} \rangle \mathbf{I})\mathbf{w}\|^2 \tag{6.14}$$

$$= \|\mathbf{A}\mathbf{w}\|^2 = \sum_{i,j=1}^{k} r_i r_j \langle \mathbf{A}\mathbf{w}_i, \mathbf{A}\mathbf{w}_j \rangle. \tag{6.15}$$

Let $\delta_{i,j} := \mathbb{I}\{i = j\}$ denote the Kronecker delta function. For each $i, j \in [d]$,

$$\langle \mathbf{A}\mathbf{w}_i, \mathbf{A}\mathbf{w}_j \rangle = \langle (\mathbf{A} - \eta_i \mathbf{I})\mathbf{w}_i, (\mathbf{A} - \eta_j \mathbf{I})\mathbf{w}_j \rangle + (\eta_i + \eta_j)\langle \mathbf{A}\mathbf{w}_i, \mathbf{w}_j \rangle - \eta_i^2 \delta_{i,j}, \tag{6.16}$$

while

$$\langle \mathbf{A}\mathbf{w}_i, \mathbf{w}_j \rangle = \langle \mathbf{E}\mathbf{w}_i, \mathbf{w}_j \rangle \text{ for } i \neq j. \tag{6.17}$$

It will also prove useful to recognize the expansion

$$\eta = \langle \mathbf{A}\mathbf{w}, \mathbf{w} \rangle = \sum_{i=1}^{k} r_i^2 \eta_i + \sum_{1 \leq i < j \leq k} 2 r_i r_j \langle \mathbf{E}\mathbf{w}_i, \mathbf{w}_j \rangle. \tag{6.18}$$

Combining these observations yields

$$\begin{aligned}
\eta^2 + \epsilon^2 &= \sum_{i,j=1}^{k} r_i r_j \langle \mathbf{A}\mathbf{w}_i, \mathbf{A}\mathbf{w}_j \rangle \\
&= \left(\sum_{i=1}^{k} r_i^2 \langle \mathbf{A}\mathbf{w}_i, \mathbf{A}\mathbf{w}_i \rangle \right) + \left(\sum_{1 \leq i < j \leq k} 2 r_i r_j \langle \mathbf{A}\mathbf{w}_i, \mathbf{A}\mathbf{w}_j \rangle \right) \\
&= \sum_{i,j=1}^{k} r_i r_j \langle (\mathbf{A} - \eta_i \mathbf{I})\mathbf{w}_i, (\mathbf{A} - \eta_j \mathbf{I})\mathbf{w}_j \rangle \\
&\quad + \sum_{i=1}^{k} r_i^2 \eta_i^2 + \sum_{1 \leq i < j \leq k} 2 r_i r_j (\eta_i + \eta_j) \langle \mathbf{A}\mathbf{w}_i, \mathbf{w}_j \rangle.
\end{aligned}$$

An application of the Cauchy–Schwarz inequality coupled with subsequent computation yields

$$\begin{aligned}
\sum_{i,j=1}^{k} r_i r_j \langle (\mathbf{A} - \eta_i \mathbf{I})\mathbf{w}_i, (\mathbf{A} - \eta_j \mathbf{I})\mathbf{w}_j \rangle &\leq \sum_{i,j=1}^{k} r_i r_j \left(\|(\mathbf{A} - \eta_i \mathbf{I})\mathbf{w}_i\| \|(\mathbf{A} - \eta_j \mathbf{I})\mathbf{w}_j\| \right) \\
&= \sum_{i,j=1}^{k} (r_i \epsilon_i)(r_j \epsilon_j) \leq \left(\sum_{i=1}^{k} \epsilon_i |r_i| \right)^2.
\end{aligned}$$

Hence,

$$\eta^2 + \epsilon^2 \leq \left(\sum_{i=1}^{k} \epsilon_i |r_i| \right)^2 + \sum_{i=1}^{k} r_i^2 \eta_i^2 + \sum_{1 \leq i < j \leq k} 2 r_i r_j (\eta_i + \eta_j) \langle \mathbf{E}\mathbf{w}_i, \mathbf{w}_j \rangle. \tag{6.19}$$

Returning to Eq. (6.13), the numerator then becomes

$$\left(\sum_{i=1}^{k} \epsilon_i |r_i| \right)^2 + \sum_{i=1}^{k} r_i^2 \eta_i (\eta_i - \alpha) + \sum_{1 \leq i < j \leq k} 2 r_i r_j (\eta_i + \eta_j - \alpha) \langle \mathbf{E}\mathbf{w}_i, \mathbf{w}_j \rangle \tag{6.20}$$

while the denominator becomes

$$\left(\sum_{i=1}^{k} r_i^2 (\eta_i - \alpha) \right) + \left(\sum_{1 \leq i < j \leq k} 2 r_i r_j \langle \mathbf{E}\mathbf{w}_i, \mathbf{w}_j \rangle \right). \tag{6.21}$$

By a simple union bound, observe that for $t > 0$,

$$\mathbb{P}\left[\max_{1 \leq i \leq j \leq k} |\langle \mathbf{E}\mathbf{w}_i, \mathbf{w}_j \rangle| > t \right] \leq \left(k + \binom{k}{2} \right) C \exp(-c t^{\gamma}), \tag{6.22}$$

in which case with high probability,

$$\left(\sum_{i=1}^{k} r_i^2 (\eta_i - \alpha) \right) \geq \lambda_1(\mathbf{P}) - \alpha - t, \tag{6.23}$$

$$\left(\sum_{1 \leq i < j \leq k} 2 r_i r_j \langle \mathbf{E}\mathbf{w}_i, \mathbf{w}_j \rangle \right) \geq -k(k-1)t, \tag{6.24}$$

while with high probability,

$$\sum_{1\le i<j\le k} 2r_i r_j(\eta_i+\eta_j-\alpha)\langle \mathbf{E}\mathbf{w}_i,\mathbf{w}_j\rangle \le (2\lambda_k(\mathbf{P})-\alpha+2t)k(k-1)t, \tag{6.25}$$

$$\left(\sum_{i=1}^k r_i^2\eta_i\right)k(k-1)t \le (\lambda_k(\mathbf{P})+t)k(k-1)t. \tag{6.26}$$

By adding and subtracting $\left(\sum_{i=1}^k r_i^2\eta_i\right)k(k-1)t$ to the numerator of Eq. (6.13) we obtain the following bound in which the first term on the right-hand side is the leading term while the second term on the right hand side corresponds to a residual term.

$$\lambda_k(\mathbf{A}) \le \frac{\left(\sum_{i=1}^k \epsilon_i|r_i|\right)^2+\left(\sum_{i=1}^k r_i^2\eta_i(\eta_i-\alpha-k(k-1)t)\right)}{\left(\sum_{i=1}^k r_i^2(\eta_i-\alpha-k(k-1)t)\right)} + \frac{(3\lambda_k(\mathbf{P})-\alpha+3t)k(k-1)t}{\lambda_1(\mathbf{P})-\alpha-(k(k-1)+1)t}.$$

Now by the same arguments as in Kato (1950), Section 3, Eq. (22–30), the constants $\{r_i\}_{i=1}^k$ can be removed. To this end, the quantity

$$\frac{\left(\sum_{i=1}^k \epsilon_i|r_i|\right)^2+\left(\sum_{i=1}^k r_i^2\eta_i(\eta_i-\alpha-k(k-1)t)\right)}{\left(\sum_{i=1}^k r_i^2(\eta_i-\alpha-k(k-1)t)\right)} \tag{6.27}$$

is bounded above by the quantity

$$\max_{1\le i\le k}\eta_i + \left(\sum_{i=1}^k \frac{\epsilon_i^2}{\eta_i-\alpha-k(k-1)t}\right). \tag{6.28}$$

Note that $\max_{1\leq i\leq k}\eta_i \leq \lambda_k(\mathbf{P}) + t$, with high probability, while a simple computation reveals that for each $i \in [k]$,

$$\epsilon_i^2 = \|\mathbf{E}\mathbf{w}_i\|^2 - |\langle \mathbf{E}\mathbf{w}_i, \mathbf{w}_i\rangle|^2 \leq \|\mathbf{E}\mathbf{w}_i\|^2 \leq \|\mathbf{E}\|_2^2. \tag{6.29}$$

Combining these observations produces an upper bound on $\lambda_k(\mathbf{A})$ of the form

$$\lambda_k(\mathbf{A}) \leq \lambda_k(\mathbf{P}) + t + \zeta^+, \tag{6.30}$$

where $\zeta^+ := \frac{k\|\mathbf{E}\|_2^2 + (3\lambda_k(\mathbf{P}) - \alpha + 3t)k(k-1)t}{\lambda_1(\mathbf{P}) - \alpha - (k(k-1)+1)t}$.

6.3.1.2 Proof of Theorem 26: lower bound

Fix $k \in [d]$ and let $l := d - k + 1$. Define $\mathcal{M}_l$ to be the l-dimensional linear manifold

$$\mathcal{M}_l := \text{span}\{\mathbf{u}_k, \ldots, \mathbf{u}_d\}.$$

We now define a collection of "aggregate quantities" similar to the formulation in Section 6.3.1.1:

- Define $\mathbf{w}$ to be an "aggregate approximate eigenvector of $\mathbf{A}$" in the sense that $\mathbf{w} := \sum_{i=k}^d r_i \mathbf{w}_i$ for a collection of normalized coefficients $\{r_i\}_{i=k}^d$ such that $\|\mathbf{w}\|^2 = \sum_{i=k}^d r_i \mathbf{w}_i = 1$, and satisfying the under-determined linear system $\langle \mathbf{w}, \mathbf{u}_i\rangle = 0$ for $i = k+1, \ldots, d$.

- Define η to be an "aggregate approximate eigenvector of $\mathbf{A}$" in the sense that $\eta := \langle \mathbf{A}\mathbf{w}, \mathbf{w} \rangle$.
- Define ϵ to be the "aggregate residual quantity" $\epsilon := \|(\mathbf{A} - \eta \mathbf{I})\mathbf{w}\|$.

By Lemma 2 in Kato (1950), the interval $\left[\eta - \frac{\epsilon^2}{\beta - \eta}, \beta\right)$ contains a point in the spectrum of $\mathbf{A}$. Note that by construction, $\mathbf{w} \in \mathcal{M}_{l-1}^{\perp} =: \mathcal{N}_{l-1}$; moreover, $\mathbf{A}\mathbf{w} \in \mathcal{N}_{l-1}$ as a function of $\{r_i\}_{i=k}^{d}$. In the Hilbert space $\mathcal{N}_{l-1}$, however, the spectrum of $\mathbf{A}$ does not contain $\lambda_{k+1}(\mathbf{A}), \ldots, \lambda_d(\mathbf{A})$ since $\mathbf{u}_{k+1}, \ldots, \mathbf{u}_d \notin \mathcal{N}_{l-1}$. Thus, by another application of Lemma 2 in Kato (1950), the eigenvalue of $\mathbf{A}$ in the interval $\left[\eta - \frac{\epsilon^2}{\beta - \eta}, \beta\right)$ must be $\lambda_k(\mathbf{A})$ with associated unit eigenvector $\mathbf{u}_k$.

Consider first the special case when $\beta = \infty$. By a simple union bound, observe that for $t > 0$,

$$\mathbb{P}\left[\max_{k \le i \le j \le d} |\langle \mathbf{E}\mathbf{w}_i, \mathbf{w}_j \rangle| > t\right] \le \left(l + \binom{l}{2}\right) C \exp(-ct^{\gamma}), \tag{6.31}$$

hence with high probability

$$\sum_{i=k}^{d} r_i^2 \eta_i \ge \min_{k \le i \le d} \eta_i \ge \lambda_k(\mathbf{P}) - t \tag{6.32}$$

and

$$\lambda_k(\mathbf{A}) \geq \eta = \sum_{i=k}^{d} r_i^2 \eta_i + \sum_{k \leq i < j \leq d} 2 r_i r_j \langle \mathbf{E}\mathbf{w}_i, \mathbf{w}_j \rangle \tag{6.33}$$

$$\geq \lambda_k(\mathbf{P}) - (l(l-1)+1)t. \tag{6.34}$$

Now suppose that $\beta < \infty$. Then for the lower bound of the above interval, one has

$$\lambda_k(\mathbf{A}) \geq \eta - \frac{\epsilon^2}{\beta - \eta} = \frac{\beta\eta - \eta^2 - \epsilon^2}{\beta - \eta} = \frac{-(\eta^2 + \epsilon^2) + \beta\eta}{\beta - \eta}.$$

Reversing the direction of the previous application of the Cauchy–Schwarz inequality in Eq. (6.19) permits the numerator to be bounded below by

$$-(\sum_{i=k}^{d} \epsilon_i |r_i|)^2 + \sum_{i=k}^{d} r_i^2 \eta_i (\beta - \eta_i) + \sum_{k \leq i < j \leq d} 2 r_i r_j (\beta - \eta_i - \eta_j) \langle \mathbf{E}\mathbf{w}_i, \mathbf{w}_j \rangle,$$

whereas the denominator has the expansion

$$\sum_{i=k}^{d} r_i^2 (\beta - \eta_i) + \sum_{k \leq i < j \leq d} 2 r_i r_j \langle \mathbf{E}\mathbf{w}_i, \mathbf{w}_j \rangle.$$

For the denominator terms, note that with high probability

$$\sum_{i=k}^{d} r_i^2(\beta - \eta_i) \geq \beta - \lambda_d(\mathbf{P}) - t,$$

$$\sum_{k \leq i < j \leq d} 2r_i r_j \langle \mathbf{E}\mathbf{w}_i, \mathbf{w}_j \rangle \geq -l(l-1)t,$$

while in the numerator, with high probability,

$$\sum_{k \leq i < j \leq d} 2r_i r_j (\beta - \eta_i - \eta_j) \langle \mathbf{E}\mathbf{w}_i, \mathbf{w}_j \rangle \geq -(\beta - \lambda_k(\mathbf{P}) + \lambda_d(\mathbf{P}) + 2t) l(l-1)t.$$

In the numerator of Eq. (6.33), add and subtract the quantity $\left(\sum_{i=k}^{d} r_i^2 \eta_i\right) l(l-1)t$ which is bounded below by $(\lambda_k(\mathbf{P}) - t)l(l-1)t$. Combining these observations yields

$$\begin{aligned}\lambda_k(\mathbf{A}) \geq & \frac{-(\sum_{i=k}^{d} \epsilon_i |r_i|)^2 + \sum_{i=k}^{d} r_i^2 \eta_i (\beta - \eta_i - l(l-1)t)}{\sum_{i=k}^{d} r_i^2 (\beta - \eta_i - l(l-1)t)} \\ & + \frac{-(\beta - \lambda_k(\mathbf{P}) + \lambda_d(\mathbf{P}) - \lambda_k + 3t) l(l-1)t}{\beta - \lambda_d(\mathbf{P}) - (l(l-1)+1)t}.\end{aligned}$$

By employing the same approach used to obtain the upper bound and taking negatives when necessary (thereby reversing the direction in which bounds hold), we obtain the lower bound for $\lambda_k(\mathbf{A})$ of the form

$$\lambda_k(\mathbf{A}) \geq \lambda_k(\mathbf{P}) - t - \zeta^-, \tag{6.35}$$

where $\zeta^- := \frac{l\|\mathbf{E}\|_2^2 + ((\beta - \lambda_k(\mathbf{P})) + (\lambda_d(\mathbf{P}) - \lambda_k(\mathbf{P})) + 3t) l(l-1)t}{\beta - \lambda_d(\mathbf{P}) - (l(l-1)+1)t}$. □

6.3.2 Proof of Theorem 27

Proof. The hypotheses imply by Lu and Peng (2013) that $\|\mathbf{A} - \mathbf{P}\|_2 = O(\sqrt{\Delta})$ with probability $1 - o(1)$ as $n \to \infty$. Set $\alpha = (C - c)\Delta/2$ and $\beta = \infty$ as Kato–Temple threshold values. Choose $\delta \in (0, 1]$ and set $t = \Theta(\log^{\delta} n)$. Then in Theorem 26, for sufficiently large n, one has $\zeta^+, \zeta^- = O(t)$ where the underlying constant depends upon k, d, as well as underlying (unspecified) constants. So for $n \geq n_0$, then $|\hat{\sigma}_k - \sigma_k| \leq c_{k,d} t$ with probability $1 - o(1)$ as claimed. □

6.3.3 Proof of Theorem 30

Proof. The proof follows essentially *mutatis mutandis* as in Theorem 26 via Remark 12, Definition 28, and Lemma 29. Observe that $\langle \widehat{\tilde{\mathbf{M}}} \tilde{\mathbf{w}}_i, \tilde{\mathbf{w}}_j \rangle = \sigma_i \delta_{i,j} + \langle \tilde{\mathbf{E}} \tilde{\mathbf{w}}_i, \tilde{\mathbf{w}}_j \rangle$ for each pair i, j, while at the same time $\|\tilde{\mathbf{E}}\|_2 = \|\mathbf{E}\|_2$. □

6.3.4 Proof of Lemma 31

Proof. Let $\mathbf{E} \in \mathbb{R}^{m \times n}$ be a (C, c, γ)-concentrated random matrix. Take $\mathcal{X}$ and $\mathcal{Y}$ to be $\frac{1}{4}$-nets of the spheres S^{n-1} and S^{m-1}, respectively, with cardinalities at most 9^n

and 9^m, respectively. Then a standard net argument yields that for $t > 0$,

$$\begin{aligned}
\mathbb{P}\left[\|\mathbf{E}\|_2 > t\right] &\leq \mathbb{P}\left[2 \max_{x \in \mathcal{X}, y \in \mathcal{Y}} |\langle \mathbf{E}\mathbf{x}, \mathbf{y} \rangle| > t\right] \\
&\leq 9^{m+n} \mathbb{P}\left[|\langle \mathbf{E}\mathbf{x}, \mathbf{y} \rangle| > t/2\right] \\
&\leq C \exp((m+n)\log(9) - c(t/2)^{\gamma}) \\
&\leq C \exp(2\log(9)\max\{m,n\} - c(t/2)^{\gamma}).
\end{aligned}$$

Choose $\epsilon > 0$ such that $2 + \epsilon > 2\left(2\log(9)/c\right)^{1/\gamma}$ and set $t = (2+\epsilon)\max\{m,n\}^{1/\gamma}$. Then for $c_{\epsilon,c,\gamma} := (c(1+\epsilon/2)^{\gamma} - 2\log(9)) > 0$, we have

$$\mathbb{P}\left[\|\mathbf{E}\|_2 > (2+\epsilon)\max\{m,n\}^{1/\gamma}\right] \leq C \exp(-c_{\epsilon,c,\gamma}\max\{m,n\}).$$

If in addition $m = n$ and $\mathbf{E}$ is symmetric, then since $\|\mathbf{E}\|_2 \equiv \sup_{\|\mathbf{x}\|_2 = 1} |\langle \mathbf{E}\mathbf{x}, \mathbf{x} \rangle|$, one need only consider the $\frac{1}{4}$-net $\mathcal{X}$ for the purposes of a union bound. $\square$

6.4 Proofs and supplementary material for Chapter 5

6.4.1 Latent position geometry

All stochastic block models in Definition 33 can be formulated as instantiations of generalized random dot product graph models possessing inherent latent position (vector) structure. Earlier observations for the two-block SBM in Section 5.5 are summarized in the following table, for which the implicit underlying vector $\boldsymbol{\pi}$ may be viewed as an additional parameter space dimension that weights the latent positions $\boldsymbol{\nu}_1$ and $\boldsymbol{\nu}_2$ by π_1 and π_2, respectively.

Model geometry:	Canonical latent positions:
Positive definite $\mathbf{B}(a, b, c)$	$\boldsymbol{\nu}_1 = (\sqrt{a}, 0)^\top, \boldsymbol{\nu}_2 = (b/\sqrt{a}, \sqrt{ac - b^2}/\sqrt{a})^\top$ in $\mathbb{R}^2$
Indefinite $\mathbf{B}(a, b, c)$	$\boldsymbol{\nu}_1 = (\sqrt{a}, 0)^\top, \boldsymbol{\nu}_2 = (b/\sqrt{a}, \sqrt{b^2 - ac}/\sqrt{a})^\top$ in $\mathbb{R}^2$
Rank one $\mathbf{B}(p^2, pq, q^2)$	$\boldsymbol{\nu}_1 = p, \boldsymbol{\nu}_2 = q$ in $\mathbb{R}$

For the homogeneous balanced affinity two-block network structure investigated in Section 5.5.1.1, the latent position geometry can be equivalently reparameterized as two vectors on the circle of radius $r := \sqrt{a}$ separated by the angle $\theta := \arccos(b/a)$. This behavior generalizes to the homogeneous balanced affinity K-block model.

When $\mathbf{B} \equiv \mathbf{B}(K) \in (0, 1)^{K \times K}$ has value a on the main diagonal and value b on the off-diagonal with $0 < b < a < 1$, we can write $\mathbf{B} = \mathbf{X}\mathbf{X}^\top$ via the Cholesky

decomposition, where $\mathbf{X}$ has rows given by $\mathbf{X} = [\mathbf{x}_1|\mathbf{x}_2|\ldots|\mathbf{x}_K]^\top$. For each $i \in [K]$ let the zero-dilation of the $\mathbb{R}^K$ vector $\mathbf{x}_i$ be denoted by $\mathbf{x}_i^\circ := (\mathbf{x}_i, 0)^\top \in \mathbb{R}^{K+1}$. For $K = 2, 3, 4$, $\mathbf{X}$ is given by

$$\mathbf{X}(2) := \begin{bmatrix} \sqrt{a} & 0 \\ \frac{b}{\sqrt{a}} & \sqrt{\frac{(a-b)(a+b)}{a}} \end{bmatrix}, \tag{6.36}$$

$$\mathbf{X}(3) := \begin{bmatrix} \sqrt{a} & 0 & 0 \\ \frac{b}{\sqrt{a}} & \sqrt{\frac{(a-b)(a+b)}{a}} & 0 \\ \frac{b}{\sqrt{a}} & \sqrt{\frac{(a-b)(a+b)}{a}}\frac{b}{a+b} & \sqrt{\frac{(a-b)(a+2b)}{a+b}} \end{bmatrix}, \tag{6.37}$$

$$\mathbf{X}(4) := \begin{bmatrix} \sqrt{a} & 0 & 0 & 0 \\ \frac{b}{\sqrt{a}} & \sqrt{\frac{(a-b)(a+b)}{a}} & 0 & 0 \\ \frac{b}{\sqrt{a}} & \sqrt{\frac{(a-b)(a+b)}{a}}\frac{b}{a+b} & \sqrt{\frac{(a-b)(a+2b)}{a+b}} & 0 \\ \frac{b}{\sqrt{a}} & \sqrt{\frac{(a-b)(a+b)}{a}}\frac{b}{a+b} & \sqrt{\frac{(a-b)(a+2b)}{a+b}}\frac{b}{a+2b} & \sqrt{\frac{(a-b)(a+3b)}{a+2b}} \end{bmatrix}. \tag{6.38}$$

By induction, for $K \geq 3$, the entries of the vector $\mathbf{x}_K$ are given by

$$\mathbf{x}_K = \left(\mathbf{x}_{K-1}^1, \mathbf{x}_{K-1}^2, \ldots, \mathbf{x}_{K-1}^{K-2}, \left(\tfrac{b}{a+(K-2)b}\right)\mathbf{x}_{K-1}^{K-1}, \sqrt{\tfrac{(a-b)(a+(K-1)b)}{a+(K-2)b}}\right)^\top \in \mathbb{R}^K. \tag{6.39}$$

Only $\mathbf{I}_0^K$ and $\mathbf{I}_{K-1}^1$ are necessary with respect to combining possible inner products on account of the sign-flip involving $a-b$. Beginning with the second row in each of the $\mathbf{X}$ matrices, the first column of each matrix can be written in the more illuminating

form $\sqrt{a}\frac{b}{a}$.

For this specific K-block model, symmetry with respect to equally-spaced vectors on the $\sqrt{a}$-radius sphere in $\mathbb{R}^K$ together with block membership balancedness translates into shared covariance structure such that Eq. (5.12) reduces to Eq. (5.13). The first two rows of $\mathbf{X}$ are ideal candidates to serve as canonical latent positions for subsequent computation, since these vectors are maximally sparse in the sense of having the fewest non-zero entries and merely become zero-inflated as a function of K. These geometric considerations are crucial in the subsequent proof of Theorem 38.

6.4.2 Analytic derivations for the two-block SBM

The value of $\rho^\star$ in Eq. (5.14) for the homogeneous balanced two-block SBM can be computed by brute force; however, such an approach offers only limited insight and understanding of how the covariance structure in Theorem 36 and Theorem 37 interact to yield differences in relative spectral embedding performance as measured via Chernoff information. This section offers a different approach to understanding $\rho^\star$ as a covariance-based spectral quantity.

The following lemma is a general matrix analysis observation that establishes a correspondence between the inverse of a convex combination of 2×2 matrices and the inverses of the original 2×2 matrices. The proof of Lemma 42 follows directly from elementary computations and is therefore omitted. Extending Lemma 42 to $n \times n$ invertible matrices is intractable in general.

Lemma 42. *Let* $\mathbf{M}_0, \mathbf{M}_1 \in \mathbb{R}^{2\times 2}$ *be two invertible matrices. For each* $t \in [0,1]$ *define the matrix* $\mathbf{M}_t := (1-t)\mathbf{M}_0 + t\mathbf{M}_1$. *Provided* $\mathbf{M}_t$ *is invertible, then the inverse matrix* $\mathbf{M}_t^{-1}$ *can be expressed as*

$$\mathbf{M}_t^{-1} \equiv \frac{(1-t)\mathbf{M}_0^{-1} + \det(\mathbf{M}_1\mathbf{M}_0^{-1})t\mathbf{M}_1^{-1}}{\det(\mathbf{M}_1\mathbf{M}_0^{-1})t^2 + \mathrm{tr}(\mathbf{M}_1\mathbf{M}_0^{-1})t(1-t) + (1-t)^2}. \tag{6.40}$$

If, in the context of Lemma 42, $\det(\mathbf{M}_1\mathbf{M}_0^{-1}) = 1$, then Eq. (6.40) simplifies to

$$\mathbf{M}_t^{-1} \equiv \frac{(1-t)\mathbf{M}_0^{-1} + t\mathbf{M}_1^{-1}}{t^2 + \mathrm{tr}(\mathbf{M}_1\mathbf{M}_0^{-1})t(1-t) + (1-t)^2},$$

which is nearly a convex combination of the inverse matrices $\mathbf{M}_0^{-1}$ and $\mathbf{M}_1^{-1}$ modulo division by a degree two polynomial in the parameter t. If, in addition, $\mathrm{tr}(\mathbf{M}_1\mathbf{M}_0^{-1}) \neq -2$ (which always holds when $\mathbf{M}_0$ and $\mathbf{M}_1$ are both positive definite), then the inverse matrix at the value $t = \frac{1}{2}$ further simplifies to

$$\mathbf{M}_{1/2}^{-1} \equiv \left(\frac{2}{2 + \mathrm{tr}(\mathbf{M}_1\mathbf{M}_0^{-1})}\right)\left(\mathbf{M}_0^{-1} + \mathbf{M}_1^{-1}\right). \tag{6.41}$$

For the homogeneous balanced two-block SBM considered in Section 5.5.1.1, one can explicitly check that the above $\det(\cdot)$ and $\mathrm{tr}(\cdot)$ conditions are satisfied. Moreover, the value $t^\star = \frac{1}{2}$ achieves the supremum in both the numerator and denominator of $\rho^\star$ in Eq. (5.12). With these observations in hand, it follows by subsequent computations that for both the positive definite and indefinite regimes,

$$
\begin{aligned}
\rho^\star &= \frac{\|\boldsymbol{\nu}_1 - \boldsymbol{\nu}_2\|^2_{\boldsymbol{\Sigma}^{-1}_{1,2}(1/2)}}{\|\tilde{\boldsymbol{\nu}}_1 - \tilde{\boldsymbol{\nu}}_2\|^2_{\tilde{\boldsymbol{\Sigma}}^{-1}_{1,2}(1/2)}} \\
&= \left(\frac{\left(\frac{2}{2+\mathrm{tr}(\boldsymbol{\Sigma}(\boldsymbol{\nu}_1)\boldsymbol{\Sigma}^{-1}(\boldsymbol{\nu}_2))}\right)}{\left(\frac{2}{2+\mathrm{tr}(\tilde{\boldsymbol{\Sigma}}(\boldsymbol{\nu}_1)\tilde{\boldsymbol{\Sigma}}^{-1}(\boldsymbol{\nu}_2))}\right)} \right) \times \left(\frac{(\boldsymbol{\nu}_1 - \boldsymbol{\nu}_2)^\top (\boldsymbol{\Sigma}^{-1}(\boldsymbol{\nu}_1) + \boldsymbol{\Sigma}^{-1}(\boldsymbol{\nu}_2))(\boldsymbol{\nu}_1 - \boldsymbol{\nu}_2)}{(\tilde{\boldsymbol{\nu}}_1 - \tilde{\boldsymbol{\nu}}_2)^\top (\tilde{\boldsymbol{\Sigma}}^{-1}(\boldsymbol{\nu}_1) + \tilde{\boldsymbol{\Sigma}}^{-1}(\boldsymbol{\nu}_2))(\tilde{\boldsymbol{\nu}}_1 - \tilde{\boldsymbol{\nu}}_2)} \right) \\
&= \left(\frac{2 + \mathrm{tr}(\tilde{\boldsymbol{\Sigma}}(\boldsymbol{\nu}_1)\tilde{\boldsymbol{\Sigma}}^{-1}(\boldsymbol{\nu}_2))}{2 + \mathrm{tr}(\boldsymbol{\Sigma}(\boldsymbol{\nu}_1)\boldsymbol{\Sigma}^{-1}(\boldsymbol{\nu}_2))} \right) \times 1 \\
&= 1 + \frac{\mathrm{tr}(\tilde{\boldsymbol{\Sigma}}(\boldsymbol{\nu}_1)\tilde{\boldsymbol{\Sigma}}^{-1}(\boldsymbol{\nu}_2)) - \mathrm{tr}(\boldsymbol{\Sigma}(\boldsymbol{\nu}_1)\boldsymbol{\Sigma}^{-1}(\boldsymbol{\nu}_2))}{2 + \mathrm{tr}(\boldsymbol{\Sigma}(\boldsymbol{\nu}_1)\boldsymbol{\Sigma}^{-1}(\boldsymbol{\nu}_2))} \\
&= 1 + \frac{(a-b)^2(3a(a-1) + 3b(b-1) + 8ab)}{4(a+b)^2(a(1-a) + b(1-b))}.
\end{aligned}
$$

6.4.3 Proof of Theorem 38

This section is dedicated to proving Theorem 38 for $K \geq 2$ block SBMs exhibiting homogeneous balanced affinity structure. The proof is divided into two parts which separately evaluate the suprema in the numerator and denominator of $\rho^\star$ in Eq. (5.12). By invoking underlying symmetries in latent space and the covariance structure of the ASE and LSE limit results, respectively, we shall leverage the (considerably simpler) ASE computations (numerator) when working with LSE (denominator). Simplifying the numerator and denominator yields the more easily interpretable (shifted) expression of $\rho^\star$ provided in Eq. (5.18).

Proof: First recall the discussion of latent space geometry in Section 6.4.1, specifically that for the homogeneous balanced affinity K-block SBM, the canonical latent

positions can be arranged row-wise as a lower-triangular matrix $\mathbf{X}$ where each latent position vector has norm $\sqrt{a}$ and each pair of distinct latent position vectors has common inner-product b. This rotational symmetry implies rotational symmetry for the block-conditional covariance matrices in Theorems 36 and 37, and as such, the formulation of $\rho^\star$ in Eq. (5.18) can be reduced to simply working with the latent position pair $\{\boldsymbol{\nu}_1, \boldsymbol{\nu}_2\}$ without loss of generality. This pair is attractive, since the non-zero entries of these vectors remain unchanged for all $K \geq 2$. One need only work with the standard inner product since $d^- = 0$.

6.4.3.1 Proof of Theorem 38: ASE (numerator)

Let $g(\mathbf{x}, X_1) := \langle \mathbf{x}, X_1 \rangle (1 - \langle \mathbf{x}, X_1 \rangle)$ and for $0 < t < 1$ define

$$g_t(\mathbf{x}_1, \mathbf{x}_2, X_1) := tg(\mathbf{x}_1, X_1) + (1-t)g(\mathbf{x}_2, X_1).$$

By Theorem 36, $\boldsymbol{\Sigma}(\mathbf{x}) = \boldsymbol{\Delta}^{-1}\mathbb{E}[g(\mathbf{x}, X_1)X_1X_1^\top]\boldsymbol{\Delta}^{-1}$, and therefore

$$\boldsymbol{\Sigma}_{1,2}(t) := t\boldsymbol{\Sigma}(\boldsymbol{\nu}_1) + (1-t)\boldsymbol{\Sigma}(\boldsymbol{\nu}_2) = \boldsymbol{\Delta}^{-1}\mathbb{E}[g_t(\boldsymbol{\nu}_1, \boldsymbol{\nu}_2, X_1)X_1X_1^\top]\boldsymbol{\Delta}^{-1}.$$

Evaluating the inner expectation yields

$$\begin{aligned}
&\mathbb{E}[g_t(\boldsymbol{\nu}_1, \boldsymbol{\nu}_2, X_1) X_1 X_1^\top] \\
&\quad = \sum_{i=1}^{K} \tfrac{1}{K} (t\langle \boldsymbol{\nu}_1, \boldsymbol{\nu}_i \rangle (1 - \langle \boldsymbol{\nu}_1, \boldsymbol{\nu}_i \rangle) + (1-t)\langle \boldsymbol{\nu}_2, \boldsymbol{\nu}_i \rangle (1 - \langle \boldsymbol{\nu}_2, \boldsymbol{\nu}_i \rangle)) \boldsymbol{\nu}_i \boldsymbol{\nu}_i^\top \\
&\quad = b(1-b)\boldsymbol{\Delta} + \left(\tfrac{a(1-a) - b(1-b)}{K} \right) \left[t \boldsymbol{\nu}_1 \boldsymbol{\nu}_1^\top + (1-t) \boldsymbol{\nu}_2 \boldsymbol{\nu}_2^\top \right] \\
&\quad = b(1-b)\boldsymbol{\Delta} + \mathbf{N}(c_0 \mathbf{D}_t)\mathbf{N}^\top,
\end{aligned}$$

where $\mathbf{N} := [\boldsymbol{\nu}_1 | \boldsymbol{\nu}_2] \in \mathbb{R}^{K \times 2}$, $c_0 := \left(\tfrac{a(1-a) - b(1-b)}{K} \right)$, and $\mathbf{D}_t := \operatorname{diag}(t, 1-t)$. Clearly $c_0 \mathbf{D}_t$ is invertible, as is $\boldsymbol{\Delta}$ since the underlying distribution F is non-degenerate. Moreover, $\mathbf{X}$ is also invertible since the K-block model under consideration is also rank K. The relation $\mathbf{X}^\top \mathbf{X} = K\boldsymbol{\Delta}$ implies $\boldsymbol{\Delta}^{-1} = K\mathbf{X}^{-1}(\mathbf{X}^\top)^{-1}$ and therefore $\mathbf{X}\boldsymbol{\Delta}^{-1}\mathbf{X}^\top = K\mathbf{I}$, so $\boldsymbol{\nu}_i^\top \boldsymbol{\Delta}^{-1} \boldsymbol{\nu}_j = K \mathbb{I}_{ij}$ where $\mathbb{I}_{ij}$ denotes the indicator function for indices i and j. Thus, $(c_0 \mathbf{D}_t)^{-1} + \tfrac{1}{b(1-b)} \mathbf{N}^\top \boldsymbol{\Delta}^{-1} \mathbf{N} = (c_0 \mathbf{D}_t)^{-1} + \tfrac{K}{b(1-b)} \mathbf{I}$, which is also invertible. By an application of the Sherman–Morrison–Woodbury matrix inversion formula (Horn and Johnson (2012), Section 0.7.4), then

$$\begin{aligned}
&\mathbb{E}[g_t(\boldsymbol{\nu}_1, \boldsymbol{\nu}_2, X_1) X_1 X_1^\top]^{-1} \\
&\quad = \left(b(1-b)\boldsymbol{\Delta} + \mathbf{N}(c_0 \mathbf{D}_t)\mathbf{N}^\top \right)^{-1} \\
&\quad = \left(\tfrac{1}{b(1-b)} \right) \boldsymbol{\Delta}^{-1} - \left(\tfrac{1}{b(1-b)} \right)^2 \boldsymbol{\Delta}^{-1} \mathbf{N} \left(\tfrac{1}{c_0} \mathbf{D}_t^{-1} + \tfrac{K}{b(1-b)} \mathbf{I} \right)^{-1} \mathbf{N}^\top \boldsymbol{\Delta}^{-1}.
\end{aligned}$$

For $\boldsymbol{\nu} := \boldsymbol{\nu}_1 - \boldsymbol{\nu}_2 = \left(\frac{a-b}{\sqrt{a}}, -\sqrt{\frac{(a-b)(a+b)}{a}}, 0, \ldots, 0\right)^\top \in \mathbb{R}^K$, then $\boldsymbol{\nu}^\top \boldsymbol{\Delta} \boldsymbol{\nu} = \frac{2}{K}(a-b)^2$ and $\mathbf{N}^\top \boldsymbol{\nu} = (a-b)(1,-1)^\top \in \mathbb{R}^2$. These observations together with subsequent computations yield the following chain of equalities.

$$
\begin{aligned}
\|\boldsymbol{\nu}\|^2_{\boldsymbol{\Sigma}^{-1}_{1,2}(t)} &= \boldsymbol{\nu}^\top \left(\boldsymbol{\Delta}^{-1} \mathbb{E}[g_t(\boldsymbol{\nu}_1, \boldsymbol{\nu}_2, X_1) X_1 X_1^\top] \boldsymbol{\Delta}^{-1}\right)^{-1} \boldsymbol{\nu} \\
&= \boldsymbol{\nu}^\top (\boldsymbol{\Delta} \mathbb{E}[g_t(\boldsymbol{\nu}_1, \boldsymbol{\nu}_2, X_1) X_1 X_1^\top]^{-1} \boldsymbol{\Delta}) \boldsymbol{\nu} \\
&= \boldsymbol{\nu}^\top \boldsymbol{\Delta} \left(\tfrac{1}{b(1-b)} \boldsymbol{\Delta}^{-1} - \left(\tfrac{1}{b(1-b)}\right)^2 \boldsymbol{\Delta}^{-1} \mathbf{N} \left(\tfrac{1}{c_0} \mathbf{D}_t^{-1} + \tfrac{K}{b(1-b)} \mathbf{I} \right)^{-1} \mathbf{N}^\top \boldsymbol{\Delta}^{-1} \right) \boldsymbol{\Delta} \boldsymbol{\nu} \\
&= \boldsymbol{\nu}^\top \left(\tfrac{1}{b(1-b)} \boldsymbol{\Delta} - \left(\tfrac{1}{b(1-b)}\right)^2 \mathbf{N} \left(\tfrac{1}{c_0} \mathbf{D}_t^{-1} + \tfrac{K}{b(1-b)} \mathbf{I} \right)^{-1} \mathbf{N}^\top \right) \boldsymbol{\nu} \\
&= \left(\tfrac{1}{b(1-b)}\right) \boldsymbol{\nu}^\top \boldsymbol{\Delta} \boldsymbol{\nu} - \left(\tfrac{1}{b(1-b)}\right)^2 \boldsymbol{\nu}^\top \mathbf{N} \left(\tfrac{1}{c_0} \mathbf{D}_t^{-1} + \tfrac{K}{b(1-b)} \mathbf{I} \right)^{-1} \mathbf{N}^\top \boldsymbol{\nu} \\
&= \left(\tfrac{2(a-b)^2}{b(1-b)K}\right) - \left(\tfrac{a-b}{b(1-b)}\right)^2 (1,-1) \left(\tfrac{1}{c_0} \mathbf{D}_t^{-1} + \tfrac{K}{b(1-b)} \mathbf{I} \right)^{-1} (1,-1)^\top \\
&= \left(\tfrac{2(a-b)^2}{b(1-b)K}\right) - \left(\tfrac{a-b}{b(1-b)}\right)^2 \operatorname{tr}\left(\left(\tfrac{1}{c_0} \mathbf{D}_t^{-1} + \tfrac{K}{b(1-b)} \mathbf{I} \right)^{-1} \right) \\
&= \left(\tfrac{2(a-b)^2}{b(1-b)K}\right) \\
&\quad - \left(\tfrac{a-b}{b(1-b)}\right)^2 \left(\tfrac{(a(1-a)-b(1-b))b(1-b)t}{((a(1-a)-b(1-b))t+b(1-b))K} + \tfrac{(a(1-a)-b(1-b))b(1-b)(1-t)}{((a(1-a)-b(1-b))(1-t)+b(1-b))K} \right) \\
&= \tfrac{(a-b)^2(a(a-1)+b(b-1))}{(a(1-a)+(a(a-1)-b(b-1))t)(b(b-1)+(a(a-1)-b(b-1))t)K}.
\end{aligned}
$$

In particular,

$$
\sup_{t \in (0,1)} \left[t(1-t) \|\boldsymbol{\nu}\|^2_{\boldsymbol{\Sigma}^{-1}_{1,2}(t)} \right] = \tfrac{1}{K} \tfrac{(a-b)^2}{a(1-a)+b(1-b)}, \tag{6.42}
$$

where by underlying symmetry the supremum is achieved at $t^\star = \frac{1}{2}$ over the entire parameter region $0 < b < a < 1$.

6.4.3.2 Proof of Theorem 38: LSE (denominator)

Recall that for this model $\mathbf{I}_{d^-}^{d^+} \equiv \mathbf{I}_d$ since $d^- = 0$. From Theorem 37 for LSE, the block conditional covariance matrix for each latent position $\mathbf{x}$ can be written in the modified form

$$\tilde{\mathbf{\Sigma}}(\mathbf{x}) = \mathbb{E}\left[\left(\tfrac{g(\mathbf{x},X_1)}{\langle \mathbf{x},\boldsymbol{\mu}\rangle}\right)\left(\tfrac{\tilde{\mathbf{\Delta}}^{-1}X_1}{\langle X_1,\boldsymbol{\mu}\rangle} - \tfrac{\mathbf{x}}{2\langle \mathbf{x},\boldsymbol{\mu}\rangle}\right)\left(\tfrac{\tilde{\mathbf{\Delta}}^{-1}X_1}{\langle X_1,\boldsymbol{\mu}\rangle} - \tfrac{\mathbf{x}}{2\langle \mathbf{x},\boldsymbol{\mu}\rangle}\right)^\top\right].$$

We begin with several preliminary observations in order to define the quantities c_1, c_2, and c_3. Namely, for each latent position (row) $\mathbf{x}$ of $\mathbf{X}$,

$$\langle \mathbf{x}, \boldsymbol{\mu}\rangle = \left(\tfrac{a+(K-1)b}{K}\right) =: c_1; \tag{6.43}$$

$$\mathbb{E}[g(\mathbf{x}, X_1)] = \left(\tfrac{a(1-a)+(K-1)b(1-b)}{K}\right) =: c_2; \tag{6.44}$$

$$\mathbb{E}[g(\mathbf{x}, X_1)X_1] := \left(\tfrac{a(1-a)-b(1-b)}{K}\right)\mathbf{x} + b(1-b)\boldsymbol{\mu} =: c_3\mathbf{x} + b(1-b)\boldsymbol{\mu}. \tag{6.45}$$

Subsequent computations yield

$$\mathbf{\Delta}\mathbf{x} = \left(\tfrac{a-b}{K}\right)\mathbf{x} + b\boldsymbol{\mu};$$

$$\left(\mathbf{\Delta} - \left(\tfrac{a-b}{K}\right)\mathbf{I}\right)\mathbf{x}\mathbf{x}^\top = b\boldsymbol{\mu}\mathbf{x}^\top;$$

$$\langle \mathbf{\Delta}\mathbf{x}, \mathbf{x}\rangle = \left(\tfrac{a^2+(K-1)b^2}{K}\right);$$

$$\tilde{\mathbf{\Delta}} \equiv \mathbb{E}\left[\tfrac{1}{\langle X_1,\boldsymbol{\mu}\rangle}X_1X_1^\top\right] = \tfrac{1}{c_1}\mathbf{\Delta}.$$

The above observations allow us to write $\tilde{\mathbf{\Sigma}}(\mathbf{x})$ as

$$\begin{aligned}
&\mathbb{E}\left[\left(\tfrac{g(\mathbf{x},X_1)}{\langle \mathbf{x},\boldsymbol{\mu}\rangle}\right)\left(\tfrac{\tilde{\mathbf{\Delta}}^{-1}X_1}{\langle X_1,\boldsymbol{\mu}\rangle}-\tfrac{\mathbf{x}}{2\langle \mathbf{x},\boldsymbol{\mu}\rangle}\right)\left(\tfrac{\tilde{\mathbf{\Delta}}^{-1}X_1}{\langle X_1,\boldsymbol{\mu}\rangle}-\tfrac{\mathbf{x}}{2\langle \mathbf{x},\boldsymbol{\mu}\rangle}\right)^\top\right] \\
&\quad=\tilde{\mathbf{\Delta}}^{-1}\mathbb{E}\left[\tfrac{g(\mathbf{x},X_1)}{\langle \mathbf{x},\boldsymbol{\mu}\rangle}\left(\tfrac{X_1}{\langle X_1,\boldsymbol{\mu}\rangle}-\tfrac{\tilde{\mathbf{\Delta}}\mathbf{x}}{2\langle \mathbf{x},\boldsymbol{\mu}\rangle}\right)\left(\tfrac{X_1}{\langle X_1,\boldsymbol{\mu}\rangle}-\tfrac{\tilde{\mathbf{\Delta}}\mathbf{x}}{2\langle \mathbf{x},\boldsymbol{\mu}\rangle}\right)^\top\right]\tilde{\mathbf{\Delta}}^{-1} \\
&\quad=\tfrac{1}{c_1}\mathbf{\Delta}^{-1}\mathbb{E}\left[g(\mathbf{x},X_1)\left(X_1-\tfrac{1}{2c_1}\mathbf{\Delta}\mathbf{x}\right)\left(X_1-\tfrac{1}{2c_1}\mathbf{\Delta}\mathbf{x}\right)^\top\right]\mathbf{\Delta}^{-1}.
\end{aligned}$$

Expanding the term inside the expectation and applying linearity of expectation allows us to analyze each piece in turn. The first term in the expansion can be analyzed via the previous computations under ASE. For the second term,

$$\begin{aligned}
\mathbb{E}\left[\tfrac{1}{2c_1}g(\mathbf{x},X_1)X_1\mathbf{x}^\top\mathbf{\Delta}\right] &= \tfrac{1}{2c_1}\mathbb{E}[g(\mathbf{x},X_1)X_1]\mathbf{x}^\top\mathbf{\Delta} \\
&= \tfrac{1}{2c_1}\left(c_3\mathbf{x}\mathbf{x}^\top+b(1-b)\boldsymbol{\mu}\mathbf{x}^\top\right)\mathbf{\Delta} \\
&= \tfrac{1}{2c_1}\left(c_3\mathbf{x}\mathbf{x}^\top+(1-b)\left[\mathbf{\Delta}-(\tfrac{a-b}{K})\mathbf{I}\right]\mathbf{x}\mathbf{x}^\top\right)\mathbf{\Delta} \\
&= \left(\tfrac{1-b}{2c_1}\right)\mathbf{\Delta}\mathbf{x}\mathbf{x}^\top\mathbf{\Delta}+\left(\tfrac{Kc_3-(a-b)(1-b)}{2c_1K}\right)\mathbf{x}\mathbf{x}^\top\mathbf{\Delta} \\
&= \left(\tfrac{1-b}{2c_1}\right)\mathbf{\Delta}\mathbf{x}\mathbf{x}^\top\mathbf{\Delta}+\left(\tfrac{a(b-a)}{2c_1K}\right)\mathbf{x}\mathbf{x}^\top\mathbf{\Delta}.
\end{aligned}$$

The transpose of this matrix corresponds to the third term in the implicit expansion of interest (not shown). Finally, the fourth term simply reduces to the form

$$\mathbb{E}\left[g(\mathbf{x},X_1)\left(\tfrac{1}{2c_1}\mathbf{\Delta}\mathbf{x}\right)\left(\tfrac{1}{2c_1}\mathbf{\Delta}\mathbf{x}\right)^\top\right]=c_2\left(\tfrac{1}{2c_1}\mathbf{\Delta}\mathbf{x}\right)\left(\tfrac{1}{2c_1}\mathbf{\Delta}\mathbf{x}\right)^\top=\left(\tfrac{c_2}{4c_1^2}\right)\mathbf{\Delta}\mathbf{x}\mathbf{x}^\top\mathbf{\Delta}.$$

Thus,

$$\begin{aligned}
&\mathbb{E}\left[g(\mathbf{x}, X_1)\left(X_1 - \tfrac{1}{2c_1}\boldsymbol{\Delta}\mathbf{x}\right)\left(X_1 - \tfrac{1}{2c_1}\boldsymbol{\Delta}\mathbf{x}\right)^\top\right] \\
&= \mathbb{E}[g(\mathbf{x}, X_1)X_1X_1^\top] - \mathbb{E}[\tfrac{1}{2c_1}g(\mathbf{x}, X_1)X_1\mathbf{x}^\top\boldsymbol{\Delta}] \\
&\quad - \mathbb{E}[\tfrac{1}{2c_1}g(\mathbf{x}, X_1)X_1\mathbf{x}^\top\boldsymbol{\Delta}]^\top + \mathbb{E}[g(\mathbf{x}, X_1)(\tfrac{1}{2c_1}\boldsymbol{\Delta}\mathbf{x})(\tfrac{1}{2c_1}\boldsymbol{\Delta}\mathbf{x})^\top] \\
&= \mathbb{E}[g(\mathbf{x}, X_1)X_1X_1^\top] - \left(\tfrac{a(b-a)}{2c_1K}\right)\mathbf{x}\mathbf{x}^\top\boldsymbol{\Delta} - \left(\tfrac{a(b-a)}{2c_1K}\right)\boldsymbol{\Delta}\mathbf{x}\mathbf{x}^\top + \left(\tfrac{c_2}{4c_1^2} - \tfrac{1-b}{c_1}\right)\boldsymbol{\Delta}\mathbf{x}\mathbf{x}^\top\boldsymbol{\Delta}.
\end{aligned}$$

Let $\mathbf{M}_1 \equiv \mathbf{M}_1(t) := \mathbf{N}\mathbf{D}_t\mathbf{N}^\top$ and $\mathbf{M}_2 := \boldsymbol{\Delta}$ with respect to the notation introduced earlier in the derivation for ASE. By completing the appropriate matrix product, there are explicit constants $\{d_i\}_{i=1}^4$ depending on a, b, and K, such that

$$\begin{aligned}
\tilde{\boldsymbol{\Sigma}}_{1,2}(t) &= t\tilde{\boldsymbol{\Sigma}}(\boldsymbol{\nu}_1) + (1-t)\tilde{\boldsymbol{\Sigma}}(\boldsymbol{\nu}_2) \\
&= \boldsymbol{\Delta}^{-1}\big(d_1\boldsymbol{\Delta} + d_2\mathbf{N}\mathbf{D}_t\mathbf{N}^\top + d_3\mathbf{N}\mathbf{D}_t\mathbf{N}^\top\boldsymbol{\Delta} + d_3\boldsymbol{\Delta}\mathbf{N}\mathbf{D}_t\mathbf{N}^\top \\
&\quad + d_4\boldsymbol{\Delta}\mathbf{N}\mathbf{D}_t\mathbf{N}^\top\boldsymbol{\Delta}\big)\boldsymbol{\Delta}^{-1} \\
&= \boldsymbol{\Delta}^{-1}\left((d_1\mathbf{M}_2 + d_5\mathbf{M}_1) + (\mathbf{I} + d_6\mathbf{M}_2)(d_7\mathbf{M}_1)(\mathbf{I} + d_6\mathbf{M}_2)\right)\boldsymbol{\Delta}^{-1} \\
&=: \boldsymbol{\Delta}^{-1}\left(\mathbf{M}_3 + \mathbf{M}_4\right)\boldsymbol{\Delta}^{-1},
\end{aligned}$$

where

$$\begin{aligned}
\mathbf{M}_3 \equiv \mathbf{M}_3(t) &:= d_1\mathbf{M}_2 + d_5\mathbf{M}_1(t); \\
\mathbf{M}_4 \equiv \mathbf{M}_4(t) &= (\mathbf{I} + d_6\mathbf{M}_2)(d_7\mathbf{M}_1(t))(\mathbf{I} + d_6\mathbf{M}_2).
\end{aligned}$$

Note that $\tilde{\boldsymbol{\nu}}_k := \left(\frac{1}{\langle \boldsymbol{\nu}_k, \boldsymbol{\mu} \rangle}\right)^{1/2} \times \boldsymbol{\nu}_k = \left(\frac{K}{a+(K-1)b}\right)^{1/2} \times \boldsymbol{\nu}_k$ for $k = 1, 2$, so

$$\|\tilde{\boldsymbol{\nu}}\|^2_{\tilde{\boldsymbol{\Sigma}}^{-1}_{1,2}(t)} = \tilde{\boldsymbol{\nu}}^\top \tilde{\boldsymbol{\Sigma}}^{-1}_{1,2}(t) \tilde{\boldsymbol{\nu}} = \left(\frac{K}{a+(K-1)b}\right) \boldsymbol{\nu}^\top \boldsymbol{\Delta} \left(\mathbf{M}_3 + \mathbf{M}_4\right)^{-1} \boldsymbol{\Delta} \boldsymbol{\nu}.$$

The above matrix inversion can again be carried out via the Sherman–Morrison–Woodbury formula. We omit the algebraic details. Subsequent computations and simplification yield

$$\begin{aligned} &\sup_{t \in (0,1)} \left\{ t(1-t) \|\tilde{\boldsymbol{\nu}}\|^2_{\tilde{\boldsymbol{\Sigma}}^{-1}_{1,2}(t)} \right\} \\ &\quad = \tfrac{4(a-b)^2(a+(K-1)b)^2}{4(a(1-a)+b(1-b))(a+(K-1)b)^2K+(a-b)^2K(3a(a-1)+3b(b-1)(K-1)+4abK)}, \end{aligned} \tag{6.46}$$

where by underlying symmetry the supremum is achieved at $t^\star = \frac{1}{2}$ over the entire parameter region $0 < b < a < 1$. Taken together, Eq. (6.42) and Eq. (6.46) simplify to yield $\rho^\star$ as in Eq. (5.18), thereby completing the proof. $\square$

Bibliography

Abbe, E. (2018). Community detection and stochastic block models: recent developments. *Journal of Machine Learning Research 18*(177), 1–86.

Abbe, E., J. Fan, K. Wang, and Y. Zhong (2017). Entrywise eigenvector analysis of random matrices with low expected rank. *preprint arXiv:1709.09565*.

Airoldi, E. M., D. M. Blei, S. E. Fienberg, and E. P. Xing (2008). Mixed membership stochastic blockmodels. *Journal of Machine Learning Research 9*, 1981–2014.

Alon, N., M. Krivelevich, and V. Vu (2002). On the concentration of eigenvalues of random symmetric matrices. *Israel Journal of Mathematics 131*(1), 259–267.

Arias-Castro, E. and N. Verzelen (2014). Community detection in dense random networks. *Annals of Statistics 42*(3), 940–969.

Athreya, A., D. E. Fishkind, M. Tang, C. E. Priebe, Y. Park, J. T. Vogelstein, K. Levin, V. Lyzinski, Y. Qin, and D. L. Sussman (2018). Statistical inference

on random dot product graphs: a survey. *Journal of Machine Learning Research 18*(226), 1–92.

Athreya, A., C. E. Priebe, M. Tang, V. Lyzinski, D. J. Marchette, and D. L. Sussman (2016). A limit theorem for scaled eigenvectors of random dot product graphs. *Sankhya A 78*(1), 1–18.

Avrachenkov, K., L. Cottatellucci, and A. Kadavankandy (2015). Spectral properties of random matrices for stochastic block model. In *Modeling and Optimization in Mobile, Ad Hoc, and Wireless Networks (WiOpt), 2015 13th International Symposium on*, pp. 537–544. IEEE.

Bai, Z. and J. W. Silverstein (2010). *Spectral analysis of large dimensional random matrices*, Volume 20. Springer.

Benaych-Georges, F. and R. R. Nadakuditi (2011). The eigenvalues and eigenvectors of finite, low rank perturbations of large random matrices. *Advances in Mathematics 227*(1), 494–521.

Bhatia, R. (1997). *Matrix analysis*, Volume 169. Springer-Verlag.

Bickel, P. J. and P. Sarkar (2013). Hypothesis testing for automated community detection in networks. *preprint arXiv:1311.2694*.

Bollobás, B., S. Janson, and O. Riordan (2007). The phase transition in inhomogeneous random graphs. *Random Structures and Algorithms 31*(1), 3–122.

BIBLIOGRAPHY

Cai, T. T. and A. Zhang (2018). Rate-optimal perturbation bounds for singular subspaces with applications to high-dimensional statistics. *Annals of Statistics 46*(1), 60–89.

Candès, E. J. and B. Recht (2009). Exact matrix completion via convex optimization. *Foundations of Computational Mathematics 9*(6), 717.

Cape, J., M. Tang, and C. E. Priebe (2017). The Kato–Temple inequality and eigenvalue concentration with applications to graph inference. *Electronic Journal of Statistics 11*(2), 3954–3978.

Cape, J., M. Tang, and C. E. Priebe (2018). On spectral embedding performance and elucidating network structure in stochastic block model graphs. *preprint arXiv:1808.04855*.

Cape, J., M. Tang, and C. E. Priebe (2019a). Signal-plus-noise matrix models: eigenvector deviations and fluctuations. *Biometrika 106*(1), 243–250.

Cape, J., M. Tang, and C. E. Priebe (2019b). The two-to-infinity norm and singular subspace geometry with applications to high-dimensional statistics. *Annals of Statistics, to appear. preprint arXiv:1705.10735*.

Chen, L., J. T. Vogelstein, V. Lyzinski, and C. E. Priebe (2016). A joint graph inference case study: the C. elegans chemical and electrical connectomes. *Worm 5*(2), 1–8.

BIBLIOGRAPHY

Chernoff, H. (1952). A measure of asymptotic efficiency for tests of a hypothesis based on the sum of observations. *Annals of Mathematical Statistics 23*(4), 493–507.

Chernoff, H. (1956). Large-sample theory: parametric case. *Annals of Mathematical Statistics 27*(1), 1–22.

Chung, F. R. (1997). *Spectral graph theory*, Volume 92. American Mathematical Society.

Csermely, P., A. London, L.-Y. Wu, and B. Uzzi (2013). Structure and dynamics of core-periphery networks. *Journal of Complex Networks 1*(2), 93–123.

Davis, C. and W. M. Kahan (1970). The rotation of eigenvectors by a perturbation. III. *SIAM Journal on Numerical Analysis 7*(1), 1–46.

Devroye, L., L. Györfi, and G. Lugosi (2013). *A probabilistic theory of pattern recognition*, Volume 31. Springer.

Ding, X. and T. Jiang (2010). Spectral distributions of adjacency and Laplacian matrices of random graphs. *Annals of Applied Probability 20*(6), 2086–2117.

Eldridge, J., M. Belkin, and Y. Wang (2018). Unperturbed: spectral analysis beyond Davis-Kahan. In *Proceedings of Algorithmic Learning Theory*, Volume 83 of *Proceedings of Machine Learning Research*, pp. 321–358. PMLR.

Erdős, P. and A. Rényi (1959). On random graphs. *Publicationes Mathematicae (Debrecen) 6*, 290–297.

BIBLIOGRAPHY

Erdős, L., A. Knowles, H.-T. Yau, and J. Yin (2013). Spectral statistics of Erdős–Rényi graphs I: local semicircle law. *Annals of Probability 41*(3B), 2279–2375.

Fan, J., W. Wang, and Y. Zhong (2018). An ℓ_∞ eigenvector perturbation bound and its application to robust covariance estimation. *Journal of Machine Learning Research 18*(207), 1–42.

Fishkind, D. E., D. L. Sussman, M. Tang, J. T. Vogelstein, and C. E. Priebe (2013). Consistent adjacency-spectral partitioning for the stochastic block model when the model parameters are unknown. *SIAM Journal on Matrix Analysis and Applications 34*(1), 23–39.

Fortunato, S. (2010). Community detection in graphs. *Physics Reports 486*(3), 75–174.

Goldenberg, A., A. X. Zheng, S. E. Fienberg, and E. M. Airoldi (2010). A survey of statistical network models. *Foundations and Trends in Machine Learning 2*(2), 129–233.

Gower, J. C. and G. B. Dijksterhuis (2004). *Procrustes problems*, Volume 30. Oxford University Press.

Harrell, E. M. I. (1978). Generalizations of Temple's Inequality. *Proceedings of the American Mathematical Society 69*(2), 271–276.

Hoff, P. D., A. E. Raftery, and M. S. Handcock (2002). Latent space approaches to

social network analysis. *Journal of the American Statistical Association 97*(460), 1090–1098.

Holland, P. W., K. B. Laskey, and S. Leinhardt (1983). Stochastic blockmodels: first steps. *Social Networks 5*(2), 109–137.

Holme, P. (2005). Core-periphery organization of complex networks. *Physical Review E 72*, 1–4.

Horn, R. A. and C. R. Johnson (2012). *Matrix analysis*. Cambridge University Press.

Johnstone, I. M. (2001). On the distribution of the largest eigenvalue in principal components analysis. *Annals of Statistics 29*(2), 295–327.

Jolliffe, I. T. (1986). *Principal component analysis*. Springer.

Karrer, B. and M. E. J. Newman (2011). Stochastic blockmodels and community structure in networks. *Physical Review E 83*, 1–10.

Kato, T. (1950). On the upper and lower bounds of eigenvalues. *Physical Review Letters 77*, 334–339.

Kolaczyk, E. D. (2009). *Statistical analysis of network data*. Springer Series in Statistics. Springer.

Koltchinskii, V. and K. Lounici (2017a). Concentration inequalities and moment bounds for sample covariance operators. *Bernoulli 23*(1), 110–133.

Koltchinskii, V. and K. Lounici (2017b). New asymptotic results in principal component analysis. *Sankhya A 79*(2), 254–297.

Le, C. M., E. Levina, and R. Vershynin (2016). Optimization via low-rank approximation for community detection in networks. *Annals of Statistics 44*(1), 373–400.

Le, C. M., E. Levina, and R. Vershynin (2017). Concentration and regularization of random graphs. *Random Structures & Algorithms 51*(3), 538–561.

Lei, J. (2016). A goodness-of-fit test for stochastic block models. *Annals of Statistics 44*(1), 401–424.

Lei, J. and A. Rinaldo (2015). Consistency of spectral clustering in stochastic block models. *Annals of Statistics 43*(1), 215–237.

Leskovec, J., K. J. Lang, A. Dasgupta, and M. W. Mahoney (2009). Community structure in large networks: natural cluster sizes and the absence of large well-defined clusters. *Internet Mathematics 6*(1), 29–123.

Levin, K., A. Athreya, M. Tang, V. Lyzinski, and C. E. Priebe (2017). A central limit theorem for an omnibus embedding of random dot product graphs. *preprint arXiv:1705.09355*.

Liese, F. and I. Vajda (2006). On divergences and informations in statistics and information theory. *IEEE Transactions on Information Theory 52*(10), 4394–4412.

BIBLIOGRAPHY

Lu, L. and X. Peng (2013). Spectra of edge-independent random graphs. *The Electronic Journal of Combinatorics 20*(4), 1–18.

Lyzinski, V. (2018). Information recovery in shuffled graphs via graph matching. *IEEE Transactions on Information Theory 46*(5), 3254–3273.

Lyzinski, V., D. L. Sussman, D. E. Fishkind, H. Pao, L. Chen, J. T. Vogelstein, Y. Park, and C. E. Priebe (2015). Spectral clustering for divide-and-conquer graph matching. *Parallel Computing 47*, 70–87.

Lyzinski, V., D. L. Sussman, M. Tang, A. Athreya, and C. E. Priebe (2014). Perfect clustering for stochastic blockmodel graphs via adjacency spectral embedding. *Electronic Journal of Statistics 8*(2), 2905–2922.

Lyzinski, V., M. Tang, A. Athreya, Y. Park, and C. E. Priebe (2017). Community detection and classification in hierarchical stochastic blockmodels. *IEEE Transactions on Network Science and Engineering 4*(1), 13–26.

Mao, X., P. Sarkar, and D. Chakrabarti (2017). Estimating mixed memberships with sharp eigenvector deviations. *preprint arXiv:1709.00407*.

McSherry, F. (2001). Spectral partitioning of random graphs. *In Proceedings of the 42nd IEEE Symposium on Foundations of Computer Science*, 529–537.

Nadler, B. (2008). Finite sample approximation results for principal component analysis: a matrix perturbation approach. *Annals of Statistics 36*(6), 2791–2817.

BIBLIOGRAPHY

Newman, M. E. and M. Girvan (2004). Finding and evaluating community structure in networks. *Physical Review E 69*(2), 1–15.

Newman, M. E. J. (2006). Modularity and community structure in networks. *Proceedings of the National Academy of Sciences 103*(23), 8577–8582.

Nickel, C. L. M. (2006). Random dot product graphs: a model for social networks. *Ph.D. thesis, Johns Hopkins University*, 1–249.

Oliveira, R. I. (2010). Concentration of the adjacency matrix and of the Laplacian in random graphs with independent edges. *preprint arXiv:0911.0600*.

O'Rourke, S., V. Vu, and K. Wang (2018). Random perturbation of low rank matrices: improving classical bounds. *Linear Algebra and its Applications 540*, 26–59.

Paul, D. (2007). Asymptotics of sample eigenstructure for a large dimensional spiked covariance model. *Statistica Sinica 17*(4), 1617–1642.

Paul, D. and A. Aue (2014). Random matrix theory in statistics: a review. *Journal of Statistical Planning and Inference 150*, 1–29.

Priebe, C. E., J. M. Conroy, D. J. Marchette, and Y. Park (2005). Scan statistics on Enron graphs. *Computational and Mathematical Organization Theory 11*, 229–247.

Priebe, C. E., D. J. Marchette, Z. Ma, and S. Adali (2013). Manifold matching: joint optimization of fidelity and commensurability. *Brazilian Journal of Probability and Statistics 27*(3), 377–400.

BIBLIOGRAPHY

Ranshous, S., S. Shen, D. Koutra, S. Harenberg, C. Faloutsos, and N. F. Samatova (2015). Anomaly detection in dynamic networks: a survey. *WIRES Computational Statistics 7*, 223–247.

Rebrova, E. and R. Vershynin (2018). Norms of random matrices: local and global problems. *Advances in Mathematics 324*, 40–83.

Rohe, K., S. Chatterjee, and B. Yu (2011). Spectral clustering and the high-dimensional stochastic blockmodel. *Annals of Statistics 39*(4), 1878–1915.

Rubin-Delanchy, P., M. Tang, C. E. Priebe, and J. Cape (2017). A statistical interpretation of spectral embedding: the generalised random dot product graph. *preprint arXiv:1709.05506*.

Rudelson, M. and R. Vershynin (2015). Delocalization of eigenvectors of random matrices with independent entries. *Duke Mathematical Journal 164*(13), 2507–2538.

Rukhin, A. (2009). Asymptotic analysis of various statistics for random graph inference. *Ph.D. thesis, Johns Hopkins University*, 1–73.

Rukhin, A. and C. E. Priebe (2011). A comparative power analysis of the maximum degree and size invariants for random graph inference. *Journal of Statistical Planning and Inference 141*, 1041–1046.

BIBLIOGRAPHY

Sarkar, P. and P. J. Bickel (2015). Role of normalization in spectral clustering for stochastic blockmodels. *Annals of Statistics 43*(3), 962–990.

Silverstein, J. W. (1984). Some limit theorems on the eigenvectors of large dimensional sample covariance matrices. *Journal of Multivariate Analysis 15*(3), 295–324.

Silverstein, J. W. (1989). On the eigenvectors of large dimensional sample covariance matrices. *Journal of Multivariate Analysis 30*(1), 1–16.

Stewart, G. W. and J.-g. Sun (1990). *Matrix perturbation theory*. Academic Press.

Sussman, D. L., M. Tang, D. E. Fishkind, and C. E. Priebe (2012). A consistent adjacency spectral embedding for stochastic blockmodel graphs. *Journal of the American Statistical Association 107*(499), 1119–1128.

Sussman, D. L., M. Tang, and C. E. Priebe (2014). Consistent latent position estimation and vertex classification for random dot product graphs. *IEEE Transactions on Pattern Analysis and Machine Intelligence 36*(1), 48–57.

Tang, M., A. Athreya, D. L. Sussman, V. Lyzinski, Y. Park, and C. E. Priebe (2017). A semiparametric two-sample hypothesis testing problem for random graphs. *Journal of Computational and Graphical Statistics 26*(2), 344–354.

Tang, M., A. Athreya, D. L. Sussman, V. Lyzinski, and C. E. Priebe (2017). A nonparametric two-sample hypothesis testing problem for random graphs. *Bernoulli 23*(3), 1599–1630.

BIBLIOGRAPHY

Tang, M., J. Cape, and C. E. Priebe (2017). Asymptotically efficient estimators for stochastic blockmodels: the naive MLE, the rank-constrained MLE, and the spectral. *preprint arXiv:1710.10936*.

Tang, M., Y. Park, N. H. Lee, and C. E. Priebe (2013). Attribute fusion in a latent process model for time series of graphs. *IEEE Transactions on Signal Processing 61*, 1721–1732.

Tang, M. and C. E. Priebe (2018). Limit theorems for eigenvectors of the normalized Laplacian for random graphs. *Annals of Statistics 46*(5), 2360–2415.

Tang, M., D. L. Sussman, and C. E. Priebe (2013). Universally consistent vertex classification for latent positions graphs. *Annals of Statistics 41*(3), 1406–1430.

Vershynin, R. (2018). *High-dimensional probability: an introduction with applications in data science*, Volume 47. Cambridge University Press.

Verzelen, N. and E. Arias-Castro (2015). Community detection in sparse random networks. *Annals of Applied Probability 25*(6), 3465–3510.

Von Luxburg, U. (2007). A tutorial on spectral clustering. *Statistics and Computing 17*(4), 395–416.

Wang, H., M. Tang, Y. Park, and C. E. Priebe (2014). Locality statistics for anomaly detection in time series of graphs. *IEEE Transactions on Signal Processing 62*(3), 703–717.

BIBLIOGRAPHY

Weyl, H. (1912). Das asymptotische Verteilungsgesetz der Eigenwerte linearer partieller Differentialgleichungen (mit einer Anwendung auf die Theorie der Hohlraumstrahlung). *Mathematische Annalen 71*(4), 441–479.

Young, S. J. and E. R. Scheinerman (2007). Random dot product graph models for social networks. *International Workshop on Algorithms and Models for the Web-Graph 4863*, 138–149.

Yu, Y., T. Wang, and R. J. Samworth (2015). A useful variant of the Davis–Kahan theorem for statisticians. *Biometrika 102*(2), 315–323.

Zhang, X., R. R. Nadakuditi, and M. E. J. Newman (2014). Spectra of random graphs with community structure and arbitrary degrees. *Physical Review E 89*, 1–8.

Zhao, Y., E. Levina, and J. Zhu (2012). Consistency of community detection in networks under degree-corrected stochastic block models. *Annals of Statistics 40*(4), 2266–2292.

Zhu, M. and A. Ghodsi (2006). Automatic dimensionality selection from the scree plot via the use of profile likelihood. *Computational Statistics & Data Analysis 51*(2), 918–930.

Vita

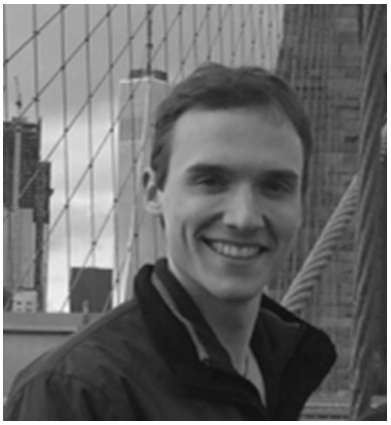

Joshua R. Cape received his Bachelor of Arts degree *summa cum laude* in Mathematics and Economics from Rhodes College in the spring of 2014. In the fall of 2014, Joshua enrolled in the Applied Mathematics and Statistics (AMS) Ph.D. program at Johns Hopkins University, where he completed his AMS Master of Science in Engineering degree in 2016. Joshua's doctoral studies were supported in part by a GAANN Fellowship (via the U.S. Department of Education), the Charles and Catherine Counselman Fellowship at Johns Hopkins University, and an AMS Research Fellowship. Joshua is also a recipient of the Campbell Award by Campbell & Company, Inc., the Acheson J. Duncan Fund for the Advancement of Research in Statistics Travel Award, and the Professor Joel Dean Award for Excellence in Teaching, all at Johns Hopkins University.